

Synthesis and Reactivity of Gold(III) Complexes with Pincer Ligands

Dragoş-Adrian Roşca

A thesis submitted in part fulfilment of the requirements for the degree
of Doctor of Philosophy



School of Chemistry

University of East Anglia, Norwich

February 2014

Supervised by Prof Manfred Bochmann

© This copy of the thesis has been supplied on condition that anyone who consults it is understood to recognise that its copyright rests with the author and that use of any information derived there-from must be in accordance with current UK Copyright Law. In addition, any quotation or extract must include full attribution

STATEMENT OF ORIGINAL WORK

The research described in this thesis has been conducted by the author, Mr Dragoş-Adrian Roşca, and is, to the best of his knowledge, original. Where other people's work has been referred to, this has been cited by corresponding references. Any materials used that were not synthesised by the author have also been detailed as such in the Experimental section in Chapter 5.

Dragoş-Adrian Roşca

ABSTRACT

This thesis explores the synthesis, characterisation and reactivity of catalytically relevant gold(III) species supported by pincer ligands. The tridentate diphenylpyridine ligand was found to stabilise monomeric, terminal hydroxides of gold(III) which are reactive synthons for new metal complexes.

Chapter 1 explores the chemistry of terminal gold(III) hydroxides and their usefulness in the synthesis of photoluminescent materials.

In Chapter 2 we show that pincer-supported terminal gold(III) hydroxides can also be used in combination with a hydride source to access gold(III) hydride complexes, a fundamentally important complex type which has until now eluded isolation and characterisation. We show that gold(III) hydrides can also be readily reduced to give dimeric, gold(II) complexes with an unsupported Au-Au bond, which possess unprecedented thermal stability. A comparison with the one electron reduction of gold(I) hydrides is also presented.

Gold(III) hydroxides are useful synthons for preparation of gold(III) peroxide complexes, another class of gold complexes which are hitherto unexplored. Chapter 3 presents the first data on the characterisation and chemistry of these species. While studying their reactivity, we found that gold(III) peroxides can be converted into gold(III) hydrides *via* successive phosphine mediated oxygen transfer reactions. Since this type of reactivity was not known for any other metal, kinetic investigations are presented. We show that in contrast to gold(III) hydrides, NHC supported gold(I) hydrides undergo the reverse reaction, namely oxygen insertion into the Au—H bond, giving rise to gold(I) peroxides.

In the last chapter of this work, Chapter 4, we show that tridentate pincer ligands can stabilise gold(III) cations in the presence of olefin complexes. We present for the first time strong NMR evidence of the existence of gold(III) olefin complexes and reactivity studies towards nucleophiles. Chapter 4 also describes the synthesis of gold(III) azides and our attempts to use highly fluorinated β -diketiminato ligands in gold(III) chemistry.

ACKNOWLEDGEMENTS

This work would have not been possible without the support and guidance of my research supervisor, Prof Manfred Bochmann to whom I would like to express my heartfelt gratitude. Over the years I have learnt not only a lot of chemistry from Manfred but how to think about chemistry. He allowed me freedom to work on projects that fascinated me and also provided direction when I got stuck. His dynamism and frankness have shaped the way I think as a scientist.

I would like to thank Dr Dan Smith, not only for his generous advice concerning this work but also for his constant moral support, friendship and for brightening up the lab with his fluorescent lab coat. Dan arrived as a postdoc just as the gold(III) project was striving to begin to work and his enthusiasm, good cheer and intellectual contributions were essential in bringing this project to fruition.

Many thanks also to Dr Joseph Wright for providing a greater understanding of this work through DFT calculations and for always having something up his sleeve when a piece of equipment decided to kick up a fuss. I am also grateful to Dr Gregory Wildgoose and Thomas Dann for an excellent collaboration and for helping to shed light into the parts of this work through electrochemistry studies.

The outcome of this project depended heavily on X-ray crystallography so I would like to thank Dr Mark Schormann for having the patience to teach me the basics of operating a diffractometer and solving X-ray structures. I would also like to thank Dr David Hughes for his tremendous help when I got stuck refining crystallographic data and battling to get the diffractometer up and running during its numerous downtimes. Thank you also to the team at the National Crystallography Service, Southampton for helping with the data collection of a few of our samples.

I am greatly in debt to all the members of Bochmann, Lancaster and Wildgoose groups for making the lab a fun place to work. I would like to thank Dr Nicky Savjani not only for finishing off the olefin work but also for his special way 'entertaining' me through molecular sieve and dry ice showers and other pranks which should probably not be mentioned. Thank you also to Elizabeth Jacobs for getting me out of the lab for 'grown-up teas' and James Woods and Angel Bajo for the frequent trips to the pub.

Before coming to UEA, I spent time in Rennes, France working with Dr Yann Sarazin. I would like to thank Yann for taking his time to teach me lab skills, to discuss ideas and also for his generous advice on good wine.

I am also grateful to my brother, Sorin Roşca who went through the effort of proof-reading my thesis and for his constant moral support during my PhD. I would also like to thank my friends in Cluj and also to apologise for driving them to despair when Sorin and I ended up talking about chemistry while they helplessly had to make sense of this strange and funny language.

Lastly I would like to thank my parents. All I have accomplished in life are a result of their patience, love and support.

Thank you all.

LIST OF ABBREVIATIONS

<	less than
>	more than
°	degrees
°C	degrees Celsius
A	anion
Å	Ångstrom
Anal.	Analytically
Approx..	approximately
BAr ^F ₃	tris(pentafluorophenyl)borane
BDE	Bond dissociation energy
br.	Broad
<i>ca.</i>	<i>circa</i>
Calcd.	Calculated
COD	cyclooctadiene
d	doublet
DCM	dichloromethane
DMAD	dimethylacetylenedicarboxylate
<i>e.g</i>	<i>exempli gratia</i>
Et	ethyl
<i>et al.</i>	et alia
<i>etc.</i>	<i>et cetera</i>
g	grams
h	hours
HOMO	Highest Occupied Molecular Orbital
<i>i.e.</i>	<i>id est</i>
IMes	N, N' -bis(2,4,6-trimethylphenyl)imidazol-2-ylidene
<i>iPr</i>	<i>iso</i> -propyl

IPr	N, N'-bis(2,6-diisopropylphenyl)imidazole-2-ylidene
IR	Infra-red
IL	intraligand
<i>J</i>	coupling constant
K	Kelvin
k_{obs}	observed rate constant
KIE	Kinetic isotope effect
L	Litre or neutral ligand
LUMO	Lowest Unoccupied Molecular Orbital
M	Molar concentration (mol/L)
<i>m</i>	multiplet <i>or</i> metre
Mm	millimolar
<i>m-</i>	<i>meta-</i>
Me	methyl
MHz	megahertz
min	minutes
MMLCT	metal-metal to ligand charge transfer
MO	molecular orbital
ⁿ Bu	<i>n</i> -butyl
nb	norbornene
NHC	N-heterocyclic carbene
<i>o-</i>	<i>ortho-</i>
OAc	acetate anion
OAc ^F	trifluoroacetate anion
OTf	triflate anion
<i>p-</i>	<i>para-</i>
Ph	Phenyl
ppm	parts-per-million

Py	Pyridine
q	quartet
r	radius or rate
RT	Room Temperature
Ref.	reference
s	seconds <i>or</i> singlet
t	triplet
tpy	p-tolylpyridine
T	Temperature
tht	tetrahydrothiophene
THF	Tetrahydrofuran
UV-Vis	Ultraviolet-visible
v	very
V.T.	Variable Temperature
<i>vs.</i>	<i>Versus</i>
X	halide
χ	electronegativity
δ	chemical shift
Φ_p	quantum yield
Δ	change
ϵ	extinction coefficient
η	hapto
μ -	bridging <i>or</i> micro
λ_{\max}	wavelength of maximum absorption or emission

TABLE OF CONTENTS

Statement of Original Work	ii
Abstract	iii
Acknowledgements	iv
List of Abbreviations	vi
INTRODUCTION	1
I.1. “Gold chemistry is different”	2
I.2 I Important consequences of relativity on the chemistry of gold	3
I.3. Gold(III) chemistry	7
I.4. Pincer <i>C, N</i> ligands in the stabilisation of gold(III) compounds	10
CHAPTER 1	
Cyclometallated Gold(III) Hydroxides as Precursors for Au—N, Au—C and Luminescent Compounds	12
INTRODUCTION	13
RESULTS AND DISCUSSION	15
1.1 Synthesis and characterisation of complexes	15
1.2 Photoluminescence studies	29
CONCLUDING REMARKS	35

CHAPTER 2	
Chemistry of Gold(III) Hydrides and Unsupported Gold(II) dimers Containing Cyclometallating Pincer Ligands	37
INTRODUCTION	38
RESULTS AND DISCUSSION	41
2.1 Synthesis and characterisation of a thermally stable Gold(III) hydride	41
2.2 Reactivity of the (C [^] N [^] C)AuH	45
2.3 Synthesis and characterisation of an unsupported Au ^{II} —Au ^{II} dimer	50
2.4 Reactivity of the Au ^{II} —Au ^{II} dimer: Synthesis of a mixed valence Au ^I ₄ /Au ^{III} ₄ macrocycle	56
2.5 Attempts to synthesise a dimeric, unsupported Au(0) complex	61
CONCLUDING REMARKS	66
CHAPTER 3	
Chemistry of Cyclometallated Gold(III) Peroxides	68
INTRODUCTION	69
RESULTS AND DISCUSSION	72
3.1 Synthesis and characterisation of the first isolated Gold peroxides	72
3.2 Reactivity of peroxides 42—45 : oxygen transfer reactions	81
3.3 Au—OH to Au—H conversion	84
3.4 Attempted synthesis of a gold(III) superoxide	94
3.5 Insertion of molecular oxygen into gold(I) hydride bond: Synthesis of gold(I) peroxides	96
CONCLUDING REMARKS AND PERSPECTIVES	101

CHAPTER 4

Gold(III) olefin complexes, gold azide complexes and attempts to use β -diketiminato ligands in gold(III) chemistry **104**

TOPIC 1. Synthesis and characterisation of Gold(III) alkene complexes **105**

INTRODUCTION 105

RESULTS AND DISCUSSION 107

4.T1.1 Initial attempts – SMe_2 reactions 107

4.T1.2 Reactions with olefins 110

4.T1.3 Olefin Hydration 114

4.T1.4 Attempted Phthalimide Route 117

CONCLUDING REMARKS AND PERSPECTIVES 118

TOPIC 2: Gold azides **119**

INTRODUCTION 120

RESULTS AND DISCUSSION 121

4.T2.1. Synthesis and characterisation of Au(I) and Au(III) azides 121

4.T2.2 Initial reactivity studies 124

CONCLUDING REMARKS AND PERSPECTIVES 126

TOPIC 3: β -Diketiminato Ligands in Gold(III) Chemistry **127**

INTRODUCTION 127

RESULTS AND DISCUSSION 129

4.T3.1. Synthesis of precursors 129

4.T3.2. Reactivity towards Au(III) 131

CONCLUDING REMARKS 135

CHAPTER 5

Experimental **136**

REFERENCES AND NOTES **180**

INTRODUCTION

I.1 “Gold chemistry is different”

This is the title of an early review article written by Schmidbaur some 20 years ago, in 1992.¹ Elemental gold has a long history in human civilisation, occupying an important role for more than 7000 years.

The physical properties of the metal have made gold attractive over the centuries. Some key features make it so versatile and thus a preferred choice over the other 117 elements in the periodic table when it comes to specific applications ranging from art to medicine, electronics or monetary exchange. Its relatively low melting point (1064 °C) makes it easy to smelt and thus easy to extract from its ores and to be obtained in high purity. Its high ductility (one gram of gold can be beaten out in a sheet of 1.0 m² only 230 atoms thick) and low electrical resistivity (23.5 nΩ m) make it ideal for applications in electronics while its distinctive colour and relatively low abundance (0.004 ppm in Earth’s crust) make it especially suitable for use in the financial market.²

Nevertheless, at a first glance, what really makes gold stand out from the rest of the metals in the periodic table is its reduced reactivity. The ‘noble’ character of gold is translated into the fact that its compounds are generally metastable and apart from the combinations with highly oxidising halogens, reduction of gold compounds to elemental gold is usually the thermodynamically preferred process. This mirrors in the fact that, with very few exceptions, in its natural deposits, the gold occurs in elemental form.³ The chemical inertness of the metal seemed to offer only very limited opportunities in terms of its chemistry and, as a consequence, until recently, gold chemistry has not been a major focus area.⁴

When gold chemistry began to be established at the end of the 19th century, it soon became obvious that rather than being a mere analogue of the other two coinage metals, copper and silver, gold has some rather unique and extreme properties. Notable differences include the specific colour of gold, the resistance towards strong oxidising agents such as nitric acid, the ability to access high oxidation states and also the facile *reduction* of the metal in the presence of caesium, to form stable auride salts, such as Cs⁺Au⁻, which were reported as early as the 1930s.⁵ Nevertheless, these properties were only understood with the advent of the concept of relativity in the quantum theory which was adopted in the theoretical chemistry circles in the 1970s.⁶

As the nuclear charge increases ($Z > 70$), electrons that penetrate to the nucleus (the *s* electrons and to a lesser extent the *p* electrons) increase their average velocity, which, according to the theory of relativity leads to an increase in their mass. The effect leads to a **contraction of the *s* orbitals and decrease in energy** (effect called *relativistic contraction*)

in heavier elements when compared to lighter elements which are not affected. This determines the electrons located in the contracted s orbitals to be more strongly bound and to screen the nuclear charge from other electrons (especially d and f electrons) more effectively than if the relativistic effects were absent. An indirect consequence is therefore that **the d and f orbitals expand in size and increase in energy** (effect called *relativistic expansion*) in heavier elements.⁷ (Figure 1, left)

The contraction of the s orbital increases considerably while the $4f$ orbitals is being filled (also because of the lanthanide contraction) and more drastically when the $5d$ orbitals are filled. The maximum contraction occurs in the case of gold (ground state electron configuration $[\text{Xe}]4f^{14}5d^{10}6s^1$), with platinum ($5d^96s^1$) and mercury ($5d^{10}6s^2$) also experiencing significant contributions from relativistic contraction effects.^{7,8} (Figure 1, right)

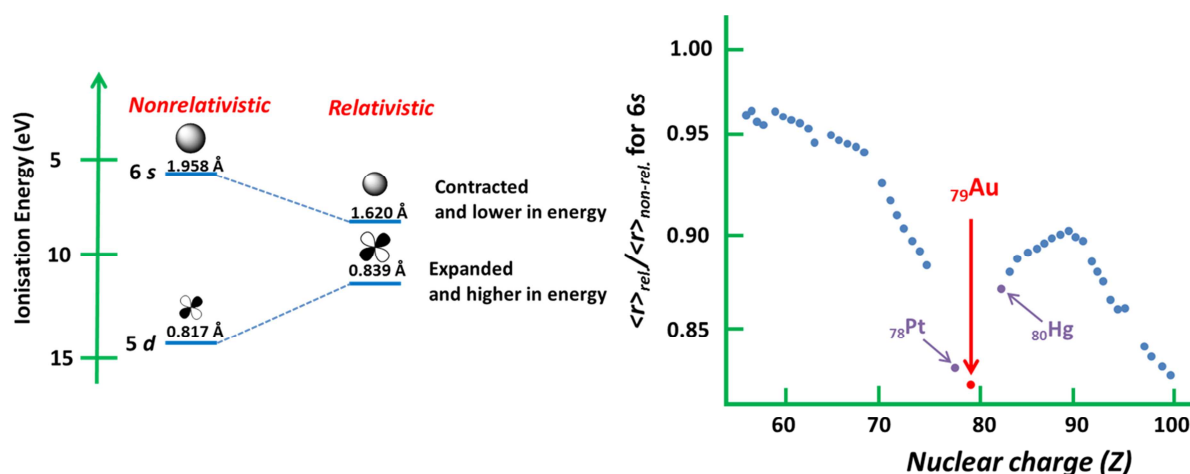


Figure 1 Comparison of calculated sizes and energies of $6s$ and $5d$ orbitals of gold with and without relativistic effects (*left*, adapted from reference⁹); Calculated relativistic contraction of the $6s$ orbital radii, underlying Pt, Au and Hg as markedly influenced (*right*, adapted from reference⁷)

I.2 Important consequences of relativity on the chemistry of gold

The most obvious effect of the $6s$ orbital contraction and $5d$ orbital expansion is on the optical properties of gold especially when compared to silver. Since the $6s$ shell is stabilised (decreases in energy) and the $5d$ shell is destabilised (increases in energy), the gap between the energy levels of the two frontier orbitals is smaller accounting for the absorption of light corresponding 2.38 eV (blue light) thus reflecting yellow light. In the case of silver, the contraction and stabilisation of the $5s$ orbital is not significant, thus the related absorption is 3.7 eV (ultraviolet light).¹⁰

The sum of the three effects (a) stabilisation and contraction of 6s orbitals (b) destabilisation and expansion of 5d orbitals and (c) smaller energy gaps between the energy levels of 5d, 6s and 6p orbitals which as a consequence can favourably intermix and overlap, has profound influences on the chemistry of gold. These influences have been extensively analysed employing computational methods by Pyykkö^{7,11} and a number of the consequences on the chemistry of gold are summarised below:

§1 Because of the pronounced stabilisation of the 6s orbital, the *first ionisation energy of gold is very high* (9.23 eV).⁸ A direct consequence of this is that the **reduction potential of gold is higher than the one of any other metal** ($\text{Au}^+/\text{Au}^0 +1.83 \text{ V}$)¹² making most gold compounds metastable and prone to reduction.

§2 The drop in energy of the 6s orbital also means that unlike most metals, gold can easily *accept an electron*, forming the auride anion Au^- ($5d^{10}6s^2$). This implies that gold has a high electron affinity (2.039 eV compared to 1.202 eV for Ag),¹⁰ which in fact ranks the highest amongst metals. This also makes gold **the most electronegative metal** ($\chi_{\text{Pauling}} 2.54$), placing it close to iodine ($\chi_{\text{Pauling}} 2.66$) and carbon ($\chi_{\text{Pauling}} 2.55$).¹¹ As a result, **Au—H and Au—C bonds have low polarity and are highly covalent**.^{7,13}

§3 In the gas phase, gold exhibits a halogen-like behaviour, forming stable dimeric Au_2 molecules with a dissociation energy of 228 kJ mol⁻¹ and bond length of 2.472 Å.¹⁴ The tendency towards association is more obvious in the solid state where **gold tends to associate in cluster compounds**, ($\text{Au}_{n>4}$)^{m+} typically stabilised by phosphine ligands, where the oxidation state of gold is intermediate between (+1) and (0). Gold clusters have proved to be very efficient as oxidation catalysts, most notably the low temperature oxidation of CO which is currently one of the most extensively studied areas in gold chemistry.¹⁵

§4 Similar to the other coinage metals, gold typically forms complexes in the oxidation state +1 (d^{10}). However, in contrast to copper and silver, because of the expansion and destabilisation of the 5d orbitals due to relativistic effects, gold can access higher oxidation states making gold(III) ($5d^8$) compounds relatively common. Furthermore, direct oxidation of gold with *aqua regia* or with halogens typically generates gold(III) compounds. ($\text{Au}^{3+}/\text{Au}^+ 1.36 \text{ V}$, $\text{Au}^{3+}/\text{Au}^0 1.69 \text{ V}$)¹²

§5 Because of the diminished gap between the 5d, 6s and 6p, **closed shell, gold(I) complexes ($5d^{10}$)**, isoelectronic and isostructural to Hg^{2+} , **typically form two-coordinated complexes which adopt linear coordination geometries**. This geometry can be rationalised in terms of *sd* hybridisations at the gold(I) centre.¹⁶ (see also §11)

Open shell gold(III) complexes (d^8) are isoelectronic and isostructural with platinum(II) complexes and adopt a square planar geometry around the metal centre.
(Figure 2)

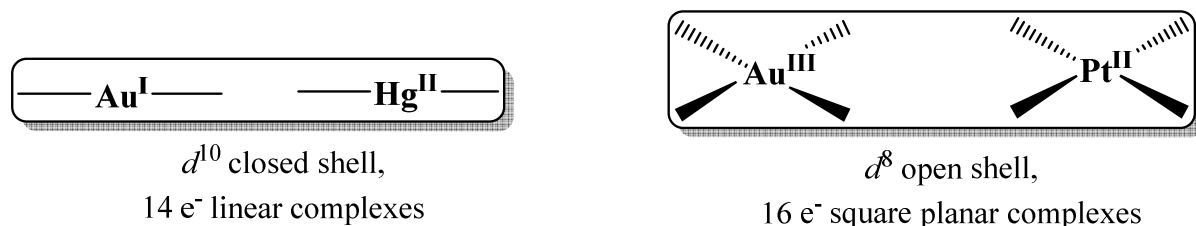


Figure 2 Comparison between geometries around gold(I), mercury(II), gold(III) and platinum(II)

§6 **Gold(I) derivatives**, especially the $\text{Au}(\text{PR}_3)$ fragment **can form hypervalent compounds** of main group elements and species such as $[\text{C}\{\text{Au}(\text{PPh}_3)\}_6]^{2+}$, $[\text{N}\{\text{Au}(\text{PPh}_3)\}_5]^{2+}$ or $[\text{O}\{\text{Au}(\text{PPh}_3)\}_4]^{2+}$ have been long known.¹⁷⁻¹⁹ These complexes exhibit short $\text{Au}\cdots\text{Au}$ interactions which can be rationalised on the basis of the small energy gap between the HOMO ($5d$) and LUMO ($6s$) in the Au^+ fragments so that overlap between the HOMO and LUMO of neighbouring gold(I) centres is favourable. Thus, **intra- and intermolecular “closed-shell interactions” between two positively charged Au^+ centres are common and are called *aurophilic interactions***. They may overrule substantial repulsive forces and are typically between 2.8 – 3.5 Å long, well below the sum of the van der Waals radii (*ca.* 3.6 Å). Their strength is comparable to the one of hydrogen bonding (typical measurements range from 21 – 63 kJ dimer⁻¹) and while they are typically encountered in solid state, in some selected cases they are retained even in solution.^{6,19} These **interactions** are thought to be **responsible for the photoluminescent properties** of some gold(I) complexes, where emission has been assigned to metal-metal-to-ligand charge-transfer (MMLCT) excited states.²⁰

On the other hand, aurophilic interactions involving open shell, gold(III) centres are a matter of debate, especially when compared to $\text{Au}(\text{I})\cdots\text{Au}(\text{I})$ or $\text{Pt}(\text{II})\cdots\text{Pt}(\text{II})$ interactions,^{19,21} despite the fact that intermolecular $\text{Au}(\text{III})\cdots\text{Au}(\text{III})$ short contacts have been predicted by Pyykkö and co-workers.²² Since metallophilic interactions play an important role in determining the photoluminescent properties of the complexes, this suggests that **gold(III) complexes showing photoluminescent behaviour are more scarce than those of Au(I) and Pt(II)**. Nevertheless, the study of the photoluminescent properties of gold(III) complexes is one of the emerging areas of research in gold chemistry.²³

§7 Due to “relativistic contraction”, **the gold(I) cation** falls between copper and silver. ($r_{\text{Au}(\text{I})} = 1.25$ Å, $r_{\text{Ag}(\text{I})} = 1.33$ Å, $r_{\text{Cu}(\text{I})} = 1.13$ Å)^{6, 24} If the size of gold(I) were only

affected by the lanthanide contraction, the radii of Au(I) and Ag(I) would have been merely equal or comparable, similar to the situation of Zr and Hf. **A comparison between the radii of Au(III) and Ag(III) was not possible experimentally** since silver does not typically form compounds in oxidation states +III.⁶

§8 Since the *5d* orbitals are more diffuse in the case of gold, there is a decreased electron/electron repulsion which implies that the *5d* electrons are held with greater energy when compared to the case of the *4d* electrons in Ag or *3d* electrons in Cu. This translates into a **smaller degree of nucleophilicity of gold compared to the other coinage metals**, which makes them less susceptible to oxidative addition reactions. This is also mirrored in the high oxidation potential of gold(I) (see also §1 and §4) and, as a consequence, **gold does not typically cycle between +I and +III oxidation states**, even though some exceptions have been reported.²⁵

§9 A consequence of the *6s* (LUMO in the case of Au(I)) and *6p* orbital contraction and stabilisation (Figure 1) is also **the increased Lewis acidity in Au(I) complexes**, which is much more pronounced than the one of the other coinage metals. The strong Lewis acidity is also mirrored in the high electronegativity of gold.²⁵ (See also §2) Also, computational studies performed on the (PH₃)Au⁺ fragment suggest rehybridisation of the phosphineAu(I) molecular orbitals so that the occupancy of the *6s* orbital is greatly increased. (see also §11 and Figure 3) Since the Au(I) cation is also large and shares the positive charge with the ligand, it is likely that orbital, rather than charge interactions would be dominant in binding a second ligand, thus making **Au(I) a ‘soft’ Lewis acid**.

Since interaction of gold(I) centres with ‘soft’ electrophiles is favourable, gold(I) complexes have become catalysts of choice for the activation of π -systems, with the most popular substrates being alkynes. The versatility of gold(I) reagents together with their resistance to oxygen and moisture has made them indispensable for an important number of transformations such as hydration, hydroamination, hydrogenation or oxidation reactions.³⁰ The increased attention given to gold homogenous and heterogeneous catalysis from both the organic and organometallic communities has led to the coining of the phrase “21th century gold rush”.²⁶

Gold(III) on the other hand is comparatively ‘harder’ Lewis acid. Historically, the activation of π -systems by gold has first been attempted using simple gold(III) compounds such as AuCl₃ and HAuCl₄ or its salts which are commercially available.²⁷ The first experiments have been reported as early as 1976 which involved the reaction of alkynes with methanol/water in the presence of substoichiometric amounts of HAuCl₄ to give the corresponding ketones.²⁸ The applications were extended to the hydrochlorination of

acetylene in the presence of HAuCl_4 to give vinyl chloride. In this case, the gold catalyst replaced HgCl_2 which is more toxic.²⁹ **In contrast to gold(I) mediated catalysis, gold(III) catalytic chemistry is less developed.** Nevertheless, since gold(III) complexes adopt tetracoordinate square-planar geometry, a larger choice from influences from neutral or anionic ligands in *cis*- or *trans*- positions relative to the incoming substrate would be available.²⁷

§10 The relativistic contraction of $6s$ orbitals has also been invoked for the shortening of the Au—L bonds ($\text{L} = \text{ligand}$).²⁵ There is limited data for **ligand exchange processes both in gold(I) and gold(III) chemistries**, but the information available supports the notion that an **associative mechanism is favoured**. In the case of Au(III) , the rate of ligand exchange has been reported to be lower than the corresponding palladium and platinum but higher than the corresponding nickel complexes.³⁰

§11 Since the frontier orbitals of Au(I)^+ units are typically regarded as σ -symmetry sp_z or sd_{z^2} hybrids, these fragments **are related to a proton H^+ (s orbital) through isolobality**. In the case of the frontier orbitals of both Au^+ and the H^+ , similar symmetries, shapes and comparable energies are present.¹⁶(Figure 3)

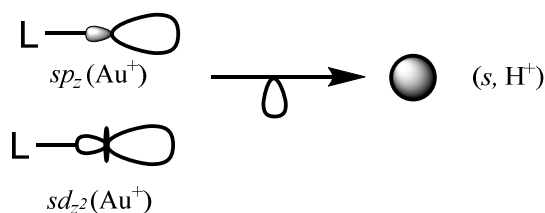


Figure 3. Isolobal analogies between the frontier orbitals of Au(I)^+ and H^+

I.3. Gold(III) chemistry

As a result of the vast interest in gold(I) mediated homogenous catalysis (See §9), major progress has been made in the coordinative chemistry of Au(I) in order to facilitate the understanding of various reaction mechanisms and to propose the structures of the active species. With the development of suitable stabilising ancillary ligands for gold(I) chemistry such as N-heterocyclic carbenes or phosphines, only recently have examples of gold(I) hydrides, arenes or terminal hydroxides been reported. (Table 1) Most of these species proved to be highly active catalysts or useful catalytic models for various transformations.³¹

In contrast, the coordination chemistry of gold(III) is far less developed³² despite the fact that gold(III) organometallic compounds are among the oldest ever to be reported, some more than 100 years ago. Since the +III oxidation state was readily accessible by dissolving

gold in *aqua regia* to obtain HAuCl_4 , (see §4) the very first examples contain exclusively gold(III) centres.

Generally, four methods can be summarised for the synthesis of gold(III) complexes:³²

(i) *Transmetallation reactions.* Initially, transmetallation agents such as alkyllithium or Grignard reagents have been used but since these complexes also facilitate electron transfer reactions, milder transmetallating agents such as organomercury, organothallium or organotin compounds have proven to give better yields.

The reports of dialkyl and trialkyl complexes of gold(III) dominated the early literature since they were readily accessible by reacting HAuCl_4 or AuX_3 ($\text{X} = \text{Cl}, \text{Br}, \text{I}$) with lithium alkyls or Grignard reagents.³³ The first reported examples were the dialkylgold(III) halide species by Pope and Gibson in 1907,³⁴ while trialkylgold complexes could only be isolated in the presence of Lewis bases such as phosphines.³⁵ All these species are susceptible to reductive elimination; for example trialkylgold complexes such as $[\text{AuMe}_3]_2$ show signs of decomposition above $-40\text{ }^\circ\text{C}$ with deposition of gold film and liberation of ethane, while phosphine adducts such as *cis*- $\text{Me}_2\text{EtAu}(\text{PPh}_3)$ undergo the same reaction only above $70\text{ }^\circ\text{C}$.³⁵

(ii) *Electrophilic substitution by gold(III) of one aromatic ring (metallation).* The first method for obtaining arylgold(III) complexes is the direct auration of aromatic derivatives with AuCl_3 to give $[\text{Ar}_2\text{AuCl}]_2$. In the absence of a stabilising Lewis base, the species then undergo reductive elimination to generate the corresponding chloroaryl derivatives.³⁶ A succession of transmetallation reactions followed by auration of a neighbouring aromatic ring is often employed for the synthesis of cyclometallated gold(III) complexes which are especially attractive because they suppress reductive elimination reactions on the metal centre.³⁷ (*vide infra*)

(iii) *Oxidative addition of halogen to the respective gold(I) complex*

(iv) *Substitution reactions on gold(III) derivatives*

The development of the chemistry of gold(III) closely followed the one of its isoelectronic and isostructural neighbour, platinum (II).^{38,39} (see also §5) Nevertheless, while there are a number of similarities between the two metals in their respective oxidation states, such as similar symmetries of their frontier orbitals, their preference for associative mechanisms in ligand exchange reactions or their reluctance to form pentacoordinated species, important differences arise in their reduction potentials. ($\text{Au}^{3+}/\text{Au}^+$ 1.36 V, $\text{Au}^{3+}/\text{Au}^0$ 1.69 V while $\text{Pt}^{2+}/\text{Pt}^0$ 1.19 V,¹² see also §4)

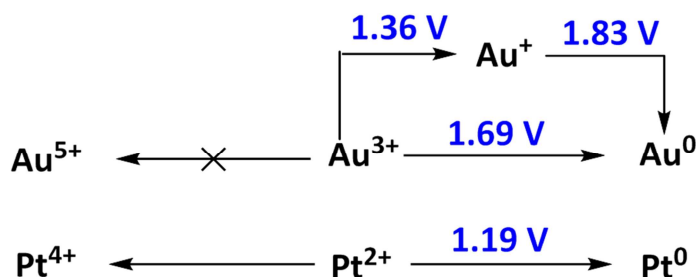


Figure 4. Standard electrode reduction potentials in acidic aqueous solutions at 25 °C

The high reduction potential of gold(III) compared to the one of platinum(II) is reflected in the timeline of some of their fundamental classes of compounds.(Table 1) Notably, π -complexes such as the platinum(II) olefin complexes reported by Zeise in 1827⁴³ and platinum(II) carbonyl complexes reported by Schützenberger in 1868⁴⁰ are the first olefin and carbonyl complexes to be reported for any metal. Platinum hydride complexes are also well known since their first report more than 50 years ago⁴¹ and since then have been thoroughly investigated.³⁸

In contrast, attempts to generate the gold(III) analogues led instead to reduction to gold metal or in some cases, to gold(I) and their successful synthesis and isolation were still unreported prior to the commencement of this work.

Table 1. Characterisation of key examples of gold(III) complexes prior to the commencement of this work^a

Pt(II)		Year	Ref	Au(I)		Year	Ref	Au(III)	
$L_nPt^{II}H$	✓	1958	41	$LAu^I H$	✓	2008	44	$L_nAu^{III}H$	X
$L_nPt^{II}(CO)_x$	✓	1868	40	$LAu^I CO$	✓	1925/1982	45	$L_nAu^{III}CO$	X
$L_nPt^{II}(\text{arene})$	✓	1973/1977	42	$LAu^I(\text{arene})$	✓	2006	46	$L_nAu^{III}(\text{arene})$	X
$L_nPt^{II}(\text{olefin})$	✓	1827/ 1954	43	$LAu^I(\text{olefin})$	✓	1966/1987	47	$L_nAu^{III}(\text{olefin})$	X

^a L denotes here both neutral and anionic ligands

Nevertheless, despite the lack of data on these complexes, they are frequently proposed as key intermediates in various gold(III) mediated organic reactions. While there are increasing reports on gold(III) complexes acting as catalysts or pre-catalysts, most investigations have followed programmes advancing by trial and error making it hard to identify any specific action or active species.²⁷ Also, in contrast to gold(I) mediated catalysis where a plethora of fine-tuned complexes have been reported for specific purposes,^{30,48} there are, to the best of our knowledge, no reports of any successful approach to a completely rational design of a gold(III) catalyst, with most reactions employing the commercially available gold trihalides or $HAuCl_4$ and its salts as (pre)catalysts.²⁷

With the recent advances in gold(III) mediated homogenous catalysis, in order to differentiate between experimental evidence and speculation, it is necessary to obtain insight into the chemistry of the proposed catalytic intermediates. In this respect, this work aims to provide spectroscopic and crystallographic data for a number of catalytically relevant intermediate models that have so far eluded isolation. We hope that the information obtained would benefit researchers working in the field of homogenous catalysis in the proposition of reaction mechanisms and in the rational design of gold(III) catalysts.

I.4 Pincer C, N ligands in the stabilisation of gold(III) compounds

In order to prevent reductive elimination reactions, chelating ligands around the gold(III) centre are commonly employed. Early reports (1939) have shown for example that O-type chelates such as κ^2 -acetylacetonato (acac) ligands can stabilise Me_2Au^+ fragments.³² More recent work focused on 2,2'-bipyridyl (N,N) or 2-phenylpyridine (C,N) type pincer ligands which have been successfully proven to be efficient in stabilising species such as bridging oxo complexes, terminal anilides, acetylides and *cis*-diarylgold(III) species and this work has been reviewed by Henderson and others.^{37,49} (Figure 5)

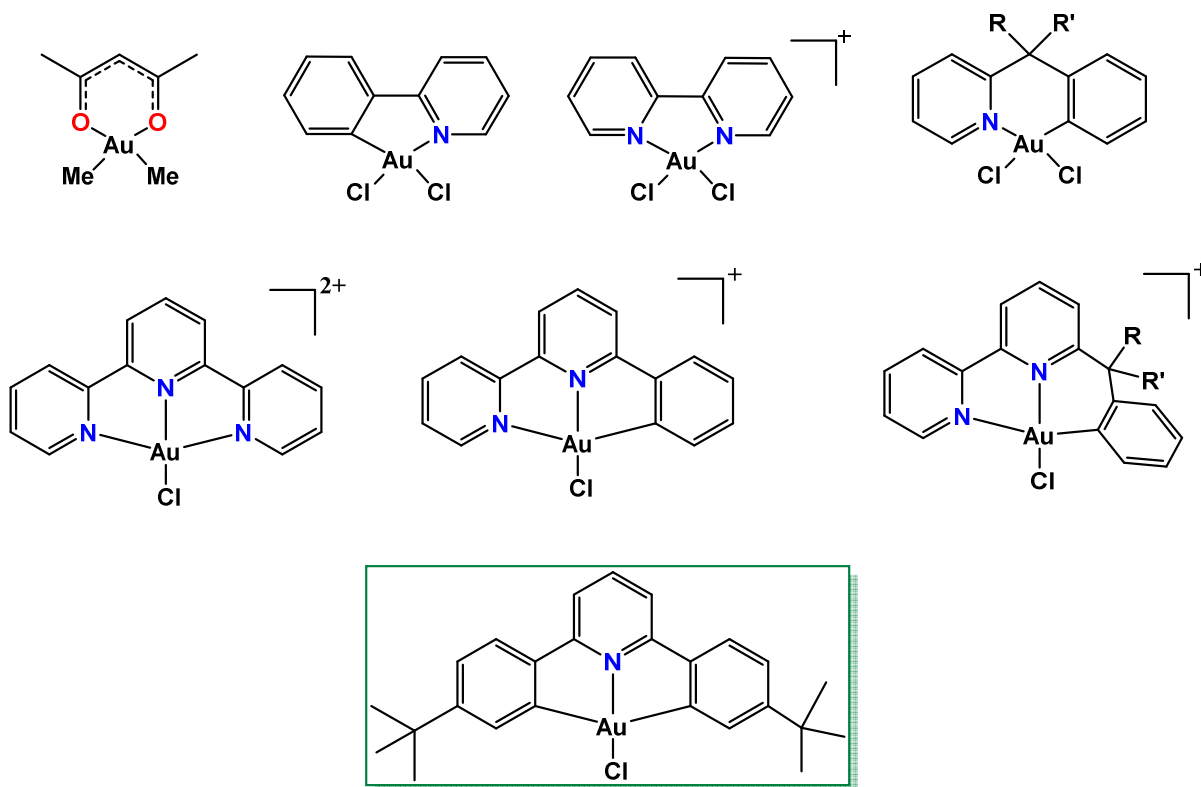


Figure 5. Selected examples of chelating ligands for the stabilisation of gold(III) centres

Among these ligands, the tridentate, 2,6-diphenylpyridine gold(III) complexes first synthesised by Che⁵⁰ and Yam⁵¹ are remarkable for their thermal stability with some

compounds withstanding reflux in toluene for more than 24 h without any decomposition. The thermal stability probably arises from the fact that the gold(III) centre is flanked by the two opposite phenyl groups which ligate the metal centre through thermodynamically stable Au—C bonds. (See also §2) Moreover, the aromatic groups are arranged in such a conformation that disfavours reductive elimination, the common decomposition pathway for gold(III) complexes. This also leaves the fourth coordination site (in Figure 5 occupied by a chloride ligand) conveniently available for functionalisation. In this respect the (C[^]N[^]C) diphenylpyridine ligand was chosen for our work. We have also decided to decorate the flanking phenyl groups with *tert*-butyl substituents in order to improve the solubility of the complexes in common organic solvents.

This work presents our investigation using tridentate diphenylpyridine ligands to stabilise gold(III) hydroxides, hydrides, peroxides and olefin complexes. Reactivity studies and in some cases comparison with gold(I) analogues and kinetic studies are also presented.

CHAPTER 1

Cyclometallated Gold(III) Hydroxides as Precursors for Au—N, Au—C and Luminescent Compounds

A portion of this chapter has appeared in print:

D.-A Roşca, D. A Smith, M. Bochmann "Cyclometallated Gold(III) Hydroxides as Versatile Synthons for Au-N, Au-C Complexes and Luminescent Compounds" *Chem. Commun.*, **2012**, 48, 7247.

D. A. Smith, D.-A. Roşca, M. Bochmann "Selective Au-C Cleavage in (C^NC)Au(III) Aryl and Alkyl Pincer Complexes" *Organometallics*, **2012**, 31, 7600.

INTRODUCTION

Late transition metals are generally considered oxophobic. The weakness of the M—OH bond is often explained by the mismatch in hard/soft interaction between the hydroxo ligand, regarded as a hard base and the metal centre which functions as a soft acid. While compared to other metal hydroxides, reports of late transition metal hydroxides are still scarce, recent studies have shown their versatility as synthons, enabling access to different classes of organometallic complexes in an expedient fashion.⁵²

Gold complexes bearing oxygen ligands have attracted a lot of attention over the years. Initial interest was prompted by the unusual properties of the synthesised complexes. Since the LAu(I)⁺ fragment is isolobal to a proton,¹⁶ special attention was attributed to species of the type [(LAu)₃O]⁺ (L = PR₃),⁵³ [(LAu)₂OH]⁺ (L = N-heterocyclic carbene⁵⁴ or phosphine^{55,56}), isolobal to H₃O⁺ and [(LAu)₄O]²⁺ (L = PR₃),⁵⁷ isolobal to the doubly protonated water, H₄O²⁺. (Figure 6) Some of the oxo-species have been found to undergo facile reduction in the presence of CO to give much sought-after small size gold clusters.⁵⁶ Surprisingly perhaps, a terminal LAu(I)OH (L = N-heterocyclic carbene) has only recently been isolated,⁵⁸ employing 1,3-bis(2,6-diisopropylphenyl)imidazole-2-ylidene (IPr) as an ancillary ligand which possesses the steric and electronic characteristics needed for stabilising such species. Both bridging and terminal gold(I) hydroxides have found applications in silver-free gold(I) mediated catalysis^{54, 59, 60} or as synthons for other classes of gold(I) complexes *e.g.* aryls⁶¹, N-heterocyclic carbenes⁶² or amides.⁶³

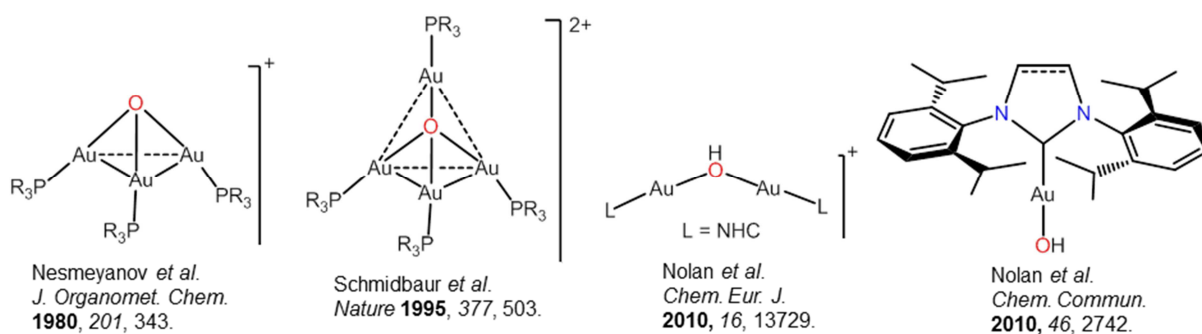


Figure 6. Examples of Gold(I) oxo and hydroxo complexes

In the case of gold(III) chemistry, gold complexes containing singly⁶⁴ and doubly bridging⁶⁵ oxygen ligands have received increasing attention recently.⁶⁶ Studies by Cinellu *et al.* have found that double oxo bridged [(bipy)Au(μ -O)₂]²⁺ complexes (Figures 7) can oxidise olefins such as styrene^{67, 68} or norbornene where the auroxoetane intermediate was isolated and structurally characterised.⁶⁸

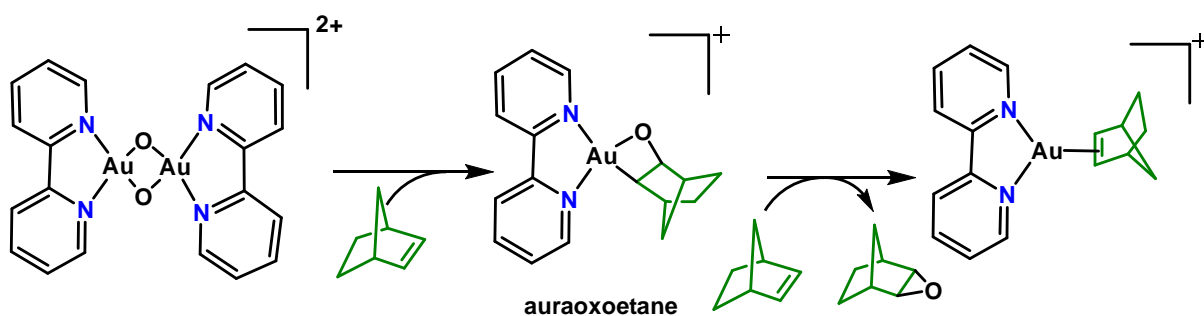


Figure 7. Gold(III) mediated olefin oxidation *via* auroxoethane species

The same group has also reported studies on *in vitro* cytotoxic activity of this class of complexes on several cancer cell lines.⁶⁹ These complexes are stable to air and moisture which also make them attractive for use in catalysis. Very recent studies report the use of the cations $[(\text{bipy})\text{Au}(\mu\text{-O})_2]^{2+}$ as catalysts for intramolecular hydroamination, with the future aim to make them suitable for asymmetric catalysis by introducing substituents in the 6,6' positions.⁷⁰

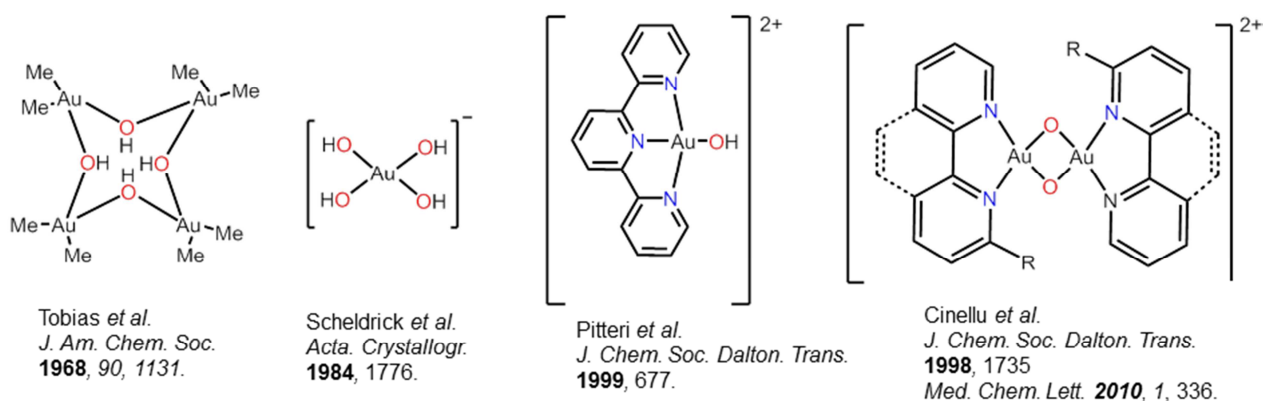


Figure 8. Gold(III) hydroxo and oxo complexes.

Compared to the gold(I) and gold (III) oxo species, gold(III) hydroxides have received less attention over the years, despite the fact that they were among the first oxygen bearing gold complexes ever to be isolated. Early examples include the tetrameric $[\text{Me}_2\text{AuOH}]_4$ which was reported to detonate easily upon impact,⁷¹ and various salts containing the $[\text{Au}(\text{OH})_4]^-$ anion.⁷² (Figure 8) Significant stabilisation was achieved by using cyclometallating ligands but reports on isolated gold(III) terminal hydroxo complexes are still scarce. Examples include the cationic hydroxides supported by bidentate $[(\text{bipy})\text{Au}(\text{OH})_2]^+$ (bipy = 2,2'-bipyridyl)⁷³ and tridentate $[(\text{N}^{\wedge}\text{N}^{\wedge}\text{N})\text{Au}(\text{OH})]^{2+}$ ($\text{N}^{\wedge}\text{N}^{\wedge}\text{N}$ = terpyridine)⁷⁴ N-donor ligands, with only the latter being structurally characterised. Both types of complexes were prepared

by ligand exchange from the corresponding chlorides and, in the case of [(bipy)Au(OH)₂]⁺, also by hydrolysis from of the di-bridging oxo complex.

Despite their potential applications as synthons for other classes of gold(III) complexes, reports on the reactivity of gold(III) hydroxides are limited. The only studies known to us include the reactions of mono- and dicationic gold(III) hydroxides or methoxides with anilines to give gold(III) amides^{75,76} or with terminal acetylenes and thiols to give gold(III) acetylides and thiolates.⁷⁶ A study is also reported on the *in vitro* cytotoxic activity of several gold(III) hydroxides against various cancer cell lines.⁷⁷

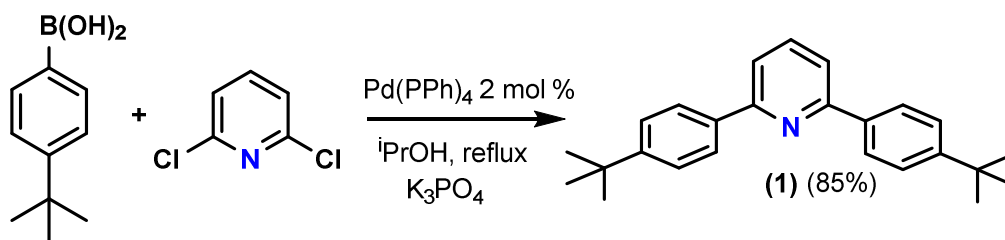
Given the reported remarkable stability of diphenylpyridine supported gold(III) species,^{50,51,78} we envisaged they would also fulfil the electronic and conformational requirements to stabilise terminal neutral gold(III) hydroxides. This chapter summarises our results on the synthesis, reactivity and applications of gold(III) hydroxides, methoxides and trifluoroacetates. The basicity of the hydroxide is explored in a series of acid-base reactions, giving rise to a plethora of gold(III) complexes containing N-heterocycle, acetylide or acetato ligands. A particularly versatile method for generating gold(III) aryl complexes by reacting gold(III) hydroxides with arylboronic acids is also described. Bis-cyclometallated pincer complexes are prone to acid mediated Au—C bond protolysis, giving rise to bidentate complexes. To illustrate the potential applications of the new classes of compounds, their photoluminescent properties have been studied.

RESULTS AND DISCUSSION

1.1 Synthesis and characterisation of complexes

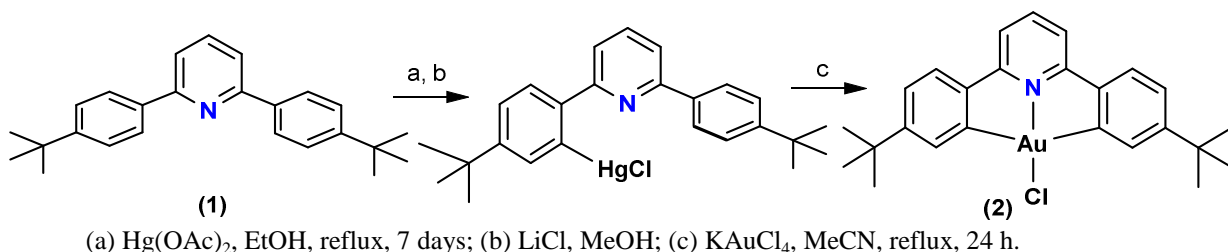
Synthesis of precursors

The reported synthesis of the pro-ligand **1** involves a four step reaction which implies the conversion of methyl ketones to substituted pyridines.⁷⁹ We have found that the same compound can be more easily synthesised in good yields (85%) *via* a single step Suzuki cross coupling of the commercially available 4-*tert*-butylphenylene boronic acid and 2,6-dichloropyridine and employing Pd(PPh₃)₄ as a catalyst. (Scheme 1)



Scheme 1. Improved synthesis for the pro-ligand **1**.

The ligand is then subjected to *ortho*-mercuration with $\text{Hg}(\text{OAc})_2$ followed by salt metathesis with LiCl to yield the organomercury(II) species $(\text{HC-N-C})\text{HgCl}$. The mercury salt then undergoes transmetalation and C-H activation with KAuCl_4 in refluxing acetonitrile following a protocol first described by Che *et al.*⁵⁰ to give the cyclometallated gold(III) chloride $(\text{C}^{\wedge}\text{N}^{\wedge}\text{C})\text{AuCl}$ **2** in moderate yield (40%). (Scheme 2)



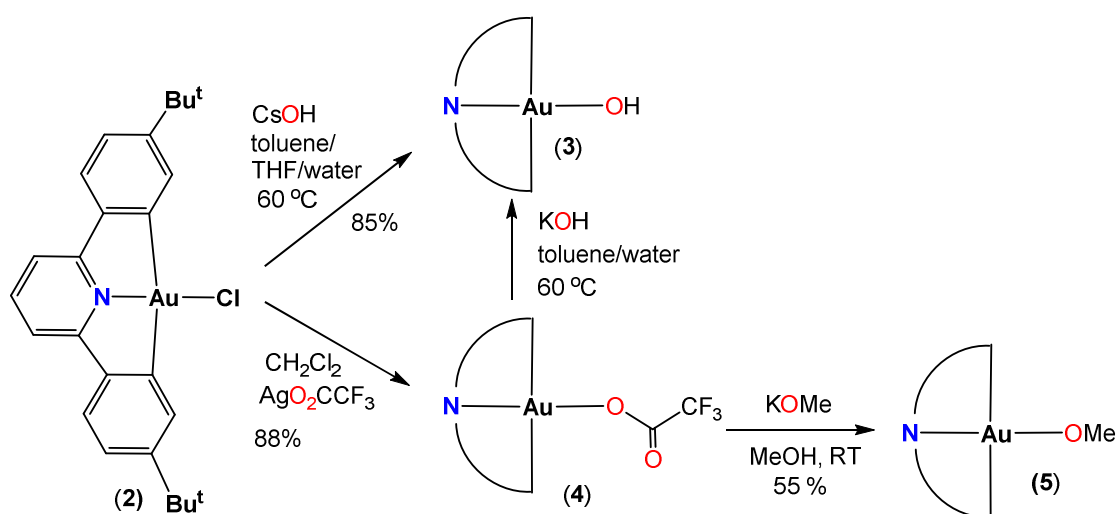
Scheme 2. Synthesis of $(\text{C}^{\wedge}\text{N}^{\wedge}\text{C})\text{AuCl}$ (**2**)

Given the established high affinity of gold ions for chloride, cyclometallated gold(III) chloride complexes are known to be resistant to reacting with various substrates under mild conditions. We envisaged that replacing the chloride ligand with more labile oxygen based ligands would overcome the inertness of **2**. The established protocol of chloride removal from gold often involves using a halide abstraction salt of soft metals such as silver or thallium which are expensive or toxic. We have found that reacting **2** with an excess of CsOH in a water/toluene/THF mixture at $60\text{ }^\circ\text{C}$ over a period of 24 h affords the desired $(\text{C}^{\wedge}\text{N}^{\wedge}\text{C})\text{AuOH}$ **3** as yellow powder in high yields (80%). (Scheme 3) The established protocol proved to be fully scalable to a 1 g scale, but in this case, owing to the heterogeneous composition of the reaction mixture, longer reaction times (3 days) are required for full conversion.

Since trifluoroacetate fragments are good leaving groups, we have also prepared the trifluoroacetate complex $(\text{C}^{\wedge}\text{N}^{\wedge}\text{C})\text{Au}(\text{OAc}^{\text{F}})$ **4**, which can be isolated in high yields (88%) as yellow-green crystals by treating the $(\text{C}^{\wedge}\text{N}^{\wedge}\text{C})\text{AuCl}$ **2** with AgOAc^{F} in CH_2Cl_2 over 24 h. Reacting **4** with potassium methoxide in dry methanol gives the gold(III) methoxide $(\text{C}^{\wedge}\text{N}^{\wedge}\text{C})\text{AuOMe}$ **5** in moderate yields (55 %). (Scheme 3) Dry solvents and inert atmosphere are required in this case to prevent the hydrolysis of **5** to **3**. Complex **4** can also be reacted with KOH in toluene/water at $60\text{ }^\circ\text{C}$ to give **3** in good yields.

Complexes **3**–**5** are thermally stable; no change in composition is observed if refluxed for 2 days in toluene. They are also stable to light for months in the solid state. Complexes **3** and **4** are stable to air and moisture while complex **5** slowly hydrolyses to **3** in the presence of moisture.

Since the triflate group is known as an even more better leaving group than the trifluoroacetate, we have also attempted the synthesis of $(C^{\wedge}N^{\wedge}C)Au(OTf)$. Reacting the $(C^{\wedge}N^{\wedge}C)AuCl$ **2** with $AgOTf$ at low temperature ($-78\text{ }^{\circ}C$ to $-30\text{ }^{\circ}C$) resulted in incomplete halide removal, and visible decomposition to colloidal gold was observed upon warming to room temperature. The decomposition is attributed to the high lability of the Au-O bond in the triflate complex which generates the $(C^{\wedge}N^{\wedge}C)Au^{+}$ cation in solution.⁸⁰ The high tendency of the triflate ion to dissociate from gold(III) is illustrated by the fact that to this date, only two complexes bearing a Au(III) centre attached to a triflate moiety have been structurally characterised, $(tpy)AuMe(OTf)$ ($tpy = 2\text{-}p\text{-tolylpyridine}$)⁸¹ and $AuMe_2(OTf)(H_2O)$.⁸²



Scheme 3. Synthesis of chloride free gold(III) starting materials.

The 1H NMR spectra of complexes **2** – **5** show the typical resonances of a symmetrically bound diphenylpyridine ligand and of a diagnostically relevant tBu group with a resonance in the δ_H 1.33 – 1.38 region. In the case of **3** the δ_H resonance of the OH moiety could not be observed by NMR but an IR (ATR) investigation showed unequivocally a band at 3480 cm^{-1} attributed to the ν_{OH} stretching mode. In the case of **5**, a typical singlet resonance for the methoxy group was observed by 1H NMR ($\delta_H = 4.14$, CD_2Cl_2) while **4** gave a characteristic CF_3 singlet resonance in ^{19}F NMR ($\delta_F = -73.74$, CD_2Cl_2).

Complexes **2** – **4** have also been characterised in the solid state by single crystal X-ray diffraction. As shown in Figure 9, the complexes show a slightly distorted square planar coordination geometry around the metal centre, as expected for a d^8 metal. Selected bond lengths and angles summarised in Table 2. The bond distances are typical for cyclometallated gold complexes.^{50, 51} $(C^{\wedge}N^{\wedge}C)Au(OH)$ **3** is a rare example of a structurally characterised Au(III) hydroxide. The Au—O bond length in **3** ($2.010(2)\text{ \AA}$) is slightly longer

than in the closely related terpyridine based $[\text{Au}(\text{terpy})\text{OH}](\text{ClO}_4)_2$ ⁷⁶ (2.000(4) Å) and in the tetrahydroxoaurate(III) salt $\text{Sr}[\text{Au}(\text{OH})_4]$ ⁷² (1.980(8) Å). The packing diagram reveals that molecules of **2**–**4** stack in a head-to-tail fashion in such a way as to minimise mutual repulsion between the sterically demanding *tert*-butyl groups. The shortest Au⋯Au distances vary between 4.673 Å in **3** to 5.620 Å in **4**, longer than the sum of the van der Waals radii (3.32 Å)⁸³ indicating insignificant gold-gold interactions in the crystal lattice. The shortest interplanar distances in **3** and **4** ranged from 3.686 Å to 3724 Å between the aromatic rings of neighbouring molecules.

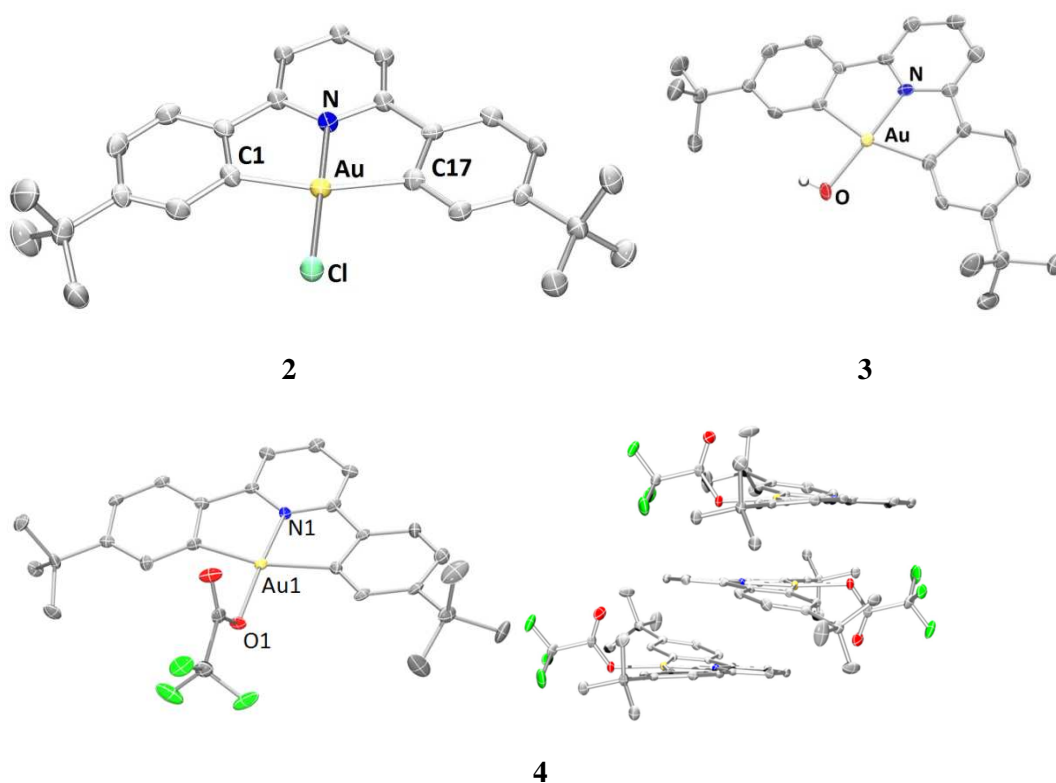


Figure 9. Molecular structures of $(\text{C}^{\wedge}\text{N}^{\wedge}\text{C})\text{AuCl}$ (**2**), $(\text{C}^{\wedge}\text{N}^{\wedge}\text{C})\text{Au}(\text{OH}) \cdot \text{H}_2\text{O}$ (**3**) and $(\text{C}^{\wedge}\text{N}^{\wedge}\text{C})\text{Au}(\text{OAc})^{\text{F}}$ (**4**) (50% probability ellipsoids shown). Hydrogen atoms (except of the OH group in **3**) and the water molecule (in **3**) were omitted for clarity. Packing in **4** depicting head-to-tail arrangements (bottom, right) .

Table 2. Selected bond lengths (Å) and angles (°) for complexes **2** - **4**

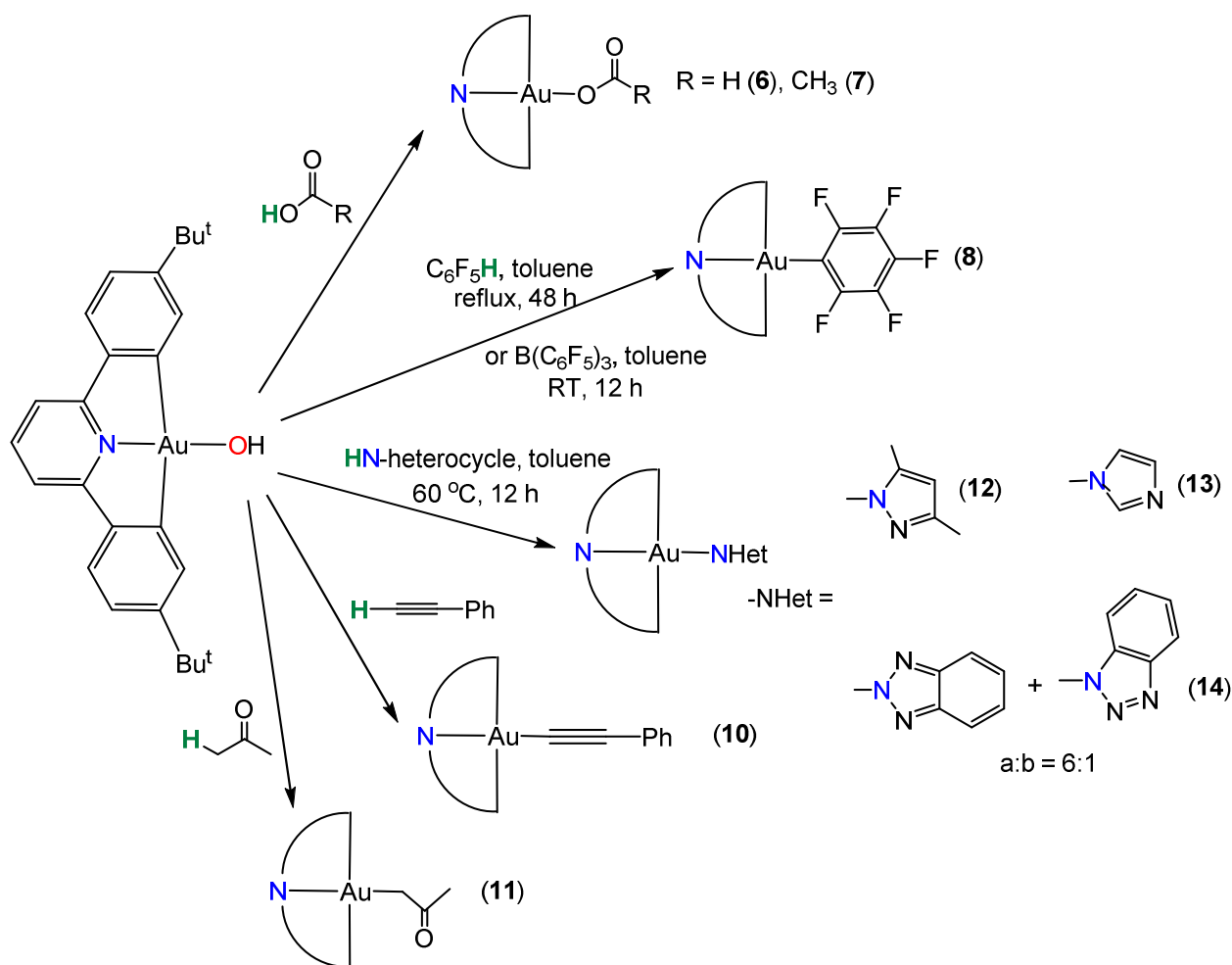
Complex	(C [^] N [^] C)AuCl (2)	(C [^] N [^] C)Au(OH) (3)	(C [^] N [^] C)Au(OAc ^F) (4) ^a
Au-E	2.279(3)	2.010(2)	2.019(3)
Au-N	1.965(10)	1.974(3)	1.959(3)
C(1)-Au	2.062(12)	2.064(3)	2.060(4)
C(17)-Au	2.052(12)	2.074(3)	2.069(4)
N(1)-Au-E^b	179.6(3)	177.89(11)	175.46(7)
(C1)-Au-C(17)	162.3(5)	163.38(14)	163.07(10)
Au...Au	4.734	4.673	5.620

^aData for one of the two molecules in the asymmetric unit. ^b E = Cl or O

The reactivity of (C[^]N[^]C)AuOH **3** as a base

An initial test of basicity involved reacting **3** with a slight excess of Brønsted acid such as acetic acid or formic acid. Rapid complete conversion to the corresponding acetate (C[^]N[^]C)Au(OOCH) **6** and formate (C[^]N[^]C)Au(OAc) **7** complexes was observed by ¹H NMR spectroscopy. (Scheme 4)

In order to establish a rough p*K*_a for **3**, the basicity was tested towards highly fluorinated benzene derivatives. The hydroxide reacts with C₆F₅H (p*K*_a 29, DMSO)^{84a} in refluxing toluene and full conversion to (C[^]N[^]C)Au(C₆F₅) **8** could be noted after 48 h by ¹H NMR spectroscopy. No reaction was observed with 1,2,4,5-tetrafluorobenzene. The methoxide **5** was found react with 1,2,4,5-tetrafluorobenzene to give **9** after 72 h in refluxing toluene. From the known p*K*_a values of the used fluoroarenes^{84a} we could estimate that **3** should be reactive towards substrates with a p*K*_a less than 29. The reactivity of the hydroxide (C[^]N[^]C)AuOH **3** resembles Nolan's (NHC)Au(I)OH⁵⁸ although **3** seems to behave as a milder base.



Scheme 4. Acid-base reactions involving (C^NC)Au(III)OH.

To test this, reactivity was attempted with phenylacetylene (pK_a in DMSO 28.8)^{84b} and the gold(III) acetylide **10** was obtained after 12 h with water as the only biproduct. Compound **10** had been previously reported by Yam *et al.*⁵¹ but its purification involved column chromatography which is not needed when employing the gold(III) hydroxide **3** as a starting material. The hydroxide **3** also reacts with refluxing acetone (pK_a in DMSO 26.5)^{84c} to give a single compound identified as the acetonato complex (C^NC)Au(CH₂COCH₃) **11** by ¹H NMR spectroscopy. An alternative route for accessing gold(III) acetonates by reacting [(N^NC)AuCl]⁺ complexes with silver salts in the presence of acetone has been reported by Minghetti *et al.*^{64, 76}

The hydroxide **3** is also capable of activating N—H bonds in N-heterocycles such as 3,5-dimethylpyrazole, imidazole or benzotriazole as exemplified by the synthesis of **12**—**14**. Compound **14** was isolated as a mixture of the 1- and 2- benzotriazolato isomers in a 6:1 ratio (by ¹H NMR spectroscopy). The 1-benzotriazolato isomer was also characterised by single crystal X-ray diffraction. (Figure 10).

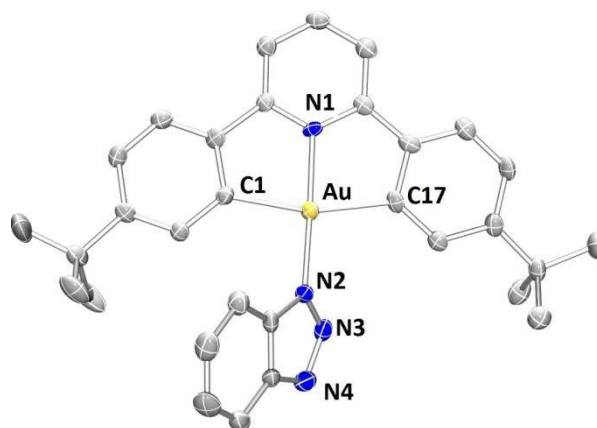
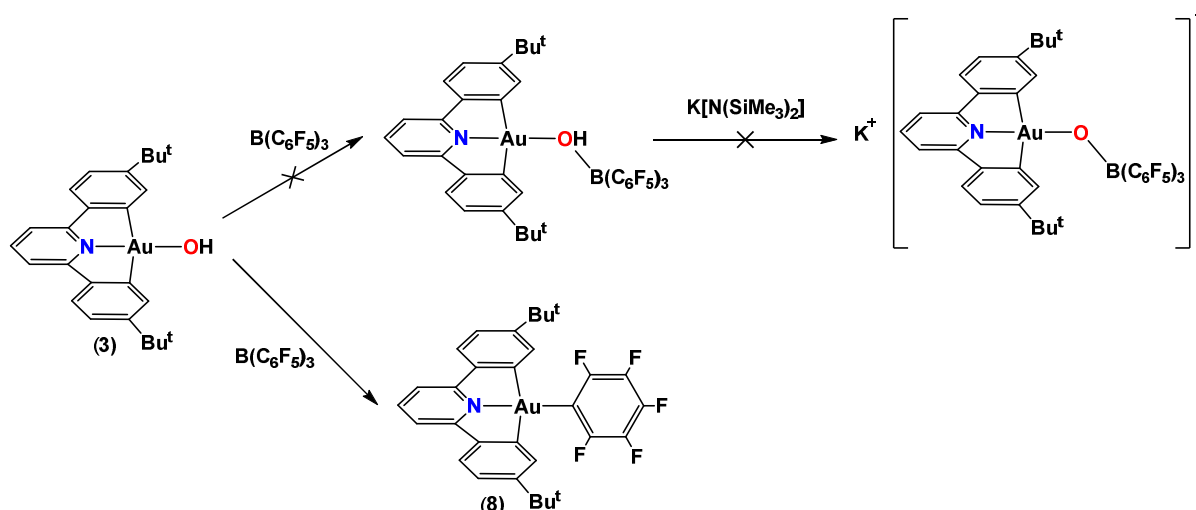


Figure 10. Molecular structure of **14** (1-benzotriazolato isomer) (50% probability ellipsoids shown) Hydrogen atoms were omitted for clarity. Selected bond lengths (Å) and angles (°): Au-N1 1.984(5); Au-N2 2.010(5); Au-C1 2.074(6); Au-C2 2.067(6); N1-Au-N2 177.02(16); C1-Au1-C17 162.5(3); Au⋯Au 5.062(4).

The formation of an adduct between **3** and $B(C_6F_5)_3$ was also attempted, which in a presence of a non-nucleophilic base such as $K[N(SiMe_3)_2]$ could give an anionic gold(III) oxo complex. (Scheme 5) Instead a C_6F_5/OH ligand exchange occurred to give cleanly the gold aryl $(C^N^C)Au(C_6F_5)$ **8**. While this seems to be the first report of an aryl transfer from fluorinated triaryl borates to a gold(III) centre, aryl transfer from boron to gold(I) has precedence. For example, the ability of Au(I) complexes to cleave B—C bonds in BPh_4^- and even $BAr^F_4^-$ ($Ar^F = 3,5$ -bis(trifluoromethyl)phenyl) has recently been reported.⁸⁵

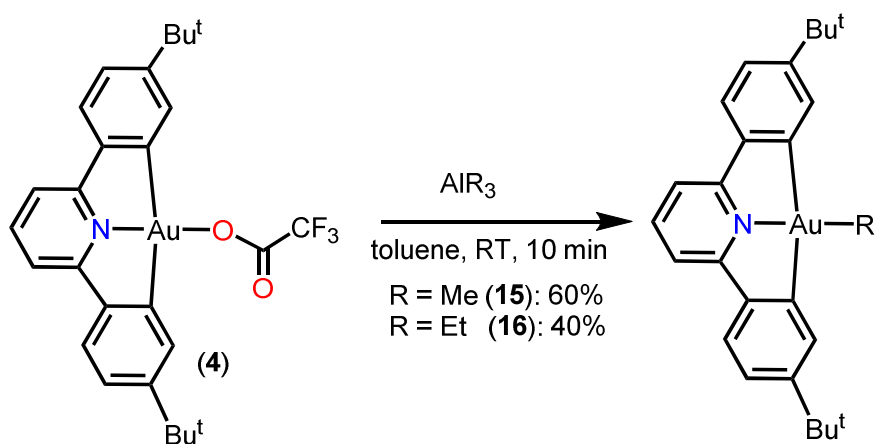


Scheme 5 Aryl transfer from $B(C_6F_5)_3$ to the $(C^N^C)Au$ fragment

Synthesis of gold(III) alkyl and aryl complexes

Since the alkylation or arylation of a gold(III) centre often involves highly toxic organomercury(II) or organotin(IV) reagents and the yields of the reactions are generally low, we decided to explore alternative pathways for accessing these classes of compounds using gold hydroxides and carboxylates as starting materials. We found that the cyclometallated gold(III) complexes containing oxygen-based ligands **3** and **4** proved indeed to be excellent and high-yielding entry points for the synthesis of gold(III) aryl and alkyl complexes.

The reaction between the trifluoroacetato complex (C[^]N[^]C)Au(OAc^F) **4** and aluminium alkyls AlR₃ (R = Me, Et) generated the corresponding gold alkyl complexes cleanly in 40–60% yields. (Scheme 6). The moderate yields are a reflection of the complexes high solubility in light petroleum (used to remove the small amount of diphenylpyridine proligand **1** generated over the course of the reaction), rather than to reduction or decomposition. The identity of compound **15** could be readily confirmed by ¹H NMR spectroscopy through the typical resonance for the Au-CH₃ protons (δ_{H} 1.33, CD₂Cl₂).

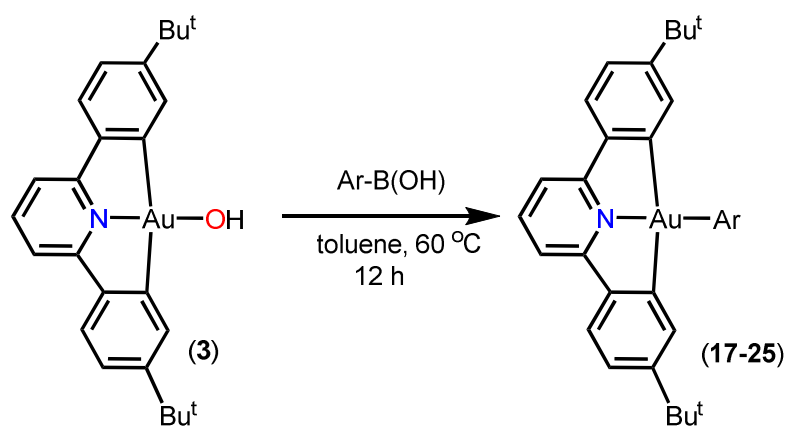


Scheme 6. General protocol for the preparation of the gold(III) alkyl complexes.

Gold(III) aryl complexes can easily be accessed in excellent yields (> 80%, Table 3) by reacting the gold hydroxide (C[^]N[^]C)Au(OH) **3** with stoichiometric amounts of arylboronic acids in toluene at 60 °C. As **3** already has a base function on board, no additional base or water addition is required for the reaction to proceed; this thus reduces the possibility of B-aryl bond hydrolysis which is often competitive with aryl transfer to the metal centre. Purification is straightforward, requiring filtration through a short silica plug only in a small number of cases. To test the generality of the method, aryl complexes **17**–**25** were synthesised (Scheme 7). It was found that the transmetalation reaction proceeds with the same efficiency both for substrates with electron donating (**19**) and electron withdrawing

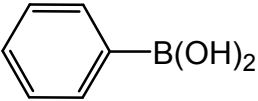
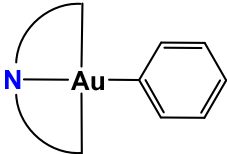
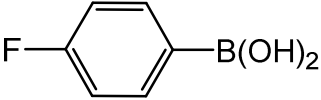
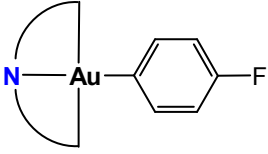
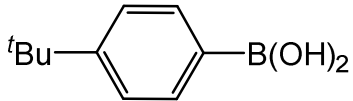
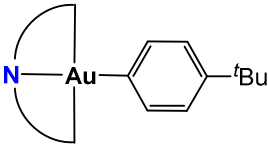
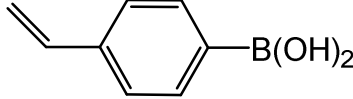
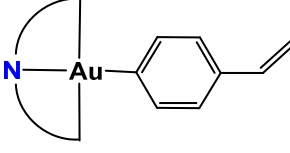
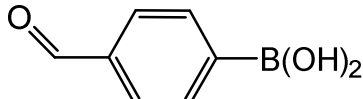
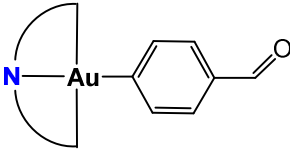
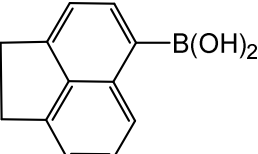
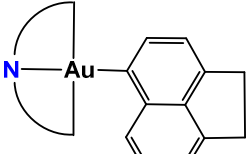
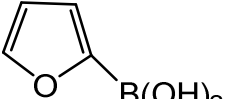
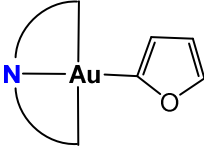
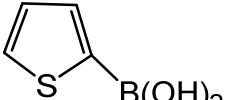
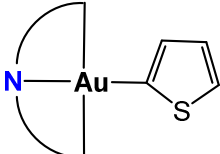
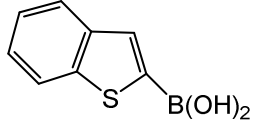
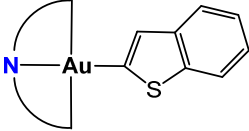
(18, 21) groups. The arylation protocol is also tolerant of functional groups such as vinyl (20) or formyl groups (21) which would otherwise exclude the use of traditional arylating agents such as organolithium or Grignard reagents. The presence of such reactive functional groups suggests the opportunity for the incorporation of cyclometallated gold(III) complexes as building blocks for various gold(III) based macromolecular complexes.

The protocol can also be extended to aromatic heterocycles as exemplified by the synthesis of 23—25. The reactions of gold(I) hydroxides or gold(I) chlorides in the presence of a base with aryl boronic acid was also explored by Nolan *et al.*⁵⁸ and Gray *et al.*⁸⁶



Scheme 7. General protocol for the preparation of the gold(III) aryl complexes

Table 3. Aryl gold(III) products, isolated yields

Boronic acid	Product		Yield
		17	90%
		18	92%
		19	92%
		20	88%
		21	85%
		22	88%
		23	85%
		24	95%
		25	92%

All synthesised alkyl and aryl complexes were isolated as air and moisture stable green-yellow powders and do not present any signs of decomposition under ambient laboratory lighting.

The new alkylation and arylation methods explored were also compared with traditional routes. Upon attempting the synthesis of (C[^]N[^]C)AuMe **15** by reacting the trifluoroacetate (C[^]N[^]C)Au(OAc^F) with the Grignard reagent MeMgBr, the bromide (C[^]N[^]C)AuBr was isolated instead alongside free ligand and colloidal gold. No reaction was observed between HgPh₂ and (C[^]N[^]C)AuCl **2**.

Complexes **15** and **18** can be readily recrystallised from a mixture of dichloromethane and light petroleum solutions. The crystals were suitable for single X-ray diffraction studies. The crystal structures are depicted in Figure 11. The geometrical parameters (Table 4) of **15** and **18** are mostly similar, showing an expected distorted square planar geometry around the metal centre. The Au—N bond (2.018(4) Å in **15** and 2.023(3) Å in **18**) is elongated when compared with oxygen-based precursors (1.974(3) Å in (C[^]N[^]C)AuOH **3** and 1.959(3) Å in (C[^]N[^]C)Au(OAc^F) **4**). This is in line with the stronger *trans* influence exerted by the methyl and phenyl groups compared to a trifluoroacetate or hydroxide moiety. In the crystal lattice, the Au⋯Au distances are longer than the sum of the van der Waals radii (4.770(2) Å for **15**, 4.524(2) Å for **18**) and the molecules are stacked in a head-to tail (**15**) or partial head-to-tail arrangement (**18**).

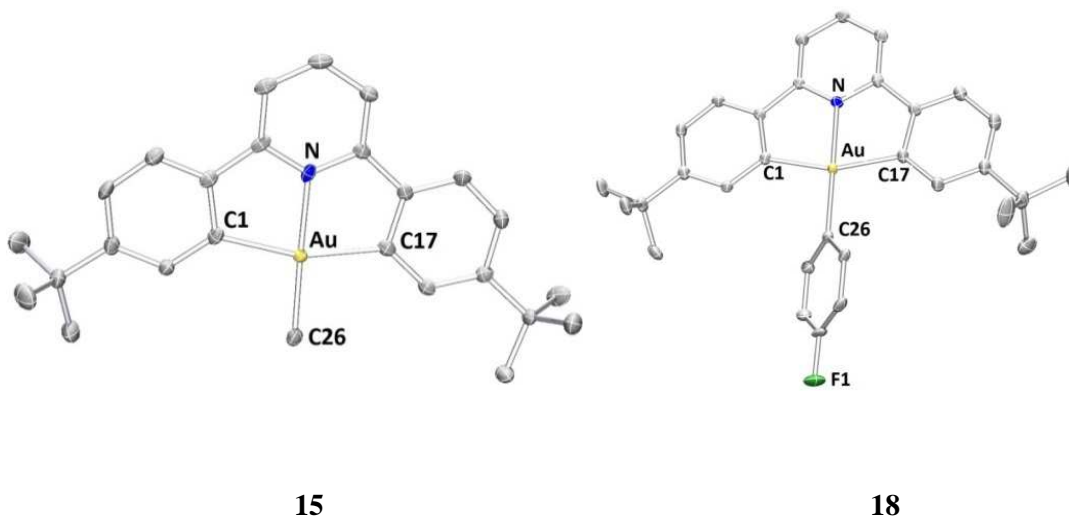


Figure 11. Molecular structures of **15** and **18**. (50% probability ellipsoids shown) Hydrogen atoms were omitted for clarity.

Table 4. Selected bond lengths (Å) and angles (°) for complexes **15** and **18**

Complex	(C [^] N [^] C)AuMe (15)	(C [^] N [^] C)Au(<i>p</i> -F-C ₆ H ₄) (18)
Au-C(26)	2.022(5)	2.014(3)
Au-N	2.018(4)	2.023(3)
C(1)-Au	2.071(5)	2.086(3)
C(17)-Au	2.077(5)	2.076(3)
N-Au-C(26)	178.03(19)	178.23(13)
C(1)-Au-C(17)	161.3(2)	161.01(14)
Au...Au	4.770(2)	4.524(2)

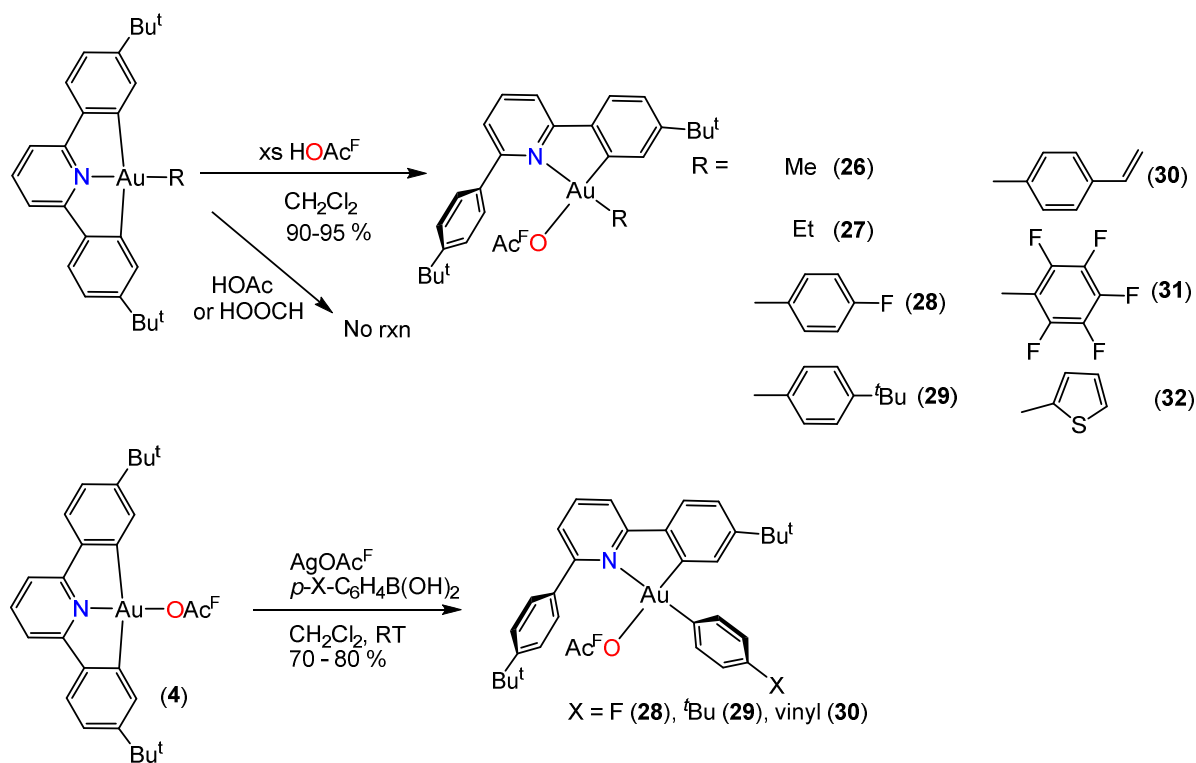
Acid mediated Au—C bond cleavage: Synthesis of cyclometallated bidentate gold complexes

Cyclometallated gold(III) complexes bearing a (C[^]N[^]C) tridentate ligand are remarkable for their thermodynamic and kinetic stability and in some particular cases resist decomposition even in refluxing toluene for 72 h (*vide supra*). The stability is enhanced by the ability of the ligand to block reductive elimination pathways. Despite this, we have also found that these robust tridentate systems can be used as precursors for the synthesis of more labile and thus more reactive gold systems in which the ligand coordinates in a bidentate fashion.

Treatment of (C[^]N[^]C)AuR (R = Alkyl, Aryl) with an excess of trifluoroacetic acid (HOAc^F) leads to Au—C bond protolysis, to yield the bidentate systems (HC-C[^]N)AuR(OAc^F). Clean and instantaneous conversion could be observed by ¹H NMR spectroscopy. The electrophilic attack occurs exclusively on the Au—C bond of the pincer ligand, while the Au—C bond *trans* to the pyridine is not attacked. Once Au—C bond protolysis has occurred, the generated bidentate systems are stable in neat HOAc^F for several hours at room temperature. Indeed, generally Au—C bonds are known to be resistant to protolysis and some protocols for the synthesis of bidentate phenylpyridine gold bearing systems even employ trifluoroacetic acid as a reaction solvent at high temperatures.⁸⁷ In the case of the (C[^]N[^]C)Au(III) systems, Au—C bond protolysis only occurs with stronger acids such as HCl or HOAc^F. No reaction was observed with weaker acids such as acetic, formic or benzoic acid. The reactivity of several tridentate gold alkyl and aryl complexes towards HOAc^F was tested and the outcome is summarised in Scheme 8.

To our surprise, complexes **28—30** can also be obtained by reacting (C[^]N[^]C)Au(OAc^F) **4** with aryl-boronic acids in the presence of AgOAc^F. (Scheme 8) No reaction occurred in the

absence of AgOAc^{F} . While the role of AgOAc^{F} is not clear, we believe that the cleavage reaction can be explained by the generation of HOAc^{F} in the presence of adventitious water. The reaction proceeded only with specific boronic acids; for example, while reaction of the trifluoroacetato complex **4** with *p*-fluorophenyl- or *p*-*t*Bu-phenylboronic acids is straightforward, treatment of **4** with 2-thienylboronic acid in the presence of AgOAc^{F} failed to give $(\text{HC-N}^{\wedge}\text{C})\text{Au}(\text{C}_4\text{H}_3\text{S})(\text{OAc}^{\text{F}})$ **32** after stirring for 7 days at room temperature and the starting materials were recovered unchanged. The origin of this variation is yet unclear.



Scheme 8. H^+ and Ag^+ mediated Au—C cleavage in tridentate gold(III) complexes

Compounds **26** and **28** were recrystallised by evaporation of a benzene solution and dichloromethane/light petroleum mixtures, respectively. The crystal structures (Figure 12) confirm the regioselectivity of the electrophilic attack, leading to the isomer where the methyl or *p*-fluorophenyl substituent is *trans* to the pyridine donor. The selectivity is a consequence of the stronger *trans* influence exerted by the *t*-butylphenyl fragment when compared to the pyridyl fragment. As a result, the Au—O(1) bond in both complexes (2.112(2) Å in **26** and 2.130(5) Å in **28**) is significantly elongated when compared to the tridentate trifluoroacetate $(\text{C}^{\wedge}\text{N}^{\wedge}\text{C})\text{Au}(\text{OAc}^{\text{F}})$ **4** (2.019(3) Å) suggesting a significant weakening of the gold—trifluoroacetate interaction. (Table 5) The Au—O(1) bond length is comparable to the one found in the closely related $(\text{tpy})\text{Au}(\text{Me})(\text{OTf})$ (2.1382(17) Å) ($\text{tpy} = p\text{-tolylpyridine}$)⁸¹ or in the bis(trifluoroacetato) gold complex $(\text{tpy})\text{Au}(\text{OAc}^{\text{F}})$ (OAc^{F} group

trans to the phenyl group 2.111(5) Å).⁸⁷ The Au—N bond in the bidentate complexes is also labilised by the *trans* influence of the strong methyl and *p*-fluorophenyl σ -donors. This is illustrated by the elongation of the Au—N in **26** (2.158(3) Å) and **28** (2.164(6) Å) when compared to the tridentate analogues **15** (2.018(4) Å) and **18** (2.023(3) Å). As a consequence, the bidentate gold(III) systems generally exhibit reduced thermal stability compared to their tridentate analogues (*vide infra*). In the extended structure of **28**, the molecules are associated as dimers through H··F contacts (2.606 Å, $\sum_{\text{vdw}}(\text{H}, \text{F}): 2.67 \text{ Å}$)⁸³ between the fluorine group of the *p*-C₆H₄ group and the hydrogen atom which neighbours the fluorine atom in the *p*-C₆H₄ group of an adjacent molecule. There are also short stacking interactions (3.685 Å) between the planes of the phenylpyridine fragments.

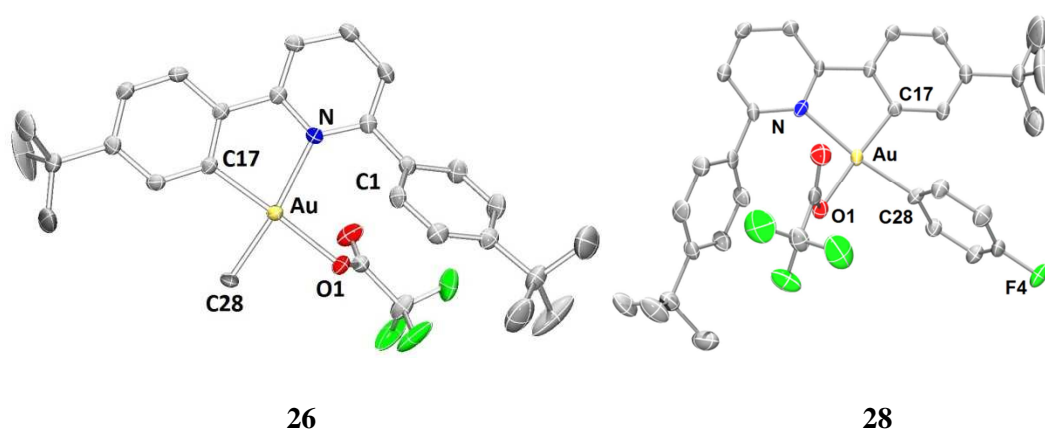
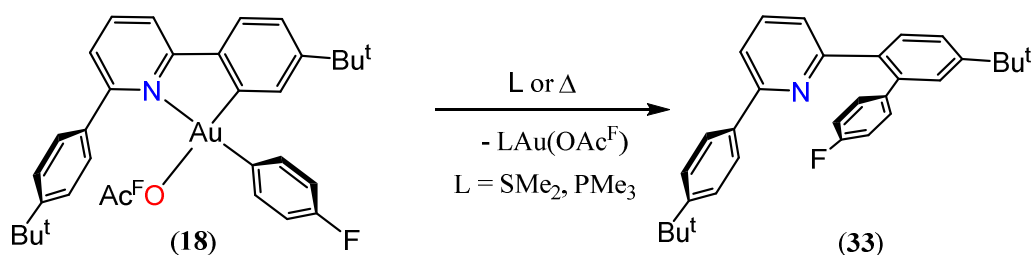


Figure 12. Molecular structures of **26**·CH₂Cl₂ and **28**. (50% probability ellipsoids shown) Hydrogen atoms and co-crystallised solvents were omitted for clarity.

Table 5. Selected bond lengths (Å) and angles (°) for complexes **26** and **28**

Complex	26 ·CH ₂ Cl ₂	28
N-Au	2.158(3)	2.164(6)
Au-C(28)	2.031(4)	2.029(7)
Au-O(1)	2.112(2)	2.130(5)
Au(C17)	2.011(3)	2.017(7)
N-Au-C(28)	172.12(13)	172.4(2)
C17-Au-O(1)	177.08(12)	174.4(2)
Au··Au	6.911	6.957

All complexes were isolated as pale yellow (**31**, **32**) or colourless (**26**–**30**) solids. They are air and moisture stable at -5 °C in the dark for months but slowly degrade if exposed to light. Deposition of gold film can be observed over the course of 16 h at room temperature. The decomposition pathway most likely involves aryl transfer from the gold centre to the phenylpyridine backbone and reductive elimination to gold(I) trifluoroacetate which further undergoes reduction to gold metal. The reaction is accelerated by the presence of neutral donor ligands. Treating dichloromethane solutions of (HC-N[^]C)Au(*p*-F-C₆H₄)(OAc^F) **28** with excess PMe₃ or SMe₂ quickly gives the C—C coupling product (HC-N-C)(*p*-F-C₆H₄) **33** concomitant with the loss of ligated gold. (Scheme 9).



Scheme 9. Reductive elimination of cyclometallated bidentate gold(III) complexes

The molecular structure was also confirmed by X-ray crystallography. (Figure 13)

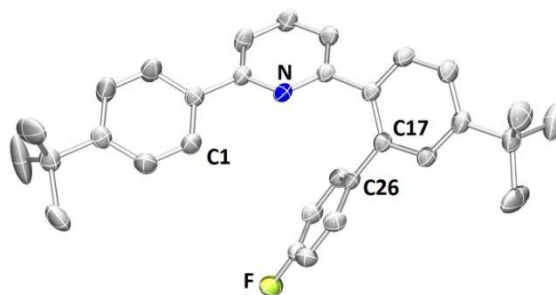


Figure 13. Molecular structure of **33**. (50% probability ellipsoids shown) Hydrogen atoms were omitted for clarity.

1.2 Photoluminescence studies

Traditionally, gold(III) complexes have been rarely observed to exhibit photoluminescent properties at room temperature. The probable reason resides with high electrophilicity of the gold centre and as a consequence renders low-energy metal centred d—d ligand field states which would quench luminescence excited states via non-radiative decay.^{23, 88} Despite this, recent reports^{51, 78} show that cyclometallated gold(III) complexes have been found to exhibit photoluminescence properties at room temperature. An essential requirement however is the presence of strong σ -donors which would lead to an increase of electron density around the

metal centre and also to the rising of d—d ligand field strength. This in turn increases the chances for population of the emissive state. (Figure 14)

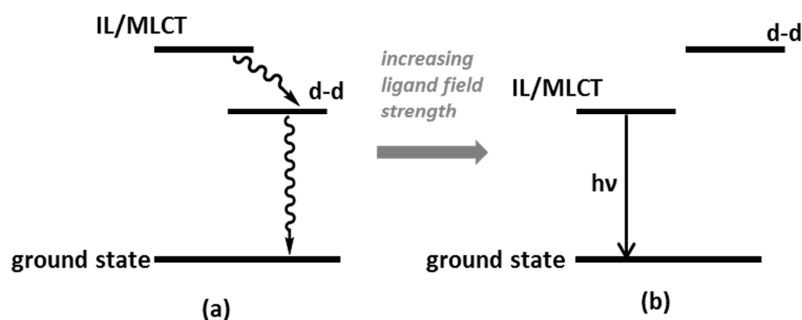


Figure 14. Energy level diagram for d-metal complexes in (a) weak field environments showing non-radiative decay and (b) strong field environments showing photoluminescent emission. Adapted from ref. 23

Photoluminescence of tridentate complexes

Most reported studies have focused on using Arduengo-type N-heterocyclic carbenes (NHCs)^{78, 89} or acetylide ligands^{51, 90-92} as strong σ -donors. Limited work has been reported on cyclometallated bidentate gold(III) systems bearing two aryl ligands;^{93,94} this is probably because the imposed *cis* configuration of the unconstrained aryl moieties around the metal centre make the complexes susceptible to reductive elimination. Given the remarkable thermal stability of the gold alkyls and aryls (C^{^N^C})AuR (**8**, **9**, **15**—**25**) and the convenient synthesis protocol developed, we decided to investigate the photophysical properties of a number of the complexes.

Since the nitrogen and oxygen based ligands are not sufficiently strong σ -donors, complexes **2**—**7** and **10**—**14** show no discernible photoemission. In contrast, most alkyl and aryl complexes exhibit photoluminescent properties at room temperature both in solid state and in dichloromethane solutions. Upon excitation at $\lambda \geq 350$ nm, the solution emission spectra of most complexes show well resolved vibronic-structured bands with maxima at similar wavelengths in the green region ($\lambda_{em} = 474 - 498$ nm). (Table 6) This correlates well with the emission wavelengths of most cyclometallated (C^{^N^C})gold(III) complexes bearing a strong σ -donor.^{51,78,90} The vibrational spacings of *ca.* 1200 cm⁻¹ (Figure 15) correlate well with the ligand-based stretching modes (C=C and C=N), suggesting a significant contribution of the diphenylpyridine ligand in the excited-state. The similarity in emission bands together with the submicrosecond lifetimes suggests that luminescence arises from a metal-perturbed ³[$\pi \rightarrow \pi^*(C^N^C)$] intraligand (IL) state. Similar assignments have also been made in other (C^{^N^C})AuX complexes.^{50,51,78} These findings suggest that the photoemission

wavelength in complexes **9**, **15**, **18**, **22** and **25** are insensitive to the nature of the aryl substituent. Similarities between the emission wavelengths irrespective of the nature of the aryl substituent were also reported by Venkatesan *et al.* for cyclometallated phenyl- and thiophenylpyridine (C^N)AuR₂ complexes (R = Ph, *p*-CF₃-C₆H₄, C₆F₅ or 2-thiophenyl).⁹⁴

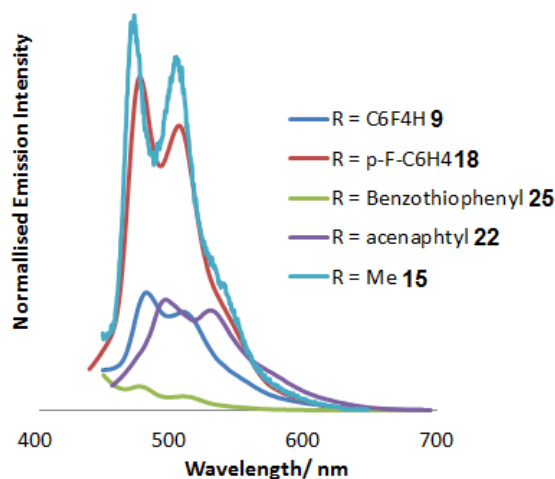


Figure 15. Emission spectra of gold(III) aryl and alkyl complexes in solution.

Unlike the aryl complexes discussed above, dichloromethane solutions of complexes **8** and **24** show significantly different emissions in the blue and yellow regions respectively ($\lambda_{em} = 439$ nm for **8** and 532 nm for **24**). (Figure 16). The considerable shift in the emission maxima as a function of the aryl substituent alongside the structureless emission band strongly suggests that photoemission process is not predominantly derived from an intraligand $^3[\pi \rightarrow \pi^* (C^N^C)]$ transition. This appears to be the first report of a strong modulation of photoluminescence response in Au(III) as a function of non-chelating σ -aryl ligands. The modulation is only observed in solution, while in the solid state the photoemission maxima of all studied complexes are at similar wavelengths, in the green region, and in these cases derive from ligand-based triplet states. Computational studies are underway to elucidate the nature of this difference. The contrast between thiophenyl **24** ($\lambda_{em} = 532$ nm, CH₂Cl₂) and benzothiophenyl ($\lambda_{em} = 482$ nm, CH₂Cl₂) is particularly striking.

Another noteworthy difference could also be observed between the thiophenyl and furanyl ligands. While the thiophenyl complex **24** displayed quite intense photoemission ($\Phi_p = 9.8 \times 10^{-2}$, CH₂Cl₂), the furanyl complex displayed negligible photoemission at room temperature both in solution and in solid state.

Table 6. Photophysical properties of (C^NC)Au(III) aryl and alkyl complexes.

	Absorbion λ_{\max}/nm ($\epsilon_{\max}/\text{dm}^3 \text{ mol}^{-1} \text{ cm}^{-1}$)	Solid state emission λ_{em} (nm)	Solution emission ^a λ_{em} (nm)	Φ_{P}^b
8	320(12997), 379 (3780), 388 (4929), 408 (4572)	445, 458, 482	439	1.04×10^{-2}
9	314(6528), 321 sh (6108), 377 sh (2045), 388 (2953), 408 (2779)	485, 516	483, 511	0.62×10^{-2}
15	320 sh (10190), 357 (3070), 378 (3040), 396 (2510)	489, 513	474, 506	2.30×10^{-2}
18	320 (19867), 365 (5165), 383 (5709), 403 (4811)	459, 479	478, 507	1.29×10^{-2}
22	315 (16084), 362 (4522), 382 (4566), 398 (4024)	458, 476	498, 531	0.50×10^{-2}
24	313 (10033), 371 sh (3188), 385 (3963), 406 (3259)	445, 458, 481	532	9.80×10^{-2}
25	310 (21471), 373 sh (7314), 386 (9006), 405 (7176)	450, 476 sh	482, 510	0.24×10^{-2}

^a In degassed dichloromethane solutions at 298 K. Emission lifetimes were determined to be <50 ns. ^b PL quantum yields recorded in degassed dichloromethane solution at 298 K using [Ru(bipy)₃]Cl₂ as standard.⁹⁵

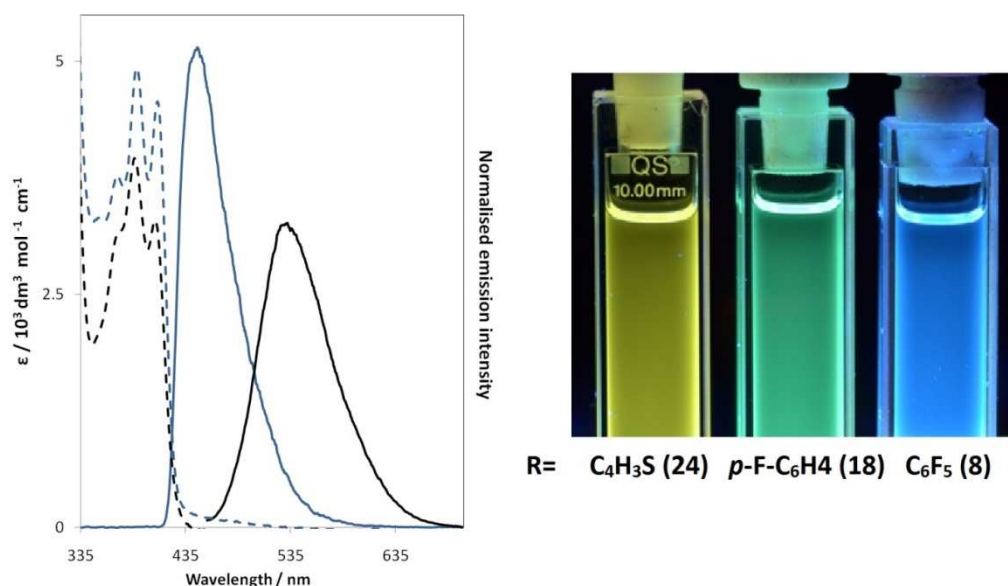


Figure 16. Absorbion (- -) and emission (-) spectra of complexes **8** (blue) and **24** (black) (left) and PL emission for **24**, **18** and **8**, λ_{exc} 365 nm (right)

The UV-Vis spectra of the studied aryl and alkyl complexes spectra in dichloromethane at 298 K are similar and were found to resemble the spectra of other (C^NC)Au(III) complexes bearing different auxiliary ligands such as phosphines,⁵⁰ carbenes⁷⁸ or acetylides.⁵¹ There is a very intense absorption band at 310 - 320 nm ($\epsilon \approx 10^5 \text{ dm}^3 \text{ mol}^{-1} \text{ cm}^{-1}$) and a moderately intense ($\epsilon > 3000 \text{ dm}^3 \text{ mol}^{-1} \text{ cm}^{-1}$) vibronic-structured absorption in the 357- 408 nm region.(Figure17 and Table 6). The position of the absorption maxima for the vibronic-structured absorption is rather insensitive to the nature of the aryl or alkyl substituent and is therefore assigned to a metal perturbed $\pi \rightarrow \pi^*$ intraligand transition of the diphenylpyridine ligand. The vibration progression of *ca.* 1200 cm^{-1} , in close agreement with C=N and C=C vibration modes of the C^NC ligands is also consistent with this assignment.

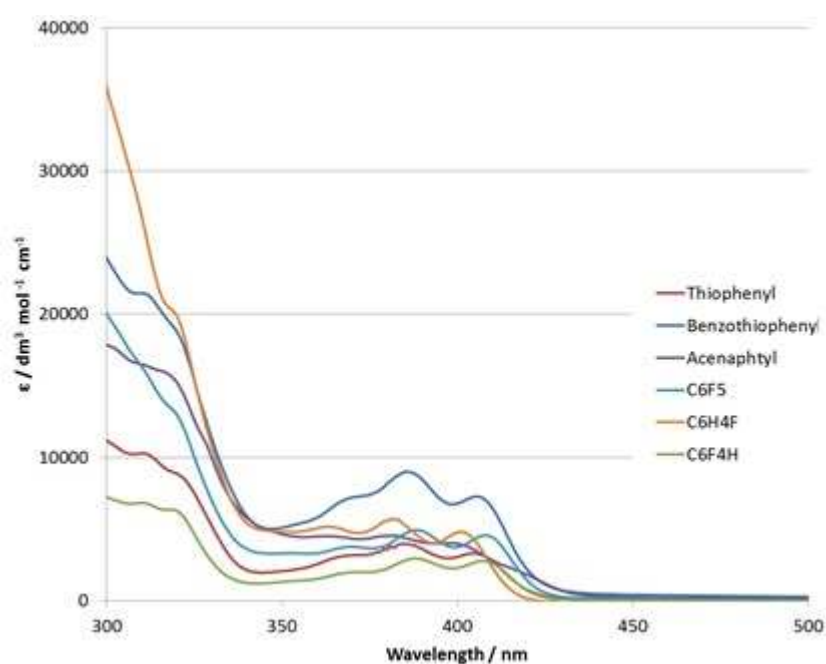


Figure 17. Absorbtion spectra of gold(III) aryl complexes

Photoluminescence of bidentate complexes

Given that the tridentate(III) aryls and alkyls displayed interesting and in some cases surprising photoluminescence properties, we decided to investigate the impact of Au—C bond cleavage on the photoemission properties. In this respect representative examples of bidentate gold complexes (HC-N^C)Au(R)(OAc^F) (R = Me **26**, *p*-F-C₆F₅ **28**) were investigated. Since in the case of the tridentate complexes, the C₆F₅ **8** and thiophenyl **24** complexes also displayed modulation of photoemission wavelength as a function of the substituent, the corresponding Au—C cleavage products (HC-N^C)Au(R)(OAc^F) (R = C₆F₅ **31** and thiophenyl **32**) were also investigated. The results are summarised in Table 7.

Table 7. Photophysical properties of bidentate gold(III) aryl and alkyl complexes

	Absorbion λ_{\max}/nm ($\epsilon_{\max}/\text{dm}^3 \text{ mol}^{-1} \text{ cm}^{-1}$)	Solid state emission $\lambda_{\text{em}}(\text{nm})$	Solution emission ^a $\lambda_{\text{em}}(\text{nm})$	Φ_{p}^b
26	341(26940)	478, 501	467, 498	7.8×10^{-2}
28	344(15040)	480, 504	477, 508	10×10^{-2}
31	320 sh (10190), 357 (3070), 378 (3040), 396 (2510)	484, 516	443	2.3×10^{-2}

^a In degassed dichloromethane solutions at 298 K. Emission lifetimes were determined to be <50 ns. ^b PL quantum yields recorded in degassed dichloromethane solution at 298 K using [Ru(bipy)₃]Cl₂ as standard.⁹⁵

In the case of complexes where R = Me or *p*-F-C₆H₄, the bidentate complexes show a surprise increase in emission intensity compared to their tridentate analogues while the photoemission wavelengths of all the complexes remain identical. The solution photoemission quantum yields increase from $\Phi_{\text{p}} = 2.3 \times 10^{-2}$ (R = Me **15**) and 1.3×10^{-2} (R = *p*-F-C₆H₄ **18**) in the tridentate complexes to $\Phi_{\text{p}} = 7.8 \times 10^{-2}$ (R = Me **26**) and 10×10^{-2} (R = *p*-F-C₆H₄ **28**) in the bidentate analogues. (Figure 18, left) By contrast, the trifluoroacetato complex (C^{N^C})Au(OAc^F) **4** which has the same number of C, N, and O donors as **28** shows no photoluminescence. The emission bands of both bidentate **26** and **28** are vibronic-structured with vibrational progression of *ca.*1200 cm⁻¹ as in the case of the tridentate analogues. We therefore tentatively assign them to metal perturbed intraligand (C^{N^C}) triplet based emission.

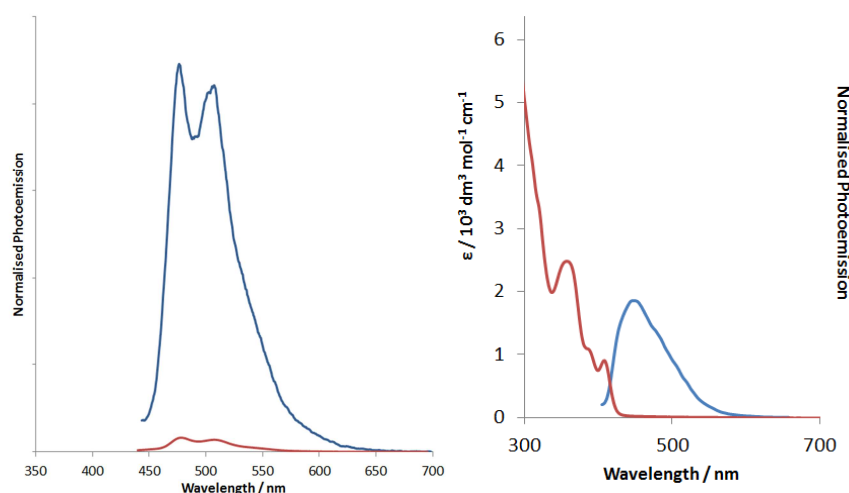


Figure 18. Normalised photoemission of tridentate (C^{N^C})*Au(*p*-F-C₆H₄) (**18**) (red) and bidentate complex **28** (blue). (left); Absorption (red) and emission (blue) spectra of bidentate C₆F₅ complex **31**.(right).

In contrast with complexes **26** and **28**, in CH₂Cl₂ solutions, the C₆F₅ bidentate complex **31** shows a *decrease* in quantum yield from $\Phi_P = 10.4 \times 10^{-2}$ in the tridentate (C^{^N^C})Au(C₆F₅) **8** to $\Phi_P = 2.3 \times 10^{-2}$ in (HC-N^{^C})Au(C₆F₅)(OAc^F) (**31**) while the thiophenyl derivative **32** does not emit at room temperature. In the case of complex **31**, the photoemission band maintains its non-vibronic structure as in the tridentate analogue **8**. (Figure 18, right). The nature of these differences is still unexplained and computational studies are underway to shed light in the photophysical mechanisms of these variations.

CONCLUDING REMARKS

The research summarised here shows that the rather inert (C^{^N^C})AuCl **2** can be converted into more reactive species by replacing the chloride ligand with oxygen ligands such as hydroxides **3**, trifluoroacetates **4** and methoxides **5**. Making use of the lability of the introduced Au—O bond, these complexes are useful synthons for other classes of gold(III) compounds. An acid-base reactivity assay showed that, in principle, (C^{^N^C})Au(OH) **3** should react with most substrates with a pK_a lower than 29 (DMSO). Treating complex **3** with substrates with an acidic proton functionality such as 5 membered N-heterocycles or acetylenes gave quantitatively the corresponding gold complexes with water as the only by-product. A particularly versatile protocol is the reaction of **3** with boronic acids to give gold(III) aryl complexes. The high-yielding reaction can be extended from simple aryls to heterocycles and is tolerant to the presence of functional groups such as *p*-vinyl and *p*-formyl on the introduced aryl group.

Similarly, the trifluoroacetate (C^{^N^C})Au(OAc^F) **4** was found to be a useful synthon to gold(III) alkyls by transmetalation from aluminium alkyls.

The isolated aryl and alkyl groups readily undergo regioselective acid mediated Au—C bond protolysis to give the bidentate (HC-N^{^C})Au(R)(OAc^F) species.

Most aryl and alkyl containing complexes generated by the protocols described above showed photoluminescence properties. We have found that in the case of the tridentate aryl and alkyl complexes (C^{^N^C})Au(R), variation of the R substituent has no influence on the photoemission maxima ($\lambda_{em} = 474 - 498$ nm, green region). Two notable exceptions are the C₆F₅ and thiophenyl complexes which show a modulation of the photoemission wavelength in solution alone from blue ($\lambda_{em} = 439$ for R = C₆F₅ **8**) to yellow ($\lambda_{em} = 532$ for R = thiophenyl **24**). This appears to be the first report of the modulation of the photoemission wavelength in solution for gold(III) aryl complexes as a function of non-chelating σ -aryl ligands.

The cleavage of an Au—C bond does not seem to have an impact on the photoemission wavelength but leads to an increase of the photoemission intensity of some compounds (R = Me (**26**), *p*-F-C₆H₄ (**28**)) and to a decrease in others (R = C₆F₅ (**31**), thiophenyl (**32**)).

CHAPTER 2

Chemistry of Gold(III) Hydrides and Unsupported Gold(II) dimers Containing Cyclometallating Pincer Ligands

A portion of this chapter has appeared in print:

D.-A. Roşca, D. A. Smith, D. L. Hughes, M. Bochmann “A Thermally Stable Gold(III) Hydride: Synthesis, Reactivity, and Reductive Condensation as a new Route to Au^{II} Complexes” *Angew. Chem.* **2012**, *124*, 10795. *Angew. Chem. Int. Ed.* **2012**, *51*, 10643.

T. Dann, D.-A. Roşca, J. A. Wright, G. G. Wildgoose, M. Bochmann “Electrochemistry of Au^{II} and Au^{III} pincer complexes: determination of the Au^{II}-Au^{II} bond energy” *Chem. Commun.* **2013**, *49*, 10169.

INTRODUCTION

Transition metal hydrides have excited considerable interest both from the perspective of fundamental M—H bonding and also as well established key intermediates in numerous homogeneously and heterogeneously catalysed reactions.⁹⁶ Platinum(II) hydrides for example have been extensively investigated³⁸ since their first report in the late 1950s.⁴¹ However, isolable hydrides of the isoelectronic gold(III) to the best of our knowledge are unknown. Their instability was often explained by the strongly oxidising nature of the metal centre ($\text{Au}^{3+}/\text{Au}^+$ 1.36 V; $\text{Au}^{3+}/\text{Au}^0$ 1.69 V)¹² which would readily be reduced in the presence of the electron-rich hydride ligand.⁹⁷ As a consequence, the formation of gold hydrides *via* β -hydride elimination in various catalytic cycles was thought to be unfavourable, even though this pathway is readily accessible to other transition metals.⁹⁸ Nevertheless, both gold(I) and gold(III) hydrides have been long proposed to be key intermediates in gold mediated hydrogenations,⁴⁸ hydrosilylations,⁹⁹ dehydrogenative alcohol silylations,¹⁰⁰ oxidative C—C coupling reactions¹⁰¹ and other organic transformations.^{98b}

In terms of experimental data, reports on characterisation data on gold hydrides are scarce¹³ especially when compared to other transition metal hydrides. Early reports on structural data were limited to vibrational spectroscopy studies on binary hydrides such as AuH, $(\text{H}_2)\text{AuH}$, $(\text{H}_2)\text{AuH}_3$ and $[\text{AuH}_4]$, generated in frozen gas matrices below 5 K.^{97, 102}

Heterobimetallic gold- transition metal complexes featuring bridging hydride ligands have been known for a long time and their synthesis involved the reaction between M—H species (M= Ir, Rh, Pt, Co, W *inter alia*) and Au(I)^+ cations.¹⁰³ (Figure 19). More recently, Le Floch *et al.* reported well-defined examples of Xhantphos-phosphone supported cationic digold(I) complexes containing Au—H—Au fragments¹⁰⁴ which are catalytically active in dehydrogenative silylation of alcohols.¹⁰⁰

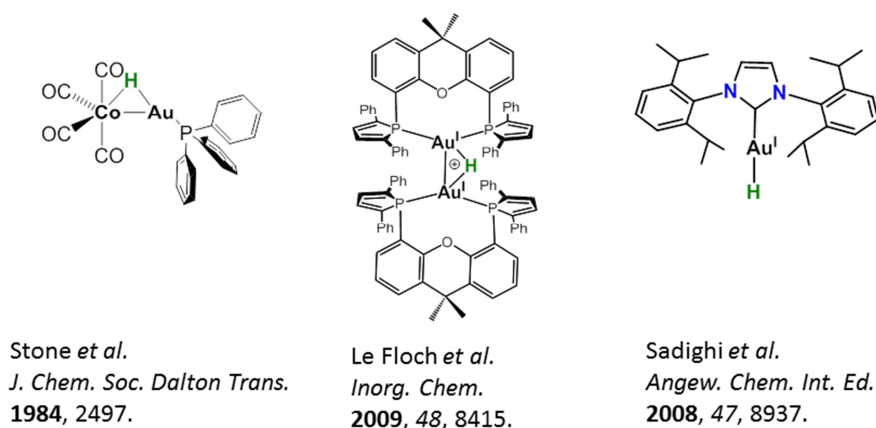
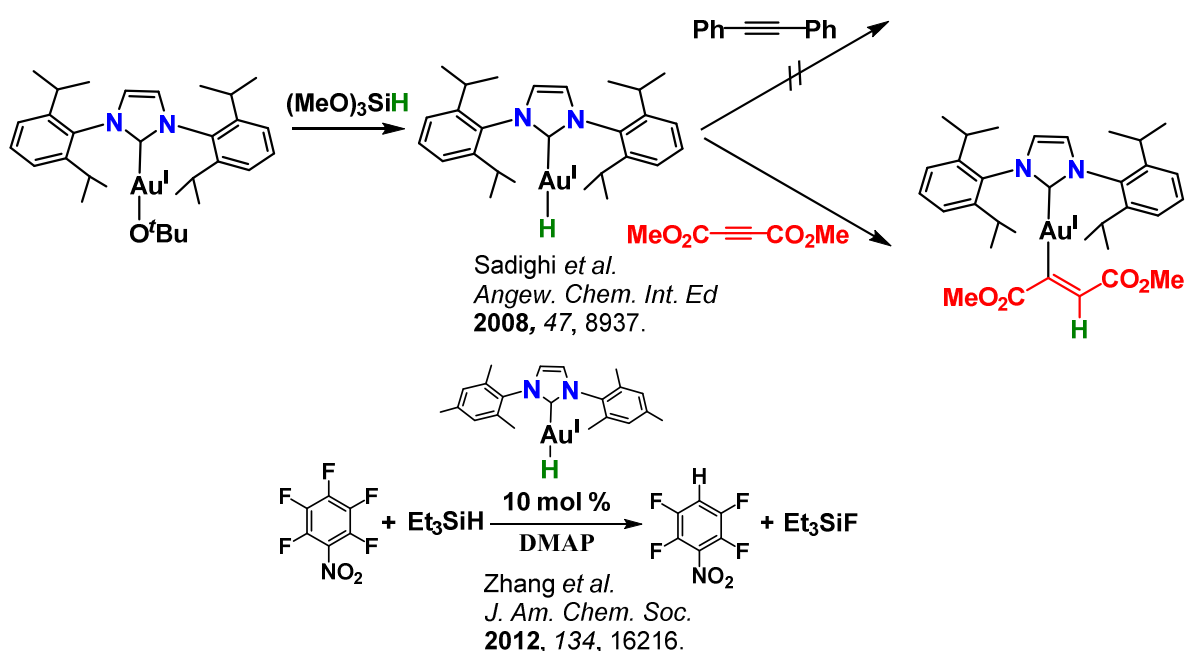


Figure 19 Examples of characterised complexes containing Au—H bonds.

Attempts to use phosphine ligands in the preparation of well-defined terminal gold(I) hydrides of the type $(R_3P)Au^I H$ resulted in reduction to Au(0), but the short-lived gold(I) hydride species could be characterised in the gas phase by mass spectrometry.¹⁰⁵ Sadighi *et al.* showed that replacing phosphine ligands with more kinetically inert and stronger σ -donating N-heterocyclic carbene ligands afforded the isolation of a thermally stable terminal Au(I) hydride which was characterised by IR, NMR and X-ray crystallography.⁴⁴ (Figure 19, right) The complex was synthesised by reacting the $(IPr)AuO^tBu$ ⁴⁴ or $(IPr)Au(OH)$ ^{58a} with a hydride source such as $(MeO)_3SiH$. (Scheme 10) Reactivity studies showed the complex to be inert towards substrates such as 1-hexyne or diphenylacetylene.⁴⁴ No reaction was reported to occur with ethylene even under elevated pressure (8 bar, RT).¹⁰⁶ The complex does however react with the more reactive dimethylacetylenedicarboxylate (DMAD) giving the *trans* insertion product.⁴⁴ Attempts to generate the $(IPr)AuH$ *via* β -hydride elimination from $(IPr)AuEt$ were unsuccessful and upon computational investigations it was concluded that the high activation barrier of this reaction (*ca.* 209 kJ mol⁻¹) would require high temperatures (>120 °C), far beyond the thermal stability limit of the product.¹⁰⁶ A recent study¹⁰⁷ showed that the N-heterocyclic carbene-supported hydride $(IPr)AuH$ can act as a C—F activation catalyst for the defluorination of perfluoroarenes in the presence of Et_3SiH as a hydride source. (Scheme 10) In the investigation of the reaction mechanism of this reaction, the authors also postulate gold(III) hydride species as possible intermediates which can be formed by oxidative addition of the fluoroarene to gold(I).¹⁰⁷



Scheme 10 Synthesis, reactivity and catalytic activity of the NHC supported Au(I) hydride

In addition to the defluorination of perfluoroarenes, Corma *et al.* proposed that gold(III) O⁺N⁻N⁻ chelates immobilised on silica supports are powerful hydrogenation catalysts and operate *via* heterolytic hydrogen activation to give rise to gold(III) hydride and dihydrogen complexes as active catalytic species. (Figure 20) These results have also been supported by computational studies.^{48c} More recently,^{98b} Alcaide *et al.* proposed the involvement of gold(III) hydride complexes formed by β -hydride elimination from gold(III) oxetane complexes in the gold(III) mediated oxycyclisation of α -allenols.

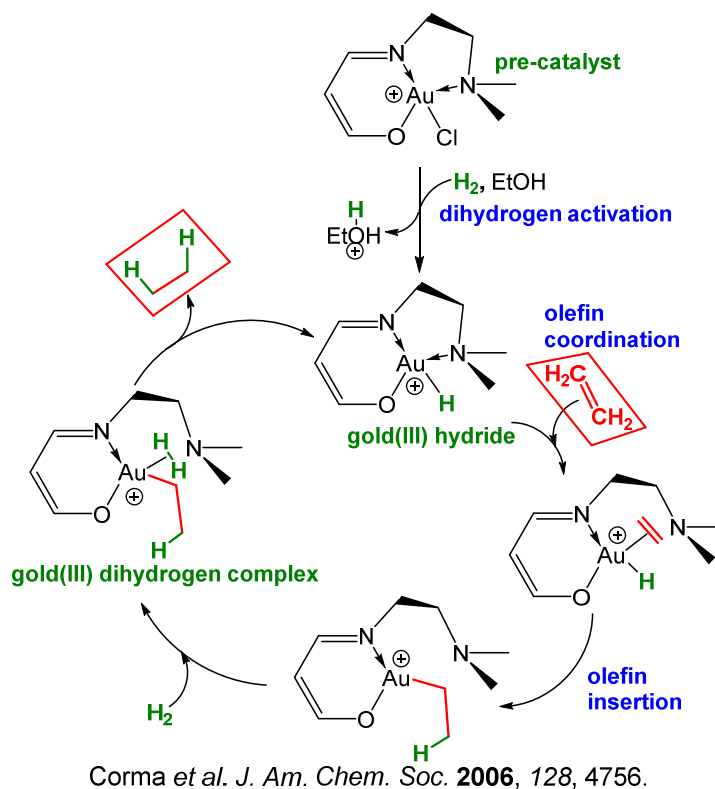


Figure 20. Proposed gold(III) hydrides as intermediates in olefin hydrogenation^{48c}

Judging from their relevance as key catalytic intermediates it is perhaps surprising that gold(III) hydrides remain unknown. Early attempts on the synthesis of AuH₃, Au₂H₆ or tetrahydridoaurates(III) M[AuH₄] by reacting AuCl₃ or HAuCl₄ with strong hydride sources such as LiBH₄ were unsuccessful, yielding colloidal gold.¹⁰⁸

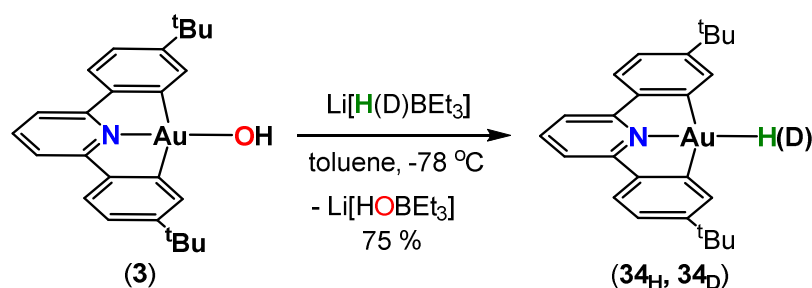
Since dianionic diphenylpyridine pincer ligands confer remarkable thermal stability to gold(III) centres by blocking reductive elimination pathways, we decided to explore their ability in stabilising gold(III) hydride species. This chapter summarises our efforts with regards to the synthesis, characterisation and reactivity of the first thermally stable gold(III) hydride. During our reactivity studies, we have observed that gold(III) hydrides also offer a convenient pathway for the synthesis of a remarkably stable, unsupported gold(II) dimer, which upon photolytic disproportionation gives rise to a unique mixed-valence Au^I₂/Au^{III}₂

macrocycle. Various aspects of the chemistry of these species explored by experimental and computational methods are discussed.

RESULTS AND DISCUSSION

2.1 Synthesis and characterisation of a thermally stable Gold(III) hydride

Treatment of (C^NC) supported gold(III) hydroxide **3** with a strong hydride source such as Li[HBET₃] in toluene at low temperature in the dark, followed by stirring for 15 minutes at room temperature rapidly yielded a single product which was identified as the gold(III) hydride (**34_H**). (Scheme 11) The complex was isolated in good yields (75 %) as air- and moisture-stable crystals. Employing a similar protocol for the synthesis of the first terminal IPrAu^IH,⁴⁴ Sadighi *et al.* reported concomitant alkyl transfer from Li[DBEt₃] to the Au(I) centre confirmed by the isolation of the LAu(I)Et as a minor product (10%). In contrast, a similar protocol for the synthesis of **34_H** produced no traces of the (C^NC)AuEt **16**.



Scheme 11. Synthesis of the (C^NC) supported gold(III) hydride

Characterisation in solution

The ¹H NMR spectrum of **34_H** displays a singlet resonance at δ_H -6.51 in CD₂Cl₂ (δ_H -5.73 in C₆D₆) while the protons attached to the carbon atom in the β position with respect to the gold centre give rise to a poorly resolved pseudo-triplet multiplicity suggesting a weak ⁴J (1 Hz) coupling to the hydride ligand. (Figure 21). The assignment was confirmed by preparing the analogous deuteride **34_D** by reacting the gold(III) hydroxide **3** with Li[DBEt₃] (Scheme 11). The ¹H NMR spectrum of **34_D** was similar to the one of **34_H** with the absence of the hydride resonance. The proton attached to the β-carbon with respect to the gold centre shows the expected doublet multiplicity (⁴J = 2 Hz). The ²H NMR spectrum of the complex shows a singlet resonance at δ_D -6.58, consistent with the hydride assignment in **34_H**.

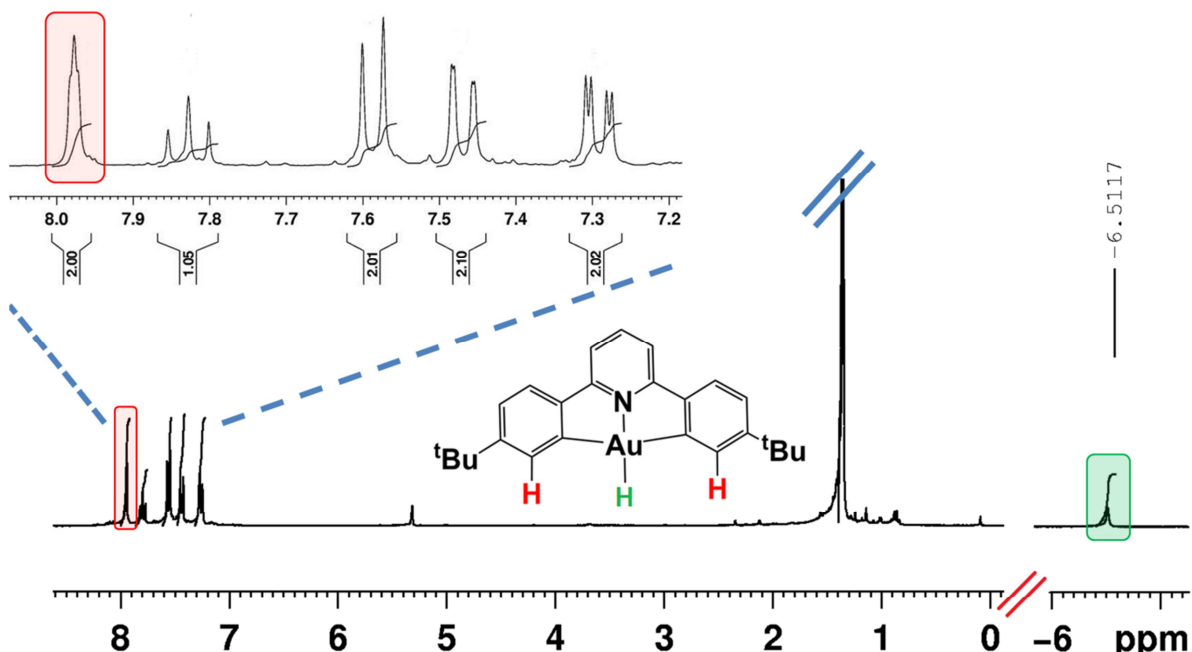


Figure 21. ^1H NMR spectrum of $\mathbf{34_H}$. (CD_2Cl_2 , 300 MHz, RT) The hydride resonance (green) and hydrogen attached to the β -carbon with respect to the gold (red) are highlighted.

By contrast, the Au—H chemical shift in $(\text{IPr})\text{Au}^{\text{I}}(\text{H})$ (IPr = 1,3-bis(2,6-diisopropylphenyl)imidazole-2-ylidene) was found at $\delta_{\text{H}} +3.38$ in CD_2Cl_2 ($\delta_{\text{H}} +5.11$ in C_6D_6),⁴⁴ about 10 ppm downfield from the resonance in gold(III) hydride $\mathbf{34_H}$. This considerable difference in chemical shifts between the gold hydrides in the two oxidation states was predicted by theoretical studies and is thought to be caused by a combination of paramagnetic ring current effects¹⁰⁹ and relativistic spin-orbit effects.¹¹⁰

Spin-orbit coupling effects are expected to have a large influence on hydrogen chemical shifts in the complexes where the hydrogen is bonded directly to heavy metal centres since the hydrogen uses exclusively its $1s$ -orbital in bonding. A dominant contribution of occupied orbitals with an approximate σ symmetry with respect to the bond between the NMR nucleus (hydrogen) and the attached heavy atom (e.g. d^{10} and d^0 metals) will cause *deshielding* spin-orbit coupling effects. At the same time, orbitals with approximate π -symmetry (e.g. in d^6 and d^8 metal complexes) will provide *shielding* contributions.^{110, 111} A consequence of the above is that the d^8 gold(III) hydride complexes, along with almost all complexes with partially filled d -shells, exhibit negative (high field) hydride NMR shifts, while complexes with fully filled d -shells (the d^{10} gold(I) included) exhibit positive (low field) chemical shifts. A comparison of the gold(I) and gold(III) hydride chemical shifts compared to other d -block metals^{44, 112} is shown in Figure 22.

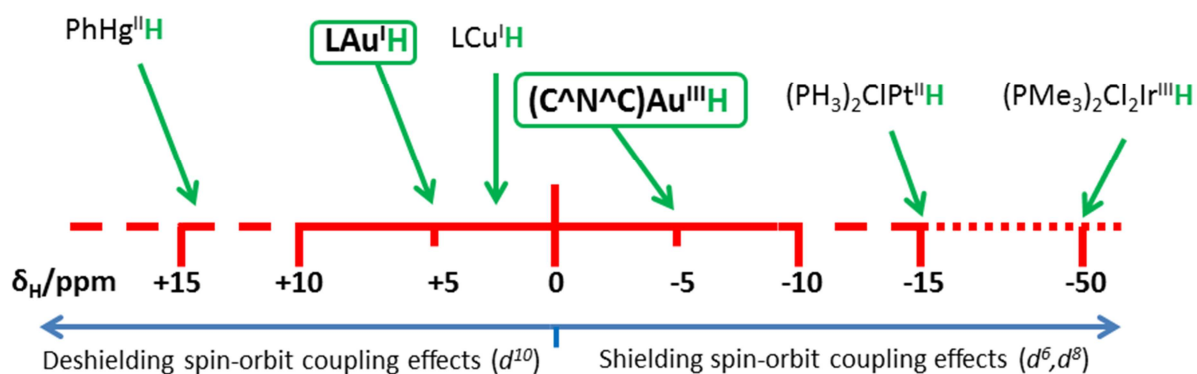


Figure 22. *d*-block metal hydrides NMR chemical shifts, based on the study by Hrobárik *et al.*¹¹⁰

Characterisation in solid state

Both hydride and deuteride **34_{H(D)}** were also investigated by IR (ATR) spectroscopy. The IR spectrum of the hydride showed a strong sharp band at 2188 cm⁻¹ which is higher than the Au—H stretch in (IPr)Au^IH (1976 cm⁻¹)⁴⁴ but similar to that reported for AuH and (H₂)AuH in frozen argon matrix (2226 and 2173 cm⁻¹ respectively),^{102a} or to the band reported for AuH in the gas phase.¹¹³ The value also compares well with the one found in the closely related platinum(II) hydrides (N[^]N[^]C)PtH (N[^]N[^]C = 6-aryl-2,2'-bipyridine) (2157-2126 cm⁻¹).¹¹⁴ The IR spectrum of the deuteride **34_D** was similar to the one of the hydride **34_H** but with the absence of the band at 2188 cm⁻¹. The Au-D stretch, expected at *ca.* 1550 cm⁻¹ was not found and is likely to be obscured by organic vibration modes. Based on the comparison with **34_D** we assign the 2188 cm⁻¹ band in **34_H** to the Au—H stretching mode.

Dichloromethane solutions of **34_H** kept at -28 °C produced single crystals suitable for an X-ray diffraction study. The solid state structure confirms **34_H** as a monomeric, terminal gold(III) hydride. (Figure 23, left) The crystal quality allowed for hydride ligand to be located on the difference density map. The Au—N bond length (2.035(3) Å) is slightly elongated when compared with the one of the starting hydroxide **3** (1.974(3) Å) (Table 2) as a consequence of the stronger *trans* influence of the hydride ligand compared to the one of the hydroxide ligand. In the crystal packing, the Au⋯Au distances are 4.635 Å and the molecules are stacked in a head-to-tail fashion with short (3.407 Å) interplanar contacts. (Figure 23, right)

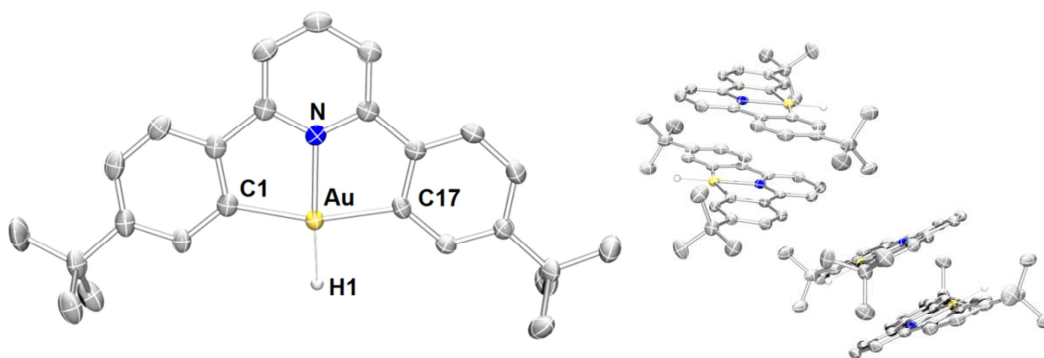


Figure 23. Molecular structure of (C^NC)AuH (**34_H**). Thermal ellipsoids are set at 50% probability level. Hydrogen atoms (except for that bound to the gold atom) are omitted. Selected bond distances (Å) and angles (°): Au-N 2.035(3), Au-C(17) 2.073(4), Au-C(1) 2.074(4), C(17)-Au-C(1) 161.63(16). Head-to-tail arrangement depicting contacts between stacking aromatic rings. (right)

Complex **34_H** is stable to moisture and air at room temperature and shows no signs of decomposition under ambient laboratory lighting for months in the solid state. However, toluene and dichloromethane solutions of **34_H** darken rapidly when exposed to light without any noticeable change in the ¹H NMR spectrum. Prolonged exposure to sunlight of a dichloromethane solution of **34_H** gave the (C^NC)AuCl **2** (*t*_{1/2} ≈ 4 h). The hydride is very soluble in polar solvents such as dichloromethane or THF, in aromatic hydrocarbons (toluene, benzene) and only sparingly soluble in light petroleum. Despite its remarkable thermal stability, heating a benzene solution of **34_H** at 60 °C for 12 h resulted in the loss of the hydride resonance by ¹H NMR spectroscopy and gave a mixture of products out of which 30 % free ligand **1** could be quantified. No products of aromatic C—H activation such as (C^NC)AuPh **17** could be identified.

It is also worth mentioning that even though β-hydride elimination has been known for *d*⁸ metals for a long time,¹¹⁵ samples of (C^NC)AuEt **17** failed to produce the hydride **34_H** under thermolysis or photolysis. The explanation probably resides with the fact that (C^NC)AuH **34_H** is coordinatively saturated,¹¹⁶ whereas a vacant coordinative site is a pre-requisite for β-hydride elimination to occur. This behaviour resembles the one of gold(I) alkyl complexes where β-hydride elimination from (IPr)Au^I(Et) has been reported to be an un-favourable process by various computational studies due to the high energy of the gold(I)-alkene-hydride intermediate.¹⁰⁶

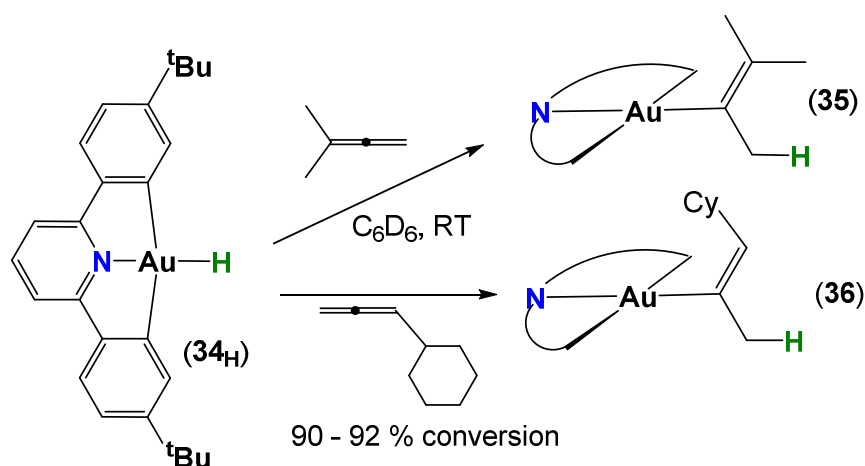
2.2 Reactivity of the (C[^]N[^]C)AuH

Reactions with unsaturated hydrocarbons

Initial reactivity screening was performed with substrates known to react with typical metal hydrides such as aldehydes or olefins.¹¹⁷ Compound **34_H** proved to be inert towards ethylene, norbornene, 3-hexyne, diphenyl acetylene, CO₂ and benzaldehyde. The reactivity of **34_H** seems to be less pronounced than of the gold(I) hydride (IPr)AuH;⁴⁴ for instance, while (IPr)AuH is reported to readily insert dimethyl acetylenedicarboxylate (DMAD) to give the gold(I) vinyl analogue via a *trans* insertion, the gold(III) hydride **34_H** displayed no reactivity towards DMAD and the starting materials could be recovered unchanged.

However, **34_H** does readily insert more reactive unsaturated hydrocarbons such as allenes to give rise to gold(III) vinyl complexes. In recent years there has been an extended interest in gold vinyl complexes. The reason lies in their ubiquitous presence as proposed intermediates in catalytic cycles involving gold(I) and gold(III) mediated transformations of unsaturated hydrocarbons. While in the case of gold(I) there have been a number of these complexes isolated and studied,¹¹⁸ reports of gold(III) vinyl complexes is still very scarce.²⁷

The reaction with 1,1-dimethylallene produced gold(III) vinyl complex **35** with >90% conversion being reached after 20 h. (Scheme 12).



Scheme 12. Reactivity of **34_H** towards allenes: synthesis of gold(III) vinyl complexes

Complex **35** could be readily recrystallised from dichloromethane solutions at -28 °C and the crystals were subjected to a single crystal X-ray investigation. The molecular structure of **35** (Figure 24) represents a rare example of a structurally characterised gold(III) vinyl complex. To the best of our knowledge, the only other reported crystal structure depicting a gold(III) vinyl complex is the gold oxazoline-based zwitterion obtained by the AuCl₃ cyclisation of a

benzamide-bearing substrate reported by Ahn *et al.*¹¹⁹ In the crystal of **35**, the vinyl moiety is disordered over two positions. The Au—C bond length (2.04(3) Å) is comparable to the one in the vinyl complex reported by Ahn (2.004(19) Å).¹¹⁹ The extended structure of **35** displays a head-to-tail arrangement with short distances between the planes (3.540 Å) and long Au⋯Au separations (6.922 Å).

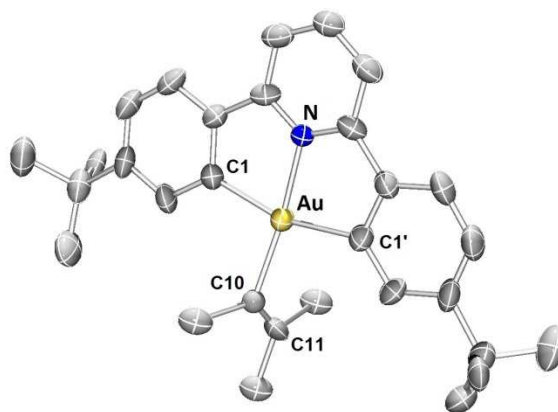


Figure 24. Molecular structure of **35**. Thermal ellipsoids are set at 30% probability level. Hydrogen atoms are omitted. Selected bond distances (Å) and angles (°): Au-N(1) 2.047(17), C(10)-C(11) 1.16(4); Au-C(10) 2.04(3); Au-C(17) 2.073(4), Au-C(1) 2.089(17), C(1)-Au-C(1') 162.8(10). N-Au-C(10) 171.1(6); C(1') is a crystallographic equivalent of C(1) generated by the operator $-x, y, \frac{1}{2}-z$. The vinyl moiety shows positional disorder. Only one position is shown.

When using cyclohexylallene as a substrate, the reaction is regioselective, producing a single compound **36**, as established by ¹H NMR spectroscopy. However, the reaction is slower, with >90% conversion noted after 3 days. Since the compound resisted crystallisation, the absolute configuration of the diastereoisomer could not be established.

The (C[^]N[^]C) supported gold hydride does not display reactivity towards functional groups such as aldehydes, common olefins or even acids (*vide infra*) In this respect, the allene insertion reaction opens the possibility for the synthesis of gold(III) vinyl complexes bearing reactive functional groups which can be further exploited.

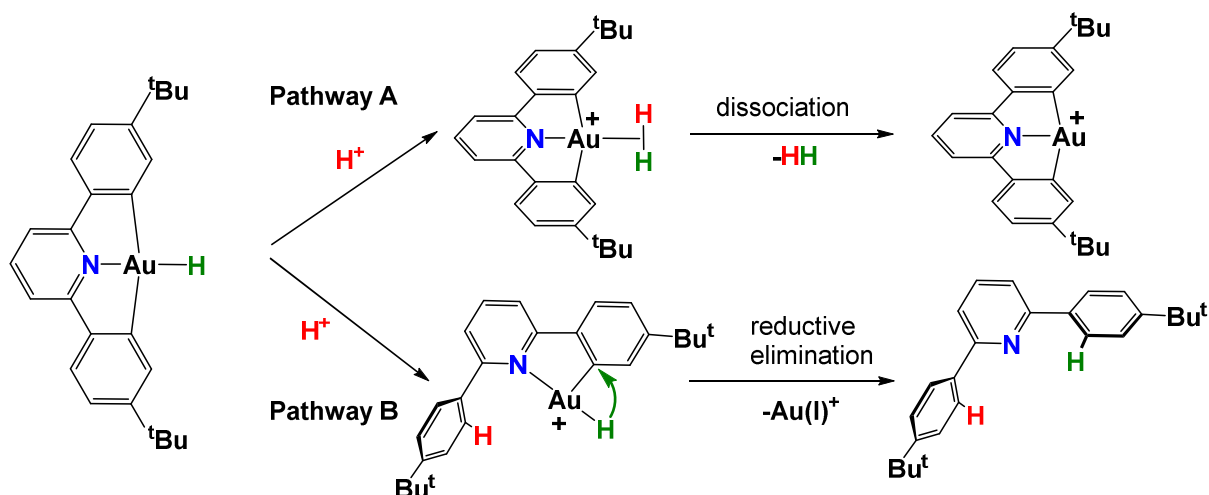
Reactivity with acids

The reaction of **34_H** with acids was also investigated. To our surprise, the hydride was stable towards weak acids such as acetic acid; adding an excess of acetic acid to solutions of **34_H** resulted in no reaction and the hydride could be recovered unchanged. On the other hand an instantaneous reaction was observed with the stronger trifluoroacetic acid (HOAc^F) to give a

mixture of products, with the expected complex $(C^{\wedge}N^{\wedge}C)AuOAc^F$ **4** not being identified among the reaction products.

Indeed, the protonation of transition metal hydrides sometimes involves processes which are more complicated than classical acid-base reactions. Depending on the protonation site, for a given metal, three reaction pathways can in principle be envisaged: hydride protonation to give a dihydrogen complex, protonation of the metal centre to give a dihydride, or proton electrophilic attack on a basic centre on the supporting ligand.¹²⁰

It was previously discussed (Section 1.1) that strong acids are capable of cleaving phenylC—Au bonds in $(C^{\wedge}N^{\wedge}C)$ tridentate pincer ligands to give rise to $(HC-N^{\wedge}C)$ bidentate environments around the metal centre. In the case of the hydride **34_H**, theoretically there are two possible sites for electrophilic attack of H^+ : (A) the Au—H bond to generate a $(C^{\wedge}N^{\wedge}C)Au^+$ cation with the liberation of H_2 or (B) the phenyl—Au bond to give the bidentate $[(HC-N^{\wedge}C)Au(H)]^+$ with the protonation of the cyclometallating ligand. (Scheme 13)



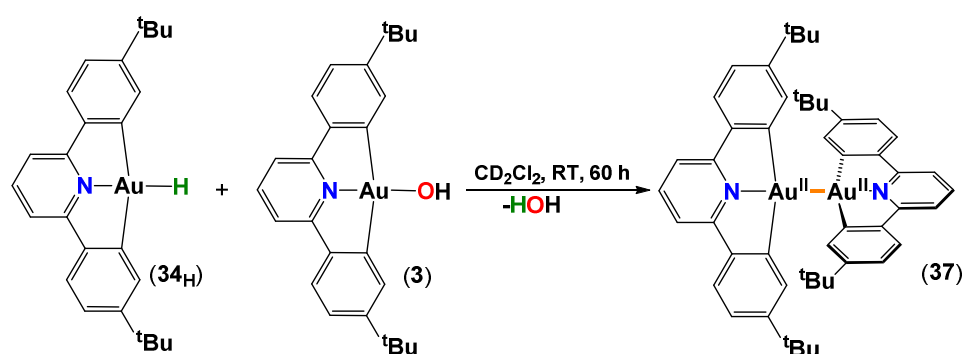
Scheme 13. Potential pathways for the reactions of gold(III) hydrides with H^+ .

Treatment of dichloromethane- d_2 or toluene- d_8 solutions of **34_H** with the Brønsted acid $[H(OEt_2)_2][H_2N\{B(C_6F_5)_3\}_2]$ ¹²¹ at low temperatures ($-70\text{ }^\circ\text{C}$) lead to the disappearance of the hydride resonance of **34_H** (δ_H -6.51 CD_2Cl_2 , -5.52 in toluene- d_8) and gave rise to a broad set of resonances which resemble the ones of the bidentate gold(III) species $[Au(HC-N^{\wedge}C)]^+$. No resonance that could be assigned to H_2 (expected δ_H 4.59 CD_2Cl_2 , 4.50 toluene- d_8) was observed. Similarly, upon reacting the deuteride **34_D** and $[H(OEt_2)_2][H_2N\{B(C_6F_5)_3\}_2]$ or $HOAc^F$ at $-70\text{ }^\circ\text{C}$ no triplet characteristic of a HD complex or of free HD was observed. Upon warming the reaction mixture up to room temperature, darkening of the solution could

be observed and a brown precipitate formed. At room temperature, the free ligand **1** was quantified as the major product (65 %). Based on the experimental evidence we propose that in the case of the (C^NC)AuH **34_H**, Au—C protolysis (Pathway B) is preferred over electrophilic attack at the Au—H bond. This preference is probably due to the strain imposed by the tridentate pincer ligand and also of the covalent nature of the Au—H bond, a consequence of the high electronegativity of the gold centre.¹²² There are no reports on gold dihydrogen complexes in any oxidation state but species of the type (H₂)AuH and (H₂)AuH₃ have been observed by vibrational spectroscopy in frozen gas matrices.^{102a}(*vide supra*)

Reactivity with (C^NC)AuOH **3**: Reductive condensation

Surprisingly, the hydride **34_H** also reacts slowly with the hydroxide **3** to give the unsupported gold(II) dimer **37**. The reaction proceeds at room temperature in the dark and full conversion is noted after 60 h. (Scheme 14). The hydride **34_H** also reacts with the trifluoroacetate (C^NC)Au(OAc^F) **4** to give **37**. After 3 minutes, the composition of the reaction mixture consisted of **37** (75 %) alongside some unidentified products (25%). The presence of secondary products is a consequence of the fact that the reaction by-product is trifluoroacetic acid (HOAc^F) which is capable of Au—C bond protolysis (See section 1.1).



Scheme 14. Reductive condensation pathway for the synthesis of the gold(II) dimer **37**

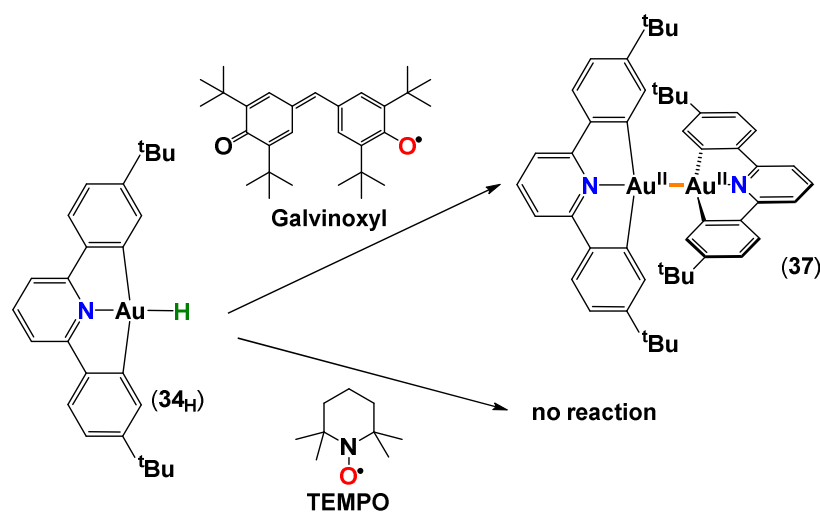
The reaction of a metal hydroxide (or carboxylate) with a metal hydride with the elimination of water (or acid) thus amounts to *reductive condensation*. Common protocols for the preparation of Au^{II}—Au^{II} dimers typically involve oxidation of a Au^I centre¹²³⁻¹²⁵ or reactions of between Au^{III} and Au^I complexes (comproportionation).¹²⁶ An inverse reaction of reductive condensation is the oxidative cleavage of a Pd^I—Pd^I bond by H₂O and NH₃ which has recently been reported by Ozerov *et al.*¹²⁷

Complex **37** was isolated as a yellow air- and moisture-stable powder and does not show any signs of decomposition in benzene and dichloromethane solutions kept in the dark over a period of at least 7 days. As a solid, **37** is stable for months at room temperature in the

presence of ambient laboratory lighting. The characterisation and chemistry of **37** will be discussed below. (Sections 2.3 and 2.4)

Bond dissociation energy in **34_H**

The dimeric Au^{II} complex **37** can also be prepared by direct H• radical abstraction from (C[^]N[^]C)AuH **34_H** mediated by radical scavengers such as galvinoxyl. The reaction is quantitative after 5 minutes as noted by ¹H NMR spectroscopy. On the other hand, the reaction does not proceed if TEMPO is employed as a radical scavenger. (Scheme 15)



Scheme 15 Reaction of gold(III) hydride **34_H** with radical scavengers

Since galvinoxyl is capable of H• abstraction while TEMPO is not, the Au—H bond dissociation energy (BDE) could be estimated experimentally. The reported BDE (measured by calorimetry) for TEMPO-H is 291.34 kJ mol⁻¹ while the BDE of galvinoxyl-H is 328.7±2.1 kJ mol⁻¹ which provides an estimate of the Au—H bond dissociation energy in **34_H** between these two values.¹²⁸ The value is consistent with the BDE determined for the diatomic compound AuH in the gas phase (292±2 kJ mol⁻¹)¹²⁹ and is also in close agreement with the value determined by us for (C[^]N[^]C)AuH **34_H** through DFT calculations (317 kJ mol⁻¹) in collaboration with Dr Joseph Wright.¹³⁰ For comparison with Pt^{II}, we have also determined the BDE of the closely related pincer supported (N[^]N[^]C)PtH (N[^]N[^]C = 6-phenyl-bipyridyl). The determined BDE (350 kJ mol⁻¹), also in close agreement with the one determined for the diatomic molecule PtH (352 kJ mol⁻¹),¹²⁹ is comparable but slightly greater than for the one of **34_H**. The results are summarised in Table 8.

Table 8. Comparison of Au^{III} and Pt^{II} hydride complexes: Calculated and experimental bond-dissociation energies (values in kJ mol⁻¹)

Complex	Experimental BDE ^a	Calculated BDE ^b	Diatomic Compound	BDE ^c
(C [^] N [^] C)AuH	291.34 – 328.7	317	Au—H	292±8
(N [^] N [^] C)PtH	—	350	Pt—H	352

^a Approximated from the reactions with H· acceptors ^b Determined by DFT and taken from ref 130 ^c Determined in gas phase, taken from ref 129

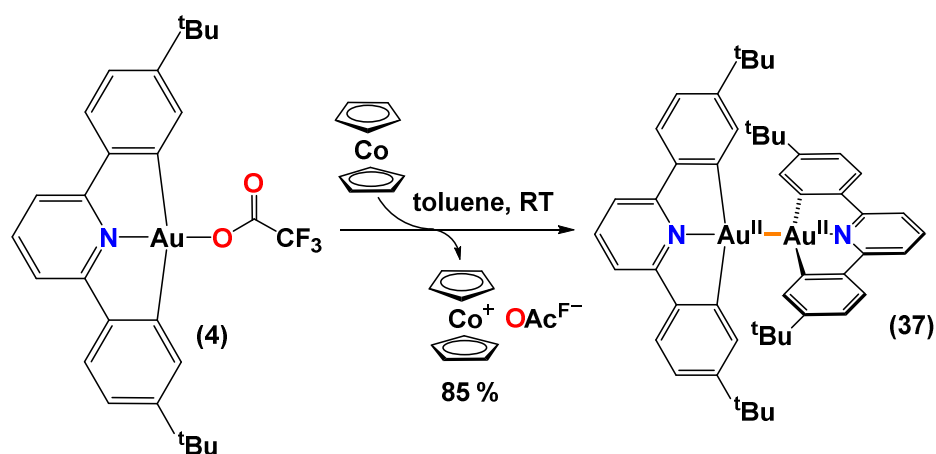
2.3 Synthesis and characterisation of an unsupported Au^{II}—Au^{II} dimer

Gold(II) complexes are still considered rather exotic and still uncommon compared to the number of compounds in oxidation states I and III. Despite this, recent reports propose that monomeric¹³¹ and dimeric¹³² gold(II) complexes play key roles in the catalytic cycles of various organic transformations such as heteroarylation of alkenes. There are very few monomeric, paramagnetic (*d*⁹) Au(II) complexes reported to this date,¹²³ but in some cases,¹³³ the assignment of the true oxidation state has been debated due to the non-innocent nature of the ligand environments.^{134,135} Unexpectedly and perhaps ironically, a ‘true’ example of structurally characterised monomeric gold(II) species, bearing non-innocent ligands, is the tetraxenogold(II) species [Au^{II}Xe₄](Sb₂F₁₁)₂.¹³⁶ The compound was synthesised by the reduction of the AuF₃ with xenon in the presence of fluoroantimonic acid and was crystallised at low temperature. These features make this a unique example of a combination of a noble metal with an inert gas where the noble metal is in an unusual oxidation state.

Most monomeric gold(II) species undergo dimerisation as a way of achieving stabilisation, to form diamagnetic complexes containing Au—Au covalent bonds frequently supported by bridging ligands. Without such ligands, disproportionation reactions of Au(II) centres to Au(I) and Au(III) becomes very facile. As a consequence, there are only a very small number of examples of compounds containing an *unsupported* Au^{II}—Au^{II} bond.^{124b,c;126;137}

From the reactivity studies of the hydride **34_H** we have found that the generation of a remarkably stable unsupported gold(II) dimer (C[^]N[^]C)Au—Au(C[^]N[^]C) **37** was quite facile. In fact, the formation of **37** is observed as a side reaction in several transformations of **34_H** and is possibly indicative of competing one electron reduction pathways.

The unusual stability of **37** towards disproportionation and oxidation caused us to investigate its structure and chemistry in more detail. Since the reductive condensation reaction was quite slow (60 h) (Scheme 14) and the H• abstraction route produced byproducts (GalvinoxylH) which were difficult to separate (Scheme 15) we decided to explore other synthetic routes for the generation of **37**. We have found that the one electron reduction of the trifluoroacetato (C[^]N[^]C)AuOAc^F **4** in toluene, employing cobaltocene as a reductant afforded **37** in good yields. The ionic byproduct [Cp₂Co](OAc^F) is insoluble in less polar organic solvents and can be easily separated by filtration. (Scheme 16) Complex **37** is very soluble in polar solvents such as dichloromethane and THF, in aromatic hydrocarbons (benzene, toluene) and only sparingly soluble in light petroleum.



Scheme 16. Synthesis of **37** via one electron reduction of (C[^]N[^]C)Au^{III}(OAc^F) **4**

Characterisation in solution

Investigation by ¹H NMR spectroscopy of **37** revealed a single set of typical resonances for the symmetrically bound diphenylpyridine pincer suggesting that the two (C[^]N[^]C) fragments are equivalent in solution. The proton attached to the carbon atom in the β-position with respect to the gold centre exhibits a pronounced downfield shift (δ_H 8.14) when compared to the hydride **34_H** or to other mononuclear species bearing the (C[^]N[^]C)Au fragment (δ_H 7.98 in **34_H**). A similar difference is observed for the *tert*-butyl groups which exhibit a upfield shift in the dinuclear **37** (δ_H 1.01) when compared to other mononuclear (C[^]N[^]C)Au species (δ_H 1.36 in **34_H**). (Figure 25) Indeed, this difference is also observed in other dinuclear species containing the (C[^]N[^]C)Au fragment. (See also Chapter 3)

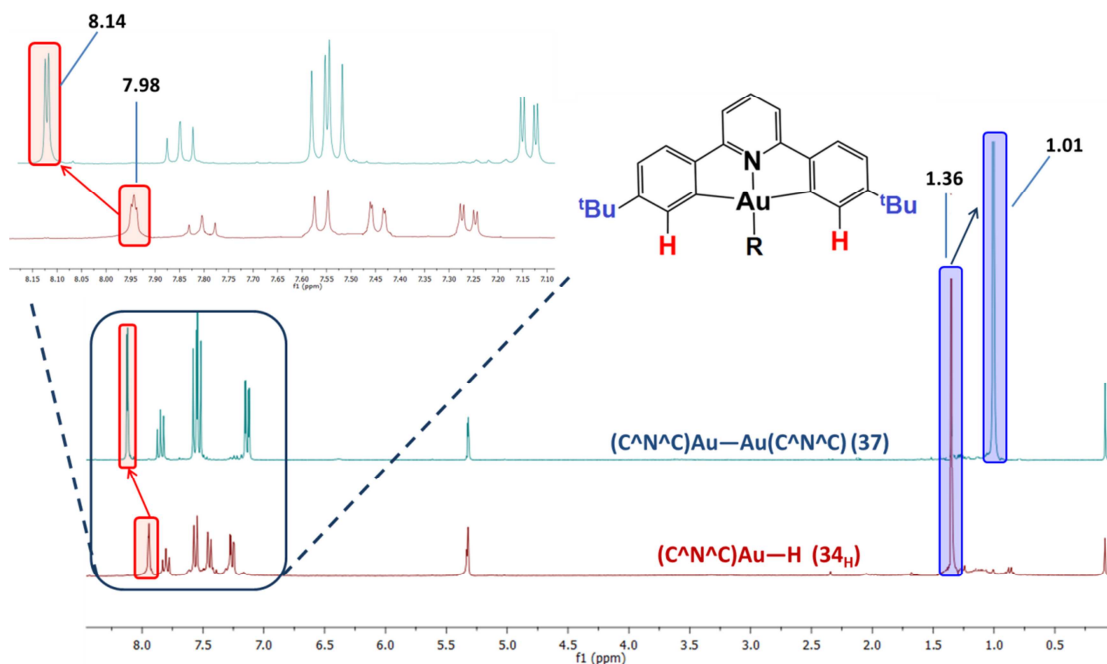


Figure 25. ^1H NMR spectra (300 MHz, CD_2Cl_2 , RT) of $(\text{C}^{\wedge}\text{N}^{\wedge}\text{C})\text{Au}-\text{H}$ **34_H** (red, bottom) and $(\text{C}^{\wedge}\text{N}^{\wedge}\text{C})\text{Au}-\text{Au}(\text{C}^{\wedge}\text{N}^{\wedge}\text{C})$ **37** (blue, top). CDHCl_2 and silicone grease also present. Hydride resonance ($\delta_{\text{H}} -6.51$) in **34_H** not shown.

The diffusion coefficient in dichloromethane solutions for compound **37** has also been measured by DOSY NMR spectroscopy and by electrochemical methods and was compared with the ones of the hydride **34_H** and the hydroxide **3**. The results are summarised in Table 9. The data confirm that complex **37** diffuses slower than complexes **34_H** and **3**, consistent with the higher nuclearity of the $(\text{C}^{\wedge}\text{N}^{\wedge}\text{C})\text{Au}-\text{Au}(\text{C}^{\wedge}\text{N}^{\wedge}\text{C})$ (**37**).

Table 9. Diffusion coefficients ($D/10^{-5} \text{ cm}^2\text{s}^{-1}$) for complexes **3**, **34_H** and **37**.

Method	$(\text{C}^{\wedge}\text{N}^{\wedge}\text{C})\text{AuOH}$ 3	$(\text{C}^{\wedge}\text{N}^{\wedge}\text{C})\text{AuH}$ 34_H	$[(\text{C}^{\wedge}\text{N}^{\wedge}\text{C})\text{Au}]_2$ 37
DOSY NMR ^a	1.24 ± 0.1	1.13 ± 0.1	0.87 ± 0.1
Electrochemistry ^b	1.51 ± 0.1	1.60 ± 0.1	0.7 ± 0.1

^aAverage of the values of D_i found for 3 or more separate peaks in the DOSY NMR spectrum using dioxane/ D_2O as standard ^bData obtained from digital simulations based on electrochemical data by Dr Gregory Wildgoose.¹³⁸

Characterisation in solid state

Complex **37** could be recrystallised from benzene solutions and the crystals were subjected to a single crystal X-ray diffraction study. The molecular structure confirms **37** as an unsupported gold(II) dimer with a short $\text{Au}^{\text{II}}-\text{Au}^{\text{II}}$ bond ($2.5169(4) \text{ \AA}$). (Figure 26, left). The geometry around the gold centre is slightly distorted square-planar with an almost

perfect linear N(1)—Au(1)—Au(2) ($179.39(11)^\circ$) arrangement. In the extended crystal lattice, the molecules are stacked in a head-to-tail fashion with short interplanar distances (3.503 \AA). (Figure 26, right) The shortest intermolecular Au \cdots Au separations between neighbouring molecules in the crystal are 6.694 \AA .

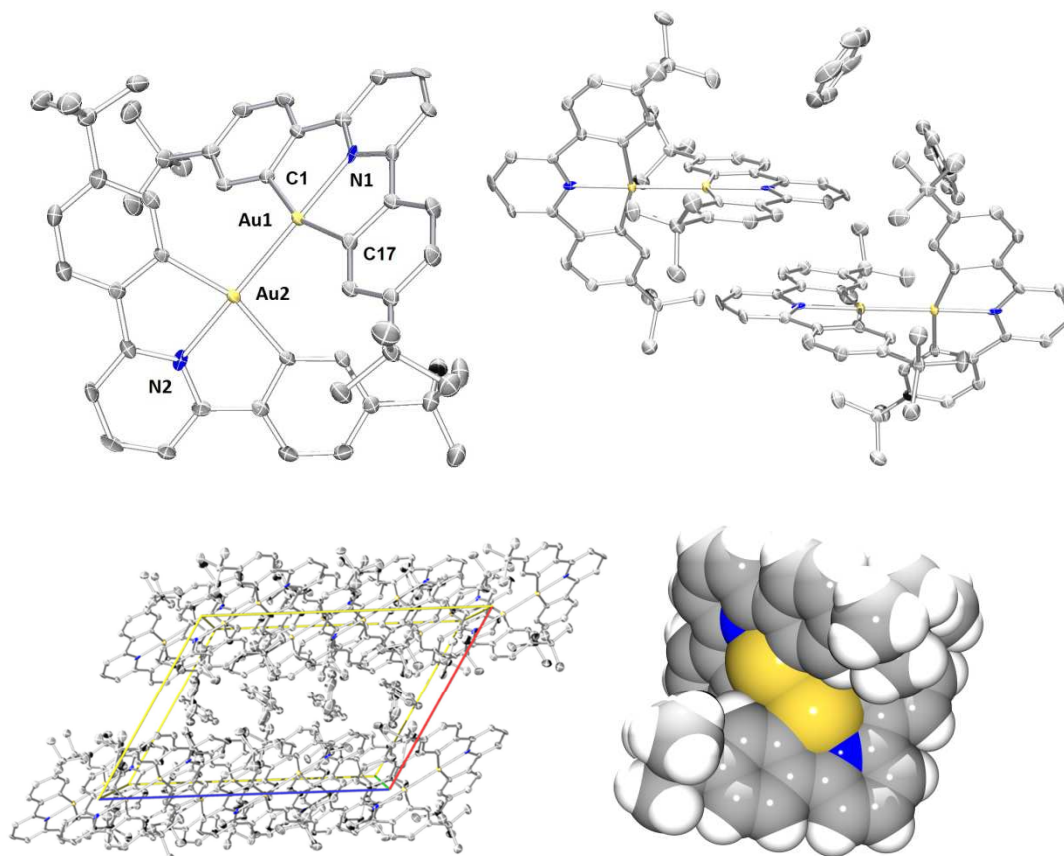


Figure 26. Molecular structure of $37 \cdot 2C_6H_6$. Thermal ellipsoids are set at 50% probability level. Hydrogen atoms are omitted. Selected bond distances (\AA) and angles ($^\circ$): Au(1)—Au(2) $2.5169(4)$; Au(1)—N(1) $2.071(4)$; Au(1)—C(17) $2.071(5)$, Au(1)—C(1) $2.080(5)$, C(1)—Au—C(17) $160.99(18)$; N(1)—Au(1)—Au(2) $179.39(11)$ (top-left); head-to-tail arrangement between stacking aromatic rings. (top-right); packing along the *b*-axis (bottom, left); space fill representation (bottom right)

Gold—Gold distances in Au(II) complexes range from 2.447 \AA — 2.501 \AA in some selected supported Au(II) complexes^{124d,e;139} to $2.5062(9) - 2.6405(8) \text{ \AA}$ in unsupported Au(II) systems. (Table 10). In general, gold—gold bonds tend to be shorter in supported systems due to the effect of the bridging ligands. In unsupported systems, an important influence on Au—Au distance is exerted by the ligand *trans* to the metal centres. As a consequence, Au(II) complexes with nitrogen donors in the *trans* positions (pyridines or quinolones, weak *trans* influence) (entries 1-3 Table 10) tend to be shorter ($2.5062(9) - 2.5355(5) \text{ \AA}$). At the same time, the Au—Au bond is elongated ($2.5679(7) - 2.6405(8) \text{ \AA}$) in complexes with

sulphur or phosphorus donors in *trans* position (tht or dppn, stronger *trans* influence) with respect to the metal centre (entries 4-7 Table 10).

In the light of the above, complex **37** shows a short Au—Au bond (2.5169(4) Å) for an unsupported dimeric gold(II) system which is in line with the weaker *trans* influence of the pyridine ligand. A theoretical Au—Au distance can be estimated based on the crystallographic data for the (C[^]N[^]C)AuMe **15**. The effective covalent radius of the (C[^]N[^]C)Au fragment can be deduced by subtracting 0.77 Å (covalent radius of CH₃ as half of C—C distance in ethane) from the Au—CH₃ distance (2.022(5) Å) in **15**. Thus, the expected Au—Au in the dimer should be *ca.* 2.504 Å. The experimental value of 2.5169(4) Å is in close agreement with the predicted one and the slight deviation can be rationalised in terms of steric repulsion of the *tert*-butyl substituents of the cyclometallated backbone.¹⁴⁰ The bond length in **37** (2.5169(4) Å, Table 10, entry 2) is very similar to the one in [Au₂(CF₃)₄(Py)₂]¹³⁷ (2.5062(9) Å, Table 10, entry 1) which suggests that the repulsion effects of the ^tBu groups of the (C[^]N[^]C)Au fragments exerts only a small influence on the Au—Au bond length.

Table 10. Au—Au bond lengths observed in the reported unsupported dimeric gold(II) compounds.

No.	Compound	Donor on <i>trans</i> to Au	d(Au, Au) (Å)	Reference
1	[Au ₂ (CF ₃) ₄ (Py) ₂]	N (Pyridine)	2.5062(9)	137
2	[Au ₂ (C [^] N [^] C) ₂] 37	N (Pyridine)	2.5169(4)	This work
3	[Au ₂ Cl ₂ (quinolin-8-ylthio) ₂]	N (quinoline)	2.5355(5)	141
4	[Au ₂ (C ₆ F ₅) ₂ (tht) ₂]	S (tht)	2.5679(7)	126
5	[Au ₂ Br ₂ (dppn) ₂][PF ₆] ₂	P (PAr ₃)	2.6035(8)	125c
6	[Au ₂ Cl ₂ (dppn) ₂][PF ₆] ₂	P (PAr ₃)	2.6112(7)	124b
7	[Au ₂ I ₂ (dppn) ₂][PF ₆] ₂	P (PAr ₃)	2.6405(8)	125c

(dppn = 1, 8-bis(diphenylphosphino)naphthalene, tht = tetrahydrothiophene, Py = Pyridine)

Gold—Gold bond dissociation energy in **37**

In order to understand better the unusual stability of **37** compared to other unsupported gold(II) dimers we were interested in determining the Au—Au bond dissociation energy (BDE) in (C[^]N[^]C)Au—Au(C[^]N[^]C).

Initial reports obtained by effusion mass spectrometry predict an atomisation energy of Au₂ molecules in the gas phase of 226.2±0.5 kJ mol⁻¹. (Table 11). This positions the value of the

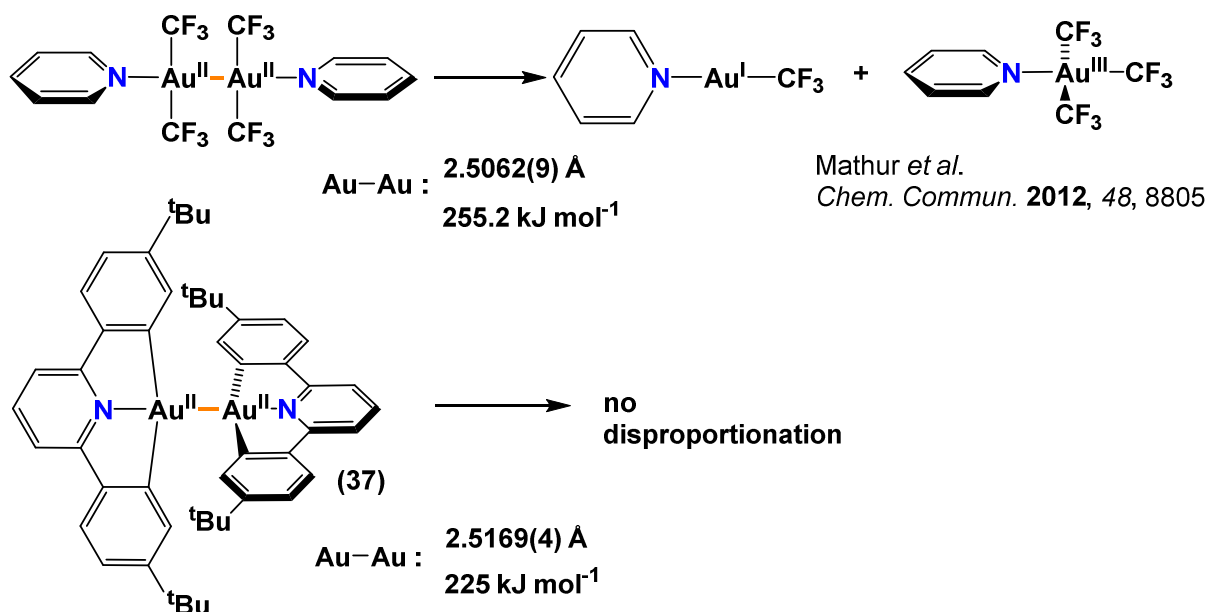
Au—Au bond dissociation energy between the ones of the Pt—Pt bond ($306.7 \pm 1.9 \text{ kJ mol}^{-1}$) and the one of Pd—Pd bond ($\approx 136 \text{ kJ mol}^{-1}$) obtained by the same methods.

Table 11. M—M bond dissociation energies measured in the gas phase by mass spectrometry of diatomic Au₂, Pt₂, Ag₂ and Pt₂ molecules.

Compound	BDE (kJ mol ⁻¹)	Reference
Au—Au	226.2±0.5	14, 142
Pt—Pt	306.7±1.9	143
Ag—Ag	162.9±2.9	143
Pd—Pd	≈136	143

The bond dissociation energy (BDE) of the Au—Au bond for **37** could be estimated experimentally employing electrochemical methods in a collaboration with Dr Gregory Wildgoose. Based on formal reduction potentials obtained from cyclic voltametric data on (C[^]N[^]C)AuOH (**3**) and (C[^]N[^]C)AuH (**34_H**) and digital simulations, the Au^{II}-Au^{II} bond enthalpy in **37** could be estimated to be $198 \pm 1 \text{ kJ mol}^{-1}$.¹³⁸ The value compares well with the value determined by DFT methods for the same system (225 kJ mol^{-1})¹³⁸ and is also in line with the value reported by Xiong and Pyykkö¹⁴⁴ for the structurally similar [Au^{II}X₂(Py)₂]¹³⁷ systems ($\approx 200 \text{ kJ mol}^{-1}$). These values are also very similar to the atomisation energies of gaseous Au₂ molecules.^{14,142,143} (Table 11).

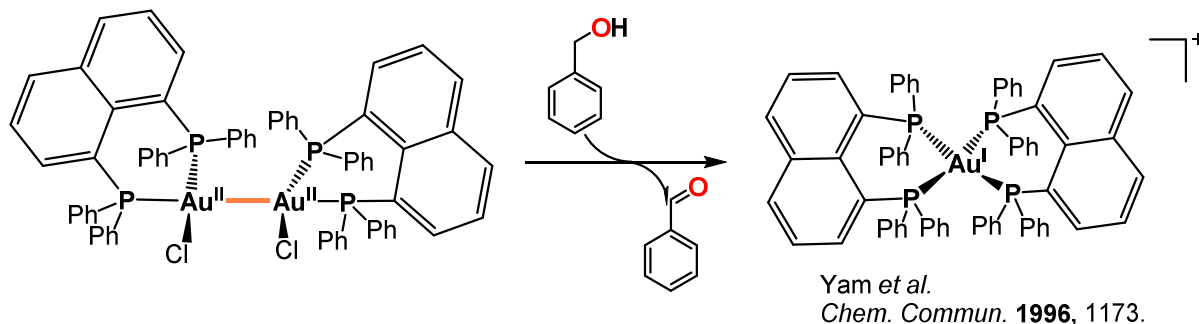
Despite the fact that both the systems reported by Mathur *et al.*¹³⁷ [Au₂(CF₃)₂(Py)₂] and the one reported by us [Au₂(C[^]N[^]C)₂] **37** have similar Au—Au BDEs ($\approx 220\text{—}225 \text{ kJ mol}^{-1}$ by DFT) and similar Au—Au bond lengths ($\approx 2.51 \text{ \AA}$), (entries 1 and 2 in Table 10) there is a significant difference in stability of the two systems towards disproportionation. While [Au₂(CF₃)₄(Py)₂] is reported to undergo spontaneous disproportionation into Au(I) and Au(III) in solution at room temperature (Scheme 17), [Au₂(C[^]N[^]C)₂] **37** is stable in benzene solutions for at least 4 h in the presence of ambient laboratory light and at least 5 days in the dark. In the case of **37**, for disproportionation to take place, the two necessary steps would consist of the cleavage of the Au—Au and of a Au—C bond. We propose that the remarkable inertness of **37** is explained by the thermodynamic stability offered by the rigid tridentate pincer system - under usual conditions, we do not observe Au—C cleavage other (C[^]N[^]C) Au systems. Additional kinetic stability is also conferred by the *tert*-butyl substituents which envelope the Au—Au bond. (Figure 26, bottom right)



Scheme 17. Comparison between the stability of **37** and $[\text{Au}_2(\text{CF}_3)_4(\text{Py})_2]$

2.4 Reactivity of the $\text{Au}^{\text{II}}-\text{Au}^{\text{II}}$ dimer: Synthesis of a mixed valence $\text{Au}^{\text{I}}_4/\text{Au}^{\text{III}}_4$ macrocycle

Given the reported lability in solution of unsupported Au(II) systems, limited studies of their reactivity (other than disproportionation) have so far been reported. To the best of our knowledge, the only report concerning the reactivity of such compounds was communicated by Yam *et al* and features the reduction of the $(\text{dppn})(\text{Cl})\text{Au}^{\text{II}}-\text{Au}^{\text{II}}(\text{Cl})(\text{dppn})$ ($\text{dppn} = 1, 8$ -bis(diphenylphosphino)naphthalene) with benzyl alcohol to give the $[\text{Au}^{\text{I}}(\text{dppn})_2]^+$ cation and benzaldehyde.^{124b} (Scheme 18)

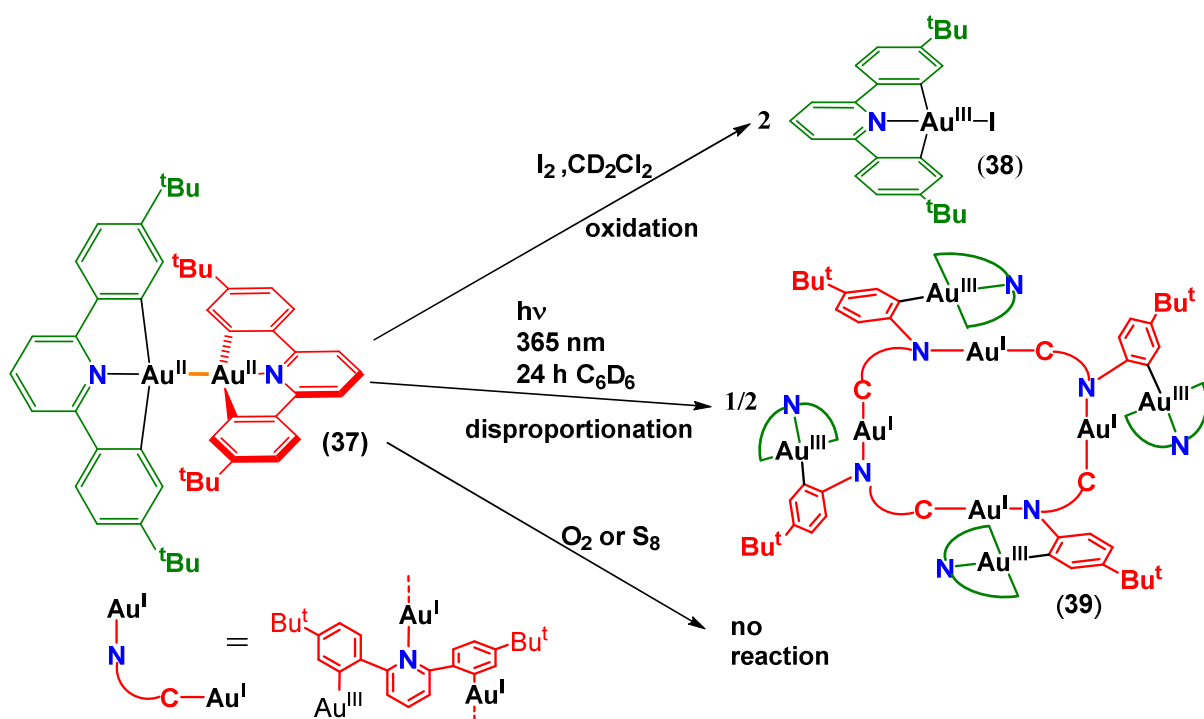


Scheme 18. Reduction of $(\text{dppn})(\text{Cl})\text{Au}^{\text{II}}-\text{Au}^{\text{II}}(\text{Cl})(\text{dppn})$ in the presence of benzylic alcohol^{124b}

Since our previous reactivity studies have shown that complexes bearing the (C[^]N[^]C)Au moiety are resistant to reduction, we decided to explore the stability of the Au—Au bond in **37** towards different oxidants. We have found that strong oxidants like iodine indeed oxidatively add across the Au^{II}—Au^{II} bond to give the (C[^]N[^]C)Au^{III}I **38** cleanly and in quantitative yield. (Scheme 19)

Despite the fact that our DFT calculations predict that the reaction with oxygen is also thermodynamically favourable to give the corresponding μ -peroxo species ($\Delta H = -136 \text{ kJ mol}^{-1}$),¹³⁰ storing **37** under O₂ (1 atm) left the starting materials unchanged, as noted by ¹H NMR spectroscopy. The lack of reactivity is probably a reflection of the steric shielding by the four *tert*-butyl substituents that envelope the Au—Au bond thus providing additional kinetic stabilisation. Nevertheless, the corresponding peroxo species could be accessed *via* an alternative route. (See Chapter 3) Oxidative addition of O₂ across metal—metal bonds has been recently reported for Pd(I) dimers.¹⁴⁵

Similarly, complex **37** does not react with sulphur in refluxing benzene over the course of 24 h probably due to the very limited solubility of S₈ in the reaction medium. A reaction was observed with Ph₃CCl and with AgOAc^F but the reaction outcome is not yet clear and the expected (C[^]N[^]C)AuCl **3** and (C[^]N[^]C)AuOAc^F **4**, respectively, were not observed among the reaction products by ¹H NMR spectroscopy.



Scheme 19. Reactivity of **37**.

The remarkable resistance towards thermal disproportionation of the pincer supported **37** vs. unsupported Au(II) complexes with non-chelating ligands has been discussed. (*vide supra*) Nevertheless, we observed that exposing C₆D₆ solutions of **37** under a nitrogen atmosphere to ambient light for long periods of time (>24 h) leads to a colour change from yellow to orange. Being interested in the structure of the photolysis product, a C₆D₆ solution of **37** was exposed to UV light (365 nm) and the reaction was monitored by ¹H NMR spectroscopy. Full conversion of **37** was noted after 24 h. By comparison, exposing a sample of **37** in C₆D₆ to ambient laboratory lighting resulted in only 30 % conversion over a period of 48 h.

The ¹H NMR spectrum of the resulting products (CD₂Cl₂) reveals the disappearance of the signal characteristic for the *tert*-butyl group of the dinuclear gold(II) species **37** (δ_H 1.01) and the appearance of two new singlets in the aliphatic region (δ_H 1.08 and 1.33) in an approximate 1:1 ratio. The conversion of **37** is also characterised by the disappearance of the high-field doublet assigned to the hydrogen attached to the carbon atom in the β-position with respect to the gold centre. (Figure 27) We envisaged that since photolysis was conducted in C₆D₆ or C₆H₆, the formation of (C^{^N^C})AuPh **17** as a result of radical attack on the reaction solvent would be possible. Nevertheless, conducting the reaction in C₆H₆ revealed no traces of the gold(III) phenyl complex (C^{^N^C})AuPh **17**.

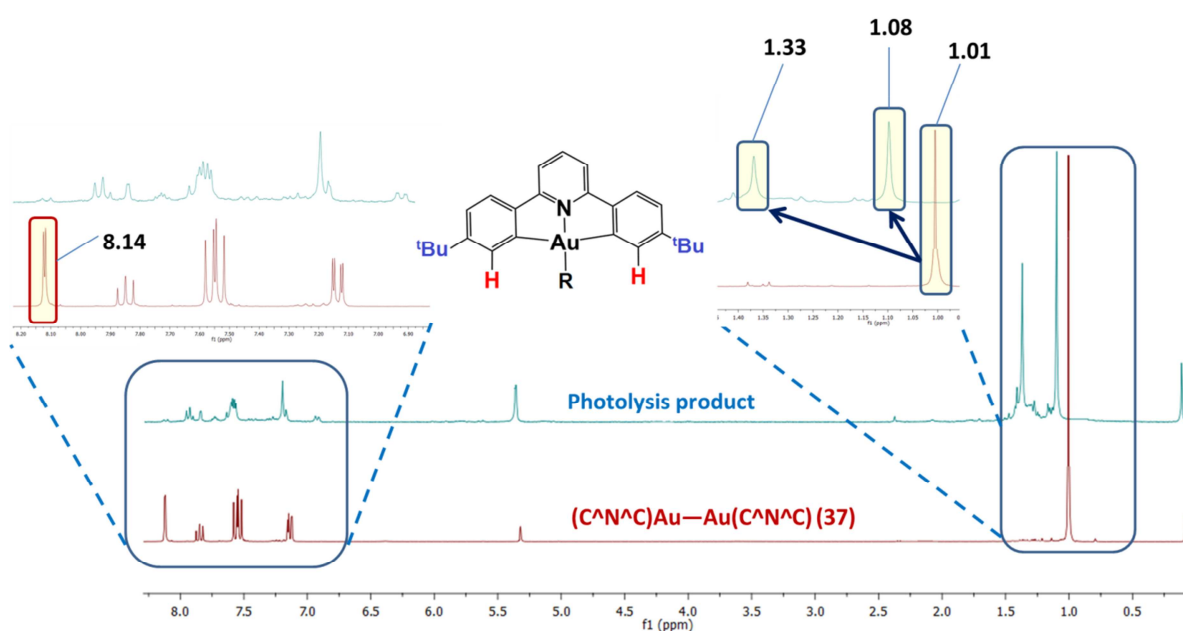


Figure 27. Stacked NMR spectra of (C^{^N^C})Au—Au(C^{^N^C}) **37** (CD₂Cl₂, RT, red) and photolysis product (CD₂Cl₂, RT, blue). Changes in the aromatic and aliphatic regions are highlighted.

The reaction solvent (C₆D₆) and the reaction conditions (nitrogen atmosphere) seem to influence the outcome of the reaction. Conducting the photolysis in dichloromethane-*d*₂

solutions quickly produces a mixture of products which exhibit photoemission in the red region upon irradiation with UV light ($\lambda_{\text{exc}} = 365 \text{ nm}$). The ^1H NMR revealed a complicated pattern suggesting a mixture of products out, although the solvent-activation product $(\text{C}^{\wedge}\text{N}^{\wedge}\text{C})\text{AuCl}$ **2** could not be found. Conducting the irradiation in C_6D_6 in the presence of air produces a mixture of products as revealed by ^1H NMR spectroscopy. The origin of these variations is still under investigation.

In our attempts to decipher the outcome of the photolysis reactions we have managed to obtain orange coloured single crystals from a photolysed sample of **37** in C_6D_6 under nitrogen atmosphere. The crystals were grown by layering a dichloromethane solution of **39** with light petroleum. An X-ray diffraction study revealed the formation of a mixed valence gold(I)/gold(III) macrocycle **39** as a result of the disproportionation of **37**. (Figure 28 and Scheme 19). Complex **39** consists of a 20-membered metallacycle formed by four pyridine-gold(I)-aryl moieties of the 2,6-diphenylpyridine ligand with one $\text{C}_6\text{H}_4^t\text{Bu}$ being decorated with a $(\text{C}^{\wedge}\text{N}^{\wedge}\text{C})\text{Au}^{\text{III}}$ fragment. The geometry around the metal centre is distorted square planar, typical for a Au(III) centre. The Au—N bond lengths in the Au^{III} fragments are comparable to the ones found in other $(\text{C}^{\wedge}\text{N}^{\wedge}\text{C})\text{Au}^{\text{III}}\text{Ar}$ (Ar = Aryl) complexes (Au(1a)—N(1a) 2.048(2) Å in **37** and 2.023(3) Å in $(\text{C}^{\wedge}\text{N}^{\wedge}\text{C})\text{Au}(p\text{-F-C}_6\text{H}_4)$ **18**).

The organic moieties that form the cavity (pyridine and aryl groups) are arranged in an alternated “up-down” orientation in order to avoid steric repulsion between the two aromatic rings. The $3\text{-}^t\text{Bu-C}_6\text{H}_4$ fragment are always pointing in the same direction, causing a narrowing of the lower rim of the cavity by the *tert*-butyl groups to about 3.9 Å. (Figure 29) The diameter of the larger rim of the cavity (defined by the distance between N(2a) and N(2c)) measures 8.7 Å and the cross channel distance $\text{Au}^{\text{I}}\cdots\text{Au}^{\text{I}}$ measures 7.7 Å. In the crystal of **39**, the cavity is probably occupied by crystallisation solvents but attempts to model the residual electron density were unsuccessful. A stacked view depicting solvent accessible channels is presented in Figure 29 (left). The pyridine-Au-aryl units are linear ($\angle \text{C}(37\text{b})\text{—Au}(2\text{c})\text{—N}(2\text{c})$ 172.98(12)°, Figure 29), in accordance with the preferred geometry of Au^{I} (d^{10}). The $\text{Au}^{\text{I}}\text{—N}$ bond lengths is significantly elongated when compared to the $\text{Au}^{\text{III}}\text{—N}$ bond lengths in the $(\text{C}^{\wedge}\text{N}^{\wedge}\text{C})\text{Au}^{\text{III}}$ fragment (Au(2a)—N(2a) 2.138(4) Å in the metallacycle and Au(1a)—Au(2a) 2.048(2) Å in the exterior $(\text{C}^{\wedge}\text{N}^{\wedge}\text{C})\text{Au}^{\text{III}}$ fragment).

The intramolecular $\text{Au}^{\text{I}}\cdots\text{Au}^{\text{III}}$ contacts (3.604(5) Å) are longer than the sum of the van der Waals radii (3.4 Å) and slightly longer than the range of general aurophilic interactions (2.50 – 3.50 Å).¹⁹ The molecule also displays long intramolecular $\text{Au}^{\text{I}}\cdots\text{Au}^{\text{I}}$ distances (5.471 Å) likely due to geometrical constraints. comparable distances can also be measured between gold(III) centres of neighbouring molecules ($\text{Au}^{\text{III}}\cdots\text{Au}^{\text{III}}$ 5.425 Å), similar to other

gold(III) bearing the cyclometallated diphenylpyridine ligand. In the crystal packing, the (C[^]N[^]C)Au^{III} planes are arranged in a head-to-tail fashion.

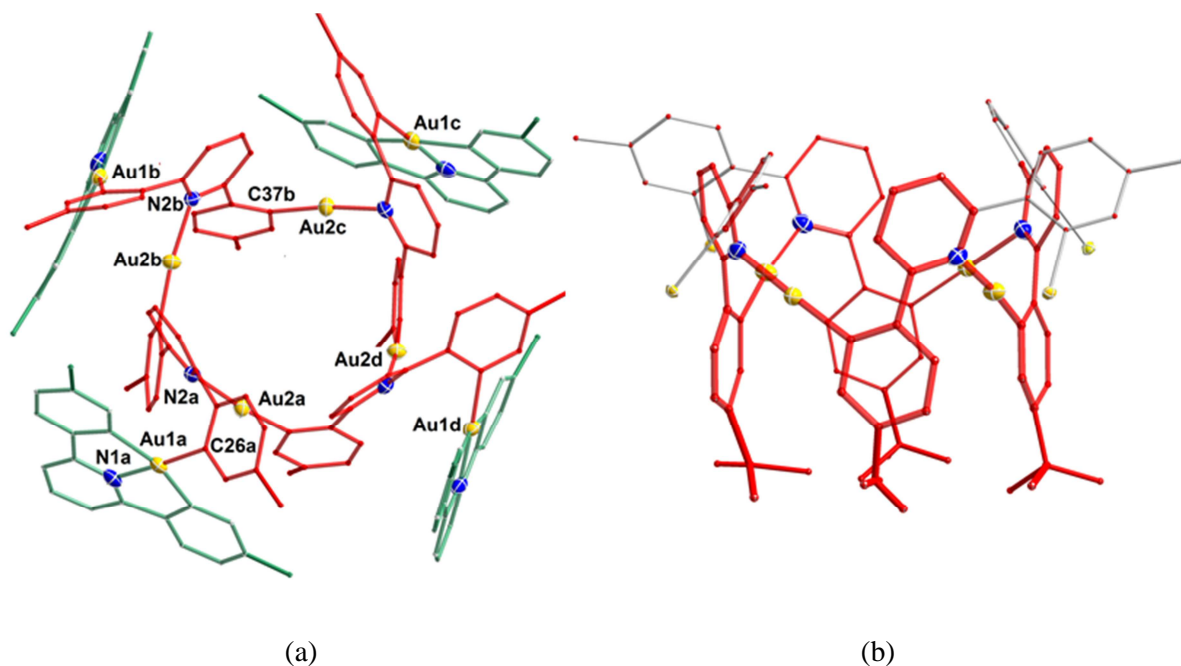


Figure 28. (a) Molecular structure of **39**. Hydrogen atoms methyl groups of *t*-butyl fragments have been omitted for clarity. Selected bond distances [Å] and angles [°]: Au(1a)-Au(2a) 3.6036(6); Au(2a)-Au(2b) 5.4708(6); Au(2a)-Au(2c) 7.7369(6); N(2a)-N(2c) 8.772(11); C37b-Au2b-N2a 173.0(4); Au(1b), Au(1c) and Au(1d) are the crystallographic equivalent of Au(1a). Au(2b), Au(3b), Au(4b) are the crystallographic equivalent of Au(2a). Symmetry operations: $\frac{1}{2}-y, x, z$; $\frac{1}{2}-x, \frac{1}{2}-y, z$; $\frac{1}{2}-x, z$. (b) View of **39** showing the alternating top-bottom arrangement of the aryl/pyridyl moieties forming the cavity together with the closing *tert*-butyl groups. Only the fragments directly taking part in the cavity are in red. The (C[^]N[^]C)Au(III) fragments have been omitted.

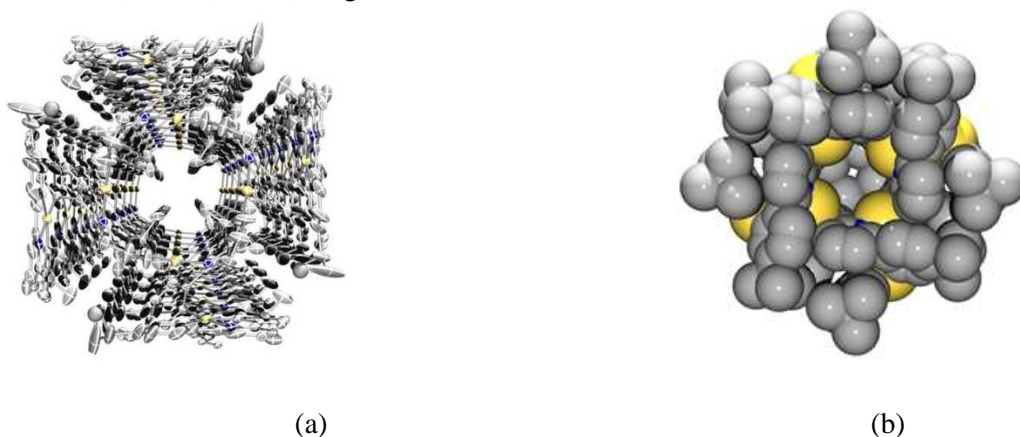


Figure 29. (a) Stacked view comprising of molecules of **37** showing solvent accessible channels. (b) Space filling view along *c* axis showing narrowing of the channel by the *t*-butyl substituents which reduce the opening to 3.9 Å.

Gold(I) macrocycles have been previously reported. Their synthesis generally involves the addition of bidentate ligands to Au(I) precursors. In some examples a supramolecular assembly *via* Au^I...Au^I aurophilic interactions holds the structure together, such as the recently reported carbido-bridged Au₄ cycle, [Au{μ-C≡W(CO)₂(Tp*)}]₄¹⁴⁶ and other thiolato- and formamidinato- containing examples.¹⁴⁷ In other reported examples, the assembly is guided by D→Au (D = Donor *i.e.* N, P, C≡C) coordinative interactions.¹⁴⁸ In this case, the larger macrocycles (containing more than four gold atoms) are characterised by the absence of Au...Au aurophilic interactions.^{148e-f} Strictly speaking, complex **39** can be viewed as an example of the latter, the donor moiety comprising of a pyridyl fragment to gold(I) with long Au...Au contacts. Nevertheless, the incorporation of gold(III) centres in the form of (C[∧]N[∧]C)Au^{III} fragments make complex **39** a unique example of a mixed valence Au^{I/III} macrocycle. Also, to the best of our knowledge, this is the first example of a gold macrocycle generated by disproportionation of a gold(II) complex.

2.5. Attempts to synthesise a dimeric, unsupported Au(0) complex

Sub-nanometre phosphine and thiol supported gold nanoclusters have found numerous applications in processes such as fluorescence sensors, catalysis and biological imaging.¹⁵ In some key chemical processes such as CO oxidation,¹⁴⁹ propene oxidation,¹⁵⁰ ethylene hydrogenation,¹⁵¹ or thiophenol oxidation¹⁵² a strong dependence of the catalytic activity was reported to be a function of the cluster size and charge. Typically, metal clusters of less than 10 atoms tend to show increased catalytic activity^{15,149,152} or enhanced selectivity¹⁵⁰ compared to larger clusters. For instance, a recent report by Corma *et al.*¹⁵² shows that while isolated gold atoms on multi-walled carbon nanotubes show no catalytic activity towards the oxidation of thiophenol, gold clusters of 5-10 atoms show high oxidation activity (TOFs ≈ 10⁵ h⁻¹). The activity clearly decreases as aggregation increases with nanoparticles of diameter ≥ 1nm showing no activity.

The use of ligands with good σ-donating properties such as N-heterocyclic carbenes or phosphines reduces the electrophilicity of the gold centre and thus prevents aggregation. Few examples of well-defined small sized cationic gold clusters have been reported in the literature. These consist of the recently reported planar trigonal Au₃⁺ cluster supported by NHC ligands,¹⁵³ and the phosphine supported tetrahedral Au₄⁺,^{57,154} and Au₈²⁺ clusters.⁵⁷ (Figure 30) Au₆²⁺ clusters have been found to arrange in either edge-sharing tetrahedral geometries,¹⁵⁵ or octahedral geometries¹⁵⁶ depending on the surrounding ligands. The formal charge in all discussed clusters is mixed-valence Au(I)/Au(0) and the bonding arises from

symmetrically adapted combinations of partially filled 6s orbitals.¹⁴ In contrast, the bonding in the Au(II) dimers (*vide supra*) arises from interactions of the half-filled d-orbitals.¹⁵⁷

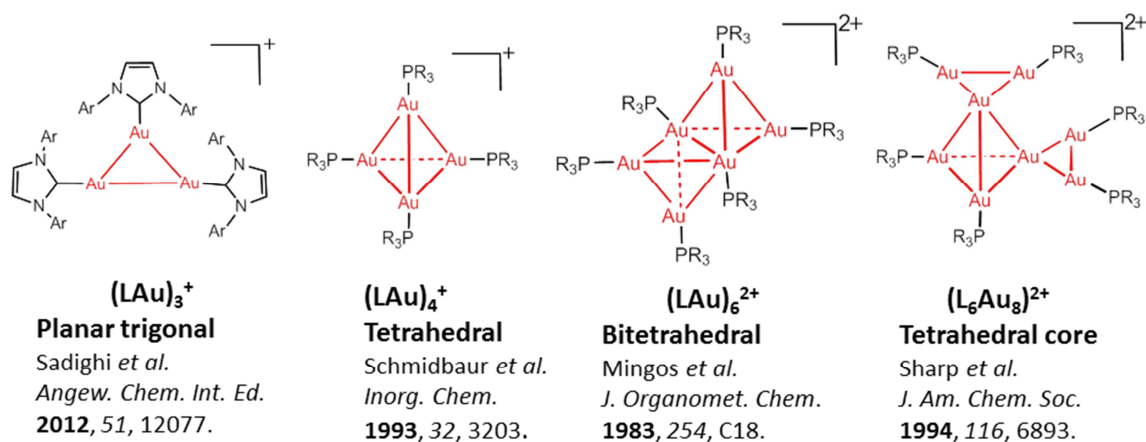
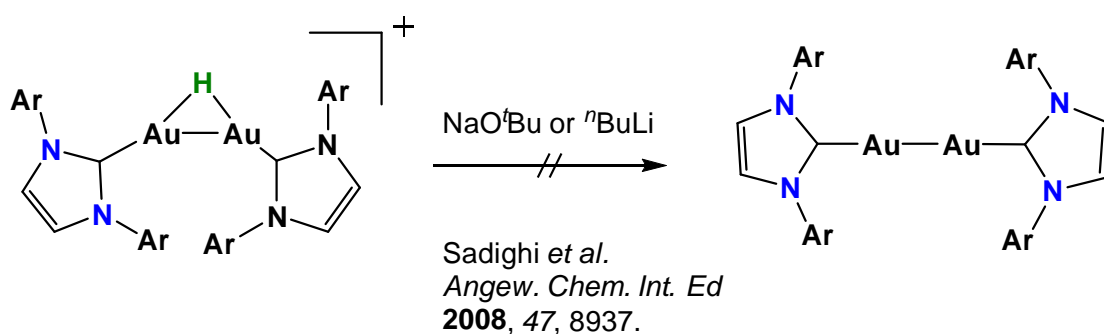


Figure 30. Examples of structurally characterised sub-nanometre cationic gold clusters.

Despite the extended interest in small size gold-nanoclusters, there were no reports on ligand-stabilised Au₂ species in formal oxidation state 0.

Attempts to generate neutral Au₂ clusters supported by N-heterocyclic carbenes involved the deprotonation of a IPr supported hydride bridging digold species.⁴⁴ Unfortunately, employing bases like NaO^tBu or ⁿBuLi failed to give the dimeric gold(0) complex. (Scheme 20) Similarly, attempted electrochemical reduction of the IPr supported Au₃⁺ produced no reduction wave within the electrochemical window of CH₃CN or THF.¹⁵³



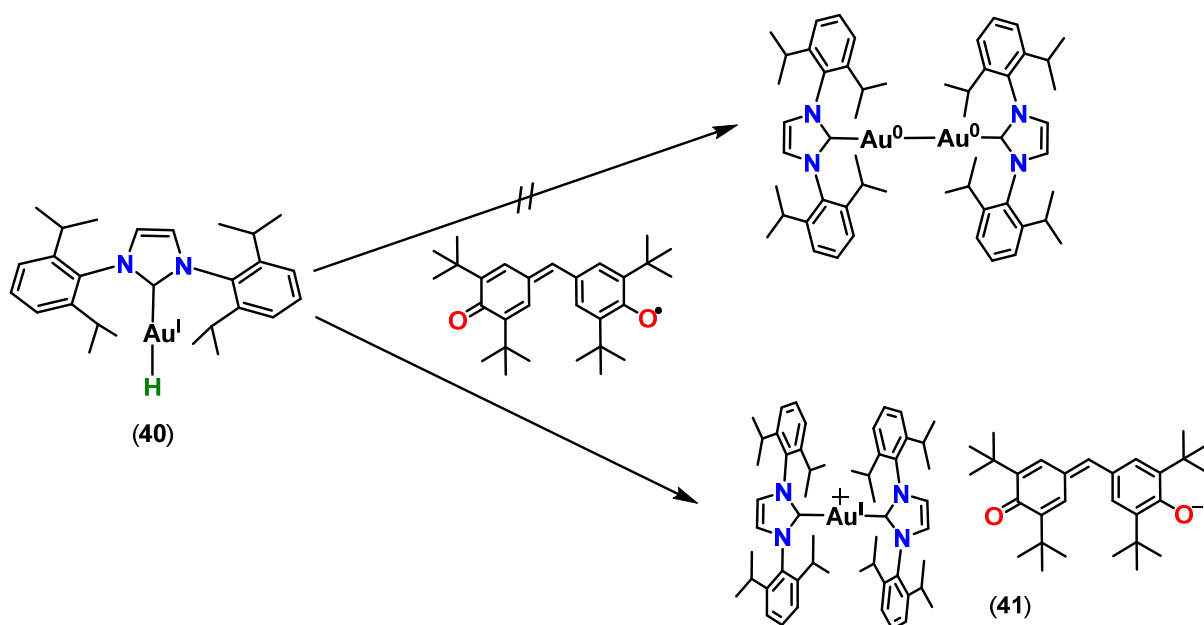
Scheme 20 Attempted deprotonation of [(IPr)₂Au₂(μ-H)]⁺

Since we have previously observed that galvinoxyl is capable of abstracting a hydride from the (C[^]N[^]C)Au^{III}(H) **34_H** to give the dimeric (C[^]N[^]C)Au^{II}—Au^{II}(C[^]N[^]C) gold(II) species **37** (Scheme 15), we envisaged that hydride abstraction by a free radical would be a suitable route for the generation of a dimeric gold(0) species. In this respect, the reaction of the

(IPr)Au^IH with galvinoxyl was attempted. (IPr = 1,3-bis(2,6-diisopropylphenyl)imidazole-2-ylidene).

Recent computational studies have confirmed that the nucleophilicity of the supporting ligand has a direct influence on the atomicity of the gold clusters.¹⁵⁸ We therefore chose the carbene IPr as an ancillary ligand. We envisaged that since IPr is more electron donating than the phosphines but less electron donating than the cyclic(alkyl)(amino)carbenes,¹⁵⁹ it may allow access to neutral clusters with two or more gold atoms. The IPr carbene was also chosen because of synthetic accessibility for our methodology: IPrAu^IH is currently the only gold(I) reported terminal hydride.⁴⁴

Treating IPrAu^IH **40** with galvinoxyl gave rise to a colour change from dark blue (galvinoxyl in C₆D₆) to purple. An initial reaction in an NMR tube in C₆D₆ also revealed the rapid disappearance of the hydride resonance for **40** (δ_{H} 5.11) and the formation of a new complex. Conducting the reaction on a larger scale and subsequent washing with petroleum ether to remove the excess galvinoxyl and the formed galvinoxylH finally afforded a purple powder. The NMR spectrum (CD₂Cl₂) of the formed complex showed no traces of the starting hydride and revealed a ratio between the carbene moiety and Galvinoxyl fragment of 2:1. (Figure 31). Based on the fact that the formed complex is insoluble in light petroleum and based on the ¹H NMR resonances, the ionic structure [(IPr)₂Au][Galvinoxyl] **41** structure seemed likely. (Scheme 21)



Scheme 21. Reactions of IPrAuH **40** with Galvinoxyl.

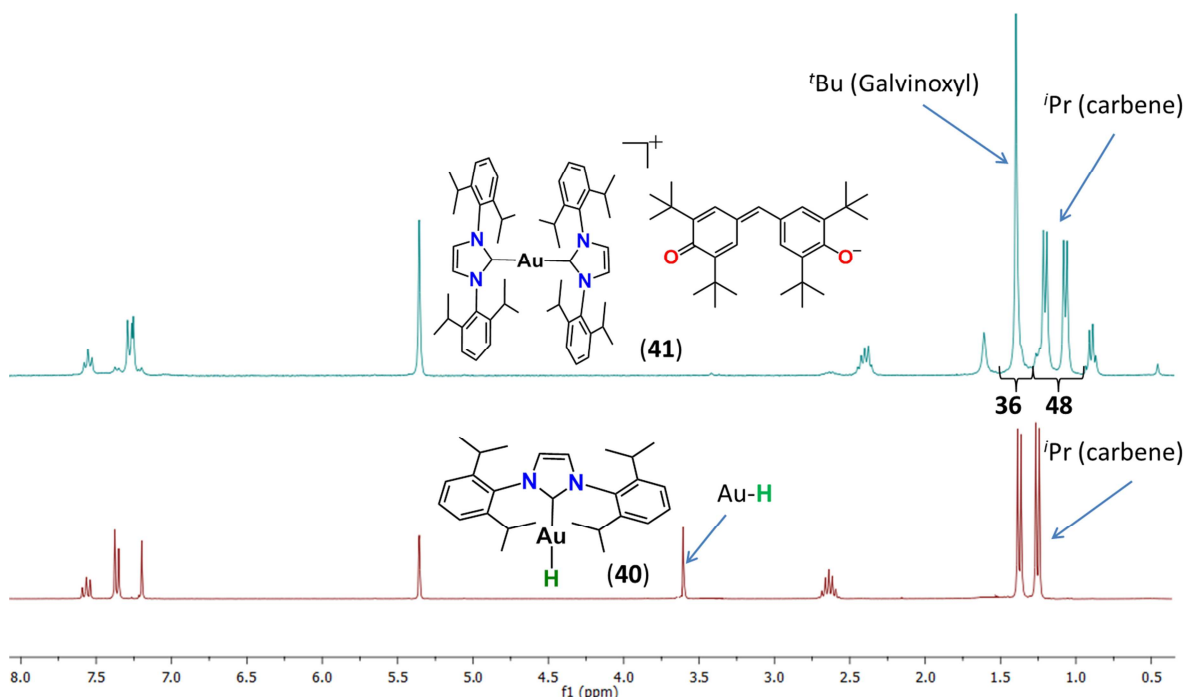


Figure 31. Stacked spectra of the (IPr)Au^IH **40** (CD₂Cl₂, RT, red) and [(IPr)₂Au](RO) (CD₂Cl₂, RT, blue)

The solid-state structure of the complex was determined by X-ray crystallography. (Figure 32) Crystals of **41**·2C₆H₆ were obtained by slow evaporation of a benzene solution of **41** at room temperature. Despite the modest quality of the crystals, unequivocal connectivity could be established and confirms complex **41** as a gold(I) cation with a Galvinoxyl phenolate acting as an anion. In the cationic fragment, the geometry around the Au(I) centre is linear ($\angle\text{C1—Au—C28 } 177.33(45)^\circ$) with the C1—Au and C28—Au of similar length (2.030(9) Å and 2.061(7) Å). The *i*Pr groups are arranged in such a fashion to minimise steric repulsion between the two carbene fragments. The torsion angle between the two imidazolyl planes is 46.6° – a reflection of the steric bulk around the metal centre. The structural parameters of the (IPr)₂Au⁺ fragment are generally similar to those of [(IPr)₂Au][BF₄] previously described by Nolan *et al.*⁶²

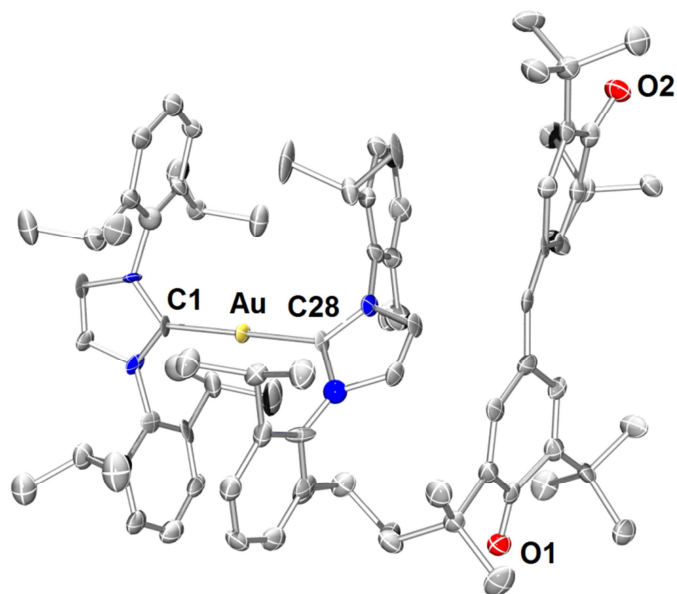
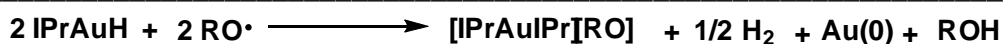
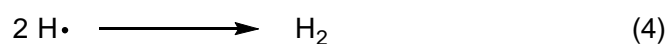
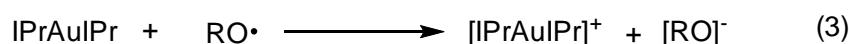
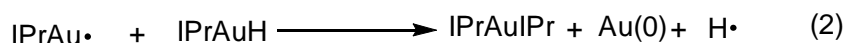
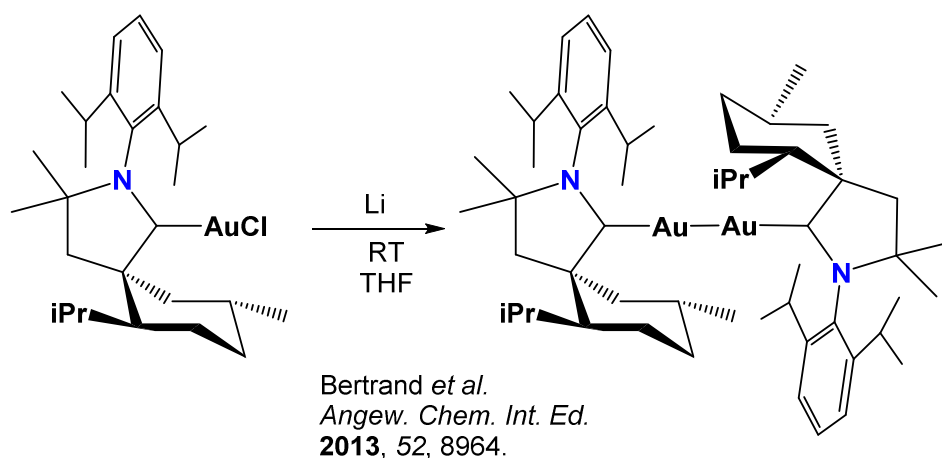


Figure 32. Molecular structure of [(IPr)₂Au][galvinoxyl] (**41**). Hydrogen atoms are omitted. Selected bond distances (Å) and angles (°): Au-C(1) 2.030(9), Au-C(28) 2.061(7), C(1)-Au-C(28) 177.33(45), N1-C1-C28-N3 46.6.

A proposed mechanism for the ligand rearrangement and formation of **41** is given below. In the first instance (1), a hydride abstraction by the radical scavenger Galvinoxyl (RO•) takes place giving rise to a short-lived monomeric Au(0) radical (IPr)Au•. In the subsequent step (2), a radical attack of the IPrAu• on the IPrAuH would promote carbene and H-dissociation from the IPrAuH fragment alongside formation of colloidal Au(0). N-heterocyclic carbenes have been known to produce tight C—Au bonds and are not generally thought to be kinetically labile, in contrast with phosphines which readily undergo dissociation and re-coordination to a metal centre. Despite that, there are some rare instances when irreversible carbene dissociation and transfer from a gold centre to another one is favourable.¹⁶⁰ The ligand supported Au(0) species (IPr)Au(IPr) then transfers one electron to another galvinoxyl radical (RO•) to give rise to the gold(I) species [(IPr)₂Au][RO] **41** (3). The mechanism thus suggests the formation of the Au(0) only as a transient species which readily oxidises in the presence of free persistent radicals.



While this work was in progress, the first examples of Au(0) complexes supported by strongly electron-donating cyclic(Alkyl)(amino)carbenes (CAACs) were reported by Bertrand and coworkers.¹⁶¹ (Scheme 22).



Scheme 22. Synthesis of the first dimeric Au(0) species supported by CAAC ligands.

CONCLUDING REMARKS

In conclusion, we have shown that gold(III) hydrides are indeed isolable and thermally stable provided a rigid ligand capable of blocking reductive elimination pathways is employed. In the case presented, the tridentate diphenylpyridine ligand fulfils these requirements. The gold(III) hydride (C[^]N[^]C)AuH **34_H** can be accessed by treating the corresponding hydroxide (C[^]N[^]C)AuOH **3** with a strong hydride source.

Reactivity studies show that while the hydride is resistant towards substrates such as simple olefins or aldehydes, it does readily insert allenes regioselectively giving rise to gold(III) vinyl complexes. The 1,1'-dimethylallene insertion product, **35** represents a rare example of a gold(III) vinyl complex characterised by X-ray crystallography. The resistance of the hydride **34_H** towards simple olefins also illustrates the high covalent nature of the Au—H bond. Since the reactivity of the metal hydride is also highly dependent on the choice of the stabilising ligand, it can be envisaged that replacing the pyridine donor with a ligand with a much stronger *trans* influence might labilise the Au—H bond enough to undergo insertion reactions with simpler substrates.

The gold(III) hydrides have also proved to be useful synthons for accessing unsupported gold(II) dimers such as (C[^]N[^]C)Au—Au(C[^]N[^]C) **37** via a reductive condensation reaction with gold(III) hydroxides. The remarkable stability of the gold(II) dimer **37** suggests that if

disproportionation pathways are blocked by employing a rigid tridentate ligand, unsupported gold(II) dimeric species are very stable at room temperature under normal conditions. Under more forceful conditions such as irradiation with UV light, the complex does however undergo disproportionation reactions to give a mixed valence $\text{Au}^{\text{I}}_4/\text{Au}^{\text{III}}_4$ macrocycle which represents the first gold macrocycle obtained *via* disproportionation of a gold(II) species.

In an effort to synthesise a N-heterocyclic carbene supported gold(0) dimer, hydride abstraction from the gold(I) hydride $(\text{IPr})\text{Au}^{\text{I}}\text{H}$ **40** in the presence of a radical scavenger such as galvinoxyl was attempted. Our studies show that the short lived gold(0) species $(\text{IPr})\text{Au}^{\cdot}$ undergoes rapid rearrangement to give the ionic species $[(\text{IPr})_2\text{Au}][\text{RO}]$ **41** where the galvinoxyl acts as an anion, suggesting that perhaps more electron donating N-heterocyclic carbenes are required to stabilise dimeric gold(0) species.

CHAPTER 3

Chemistry of Cyclometallated Gold(III) Peroxides

A portion of this chapter has appeared in print:

D.-A. Rosca, J. A. Wright, D. L. Hughes, M. Bochmann “Gold peroxide complexes and conversion of hydroperoxides into gold hydrides by successive oxygen-transfer reactions” *Nat. Commun* **2013**, *4*, 2167. doi: 10.1038/ncomms3167

INTRODUCTION

The chemistry of late transition metal complexes containing M—O bonds has been studied extensively due to their involvement in biological or biomimetic oxidations.¹⁶² More specifically, late transition metal oxo, peroxy and superoxo complexes (Figure 33) have been found to be efficient oxygen atom transfer agents leading to oxidation of various substrates such as alkenes, alcohols or to C—H activation reactions.¹⁶³⁻¹⁶⁵

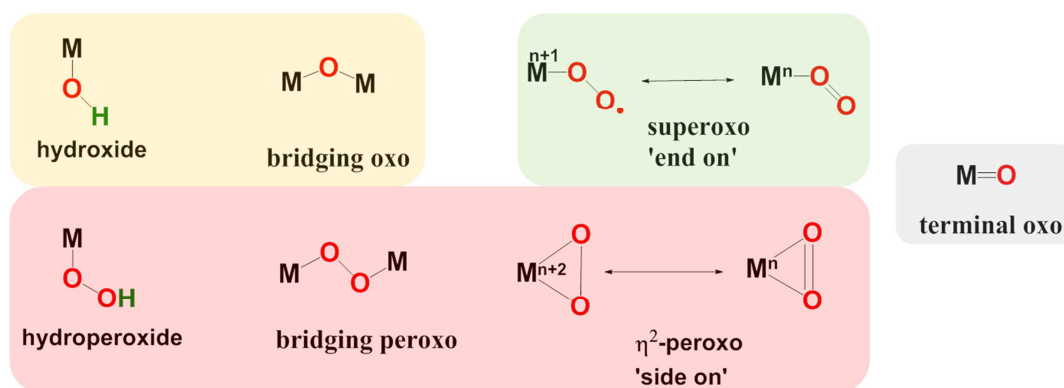


Figure 33 Coordination modes for Metal-Oxygen species.

However, reports of late transition metals bearing M—O fragments still remain scarce when compared to early transition metal compounds with M—O bonds. This can be explained by the fact that oxygen atoms are hard Lewis bases while late transition metals are soft Lewis acids.¹⁶⁶ In the case of early transition metals, M—O bonds are stabilised by the delocalisation of oxygen lone pairs into the vacant *d* orbitals of the metal (π – donation).¹⁶⁷ However, with the increase of electron count and electronegativity of the metal centre, the stabilisation of the M—O bond through oxygen-to-metal π -donation decreases because of the repulsion between the oxygen lone pairs and the filled metal *d* orbitals. This causes the stability of the M—O bond to decrease and its reactivity to increase as one moves from left to right across the transition metals in the periodic table.

This effect is even better reflected in the case of terminal metal oxo M=O complexes which are thought to be stabilised at metal centres with no more than four *d* electrons.¹⁶⁷ In this respect, while early transition metal oxo complexes are a common occurrence and quite unreactive, late transition metals are behind the ‘oxo wall’ (group 8 elements) and terminal M=O bonds are usually thought to be too unstable to exist. In 2008, Milstein *et al.* reported a (P[^]C[^]N) stabilised Pt(IV)O species (*d*⁶) characterised by spectroscopic methods in solution at low temperature.¹⁶⁸ By contrast, earlier claims of room temperature stable polyoxometallate stabilised *d*⁸ metal oxo species such as Pd=O, Pt=O and Au=O have recently been retracted.¹⁶⁹ Nevertheless, in the case of gold, Au=O species have been

proposed as intermediates in a variety of gold-mediated organic transformations such as oxidative C—C couplings¹⁰¹ or olefin epoxidations.^{68,170}

Even though there are no reports of terminal Au=O complexes, oxo complexes containing singly or doubly-bridging oxygen ligands have been isolated^{64,65} and their ability to oxidise olefins has been tested.^{67,68} (See Introduction to Chapter 1)

Perhaps the most important reaction that is proposed to involve intermediates with Au-O-Au, Au—O—O—Au or Au—O—O linkages is the low temperature oxidation of CO mediated by gold nanoclusters. Since the first report in 1987 by Haruta *et al.*,¹⁷¹ the research in gold mediated oxidation catalysis using molecular oxygen as an oxidant has grown dramatically.^{98a,172} The activity of the gold nanoclusters is thought to be dependent on multiple factors, such as the support deposition method, the size of the nanoparticles (See also Section 2.5), cluster charge and other factors.^{15,152,173}

While ¹⁸O/¹⁶O isotope labelling studies recently showed that specific gold nanoparticles-support interactions play an important role in O₂ activation,¹⁷⁴ the mechanism of oxygen activation on the gold surface still remains unclear. Since Au—O bonds are considered to be intrinsically unstable,¹⁷⁵ the absorption of dioxygen on gold surfaces is thought to be limited.¹⁷⁵ Effort to construct catalytic cycles for the oxidation of CO on gold surfaces have led to the proposition that in the case of O₂ activation by negatively charged gold clusters, O₂ absorption can be enhanced by electron transfer from gold to the π^* orbital of O₂, thus weakening the O—O bond and leading to surface bound superoxo-bound species.^{149b,176} This mode of activation has been supported by vibrational spectroscopy; while free O₂ displays a stretching frequency of 1556 cm⁻¹, the formation of a superoxo species is characterised by a lowering of the frequency to 1074 cm⁻¹ (for a superoxo species O₂⁻). Some reports also postulate the formation of bridging peroxo species as alternative modes for activating O₂ in larger clusters (n = 4, 5), as postulated by a computational study.^{176b} (Figure 34, right)

The bound activated oxygen species are then susceptible to nucleophilic attack by a CO molecule leading to a bound carbonate species which upon reaction with an extra CO molecule releases two equivalents of CO₂ and regenerates the Au₂⁻ fragment. (Figure 34, left) The steps of this mechanism have been addressed computationally and spectroscopically.^{176a} A similar mode of activation was proposed by neutral gold clusters where a charge transfer from the central metal induces a positive charge on the gold centre which binds a superoxo fragment.¹⁷⁷ A cooperation between positively charged (Au⁺ and Au³⁺) and neutral gold nanoparticles is also supported by X-ray absorption studies.^{151,173b,178}

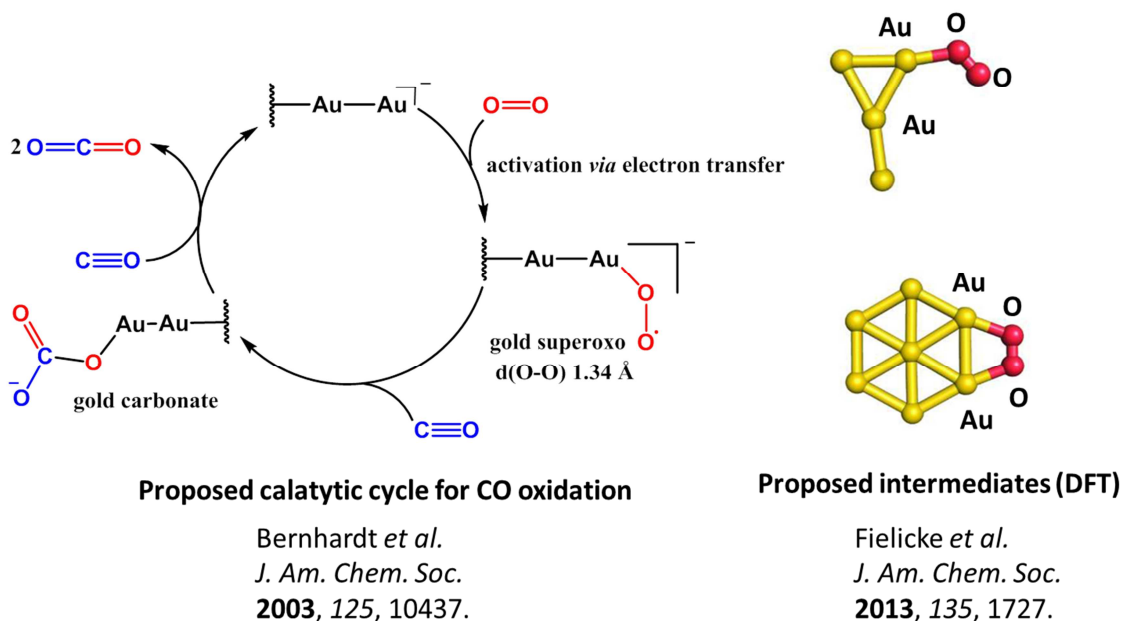


Figure 34. Proposed mechanism for the O₂ mediated CO oxidation by gold nanoparticles. (left)^{176a} Computational models of the active species involved in gold nanoparticles oxidation catalysis. (right) (reproduced from ref 177)

The presence and interconversion of surface bound peroxides, superoxides and oxides on gold nanoclusters have been invoked in a number of other important oxidation reactions such as propene oxidation,¹⁷⁹ alcohol oxidation^{152,180} and water splitting.¹⁸¹

Since the interaction between molecular oxygen and gold nanoparticles is difficult to investigate using the available techniques, the synthesis of molecular models of the key surface species is highly desirable. However, to the best of our knowledge, isolable gold species with Au—OOH, Au—OO or Au—O—O—Au linkages are unknown.

We have shown that despite the intrinsic instability of the Au—O bond, gold(III) hydroxides supported by tridentate pincer ligands such as diphenylpyridine can be synthesised and are in fact useful synthons for the preparation of gold(III) aryl and N-heterocyclic complexes (Chapter 1). We have also shown that employing the (C[^]N[^]C)AuOH **3** as a starting material, we can access gold(III) hydrides, a type of compounds which was long thought to be thermally unstable (Chapter 2). The present chapter presents the synthesis, characterisation and reactivity of the first reported gold peroxides. Our investigation on the oxygen transfer reactions involving gold peroxides revealed that even gold(III) hydroxides can undergo oxygen transfer reactions yielding gold(III) hydrides. Various mechanistic aspects of the chemistry of these species have also been explored by spectroscopic and computational methods.

Towards the end of the chapter we also report our investigations in the ability of gold(I) and gold(III) hydrides to activate oxygen which lead to the isolation of a NHC supported bridging gold(I) ($\mu\text{-}\kappa^1:\kappa^1$) peroxide. Our interest was fuelled by the fact that the O₂ activation by an oxophilic metal such as gold would make the resulting peroxo complexes efficient oxygen transfer catalysts. Since molecular oxygen is inexpensive, environmentally friendly and abundant, it is in many ways regarded as an ideal oxidant, especially on an industrial level. However, often the reactivity of oxygen is difficult to control leading to overoxidation or low selectivity.^{182c} In this respect, selectivity could be achieved by the activation of dioxygen by transition metal complexes to give transition metal peroxides and subsequent oxygen atom transfer to various substrates.

The interest in *d*-block elements mediated oxidation employing molecular oxygen as a sole oxidant is illustrated by the development of different catalytic systems where the oxygen insertion into a M—H bond (typically Pd^{II} or Ru) is a key step.^{164,182c} For a number of *d*⁶ and *d*⁸ elements, the M—H \rightarrow M—OOH transformation has been studied by spectroscopic^{182,183} and computational methods.¹⁸⁴

RESULTS AND DISCUSSION

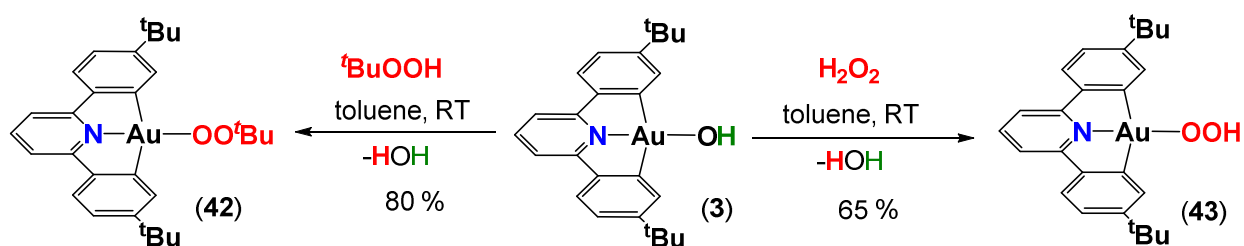
3.1. Synthesis and characterisation of the first isolated Gold peroxides

In Section 1.1 it was shown that the cyclometallated gold(III) hydroxide (C^NC)Au(OH) **3** can react with weak acids such as acetylenes, arylboronic acids (phenylboronic acid pK_a 8.83)¹⁸⁵ or N-heterocycles to give the corresponding Au—C or Au—N complexes. Since hydrogen peroxide (pK_a 11.75)¹⁸⁶ and *tert*-butyl peroxide (pK_a 12.25)¹⁸⁶ can also act as weak acids, we envisaged that the gold(III) hydroxide **3** would be a good synthon for these species.

Treatment of toluene solutions of **3** with a slight excess (1.4 eq) of *tert*-butyl hydroperoxide in toluene at room temperature resulted in water elimination and formation of the corresponding gold(III) *tert*-butyl peroxide (C^NC)Au(OO^tBu) **42** which was isolated as a yellow crystalline solid. (Scheme 23) The identity of the complex was confirmed by ¹H NMR spectroscopy where a characteristic singlet for the ^tBu group of the gold peroxo moiety (δ_H 1.40, CD₂Cl₂) could be observed. The value of the chemical shift is *ca.* 0.2 ppm downfield from the resonance of the ^tBu group in the *tert*-butyl hydroperoxide starting material (δ_H 1.22, CD₂Cl₂).

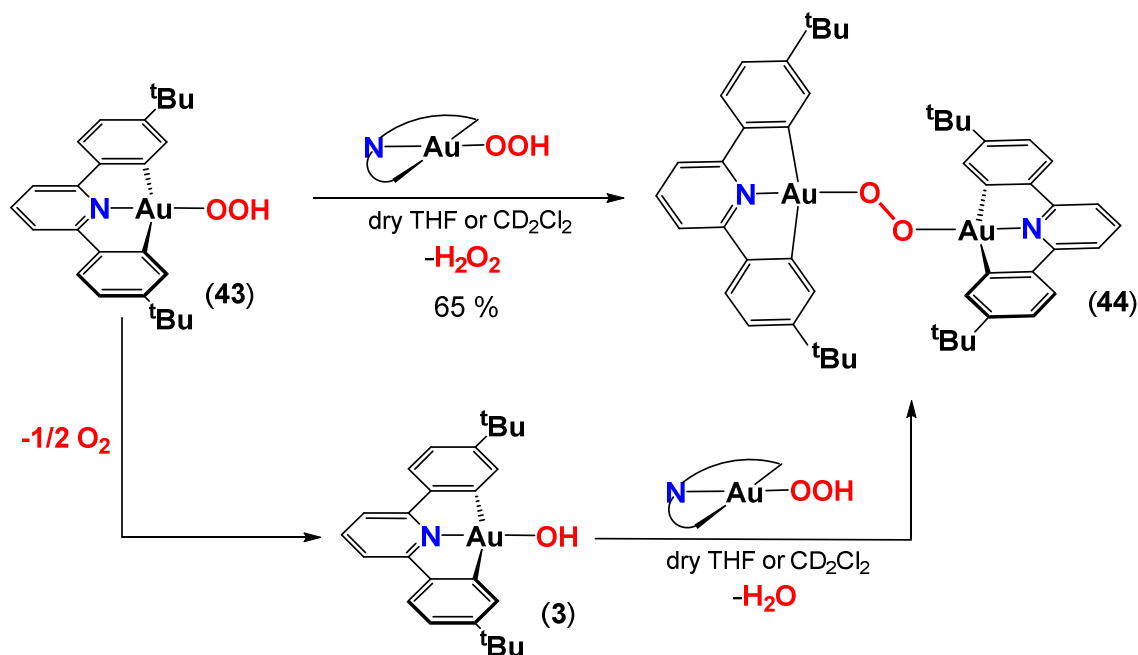
Very recently, Nolan *et al.* reported the isolation of the NHC supported gold(I) *tert*-butyl peroxide, (IPr)Au^I(OO^tBu), made by the same method.¹⁸⁷ Here the chemical shift for the ^tBu group was observed *ca.* 0.3 ppm *upfield* of free *t*-butyl hydroperoxide (δ_{H} 0.87 vs. 1.22, CD₂Cl₂).

An analogous reaction of solution of **3** in toluene with an excess of 30% aqueous hydrogen peroxide rapidly gave rise to the formation of a (C[^]N[^]C)Au(OOH) **43** as a yellow precipitate (Scheme 23) which was washed with toluene and acetonitrile in order to remove trace amounts of the starting materials. The ¹H NMR spectra of **3** and **43** are very similar, with the notable exception that fresh samples of **43** display a broad resonance at δ_{H} 8.26 (CD₂Cl₂) which is absent in the case of (C[^]N[^]C)Au(OH) **3**. The resonance, which disappears upon addition of D₂O, was assigned to the OOH group of the (C[^]N[^]C)Au(OOH) **43**. A δ_{H} resonance for the starting gold(III) hydroxide (C[^]N[^]C)Au(OH) **4** could not be located by ¹H NMR spectroscopy. (See Section 1.1) The chemical shift of the peroxo moiety in other *d*⁸ metal hydroperoxides range from 4.43 ppm in *trans*-(PPh₂Me)₂Pt(Ph)(OOH)¹⁸⁸ to 8.93 ppm in (Tp)(PPh₃)Pd(OOH) (Tp = hydrotris(pyrazolyl)borate).¹⁸⁹



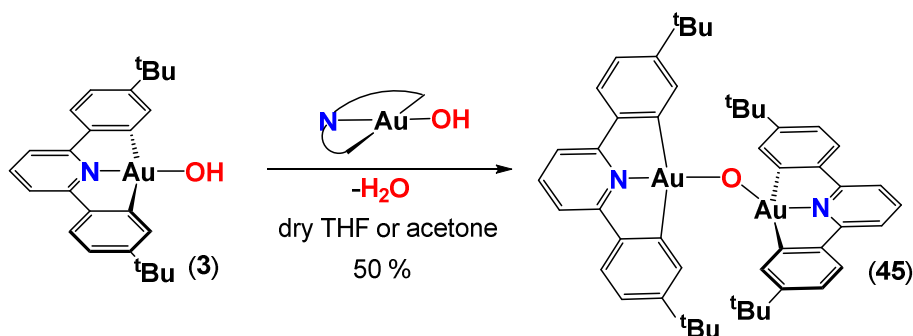
Scheme 23 Synthesis of the alkylperoxo **42** and hydroperoxo **43** gold(III) complexes

Storing the hydroperoxide **43** in dry CD₂Cl₂ or THF produces yellow crystalline blocks identified as the bridging (μ - κ^1 : κ^1) peroxide (C[^]N[^]C)Au—OO—Au(C[^]N[^]C) **44**, which is produced by a condensation reaction. Since late transition metal hydroperoxides commonly undergo disproportionation to give the corresponding hydroxides and molecular oxygen,¹⁸² we can envisage two possible pathways for the condensation reaction to yield **44**: *i*) the reaction between two molecules of hydroperoxide **43** to give **44** and hydrogen peroxide or *ii*) disproportionation of **43** into O₂ and the gold(III) hydroxide (C[^]N[^]C)AuOH **3** which reacts with the starting hydroperoxide **43** to give water and **44**. (Scheme 24) The condensation reaction is however reversible and storing **44** in water-saturated CD₂Cl₂ solutions regenerates **43** and **3** as indicated by ¹H NMR spectroscopy.



Scheme 24 Possible hydroperoxide condensation pathways to give **44**

A similar condensation reaction takes place when the hydroxide **3** is stored in dry acetone or THF where the bridging oxide ($\text{C}^{\wedge}\text{N}^{\wedge}\text{C}$)Au-O-Au($\text{C}^{\wedge}\text{N}^{\wedge}\text{C}$) **45** precipitates. (Scheme 25) The reaction is reversible, and storing the oxide **45** in water-saturated CH_2Cl_2 solution regenerates the hydroxide **3**.



Scheme 25. Hydroxide condensation reaction to give **45**

Compounds **44** and **45** were characterised by NMR spectroscopy. The ^1H NMR spectrum for both digold species showed a single set of resonances for the symmetrically bound pincer ligand, suggesting that both ($\text{C}^{\wedge}\text{N}^{\wedge}\text{C}$) fragments are equivalent in solution. The proton attached to the carbon atom in the β -position with respect to the gold centre exhibits a significant downfield shift (δ_{H} 8.23 in **44** and 8.32 in **45**) compared to **3** (δ_{H} 7.62, red highlight in Figure 35). A similar effect is observed for the *tert*-butyl groups which exhibit an upfield shift in the dinuclear species (δ_{H} 1.14 in **44** and 1.08 in **45**) compared to **3**

(δ_{H} 1.37). The same characteristic pattern for digold species is also observed for the dimeric gold(II) complex $(\text{C}^{\wedge}\text{N}^{\wedge}\text{C})\text{Au}-\text{Au}(\text{C}^{\wedge}\text{N}^{\wedge}\text{C})$ **37**. (See Section 2.3)

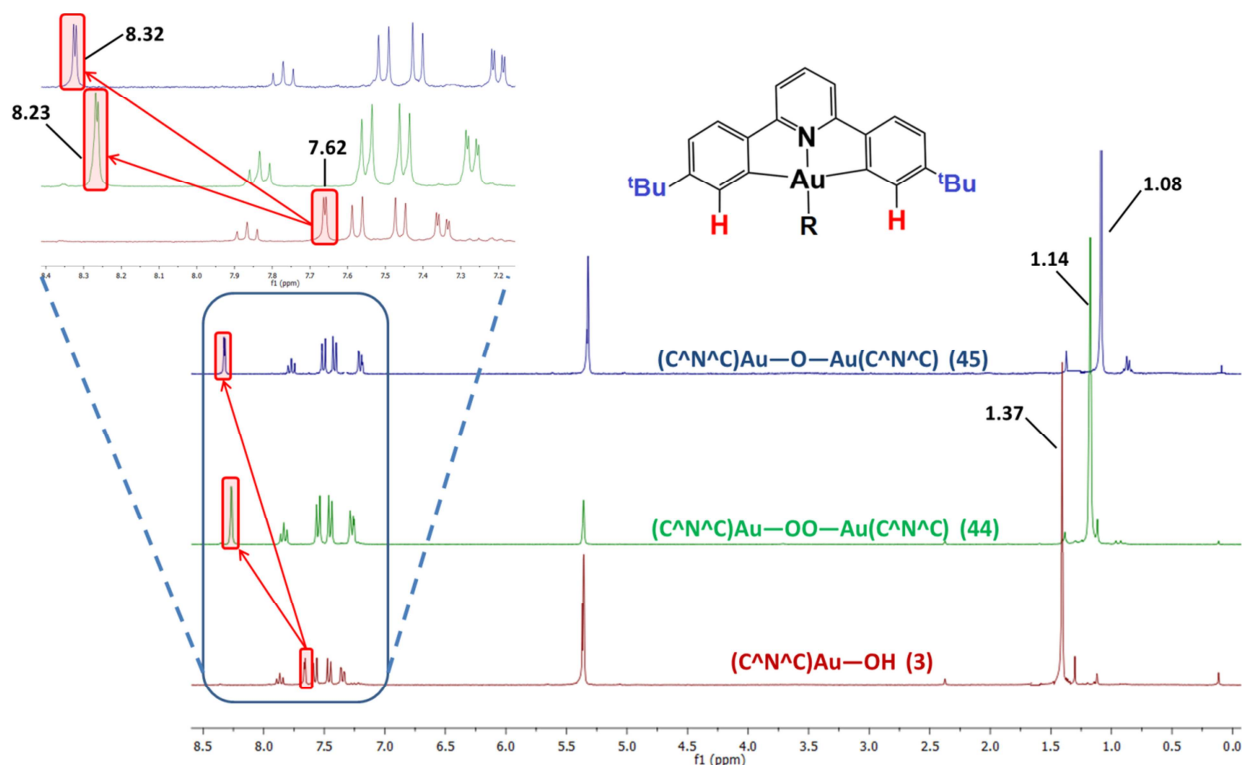
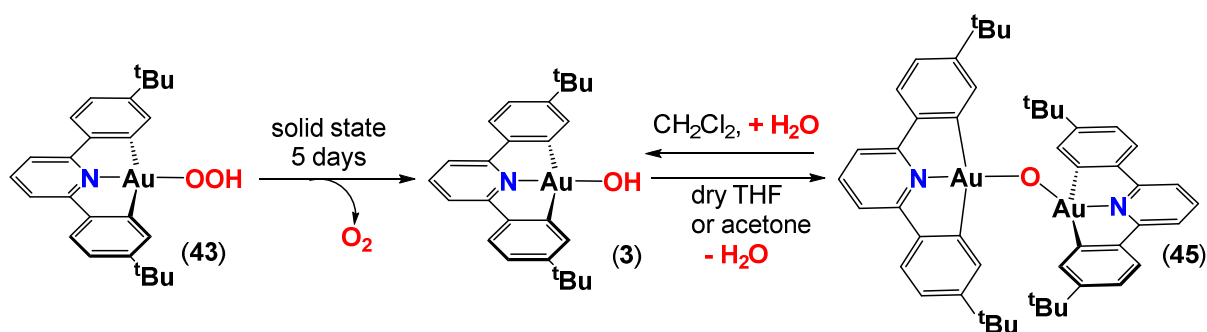


Figure 35. ^1H NMR spectra (300 MHz, CD_2Cl_2 , RT) of $(\text{C}^{\wedge}\text{N}^{\wedge}\text{C})\text{AuOH}$ **3** (red), $[(\text{C}^{\wedge}\text{N}^{\wedge}\text{C})\text{Au}]_2(\mu\text{-OO})$ (green) and $[(\text{C}^{\wedge}\text{N}^{\wedge}\text{C})\text{Au}]_2(\mu\text{-O})$ (blue)

The *tert*-butylperoxide **42** readily dissolves in polar solvents (THF, CH_2Cl_2) and aromatic hydrocarbons (toluene, benzene) and is poorly soluble in light petroleum. The hydroperoxide **43** and the digold species **44** and **45** are on the other hand only poorly soluble in aromatic hydrocarbons, which facilitates their purification from the starting gold hydroxide $(\text{C}^{\wedge}\text{N}^{\wedge}\text{C})\text{AuOH}$ **3**.

The *tert*-butylperoxide **42** and the bridging peroxide **44** show remarkable thermal stability – heating THF solution of **42** and **44** at 60 °C for 16 h leaves the compounds unchanged as verified by ^1H NMR spectroscopy. Similar stability is also observed towards ambient laboratory lighting with solid samples of **42** and **44** showing no obvious signs of decomposition.

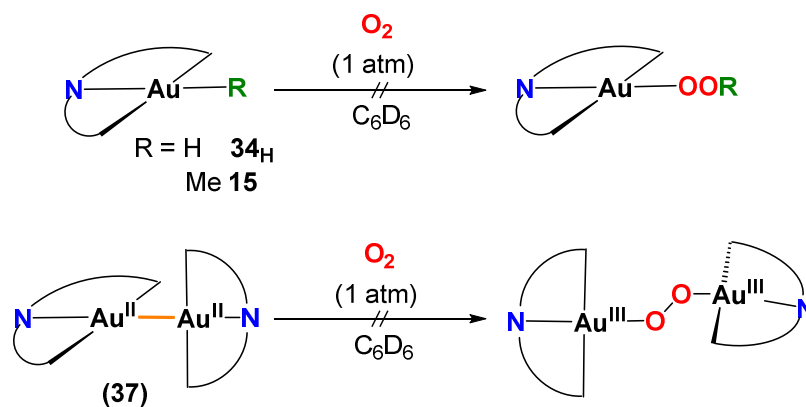
The hydroperoxide **43** shows only moderate stability both in solid state and in solution. Storing solid samples of **43** for 5 days at room temperature followed by dissolution in dry acetone or THF produces the bridging oxide **45** as the only identified complex by ^1H NMR spectroscopy, suggesting that **43** readily undergoes disproportionation to give **3** which condenses to the bridging oxide **45**. (Scheme 26)



Scheme 26 Disproportionation of **43** followed by condensation to give **45**

Direct O₂ insertions into metal-hydrogen,^{182a,b;183} metal-carbon^{165,190} or metal-metal¹⁴⁴ bonds are well established pathways for the synthesis of transition metal peroxides. Activation of molecular oxygen by late transition metals is particularly appealing because their low oxophilicity makes them reactive towards O-transfer to substrates like olefins.¹⁶⁹ The resulting peroxo complexes would be key intermediates in transition metal catalysed oxygenation reactions using molecular oxygen as an sole oxidant.^{182c} (See also section 3.5).

There are numerous examples of O₂ insertion reactions of Pt(II) and Pd(II) complexes.^{182c} By contrast, no reaction was observed between (C^{^N^C})AuH **34_H**, (C^{^N^C})AuMe **15** and (C^{^N^C})Au—Au(C^{^N^C}) **37** and molecular oxygen (1 atm), and the gold complexes could be recovered unchanged. (Scheme 27) While in the case of **34_H**, the resistance of the O₂ insertion into the Au—H bond may be a reflection of the high BDE of Au—H, (317 kJ mol⁻¹, see Table 8), computational studies suggest that O₂ insertion into the Au—Au bond is thermodynamically favourable ($\Delta H = -136$ kJ mol⁻¹).¹³⁰ It is likely that the kinetic shielding of the *tert*-butyl groups of the (C^{^N^C}) supporting ligand is responsible for this lack of reactivity.



Scheme 27 Attempted O₂ insertion reactions into the Au—H, Au—C and Au—Au bonds

IR Spectroscopy

Since the O—O stretching vibration is of interest in the study of O₂ activation by gold nanoclusters, (See Introduction to the Chapter) the gold peroxides **42** – **44** have been characterised by IR (ATR) spectroscopy. The results are summarised in Table 12. The IR spectrum of the hydroperoxide **43** is very similar to that of the hydroxide **3**, but shows an additional medium intensity band at 825 cm⁻¹. The *tert*-butylperoxo complex **42** and the (μ-κ¹:κ¹-peroxo)digold complex **44** show three weak vibration modes in the O—O stretching region (Table 12, entries 1 and 3). The observed values are similar to the O—O stretching vibrations reported for the carbene supported gold(I) alkyl peroxides,¹⁸⁷ palladium(II)¹⁸⁹ and platinum(II)¹⁸⁸ peroxo complexes and to the vibration modes reported for hydrogen peroxide.¹⁹¹ A recent study on gold nanocluster catalysis reported by Yeo *et al.*¹⁹² also assigned a Raman band at 820 cm⁻¹ to surface-bound OOH species (Table 12, entry 8) which is in excellent agreement to the band we tentatively assigned to the O—O stretch in (C[^]N[^]C)Au(OOH) **43**.

Table 12. Selected O—O IR stretching frequencies in Au, Pt and Pd peroxo compounds

No.	Complex	$\nu_{\text{O-O}}$ (cm ⁻¹)	Reference
1	(C [^] N [^] C)Au(OO ^t Bu) 42	831, 844, 878	This work
2	(C [^] N [^] C)Au(OOH) 43	825	This work
3	[(C [^] N [^] C)Au] ₂ (μ-OO) 44	823, 828, 844	This work
4	(IPr)Au(OO ^t Bu)	803	187
6	[(Tp)(Py)Pd] ₂ (μ-OO) ^a	838	189
7	<i>trans</i> -(PPh ₃)(Ph)Pt(OO ^t Bu)	890	188
8	Au(OOH) <i>nanocluster surface</i> ^a	820	192
9	H ₂ O ₂	866	191

^aRaman stretch

X-ray crystallography

The structures of complexes **42** — **45** have been confirmed by X-ray crystallography and relevant bond lengths and angles are summarised in Table 13. Compounds **42** — **44** represent the first gold peroxide complexes (in any oxidation state) to be characterised. The O—O bond distances in **42** and **44** (1.416(6) Å and 1.448(4) Å respectively) are within the typical range of distances recorded for transition metal peroxo complexes.^{182,183,187-190} The Au—N in complexes **42**, **44** and **45** vary from 1.985(4) Å (in **42**) to 2.001(4) Å (in **44**), and slightly shorter but comparable distances are found in other (C[^]N[^]C)Au-O compounds (1.974(3) Å in (C[^]N[^]C)AuOH **3** and 1.959(3) Å in (C[^]N[^]C)AuOAc^F **4**, Table 2).

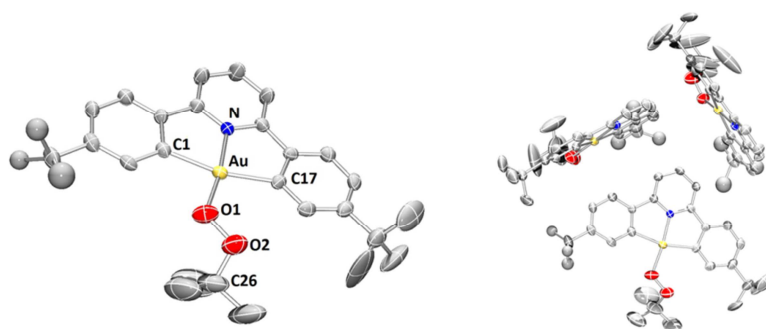


Figure 36. Molecular structure of $(C^N^C)Au(OO^tBu)$ **42**·0.3 CH_2Cl_2 (50% probability ellipsoids shown). Hydrogen atoms and solvent molecule omitted. (left) Depiction of the asymmetric unit of **42** showing the normal to the planes of the three $(C^N^C)Au$ fragments mutually perpendicular. (right) Disordered tBu groups which contain atoms which have less-than-complete occupancies were refined isotropically.

Crystals of **42**·0.3 CH_2Cl_2 were obtained by layering a dichloromethane solution of **42** with light petroleum at -20 °C. The complex crystallises as three independent molecules per asymmetric unit with slight variations in the Au—O—O—C torsion angles at $-119.8(6)^\circ$, $115.1(6)^\circ$ and $-129.3(4)^\circ$ in the three molecules. (Figure 36) The normal of the three $(C^N^C)Au$ planes are mutually approximately perpendicular. The arrangement is different from most complexes bearing a (C^N^C) fragment where the stacking between the $(C^N^C)Au$ planes with a head-to-tail arrangement is usually preferred. The O—O bond length ($1.416(6)$ Å) appears to be significantly shorter than the ones in the recently reported gold(I) alkylperoxides $(IPr)Au(OO^tBu)$ and $(SIPr)Au(OO^tBu)$ ¹⁸⁷ ($1.496(16)$ Å and $1.51(2)$ Å, respectively) most probably due to the smaller size of the Au^{3+} centre compared to the Au^+ centre.

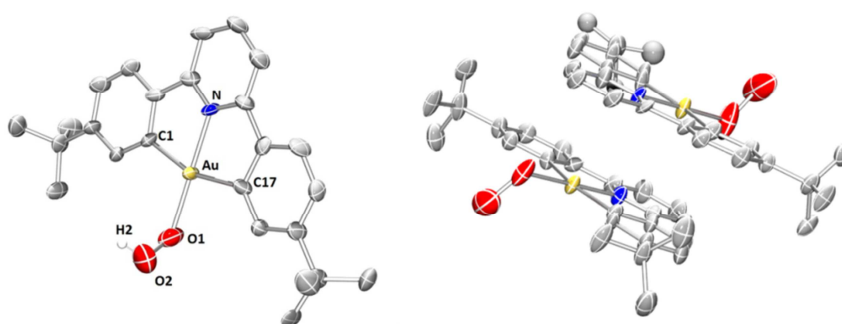


Figure 37. Molecular structure of $(C^N^C)Au(OOH)$ **43** (50% probability ellipsoids shown). Hydrogen atoms (with the exception of the OOH) are omitted. (left) Depiction of the asymmetric unit of **43** showing stacking between the $(C^N^C)Au$ fragments. All hydrogen atoms are omitted (right)

The hydroperoxide **43** was crystallised from dichloromethane solutions kept at -20 °C. Despite the modest quality of the crystals which suffered from possible twinning, unequivocal connectivity could be established. (Figure 37) The asymmetric unit consists of two molecules of **43** which are stacked in a head-to-tail fashion. The proton of the OOH moiety does not seem to be involved in hydrogen bonding. Repeated attempts to obtain better quality crystals of **43** resulted in the crystallisation of the bridging peroxide $(C^{\wedge}N^{\wedge}C)Au-OO-Au(C^{\wedge}N^{\wedge}C)$ **44**, as a result of the facile condensation reaction involving **43**. (See Scheme 27)

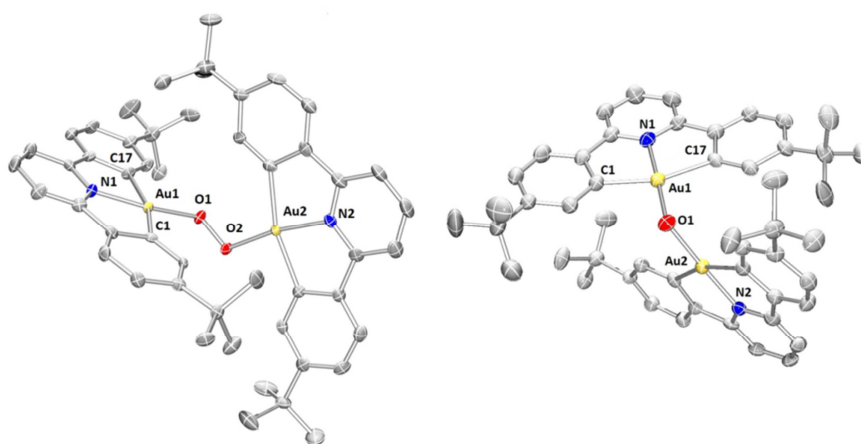


Figure 38 Molecular structure of the digold peroxide $[(C^{\wedge}N^{\wedge}C)Au]_2(\mu-OO)$ **44**·0.56 CH_2Cl_2 (left) and oxide $[(C^{\wedge}N^{\wedge}C)Au]_2(\mu-O)$ **45** (right) (50% probability ellipsoids shown). Hydrogen atoms and disordered solvent molecules are omitted

Crystals of the peroxide **44** were obtained from dry THF solution. (Figure 38, right) The O—O distance (1.448(4) Å) and the Au—O—O—Au torsion angle ($-102.2(2)^\circ$) are similar to the ones reported for H_2O_2 (1.49 Å and 120°).¹⁹³ There is no stacking of parallel $(C^{\wedge}N^{\wedge}C)Au$ fragments in the crystal.

The oxide **45** (Figure 38, left) has a bent structure with an Au—O—Au angle of $113.5(2)^\circ$, typical for an sp^3 hybridised oxygen atom. These results suggest negligible Au—O π interactions, a feature also confirmed by computational studies (*vide infra*). A similar value of the Au—O—Au angle ($121.2(2)^\circ$) was also reported by Cinellu *et al.*⁶⁴ for the cationic 6-benzyl-2,2'-bipyridine supported gold(III) bridging oxide $[(N^{\wedge}N^{\wedge}C)Au](\mu-O)]^{2+}$. For a general review on the influence of M—O π contribution on the M—O—M angles in transition metals, see ref.167

Table 13. Comparison of geometric parameters of gold(III) peroxide and oxide complexes

	(C ^N C)AuOO ^t Bu (42)	(C ^N C)AuOOH (43) ^a	[(C ^N C)AuO] ₂ (44)	[(C ^N C)Au] ₂ O (45)
Au1-O	1.983(4)	2.085(9)	1.975(3)	1.992(5)
Au2-O			1.977(3)	1.989(5)
N-Au	1.985(4)	2.052(8)	2.001(4)	1.993(6)
O1-O2	1.416(6)	1.555(18)	1.448(4)	
N-Au1-O	172.84(17)	178.8(4)	170.92(15)	177.2(2)
Au1-O1-O2	115.4(3)	111.9(8)	116.0(2)	
Au-O-Au				113.5(2)
Au1...Au2			4.204(4)	3.3301(4)

^a Crystals of **43** suffered from modest quality possible twinning.

Bonding in the gold peroxides: DFT insights (collaboration with Dr Joseph Wright)

The structures and bonding of complexes **3**, **42** - **45** was further investigated by computational modelling using density functional theory (DFT) methods. Optimisation of the gas phase geometries of compounds allowed calculation of Au—O and O—O bond energies (Table 14).

The Au—O bonds in the peroxides **42**—**44** (126 – 168 kJ mol⁻¹) are significantly weaker than for the gold(III) hydroxide **3** and oxide **45** (279 and 206 kJ mol⁻¹ respectively). For the peroxides **42** - **44**, the O—O bonds weaken with increasing electron donation of the substituents. (Table 14) A similar trend was found for the O-O bond strengths in the series H₂O₂ > MeOOH > MeOOME (204, 186 and 158 kJ mol⁻¹, respectively).¹⁹⁴

Table 14. Calculated Bond Energies (kJ mol⁻¹) of gold(III) peroxide and oxide complexes

Compound	3	42	43	44	45
Au-O	279	150	168	126	206
AuO-O	-	130	166	138	-

A consideration of the molecular orbitals shows that the HOMOs do not show a consistent Au—O bonding component, whilst the HOMO-1 orbitals show a variety of out-of-phase relationships between the oxygen lone pairs and the gold *d*-orbitals, *i.e.* the interactions are anti-bonding (Figure 39). This confirms the absence of π -interactions between the metal and the oxygen ligands that were already suggested by the acute Au-O-Au and Au-O-O angles in the solid state structures. (*vide supra*) This observation is in line with the fact that, in general, for late transition metals M—O complexes, oxygen *p*-electron delocalisation into

vacant *d* orbitals on the metal is disfavoured due to electron repulsion between the oxygen electrons and the filled metal *d* orbitals.¹⁶⁷

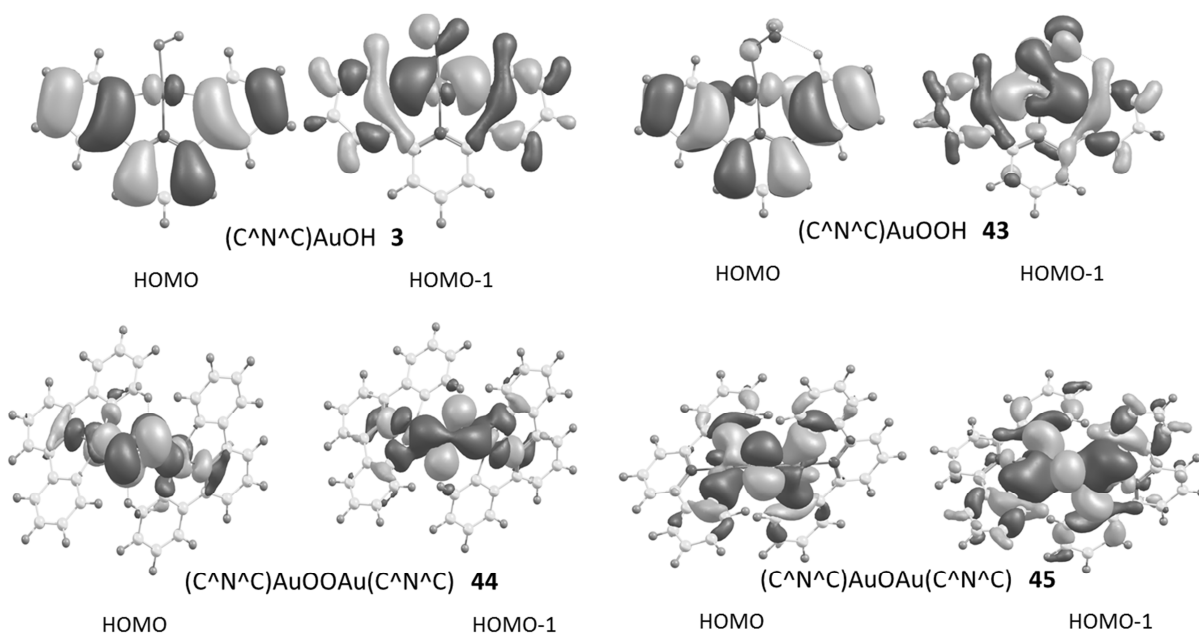


Figure 39. HOMO (left) and HOMO-1 (right) depictions of complexes **3**, **43** – **45**

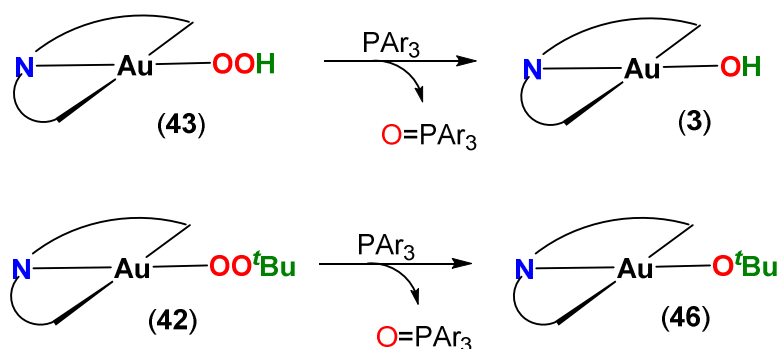
3.2 Reactivity of peroxides **42**—**45**: oxygen transfer reactions

Since the Au—O and O—O bonds are relatively weak in the peroxides **42**—**44**, we envisaged they would efficiently transfer an oxygen atom to an oxidisable substrate such as phosphines. In this respect, the reactivity of compounds **42** – **45** towards $P(p\text{-tolyl})_3$ as reductant was tested. Treating the hydroperoxide **43** with the phosphine (0.8 equivalents)¹⁹⁵ in CD_2Cl_2 solutions instantly led to the disappearance of the peroxo OOH resonance (δ 8.26) and formation of $O=P(p\text{-tolyl})_3$ alongside the hydroxide **3**, as observed by 1H NMR spectroscopy. (Scheme 28) The oxygen transfer was also confirmed by $^{31}P\{^1H\}$ NMR spectroscopy where reaction with **43** led to a shift from δ_p -8.1 (for $P(p\text{-tolyl})_3$) to δ_p 30.5 (for $O=P(p\text{-tolyl})_3$).

Similarly, treatment of the *tert*-butylperoxide **2** with one equivalent of phosphine led to the formation of the phosphine oxide together with $(C^{\wedge}N^{\wedge}C)AuO^tBu$ (**46**). The reaction was found to be much slower than in the case of **43** and full conversion was reached only after 16 h. The conversion could be monitored by the disappearance of the singlet signal characteristic for the *tert*-butyl group of the OO^tBu group in $(C^{\wedge}N^{\wedge}C)AuOO^tBu$ **42** (δ_H 1.40,

CD₂Cl₂) concomitant with the appearance of a new singlet signal for the O^tBu group in (C[^]N[^]C)AuO^tBu **46** (δ_{H} 1.49, CD₂Cl₂).

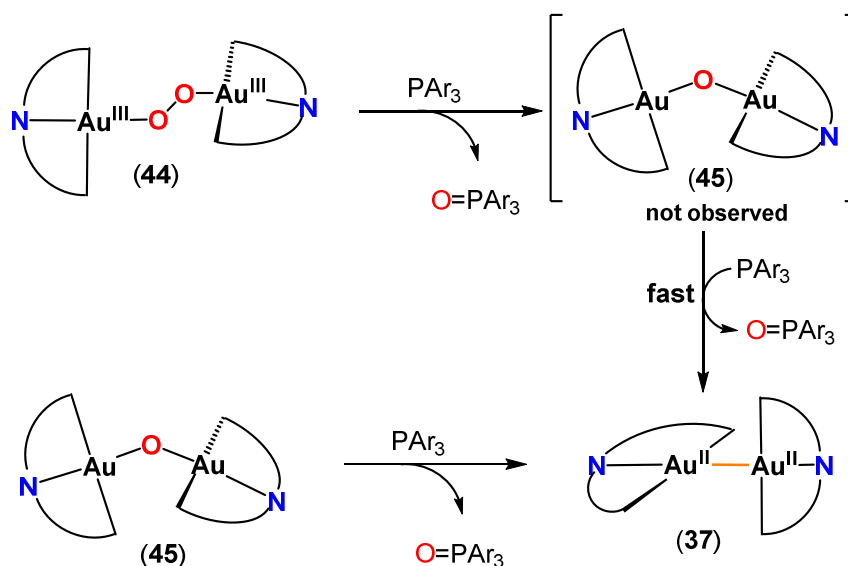
The identity of **46** was also confirmed by its independent synthesis which involved the reaction between the trifluoroacetato (C[^]N[^]C)Au(OAc^F) **4** and potassium *tert*-butoxide in ^tBuOH : toluene mixtures. (See Experimental, Chapter 5) The protocol is analogous to the one used for the methoxide derivative (C[^]N[^]C)Au(OMe) **5**. (See Section 1.1)



Scheme 28 Oxygen transfer reactions involving **42** and **43**

The (μ - κ^1 : κ^1 -peroxo)digold complex **44** in CD₂Cl₂ oxidises P(*p*-tolyl)₃ more slowly, with quantitative formation of O=P(*p*-tolyl)₃ after 36 h. (Scheme 29) After 16 h the reaction mixture showed a number of gold products, including **44** (21%), (C[^]N[^]C)AuCl **2** (17%), and the gold(II) dimer (C[^]N[^]C)Au—Au(C[^]N[^]C) (**37**) (25%), as well as other unidentified products. Interestingly, the peroxide **44** and the gold(II) dimer **37** co-exist in solution, *i.e.* the peroxide is evidently unable to oxidise the Au^{II} compound to the Au^{III} oxide.

We assume that the reaction of **44** with phosphines proceeds by stepwise O-abstraction, to give first the oxide **45**. However, monitoring the reaction by ¹H NMR spectroscopy failed to show traces of **45**, which suggests that the second reduction step to gold(II) is fast. This was confirmed independently by treating **45** with P(*p*-tolyl)₃ which cleanly gives **37** and phosphine oxide. (Scheme 29)

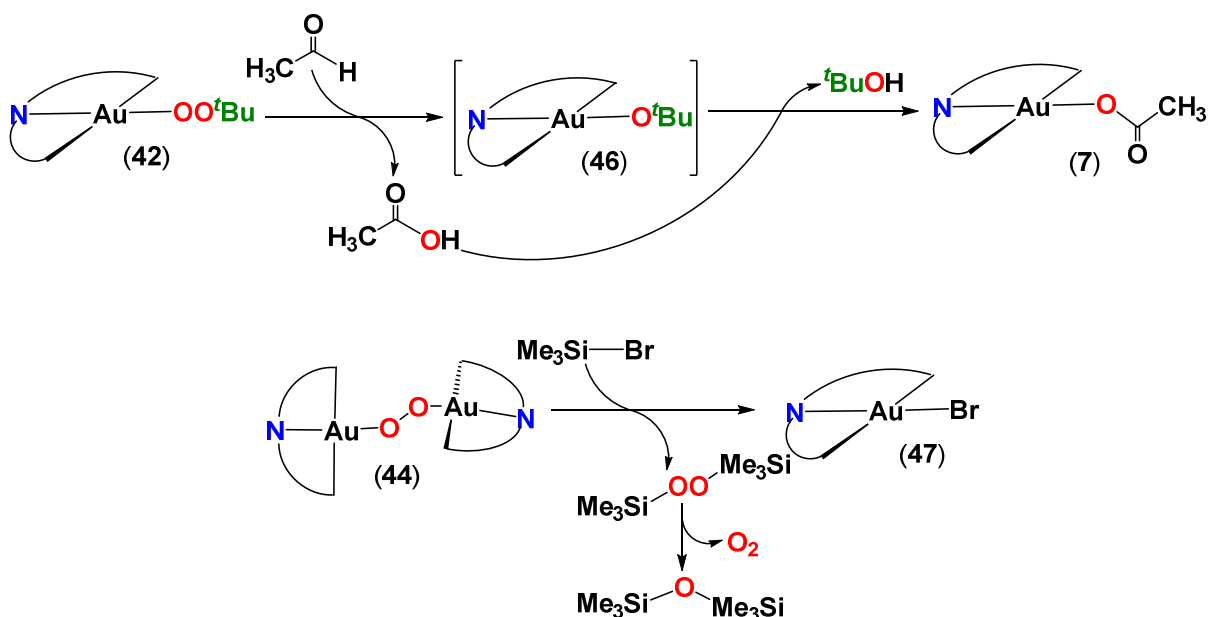


Scheme 29 Oxygen transfer reactions involving **44** and **45**

The *tert*-butylperoxide **42** in C_6D_6 at 60°C also oxidises acetaldehyde, giving initially acetic acid and $(\text{C}^{\wedge}\text{N}^{\wedge}\text{C})\text{AuO}^t\text{Bu}$ (**46**). Subsequently protolysis led to the isolation of $(\text{C}^{\wedge}\text{N}^{\wedge}\text{C})\text{AuOAc}$ **7**, the identity of which was confirmed by its independent synthesis (see Section 1.1). (Scheme 30)

The reactivity of gold peroxides **42** and **44** was also tested olefins like 1-hexene or towards vinyl ethyl ether with the aim to obtain the corresponding epoxide or ethyl acetate respectively. Despite varying the reaction conditions (reaction time, solvent, temperature) no reactivity was observed and the starting materials could be recovered unchanged. The reactivity of **42**—**44** towards alkenes is reminiscent of the one of the $\text{Pt}^{188,196}$ and $\text{Pd}^{189,197}$ peroxides with the peroxo fragment *trans* to a group which exerts a weak trans influence.

Peroxide ligands are readily cleaved by electrophiles; *e.g.* **44** reacts instantly with Me_3SiBr to produce the $(\text{C}^{\wedge}\text{N}^{\wedge}\text{C})\text{AuBr}$ **47** along with $\text{Me}_3\text{SiOOSiMe}_3$ (65 %) and $\text{Me}_3\text{SiOSiMe}_3$ (25 %) as confirmed by ^1H NMR spectroscopy. (Scheme 30) The presence of the oxide $\text{Me}_3\text{SiOSiMe}_3$ is probably due to the disproportionation of the peroxide $\text{Me}_3\text{SiOOSiMe}_3$ in the presence of Me_3SiBr . This was also observed by others.¹⁴⁵

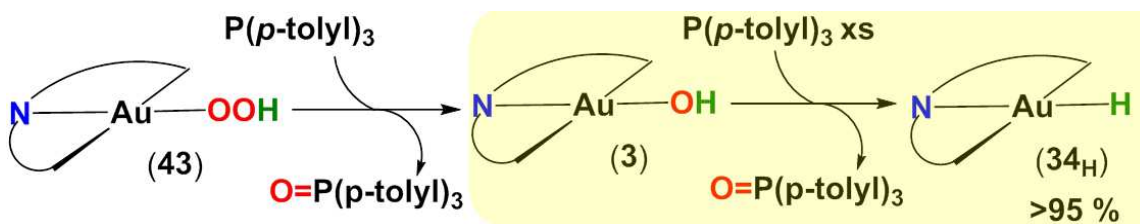


Scheme 30 Oxidation of acetaldehyde by **42** followed by electrophilic attack to give **7** (top) and electrophilic attack on **44** to give **47** (bottom).

3.3 Au—OH to Au—H conversion

Upon our initial investigation of the oxygen transfer ability of peroxides **42—44**, we carried out the reduction of the hydroperoxide **43** with an excess of phosphine (>2 eq). We could establish by ^1H NMR spectroscopy (CD_2Cl_2) that after 3 minutes, the reaction mixture was found to contain no trace of the expected gold hydroxide ($\text{C}^{\wedge}\text{N}^{\wedge}\text{C}$)AuOH **3**. Instead the composition suggested a mixture between the gold(II) dimer ($\text{C}^{\wedge}\text{N}^{\wedge}\text{C}$)Au—Au($\text{C}^{\wedge}\text{N}^{\wedge}\text{C}$) **37** and the gold hydride ($\text{C}^{\wedge}\text{N}^{\wedge}\text{C}$)AuH **34_H** in a ratio of 3:1. The latter was identified by its high-field chemical shift. (δ_{H} -6.5 in CD_2Cl_2). The same outcome was observed when ($\text{C}^{\wedge}\text{N}^{\wedge}\text{C}$)AuOH **3** was reacted with an excess of phosphine.

We have found that the selectivity of the reaction towards the formation of the gold hydride **34_H** could be increased to 95% by (i) exchanging the polar CH_2Cl_2 reaction solvent for a less polar solvent (toluene) (ii) lowering the reaction temperature to $-10\text{ }^\circ\text{C}$ or below, and (iii) using a larger excess of phosphine (> 5eq). High selectivity was also achieved at room temperature but a larger excess of phosphine (>30 eq) was necessary. (Scheme 31)



Scheme 31 Oxygen transfer reactions linking Au—OOH to Au—H (reaction carried in toluene)

The formation of metal hydrides from oxygen-bound ligands is known. For example, in palladium methoxides β -H elimination of formaldehyde leads to Pd-H species,¹⁹⁸ while in rhenium hydroxides, the isomerisation of a hydroxide into a metal oxo-hydride product, as in the conversion of $(\text{C}_2\text{Et}_2)_3\text{ReOH}$ into $(\text{C}_2\text{Et}_2)_3\text{Re}(\text{H})(\text{O})$ was observed.¹⁹⁹ Other examples also include generation of palladium(II) hydrides from metal hydroxides or alkoxides by reaction with dihydrogen.²⁰⁰

The simple transformation of a metal hydroxide to a metal hydride presents interest as a potential key step in a water splitting cycle. Traditionally, metal mediated water splitting catalytic cycles were based on the metal ability to readily change its oxidation states.²⁰¹ In this case, the formation of a metal hydrido hydroxide $\text{M}(\text{H})(\text{OH})$ is a key step, as realised by Milstein *et al.* using ruthenium pincer complexes [$\text{M} = (\text{PNN})\text{Ru}$; $\text{PNN} = 2,6\text{-C}_5\text{H}_3\text{N}(\text{CH}_2\text{P}^t\text{Bu}_2)(\text{CH}_2\text{NEt}_2)$] (Figure 40).²⁰²

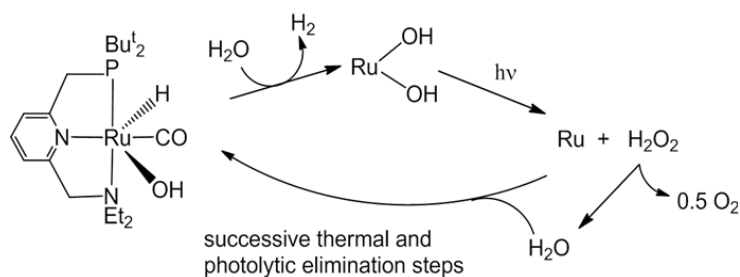


Figure 40 Redox mechanism for water cleavage.²⁰²

On the other hand, an alternative and potentially simpler pathway is available that does not require changes in oxidation states. This cycle involves the reaction of a metal cation with water to give a metal hydroxide. The following key step implies the conversion of the metal hydroxide into a metal hydride which, in the subsequent protonation step regenerates the metal cation and releases hydrogen. (Figure 41)

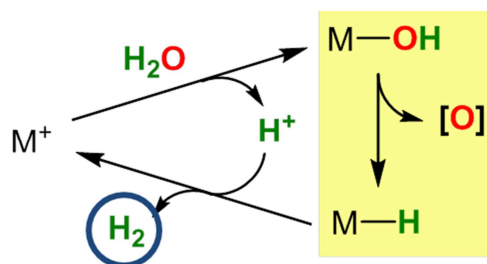


Figure 41. Non-oxidative cycle for water splitting

However, to the best of our knowledge, the report of a transformation of a metal hydroxide $M-OH$ to a metal hydride $M-H$ *via* simple oxygen atom transfer reactions has not been previously observed for any metal. This can be explained by the fact that for most metals the hydroxides are thermodynamically more stable than the hydrides, so that the $M-OH \rightarrow M-H$ transformation is not usually possible without an external hydride donor.

On the other hand, for gold, a $Au-OH \rightarrow AuH$ transformation can be envisaged since the gold centre (*i*) has a high electronegativity which is actually comparable to that of carbon and hydrogen, and (*ii*) is capable of forming highly covalent $Au-H$ and less stable $Au-O$ bonds.

Kinetic Studies

To gain more insight on the phosphine mediated $Au-OH \rightarrow AuH$ transformation, we have used kinetic studies in order to gain more insight in the reaction mechanism. The kinetic data were obtained by 1H NMR spectroscopy. In order to suppress the formation of the Au^{II} by-product $[(C^N^C)Au]_2$ **37**, the studies were conducted at low temperature (-10 to -55 °C). The conversion was followed under pseudo-first order conditions. It was convenient to monitor the disappearance of the signal corresponding to the proton attached to the β -carbon atom with respect to the gold centre in the hydroxide $(C^N^C)Au(OH)$ **3** (δ_H 8.13, see Figure 42 and 43, red highlight) and the increase of the signal corresponding to the analogous proton resonance in the hydride $(C^N^C)AuH$ **34_H** (δ_H 8.40, Figure 42 and 43, blue highlight).

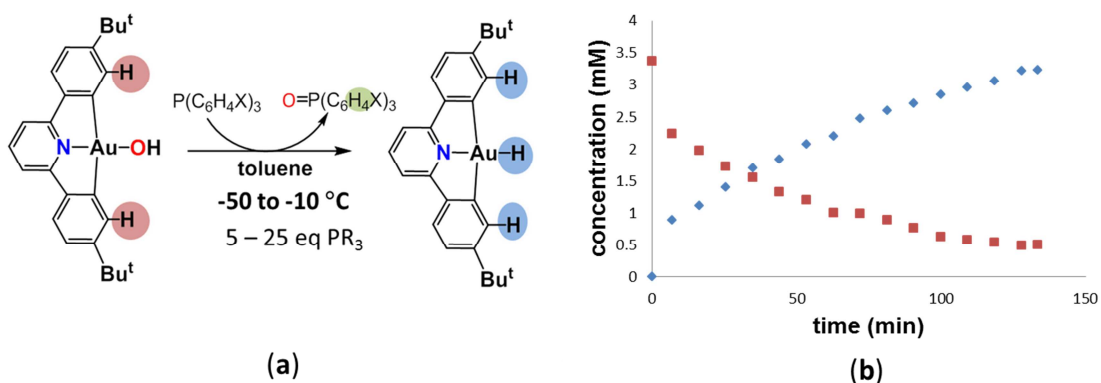
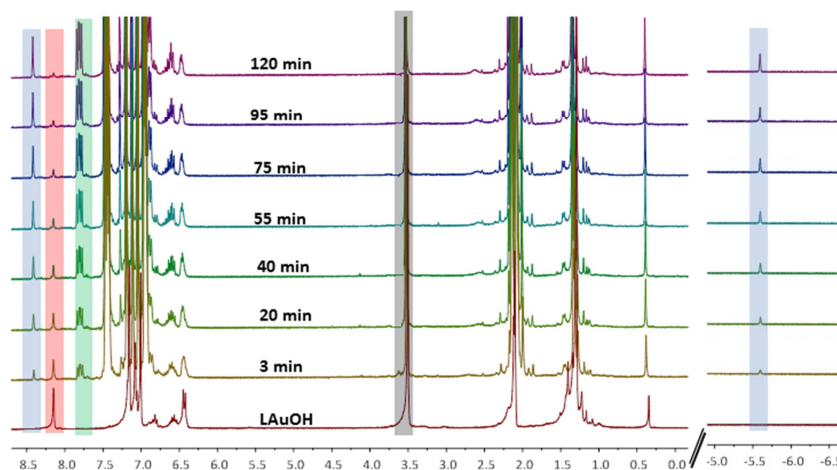
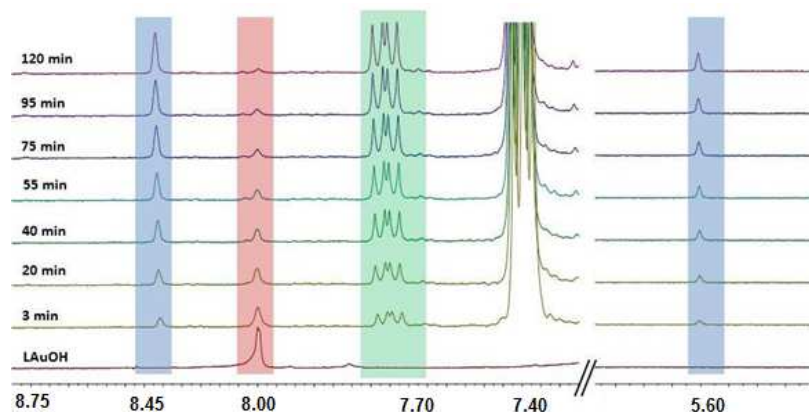


Figure 42 (a) Conversion of **3** into **34_H** and (b) Changes in the concentrations of L AuOH **1** (■) and L AuH **8** (◆) in the reaction with P(*p*-MeC₆H₄)₃ (10.6 eq) as a function of time ([Au] = 3.5 mM) at -40 °C. Due to the nature of the low temperature measurements, the first few data points could not be accurately obtained.



(a)



(b)

Figure 43 (a) Stacked plot of ¹H NMR spectra (toluene-*d*₈, -40 °C) showing the conversion of the (C^{^N^C})AuOH **3** (red highlight) into (C^{^N^C})AuH **34_H** (blue highlight) and O=P(*p*-Me-C₆H₄)₃ (green highlight) (10 fold excess PR₃). Internal standards 18-crown-6 (grey highlight) and silicone grease. (b) Detail of the aromatic (8.8 - 7.3 ppm) and hydride regions of the ¹H NMR spectra (toluene-*d*₈, -40 °C). Colour coding corresponds to the one in Figure 42

In order to establish the rate law, the conversion of **3** into **34_H** was conducted at fixed gold concentrations ($[\text{Au}]_0 = 14.4 \text{ mM}$) and under variable phosphine concentrations ($[\text{P}(p\text{-Me-C}_6\text{H}_4)_3]_0 = 150 - 600 \text{ mM}$). A first-order dependence in $[(\text{C}^{\wedge}\text{N}^{\wedge}\text{C})\text{AuOH}]$ **3** was observed in each case, suggesting a partial order in $[(\text{C}^{\wedge}\text{N}^{\wedge}\text{C})\text{AuOH}]$ of 1 (Figure 44, left). The plot of $\ln(k_{\text{obs}})$ vs. $\ln([\text{P}(p\text{-Me-C}_6\text{H}_4)_3]_0)$ was linear with a gradient of 0.94(4), suggesting that the partial order in phosphine is also 1.0, within experimental errors (Figure 44, right). Hence, this gives the rate law:

$$-d[(\text{C}^{\wedge}\text{N}^{\wedge}\text{C})\text{AuOH}]/dt = k \cdot [(\text{C}^{\wedge}\text{N}^{\wedge}\text{C})\text{AuOH}]^{1.0} \cdot [\text{P}(p\text{-Me-C}_6\text{H}_4)_3]^{1.0} \quad (\text{eq 1})$$

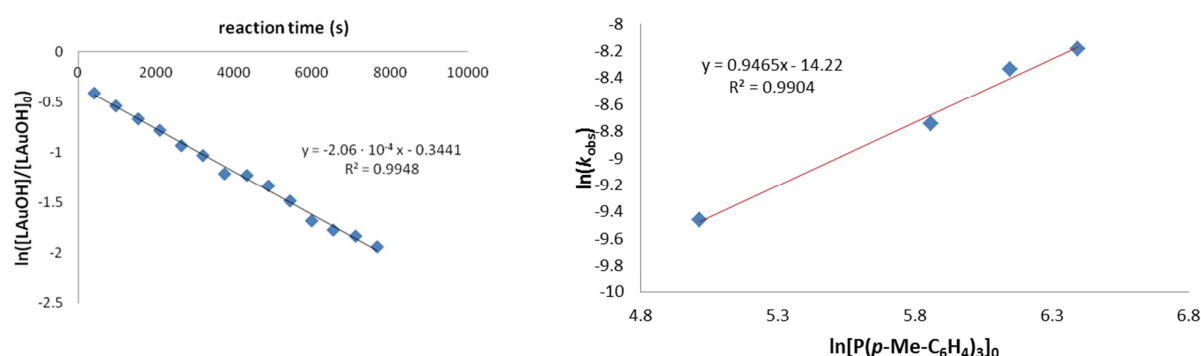


Figure 44 a) Plot of $\ln([\text{LAuOH}]/[\text{LAuOH}]_0)$ versus time at $-50 \text{ }^\circ\text{C}$. Each data point is an average of 5 measurements. b) Plot of $\ln(k_{\text{obs}})$ versus $\ln [\text{PR}_3]$ at various phosphine concentrations at $-50 \text{ }^\circ\text{C}$.

The activation parameters of the reaction were obtained by observing the conversion of $[\text{LAuOH}]$ at fixed gold and phosphine concentrations ($[\text{LAuOH}]_0 = 14.4 \text{ mM}$, $[\text{P}(p\text{-Me-C}_6\text{H}_4)_3]_0 = 152.3 \text{ mM}$) while varying the temperature ($-50 \text{ }^\circ\text{C}$ to $-10 \text{ }^\circ\text{C}$). The Eyring plot gave the activation parameters $\Delta H^\ddagger = 35.0(7) \text{ kJ mol}^{-1}$ and $\Delta S^\ddagger = -105.7(2) \text{ J mol}^{-1} \text{ K}^{-1}$. The negative value of ΔS^\ddagger implies that the reaction proceeds via an associative mechanism in the transition state. Similarly, using the Arrhenius equation, the activation energy was found to be $E_a = 36.78(8) \text{ kJ mol}^{-1}$. (Figure 45, right)

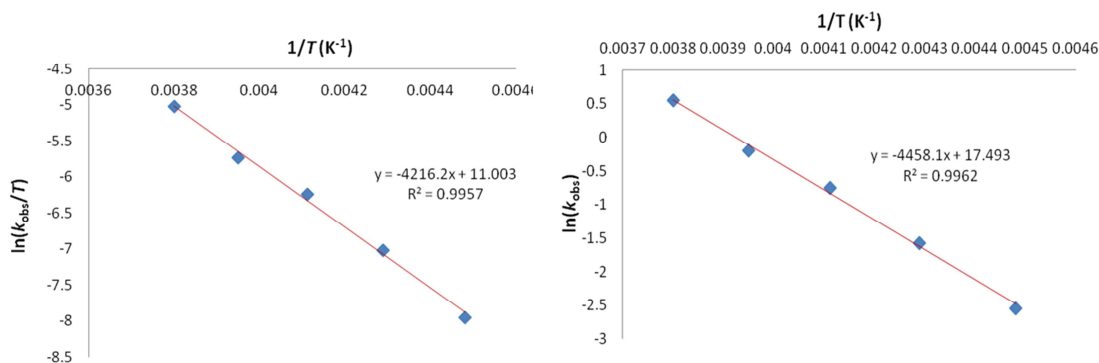


Figure 45. (a) Eyring plot of the reaction of **1** with $\text{P}(p\text{-MeC}_6\text{H}_4)_3$ in toluene- d_8 between 223 and 263 K ($[\mathbf{3}]_0 = 14.4 \text{ mM}$, $[\text{P}(p\text{-MeC}_6\text{H}_4)_3]_0 = 152.3 \text{ mM}$). (b) Arrhenius plot for the determination of the activation energy.

The reaction of the deuterio analogue **3-d₁** with P(*p*-Me-C₆H₄)₃ resulted in a slight retardation of the reaction ([LAuOH(D)]₀: [P(*p*-Me-C₆H₄)₃]₀ 1:10.8, -20 °C, $k_{\text{obs}}(\text{LAuOH}) = 8.07(6) \cdot 10^{-4} \text{ s}^{-1}$, $k_{\text{obs}}(\text{LAuOD}) = 5.49(3) \cdot 10^{-4} \text{ s}^{-1}$) which corresponds to a kinetic isotope effect ($k_{\text{H}}/k_{\text{D}}$) of 1.45(3).²⁰³ Based on the IR stretching frequencies for **3** (3476 cm⁻¹) and **3-d₁** (2553 cm⁻¹), a maximum theoretical kinetic isotope effect (KIE) at -20 °C of 14.7 could be calculated.²⁰⁴ The value of the measured KIE suggests that O-H bond cleavage is only indirectly involved in the rate determining step and implies an out-of-plane bending of the O-H bond in the rate-limiting step.²⁰⁵

The reaction rates are insensitive to the presence of radical inhibitors. No significant effect on the rate constants was observed when the reaction of (C^NC)AuOH **3** with P(*p*-Me-C₆H₄)₃ was carried in the absence (toluene-*d*₈, [(C^NC)AuOH]₀ : [P(*p*-Me-C₆H₄)₃]₀ = 10.6, -30 °C, $k_{\text{obs}} = 4.34(5) \cdot 10^{-4} \text{ s}^{-1}$) or in the presence of 2,2,6,6-tetramethyl-1-piperidinyloxy free radical (TEMPO, toluene-*d*₈, [LAuOH]₀ : [P(*p*-Me-C₆H₄)₃]₀ = 12.3, -30 °C, $k_{\text{obs}} = 5.01(9) \cdot 10^{-4} \text{ s}^{-1}$). Galvinoxyl was found to react with the hydride **2** quantitatively giving the gold(II) dimer [(C^NC)Au]₂ **37**. (See Section 2.2)

Effect of *p*-X-C₆H₄ substituents of the phosphines: Hammett correlation

We proceeded to examine the kinetics of the oxygen abstraction by using various phosphines with electron withdrawing (F) and donating (OMe, Me) *p*-substituents.²⁰⁶ The reaction rates were determined by ¹H NMR under rigorously identical conditions (-30 °C, toluene-*d*₈, ([**3**]₀ : [PR₃]₀ = 1 : 10.58). The Hammett correlation shows that the para substituent on the aryl phosphine has a major influence ($\rho = -3.15$, $R^2 = 0.94$) on the reaction rate, with electron donating groups (such as Me or OMe) substantially accelerating the reaction. (See Figure 46) The negative ρ value (-1.05 per aryl ring) suggests that positive charge is built on the reaction centre and is in good agreement with a zwitterionic transition state.

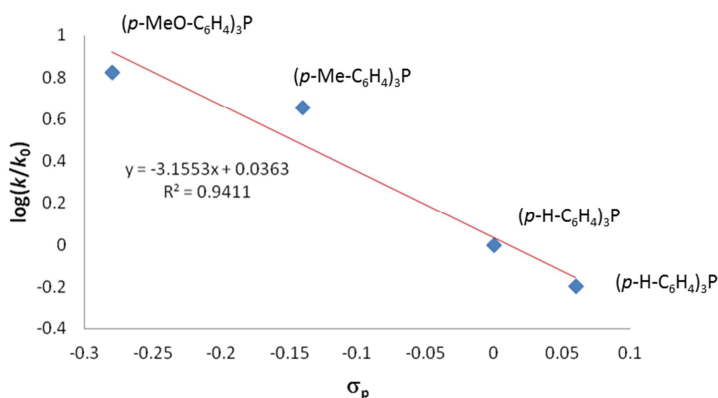


Figure 46. Hammett correlation ([LAuOH] : [PR₃] = 1 : 10.58, toluene-*d*₈, -30 °C)

Mass spectrometry

In order to establish that the oxygen atom transfer proceeds from the hydroxide **3** to the phosphine, an ^{18}O labelled sample of **3** was prepared by reacting the $(\text{C}^{\wedge}\text{N}^{\wedge}\text{C})\text{AuOAc}^{\text{F}}$ **4** with Na^{18}OH . An IR investigation showed that the ^{18}OH vibration of $\mathbf{3}^{18}\text{O}$ is shifted to lower energy by 20 wavenumbers, to 3456 cm^{-1} while the ^1H NMR spectrum was identical to **3**. $\text{P}(p\text{-Me-C}_6\text{H}_4)_3$ was reacted with $\mathbf{3}^{18}\text{O}$ and extracted with acetonitrile. The extract was subjected to APCI(+) MS analysis showing the formation of $^{18}\text{O}=\text{P}(p\text{-Me-C}_6\text{H}_4)_3$ as the predominant product.²⁰⁷ (Figure 47)

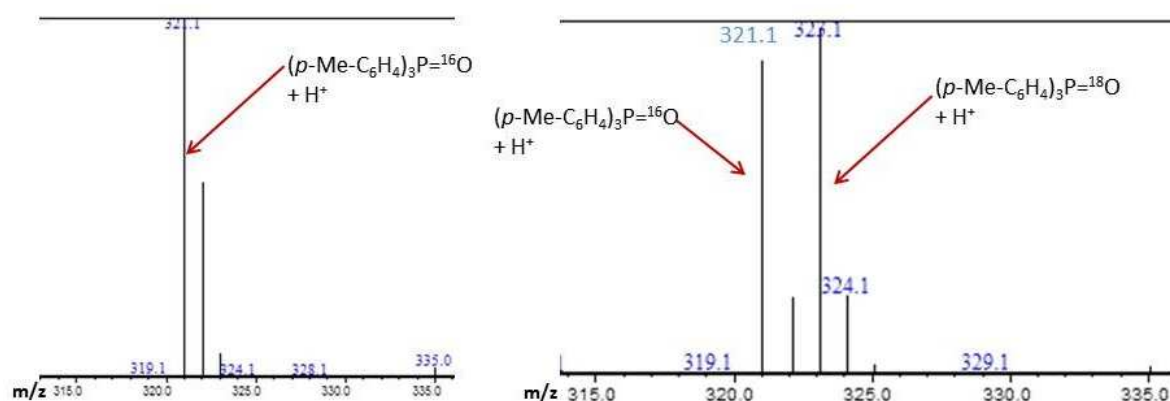


Figure 47 Mass spectrum of $^{16}\text{O}=\text{P}(p\text{-Me-C}_6\text{H}_4)_3$ (left) and mixture of $^{16}\text{O}=\text{P}(p\text{-Me-C}_6\text{H}_4)_3$ and $^{18}\text{O}=\text{P}(p\text{-Me-C}_6\text{H}_4)_3$ (right) resulted from the reaction between **3** and $\text{P}(p\text{-Me-C}_6\text{H}_4)_3$.

Bond dissociation energies (collaboration with Dr Joseph Wright)¹³⁰

A calculation of bond dissociation energies (BDE) by DFT methods also confirmed that the $\text{Au-OH} \rightarrow \text{Au-H}$ transformation is thermodynamically favourable. The results, which correlate well to the BDE gas phase measurements of the diatomic AuO and AuH molecules suggest that the Au-H bond in $\mathbf{34}_\text{H}$ (BDE 317 kJ mol^{-1}) is stronger than the Au-O bond in **3** (279 kJ mol^{-1}). (Table 15) Moreover, when the gold(III) $(\text{C}^{\wedge}\text{N}^{\wedge}\text{C})\text{Au}$ systems were compared with the closely related platinum(II) $(\text{N}^{\wedge}\text{N}^{\wedge}\text{C})\text{Pt}$ systems ($\text{N}^{\wedge}\text{N}^{\wedge}\text{C}$ = 2-phenyl-6,6'-bipyridine), the BDE calculations suggested an opposite trend. This implies that since in the case of platinum(II), the Pt-H bond (350 kJ mol^{-1}) is weaker than the Pt-O bond (367 kJ mol^{-1}), a $\text{Pt-OH} \rightarrow \text{Pt-H}$ transformation is thermodynamically unfavourable. The BDE calculations also correlate well with the gas phase measurements in the diatomic PtO and PtH molecules. (Table 15)¹²⁹ The results are perhaps surprising since the isoelectronic and isostructural gold(III) and platinum(II) were often thought to display similar chemistry.²⁰⁸

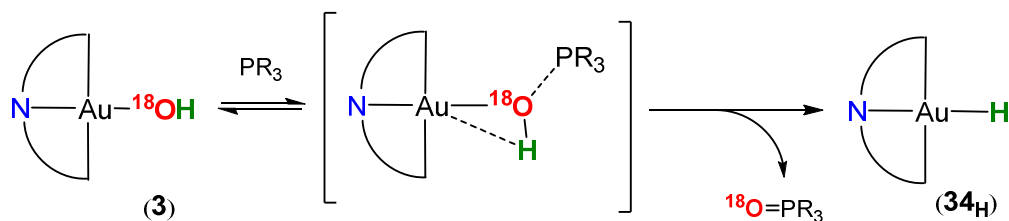
Table 15. Comparison of calculated and experimental bond dissociation energies (BDE) (kJ mol⁻¹)

Complex	Calculated BDE	Diatomic compound	BDE ^a
(C [^] N [^] C)Au ^{III} -H 34_H	317	Au-H	292±8
(C [^] N [^] C)Au ^{III} -OH 3	279	Au-O	223
(C [^] N [^] N)Pt ^{II} -H	350	Pt-H	352
(C [^] N [^] N)Pt ^{II} -OH	367	Pt-O	391

^a Data taken from ref 129

Reaction mechanism

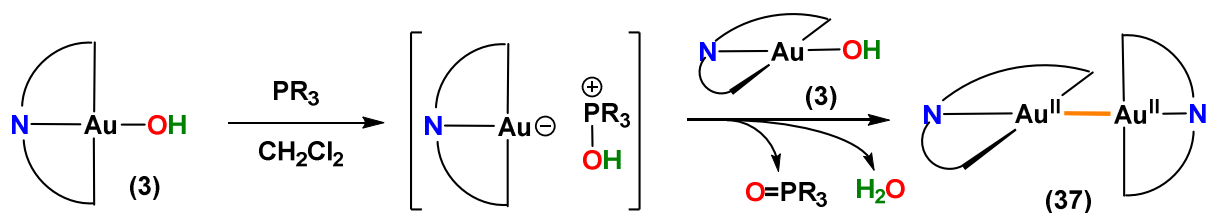
Attempts to computationally identify an intermediate in the reaction of LAuOH with PR₃, such as a 5-coordinate phosphine adduct of gold or a zwitterionic intermediate [(C[^]N[^]C)Au^(δ-)(μ-OH)-PR₃^(δ+)] were unsuccessful. The results suggest a concerted mechanism for O-abstraction by PR₃ with simultaneous hydride transfer from oxygen to gold, as would be represented by a bending mode of the Au-O-H moiety as PR₃ approaches. The formulation is in line with the observed modest kinetic deuterium isotope effect. (Scheme 32)



Scheme 32 Mechanistic pathway for the O-abstraction from gold(III) hydroxide by phosphines, based on the observed kinetic isotope effect and DFT calculations

Conducting the reaction in CH₂Cl₂

Employing the more polar CH₂Cl₂ as solvent results in the conversion to the gold(II) species [(C[^]N[^]C)Au]₂ **37** as the major product (75 %) both at 20 °C or at low temperature, regardless of the amount of phosphine used. Since (C[^]N[^]C)AuCl **2** – the product of a typical radical attack on the chlorinated solvent is not observed, a competing ionic pathway is possible, favouring the formation of the gold(II) dimer **37**. (Scheme 33)

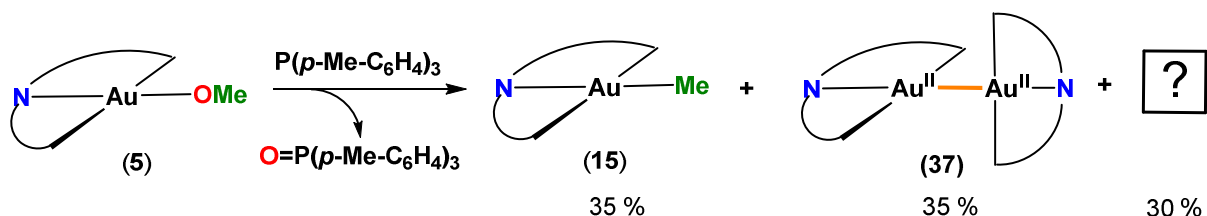


Scheme 33 Proposed ionic pathway for the reaction of **3** with phosphines (reaction carried in CH_2Cl_2)

Reaction of LAuOMe with PR_3

In the light of the facile $\text{Au—OH} \rightarrow \text{Au—H}$ phosphine mediated transformation, the reaction of the gold(III) methoxide $(\text{C}^{\wedge}\text{N}^{\wedge}\text{C})\text{Au}(\text{OMe})$ **5** with $(p\text{-tolyl})_3\text{P}$ in C_6D_6 at room temperature was also attempted.

Monitoring the reaction by $^{31}\text{P}\{^1\text{H}\}$ NMR spectroscopy (under nitrogen atmosphere) revealed a decrease in the intensity of the signal at $\delta_{\text{P}} -8.1$ (corresponding to $(p\text{-tolyl})_3\text{P}$) and the appearance of a signal at $\delta_{\text{P}} 30.6$ (corresponding to $(p\text{-tolyl})_3\text{P=O}$) suggesting the oxidation of the phosphine, with full conversion being reached after 36 h.



Scheme 34 Oxygen transfer reactions from $(\text{C}^{\wedge}\text{N}^{\wedge}\text{C})\text{AuOMe}$ **5** to phosphines

The consumption of the $(\text{C}^{\wedge}\text{N}^{\wedge}\text{C})\text{AuOMe}$ **5** could also be followed by ^1H NMR by monitoring the decrease of the resonance corresponding to the proton atoms attached to the methoxy group ($\delta_{\text{H}} 4.69$, C_6D_6). Analysing the reaction mixture after 36 h revealed the consumption of **5** and the formation of the gold methyl complex $(\text{C}^{\wedge}\text{N}^{\wedge}\text{C})\text{AuMe}$ **15** (35 % conversion) which was identified by the characteristic Au—Me resonance ($\delta_{\text{H}} 1.85$, C_6D_6). (Scheme 34) The other product appears to be the gold(II) dimer $[(\text{C}^{\wedge}\text{N}^{\wedge}\text{C})\text{Au}]_2$ **37** (35 %), alongside unidentified reaction products, as confirmed by observing the new resonances at $\delta_{\text{H}} 3.10$, 2.74 , 2.71 and 0.21 . (Figure 48)

The transformation Au—OMe \rightarrow Au—Me by an oxygen transfer reaction is still surprising since in principle it involves breaking O—CH₃ bonds are usually regarded as strong. The reaction of the methoxide (C^{^N^C})AuOMe **5** with phosphines is currently under investigation in order to elucidate the reaction mechanism and the nature of the unidentified products.

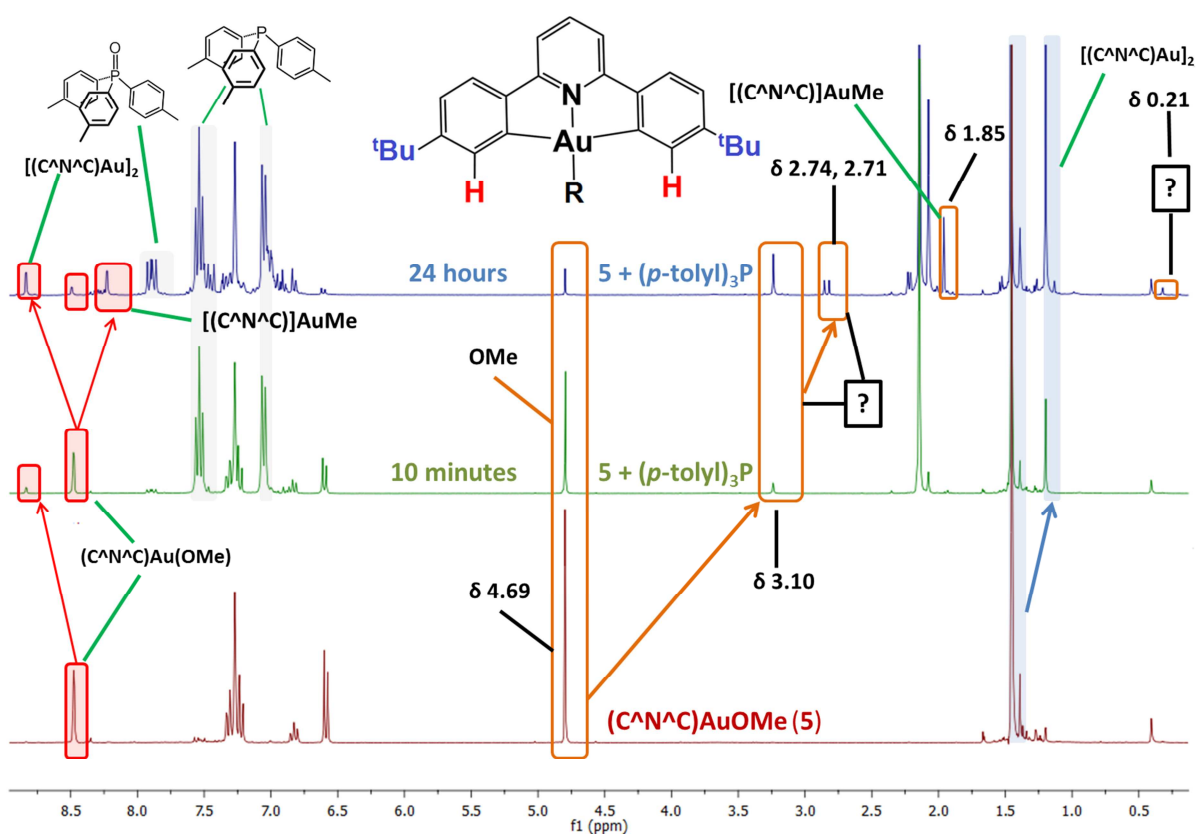
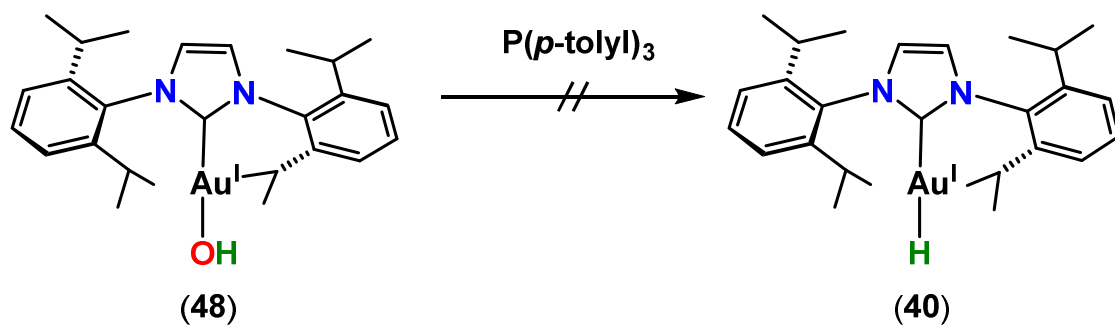


Figure 48 Stacked ¹H NMR spectra (300 MHz, C₆D₆, RT) showing the reaction of (C^{^N^C})AuOMe **5** (red) with phosphines at various reaction times.

Attempted reaction of (IPr)Au^IOH with PR₃

In order to check if the phosphine mediated Au—OH \rightarrow Au—H transformation is also possible for gold(I) centres, (IPr)AuOH **49**⁵⁸ was reacted with excess P(*p*-tolyl)₃ phosphine (25 eq) at room temperature. (Scheme 35) No reaction was observed after 24 h by ¹H and ³¹P{¹H} NMR spectroscopy.

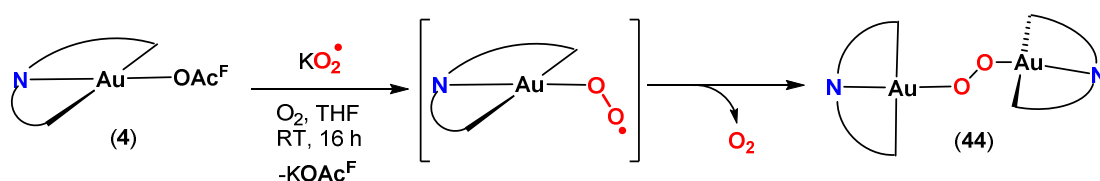
Since the nature of the donating ligand on the gold centre significantly affects the reactivity of the ligand located *trans* to the L—Au bond, the LAu^I—OH \rightarrow LAu^I—H conversion is currently under investigation by employing different ancillary ligands.



Scheme 35 Attempted oxygen transfer reactions from (IPr)Au(OH) **48**

3.4 Attempted synthesis of a gold(III) superoxide

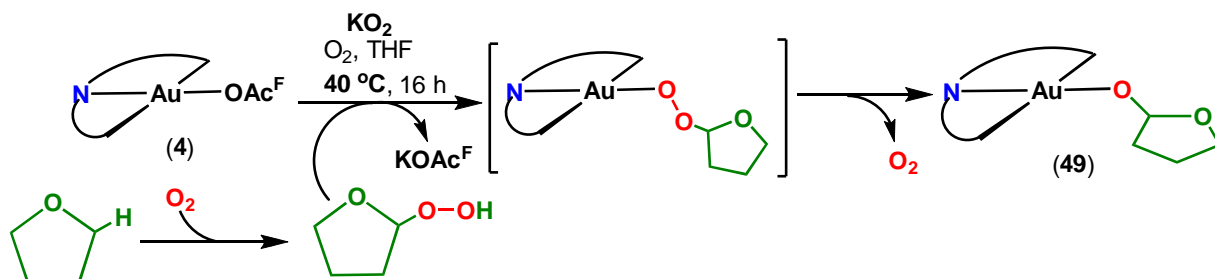
In an attempt to generate a gold(III) superoxide (C[^]N[^]C)AuOO•, the trifluoroacetate (C[^]N[^]C)Au(OAc^F) **4** was allowed to react with KO₂ in THF/toluene mixtures (1:1) under an atmosphere of dioxygen at room temperature. An ¹H NMR analysis of the crude reaction mixture reveals the formation of a mixture of compounds out of which the μ-κ¹:κ¹-peroxo)digold complex [(C[^]N[^]C)Au]₂(μ-OO) **44** could be identified. This may suggest the initial formation of the superoxide (C[^]N[^]C)AuOO• which seems to be unstable even under one atmosphere of dioxygen and undergoes disproportionation to give the the μ-κ¹:κ¹-peroxo)digold complex [(C[^]N[^]C)Au]₂(μ-OO) **44** and dioxygen. (Scheme 36). This decomposition pathway has also been reported for other late transition metal superoxide complexes under deficiency of dioxygen.¹⁴⁵



Scheme 36 Reaction of **4** with KO₂ under O₂ at RT

Upon conducting the reaction at 40 °C, a single product could be observed by ¹H NMR, which upon recrystallisation from CH₂Cl₂ : light petroleum mixtures at -20 °C produced the tetrahydrofuranolato complex (C[^]N[^]C)Au(O-C₄H₇O) **49** as yellow crystals. Its structure was confirmed by X-ray diffraction (see Figure 47). Since the reaction was carried out under one atmosphere of dioxygen in the presence of THF, O₂ insertion into one C—H bond of the α-carbon atom of THF to give a tetrahydrofuranyl hydroperoxide is plausible. The subsequent reaction of the hydroperoxide with **4** in the presence of KO₂ (base) gives the

gold(III) tetrahydrofuran-2-yl peroxide which upon disproportionation liberates O₂ and gives the tetrahydrofuranolato gold complex **49**. (Scheme 37)



Scheme 37 Reaction of **4** with KO₂ under O₂ at 40 °C

The solid state structure of (C[^]N[^]C)Au(O-C₄H₇O) **49** is depicted in Figure 49. The Au—O bond length (1.983(6) Å) is similar to the one in other (C[^]N[^]C)Au complexes with oxygen ligands (2.010(2) Å in (C[^]N[^]C)AuOH **3**, 1.975(3) Å in [(C[^]N[^]C)AuO]₂ **44**) and the Au—O—C angle between the gold centre and the furanyl moiety (116.2(8) Å) reflects the sp³ hybridisation of the oxygen atom with negligible Au—O π interactions. The molecules stack through overlapping (C[^]N[^]C)Au fragments along the *b* axis. (Figure 49, right) In the crystal packing, the intermolecular Au⋯Au distances are long (6.114(3) Å)

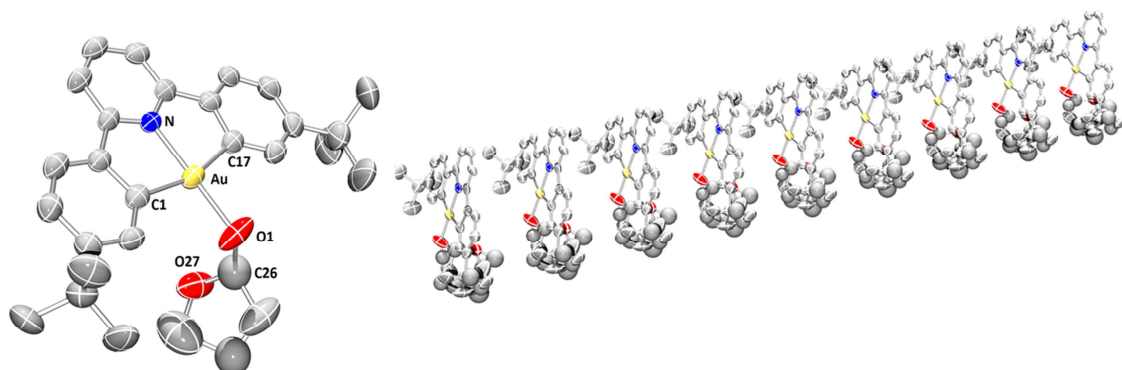


Figure 49. Molecular structure of **49**. Thermal ellipsoids are set at 50% probability level. Hydrogen atoms are omitted. Selected bond distances (Å) and angles (°): Au-N(1) 1.972(5), Au-C(17) 2.061(8), Au-C(1) 2.072(8), Au-O(1) 1.983(6), C(17)-Au-C(1) 161.63(16), N-Au-O(1) 179.1(2), Au-O(1)-C(26) 116.2(8). The C₄H₇O unit shows disorder over two orientations: only one orientation shown. Atoms with less than full occupancy were refined isotropically. (left) Stacking along the *b* axis (right)

While there are no reports of ‘side on’ (η¹-O₂) gold or platinum compounds, in 2011 the groups of Ozerov¹⁴⁵ and Hoff²⁰⁹ reported examples of palladium(II) superoxo complexes synthesised by O₂ mediated oxidation of a Pd(II) bridging peroxo complex or a carbene supported Pd(0) centre respectively.

3.5 Insertion of molecular oxygen into gold(I) hydride bond: Synthesis of gold(I) peroxides

We have shown above that despite the fact that the dioxygen insertion into the Au^{II}—Au^{II} bond would be thermodynamically favourable, ($\Delta H = 136 \text{ kJ mol}^{-1}$) (See Section 2.4) the gold(II) dimer (C^{^N^C})Au—Au(C^{^N^C}) **37** shows no reactivity towards dioxygen (1 bar). The same behaviour was observed for the gold(III) hydride (C^{^N^C})AuH **34_H**. Nevertheless, the corresponding hydroperoxide **43** and bridging ($\mu\text{-}\kappa^1:\kappa^1$) **44** were isolated *via* acid-base and dehydrocondensation reactions. Compared to the gold(III) hydride **34_H**, the NHC-supported gold(I) hydride (IPr)AuH **40** is more reactive. (See Section 2.2) Consequently, we decided to explore the reactivity of **40** towards dioxygen.

Recently, the involvement of a M—H \rightarrow M—OOH step in catalytic cycles has also been postulated in gold(I) chemistry. For example Zhu *et al.* demonstrated that bipyridine supported gold(III) cations are active in the oxidative C—C coupling from unactivated C-H bonds, using air as a sole oxidant.¹⁰¹ In the proposed catalytic cycle (Figure 50), the insertion of O₂ into the Au^IH bond is a critical step for the activation of dioxygen. However, to the best of our knowledge the insertion of dioxygen into the Au—H bond has so far not been reported.

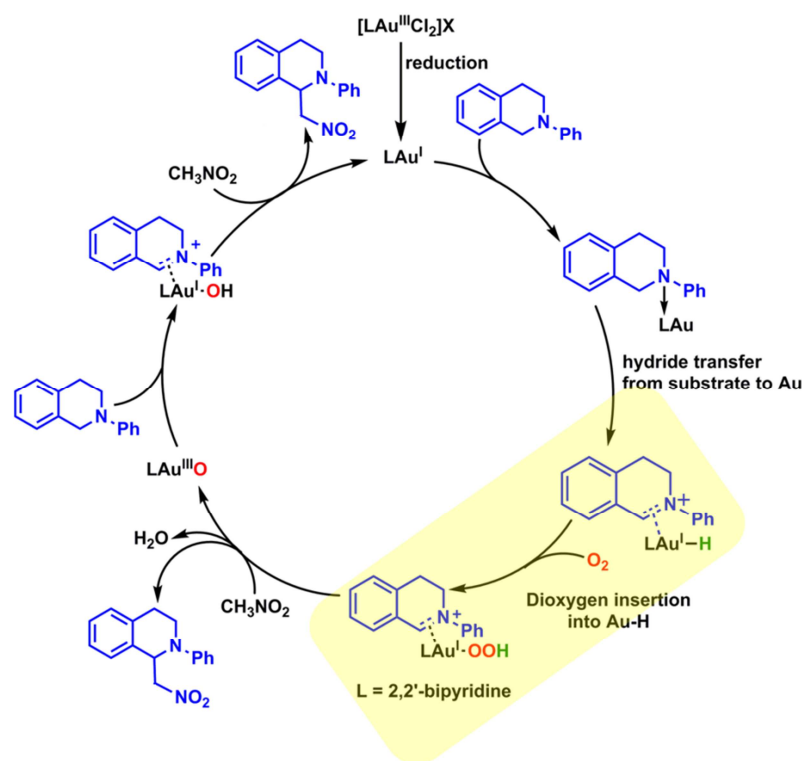
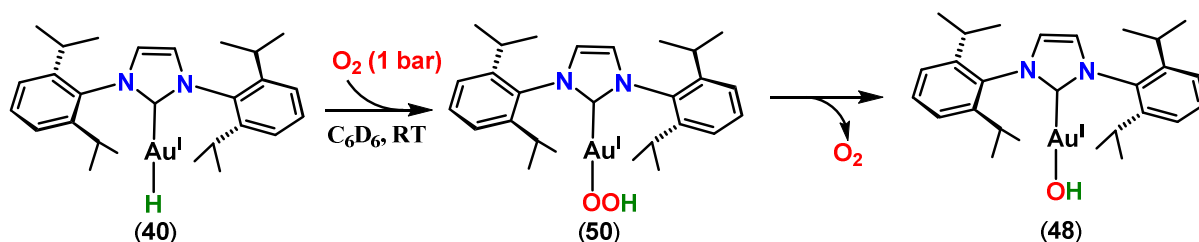


Figure 50 Proposed catalytic cycle for the gold mediated oxidative C—C coupling reaction.¹⁰¹ Dioxygen insertion step highlighted in yellow.

Exposure of a C₆D₆ solution of the gold(I) hydride⁴⁴ (IPr)AuH **40** to an atmosphere of dioxygen (1 bar) for 36 h lead to the disappearance of the resonance associated with the Au—H fragment (δ_{H} 5.11) and to the formation of a new product, the gold(I) peroxide (IPr)AuOOH **50**. The conversion of **40** into **50** can also be observed by monitoring the carbene proton resonances. (Purple highlight in Figure 51)

After the first half-life of the reaction, a resonance at δ -0.26 can be observed which is consistent with the formation of the gold(I) hydroxide⁵⁸ (IPr)AuOH **48**. The spectrum of the hydroxide **48** is very similar to the one of the hydroperoxide **50** with the notable presence of the OH at δ -0.26 in **48**. The resonance for the OOH group in **50** could not be located under the present conditions.

At full conversion of the starting Au^I hydride (IPr)AuH **40** (after 48 h), the final ratio of **50:48** is about 1:2 and ultimately, upon standing at room temperature the hydroxide **48** can be obtained quantitatively. This suggests that while **50** readily forms under 1 atmosphere of oxygen, the disproportionation reaction is facile and in time **50** converts into **48** while releasing O₂. (Scheme 38) This decomposition pathway has also been reported for similar Pd(II) and Pt(IV) hydroperoxides.^{182a,b} In those cases, the disproportionation reaction could be suppressed by increasing the dioxygen concentration.



Scheme 38 Oxygen insertion into the Au^I—H bond followed by disproportionation of the resulting hydroperoxide

The ability of the hydroperoxide **50** to transfer oxygen atoms was tested by reacting it with phosphines. Treating **50** with an excess of (*p*-tolyl)₃P (δ_{P} -8.1)(1.5 eq) showed the formation of (*p*-tolyl)₃P=O (δ_{P} 30.6) as revealed by ³¹P{¹H} NMR spectroscopy. The mechanism of the dioxygen insertion into the Au—H bond and the reactivity of the formed peroxide is currently under investigation.

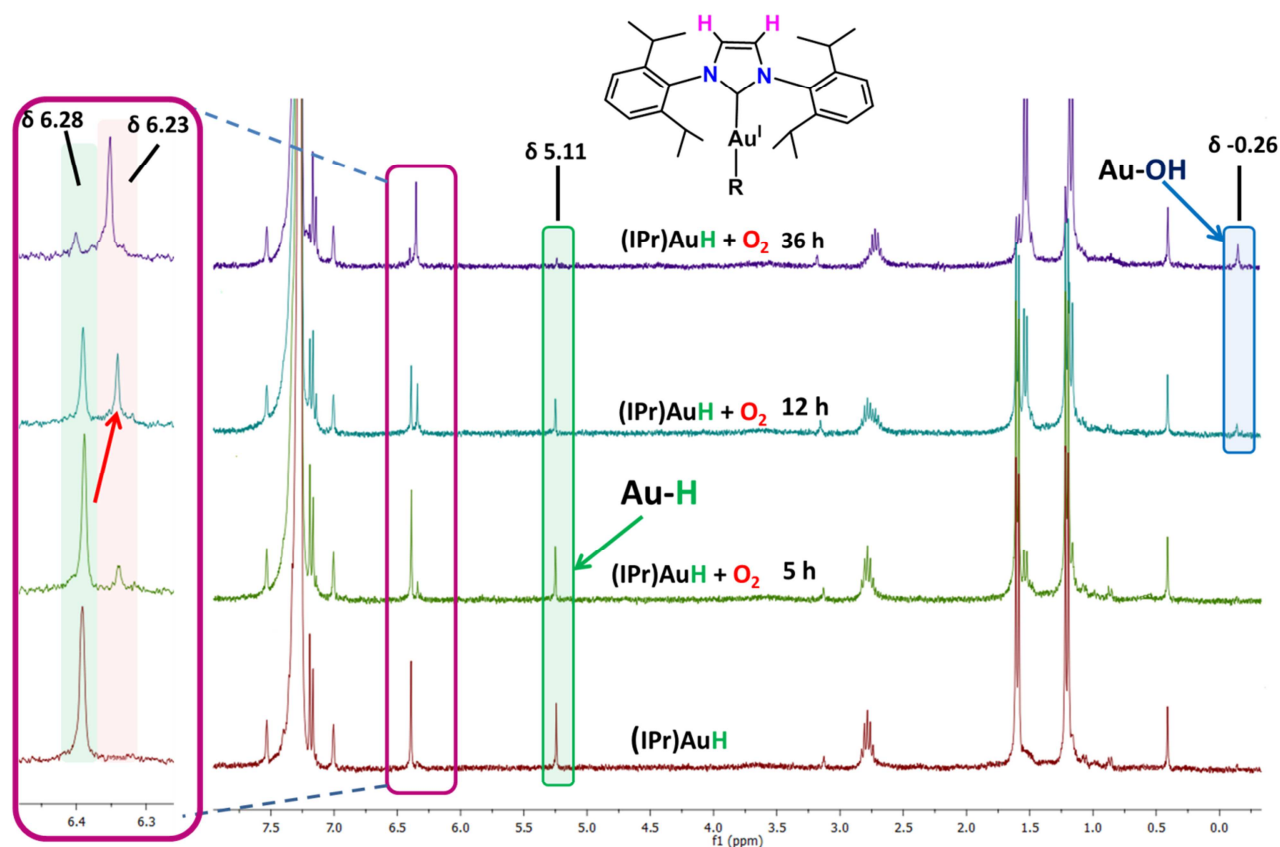
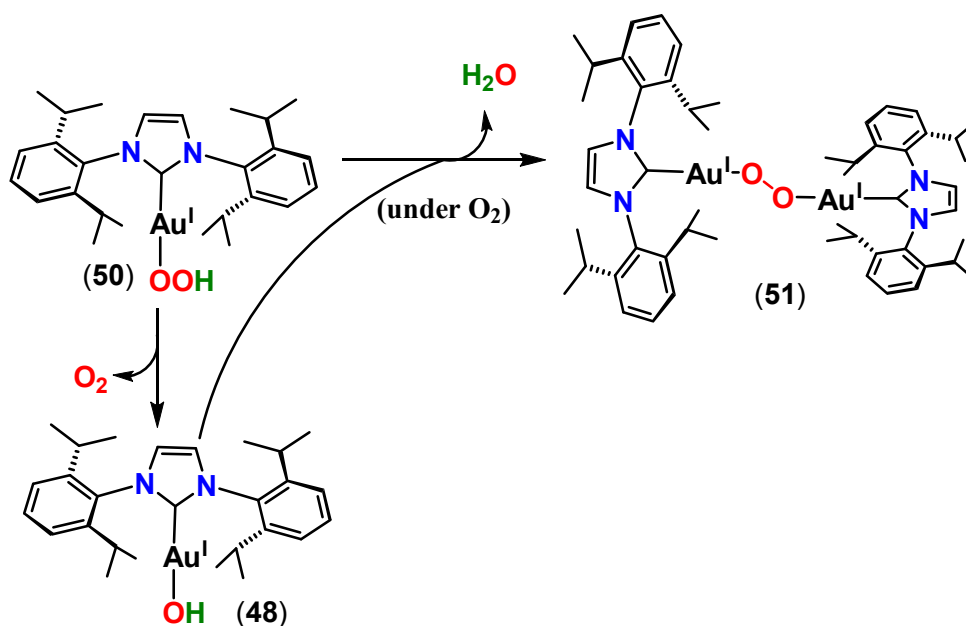


Figure 51 Stacked ^1H NMR spectra (300 MHz, C_6D_6 , RT) showing the reaction of $(\text{IPr})\text{AuH}$ **40** (red) with O_2 (1 bar) at various reaction times.

Attempts to crystallise the hydroperoxide **50** under an atmosphere of oxygen gave single crystals of the bridging ($\mu\text{-}\kappa^1\text{:}\kappa^1$) peroxide $[(\text{IPr})\text{Au}]_2(\mu\text{-OO})$ **51** instead, as confirmed by single crystal X-ray crystallography. (Figure 52) The condensation of a molecule of **50** and the corresponding hydroxide **48** obtained through disproportionation (Scheme 39) is reminiscent to the behaviour of the gold(III) hydroperoxide **43** towards the corresponding hydroxide **3** to give the bridging ($\mu\text{-}\kappa^1\text{:}\kappa^1$) peroxide $[(\text{C}^{\wedge}\text{N}^{\wedge}\text{C})\text{Au}]_2(\mu\text{-OO})$ **44**. (See Scheme 24) This behaviour is also similar to the one of other *d*-block hydroperoxides.



Scheme 39 Disproportionation of **50** followed by dehydrocondensation to give **51**

Crystals of **51**·2(C₆H₆) were obtained by storing a benzene solution of **51** under oxygen. Despite positional disorder of the carbene ligands and peroxo fragment which are disordered over two positions, the connectivity could be assigned unambiguously and confirms the identity of **51** as a digold (μ - κ^1 : κ^1) bridging peroxide. (Figure 52) However the poor quality of the data precludes any discussion of the bond lengths. For instance, the O—O bond length (1.26 Å) appears much shorter than the one of typical transition metal peroxides (1.41 - 1.50 Å).^{182, 183, 187-190} The C—Au—O fragment is linear which is a typical geometry around a gold(I) centre.

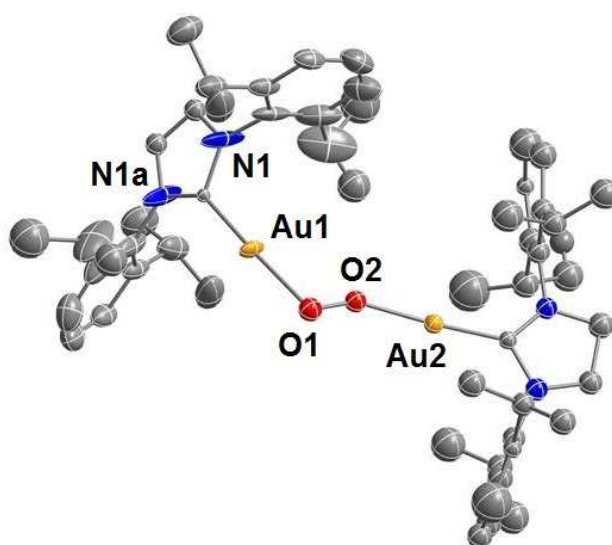


Figure 52 Molecular structure of **51**·2(C₆H₆). For disordered imidazolyl rings and peroxo groups, only one orientation is shown.

Upon attempting to obtain better quality crystals of **51** from a solution of THF under air, single crystals of the carbonate **52·3(THF)** were obtained, as confirmed by single crystal X-ray diffractometry. (Figure 53) For the bridging trigold carbonato cation $[(\text{IPrAu})_3(\mu_3\text{-CO}_3)]^+$, the geometry at the gold centre is linear as expected (C2—Au—O $176.76(32)^\circ$) and the carbonate moiety is essentially planar (O1—C1—O2 $118.93(43)^\circ$). The geometry around the oxygen atom is bent (Au1—O1—C1 $115.54(31)^\circ$). The modest quality of the reflection data did not allow for an anion to be located on the density map but it is assumed that, owing to the composition of the reaction mixture, a hydroxyl anion may be plausible.

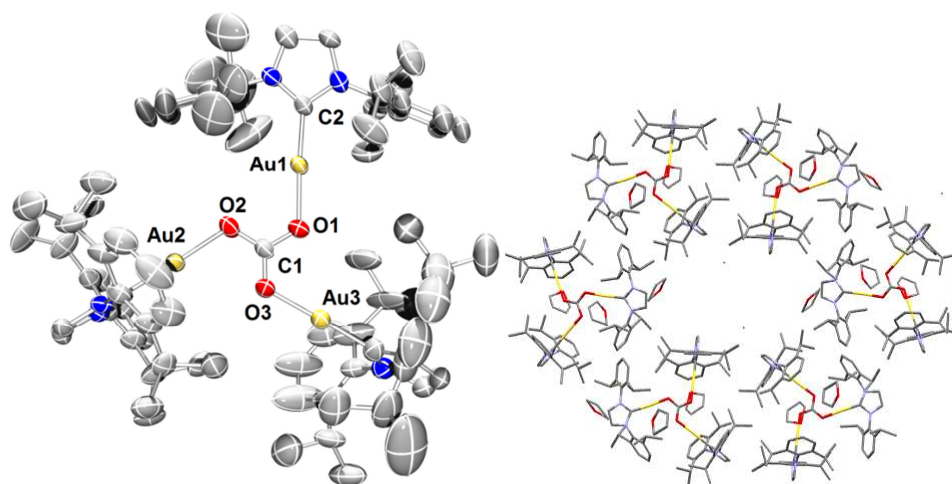
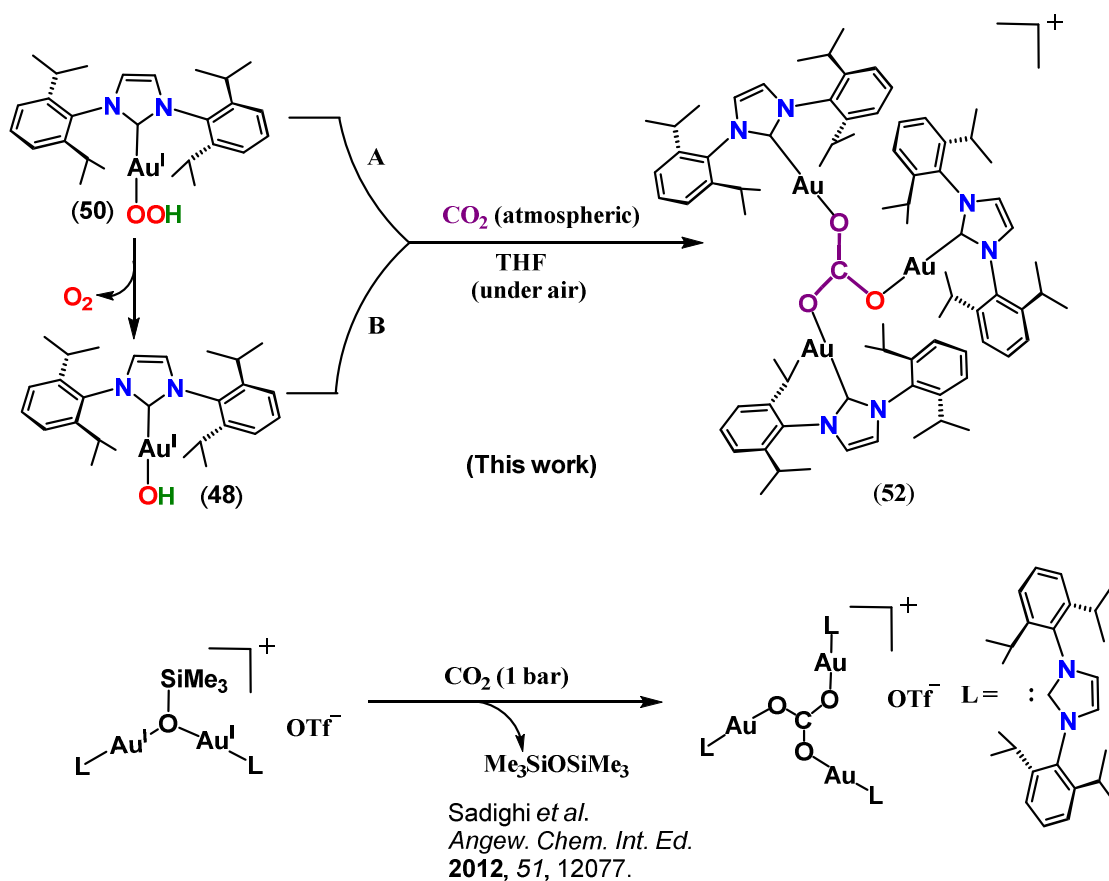


Figure 53 Molecular structure of **52**. Thermal ellipsoids are set at 50% probability level. Hydrogen atoms are omitted. The anion fragment could not be located on the difference density map. Selected bond distances (Å) and angles ($^\circ$): Au1-C(2) 1.942(3), Au1-O(1) 2.045(3), O(1)-C(1) 1.272(5), C(2)-Au(1)-O(1) $176.76(32)$, O(1)-C(1)-O(2) $118.93(43)$, Au-O(1)-C(1) $115.54(31)$. (left) View along the a axis highlighting solvent accessible voids (right)

The formation of a $(\mu_3\text{-CO}_3)$ trigold complex can be explained by the reaction of the hydroxide **48** or hydroperoxide **50** with atmospheric CO_2 which in time lead to the crystallisation of **52**. However, we cannot exclude the formation of a digold hydroxy-bridged cation⁵⁴ $[(\text{IPrAu})_2(\mu\text{-OH})]^+$ as a key intermediate. A recent report by Sadighi *et al.*¹⁵³ describes the synthesis of the same NHC supported $(\mu_3\text{-CO}_3)$ carbonato trigold cation by a different route, stabilised by a triflate anion. The synthesis proceeds from the siloxy-bridged digold cation $[(\text{IPrAu})_2(\mu\text{-OSiMe}_3)]^+$ under one bar of CO_2 . The parent siloxide $(\text{IPrAu})(\text{OSiMe}_3)$ was reported to be inert in the presence of CO_2 .¹⁵³



Scheme 40 Reaction pathways for the formation of **52**.(top) Literature method for the synthesis of **52**. (bottom)¹⁵³

CONCLUDING REMARKS AND PERSPECTIVE

We have shown for the first time that even in the case of gold, which is often regarded as very oxophobic, dioxygen activation is possible under mild conditions (1 atm) *via* insertion into the $\text{Au}^{\text{I}}\text{-H}$ bond, leading to the formation of the gold(I) hydroperoxide $(\text{IPr})\text{Au}(\text{OOH})$ **50** which readily transfers an oxygen atom unto phosphine acceptors (Steps **I** and **II** in Figure 54). A dehydrocondensation reaction involving **50** also led to the isolation of a bridging ($\mu\text{-}\kappa^1:\kappa^1$) peroxo digold complex **51**.

In the case of gold(III), the Au-H and Au-Au bonds in $(\text{C}^{\wedge}\text{N}^{\wedge}\text{C})\text{AuH}$ **34_H** and $(\text{C}^{\wedge}\text{N}^{\wedge}\text{C})\text{Au-Au}(\text{C}^{\wedge}\text{N}^{\wedge}\text{C})$ **37** proved to be resistant towards O_2 insertion under 1 atm O_2 pressure; the gold(III) peroxides were instead accessed *via* acid base reactions from the gold(III) hydroxide $(\text{C}^{\wedge}\text{N}^{\wedge}\text{C})\text{AuOH}$ **3**. The gold(III) peroxides readily transfer oxygen atoms to phosphines with low activation barriers. More surprisingly, even the gold(III) hydroxide **3**

proved capable of oxygen atom transfer and gives rise to the gold(III) hydride (C[^]N[^]C)AuH **34_H**, in the presence of phosphines, a key transformation in a potential new water splitting cycle. Mechanistic investigations suggest the reaction proceeds via an associative interchange (concerted) mechanism. DFT studies have also confirmed that while the transformation of M—OH → M—H is thermodynamically favourable for gold(III), this is not the case for the isoelectronic and isostructural platinum(II), suggesting that only in the envisaged water cleavage may only be realisable for gold.

Attempts to generate a gold(III) superoxide from the (C[^]N[^]C)AuOAc^F **4** and KO₂ in the THF under an atmosphere of oxygen resulted in the isolation of the furanolato complex (C[^]N[^]C)Au(O-C₄H₇O) **49**. The reaction produced variable amounts of the (μ-κ¹:κ¹) peroxo digold complex **44**, which suggests that if the gold(III) superoxide (CN[^]N[^]C)Au(OO•) is indeed formed, it readily disproportionates even under an oxygen atmosphere.

Based on the Au^I and Au^{III} transformations described, the catalytic cycle depicted in Figure 54 can be constructed. The first step would involve the activation of dioxygen by gold hydrides leading to the formation of gold hydroperoxides. This step has so far been demonstrated for gold(I) but not for gold(III). Future work would involve initial reaction of the (C[^]N[^]C)AuH **34_H** with dioxygen under various gas pressures to verify if the activation of dioxygen by Au^{III}—H is indeed possible. The second step, the oxygen atom transfer from peroxides to a substrate has been verified for both Au^I and Au^{III} centres. The third step, an oxygen transfer from Au—OH → Au—H, has been demonstrated for Au^{III} while IPr-supported Au^I centres do not undergo this transformation. It still remains to be established whether varying the ancillary ligand on the Au^I centre would labilise the Au—O bond in gold(I) hydroxides so that an oxygen transfer becomes favourable.

In the great majority of catalytic cycles involving metal peroxo species, one oxygen atom is transferred unto substrates whereas the other one is “lost” as water. The sequence of transformations (Figure 54) would therefore also be atom economical, since both oxygen atoms would be transferred unto substrates. It remains to be established however if (i) gold(III) hydrides could activate O₂, (ii) gold(I) hydroxides can transfer an oxygen atom unto substrates to give gold(I) hydrides and (iii) under which conditions the oxidation of oxygen-acceptor substrates which are lower in energy is possible.

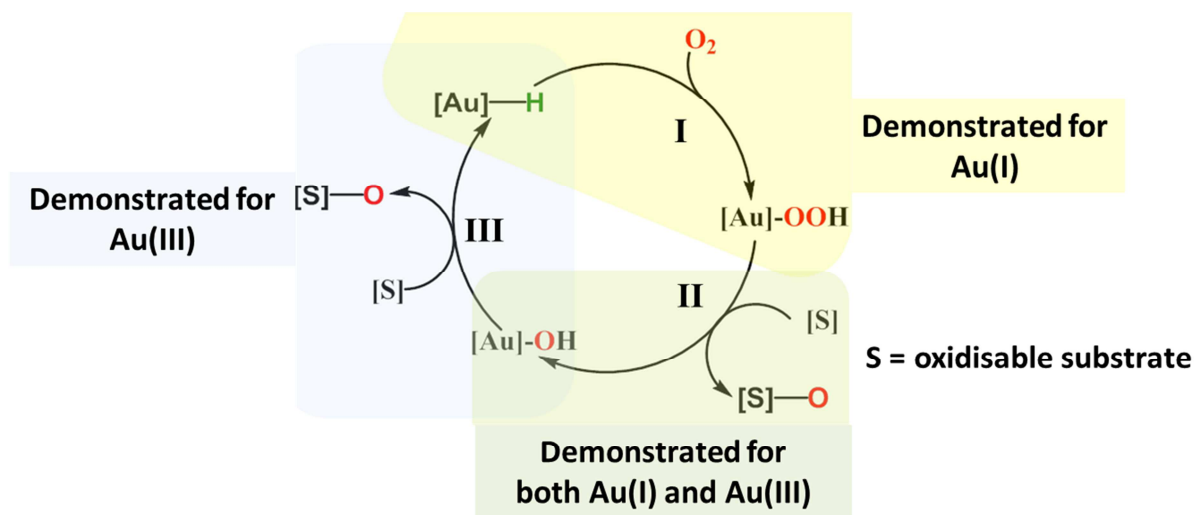


Figure 54 Proposed catalytic cycle for gold mediated oxidation reactions based on the work discussed in this chapter.

CHAPTER 4

Gold(III) olefin complexes, gold azide complexes and attempts to use β -diketiminato ligands in gold(III) chemistry

A portion of this chapter has appeared in print:

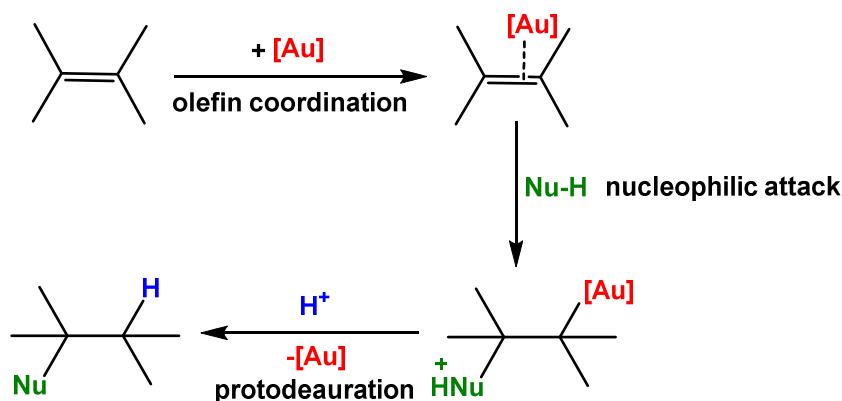
N. Savjani, D.-A Roşca, M. Schormann, M. Bochmann "Gold(III) Olefin Complexes" *Angew. Chem. Int. Ed.*, **2013**, 52, 874.

TOPIC 1. Synthesis and characterisation of Gold(III) alkene complexes

INTRODUCTION

Platinum(II) olefin complexes were amongst the first organometallic complexes ever to be reported. The very first example, known as Zeise's salt, $K[Pt^{II}Cl_3(C_2H_4)]$, was published as early as 1827 and was obtained serendipitously by refluxing an ethanol solution of $H_2[PtCl_6]$ in the presence of KCl .⁴³ Since early on it was recognised that complexation of an olefin to a metal centre leads to significant activation of the C=C bond, as illustrated by the Dewar-Chatt-Duncanson model^{210a,b} and this feature was further explored in metal mediated olefin transformations.²⁰⁸

Olefin complexes of gold(I) were isolated and structurally characterised in the 1970s and 1980s by Hüttel and others,^{47,208} and the first arene complexes of gold(I) were recently reported.⁴⁶ Since the mid-1990s the interest in π -complexes of gold underwent significant growth²⁰⁸ due to their involvement as active catalytic species in gold mediated transformation of olefins.³⁹ Most of these transformations propose the coordination of gold to the olefin as a first step of activation, followed by nucleophilic attack on the coordinated olefin and subsequent protodeauration to liberate the functionalised substrate and regenerate the catalyst.^{30a} (See Scheme 41)



Scheme 41. General scheme for gold mediated activation of olefins

In the case of gold(III), which is isoelectronic and isostructural to platinum (II), a number of organic transformations of olefins propose gold π -complexes, most notably gold alkene and alkyne complexes as key intermediates.^{27,30} Nevertheless, surprisingly, no alkene, alkyne or arene complexes of gold(III) have been isolated and characterised.²⁰⁸ Earlier attempts to generate π -complexes of gold involved treating gold(III) halides directly with olefins, but a

gold π -complex could not be identified and the outcome of the reactions was invariably reduction to gold(I) or gold metal.²⁰⁹ Claims of the synthesis of a $\text{AuCl}_3(\eta^2\text{-1,5-cyclooctadiene})$ by reacting HAuCl_4 with 1,5-cyclooctadiene^{210c} have been contested.^{208,210c} Nevertheless, gas phase calculations suggest that the formation of a $\text{AuCl}_3(\eta^2\text{-C}_2\text{H}_4)$ complex would be exothermic,²¹³ while the formation of a neutral gold(III) acetylene complex, $\text{AuCl}_3(\eta^2\text{-C}_2\text{H}_2)$ complex would be endothermic. A comparison between bond dissociation energies in Au(I) and Au(III) ethylene and acetylene complexes and relative calculated Au—C and C—C bond lengths is depicted in Table 16.

Table 16. Bond dissociation energies (kJ mol^{-1}) for gold ethylene and acetylene complexes

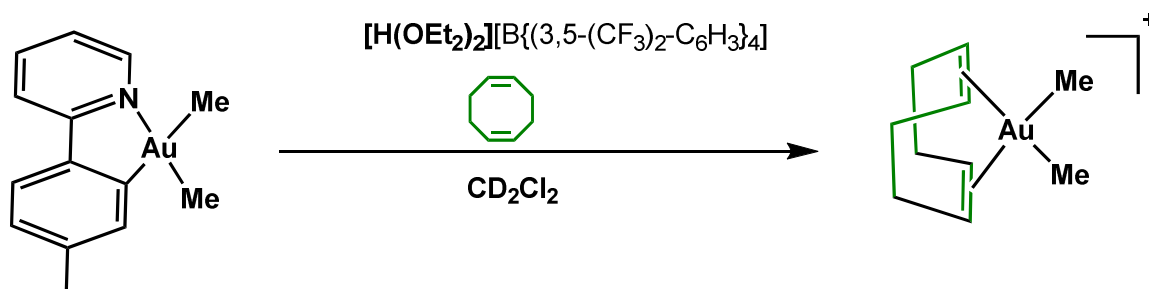
Complex	BDE	d(C, C) (Å)	d(Au,C) (Å)	Reference
C_2H_4	—	1.31(1)	—	213
$[(\eta^2\text{-C}_2\text{H}_4)\text{Au}^{\text{I}}]^+$	-259 to -297			213a
$[(\eta^2\text{-C}_2\text{H}_4)\text{Au}^{\text{I}}\text{Cl}]$	-161	1.382	2.248	213b
$(\eta^2\text{-C}_2\text{H}_4)\text{Au}^{\text{III}}\text{Cl}$	-33.1	1.377	2.364	213b
C_2H_2	—	1.202(3)	—	213b
$(\eta^2\text{-C}_2\text{H}_2)\text{Au}^{\text{I}}\text{Cl}$	-143	1.235	2.221	213b
$(\eta^2\text{-C}_2\text{H}_2)\text{Au}^{\text{III}}\text{Cl}_3$	+6.32	1.223	2.486	213b

We envisaged that since reduction of the Au(III) centre is a common pathway for the decomposition of organogold derivatives, stabilisation of a gold(III) olefin complex could be achieved if a ligand capable of blocking reductive elimination pathways is employed. We have shown that the tridentate diphenylpyridine ligand fulfils the stabilisation requirements and allowed us to isolate species that were previously considered to be too kinetically labile to be isolated such as gold(III) hydrides. (Chapter 2) We therefore decided to attempt to generate $\text{C}^{\wedge}\text{N}^{\wedge}\text{C}$ supported gold(III) cations in the presence of olefins in the hope of isolating gold(III) olefin complexes.

The present section presents the synthesis and NMR characterisation of a gold(III) norbornene complex which is the first example of a gold(III) olefin complex unambiguously characterised in solution. The reactivity of the complex with nucleophiles such as water is also explored.

After the publication of this work, Tilset *et al.* reported the first example of a crystallographically characterised cationic gold(III) alkene complex, $[(\eta^4\text{-1,5-cyclooctadiene})\text{AuMe}_2]^+$.²¹⁴ The complex was prepared by the protolysis of a Au—C bond in a $(\text{PhPy})\text{AuMe}_2$ complex in the presence of COD. (Scheme 42) Upon coordination, each olefin C=C bond is asymmetrically bonded to Au such as one Au—C bond is significantly

longer than the other. The C=C bonds in COD are also only slightly elongated upon coordination (1.364(5) and 1.348(5) in the η^4 -COD gold complex vs. 1.340(3) in free COD).



Scheme 42 Preparation of $[(\eta^4\text{-1,5-cyclooctadiene})\text{AuMe}_2]^+{}^{214}$

RESULTS AND DISCUSSION

4.T1.1 Initial attempts – SMe_2 reactions

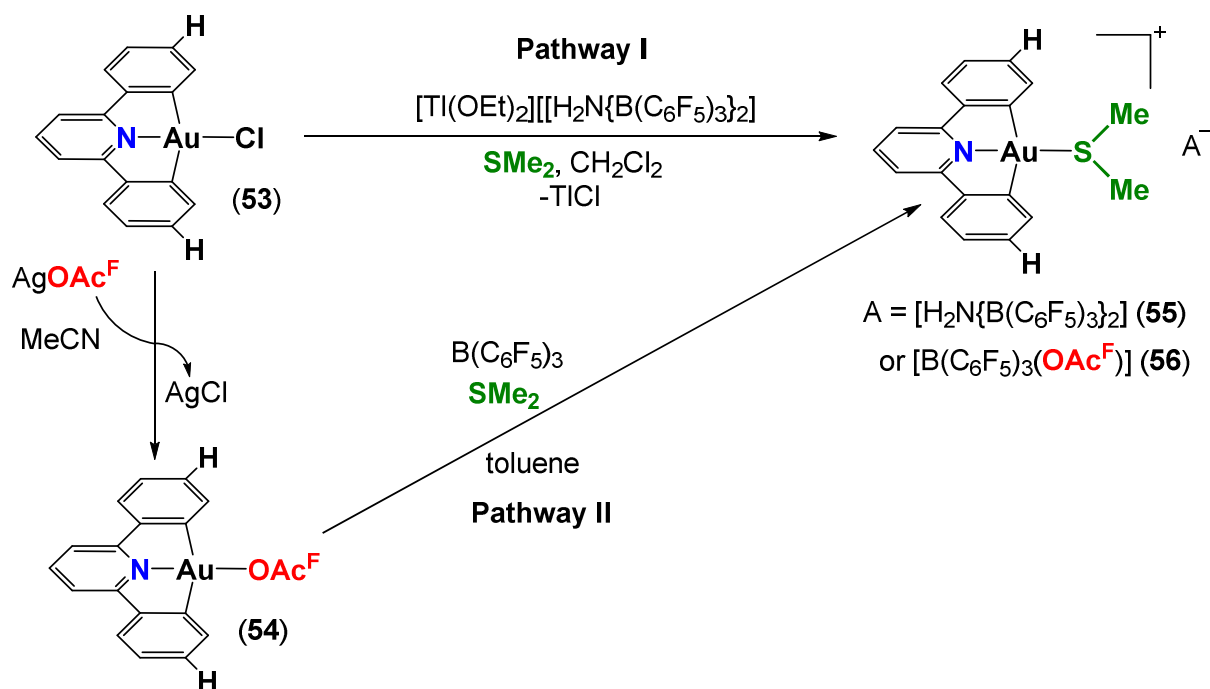
Initial attempts were made to generate gold(III) cations in the presence of weak σ -donors which can act as neutral ligands. For our initial studies, due to its commercial availability, the non-substituted 2,6-diphenylpyridine ligand was used as a cyclometallating ligand for gold(III) centres. The $(\text{C}^{\wedge}\text{N}^{\wedge}\text{C})^{\text{H}}\text{AuCl}$ (**53**) where $(\text{C}^{\wedge}\text{N}^{\wedge}\text{C})^{\text{H}}$ denotes the non-substituted diphenylpyridine ligand, was prepared in an analogous fashion to the *tert*-butyl substituted phenylpyridine supported $(\text{C}^{\wedge}\text{N}^{\wedge}\text{C})\text{AuCl}$ (**3**) following a published protocol.⁵⁰

In order to abstract the chloride ligand, two possible pathways were explored: (i) a one step chloride abstraction with thallium(I) or silver salts of non-coordinating anions in the presence of SMe_2 to give the adduct **55** (Pathway I) and (ii) a two step pathway where the chloride ligand would be removed by the silver salt of a coordinating anion such as trifluoroacetate, to give the gold(III) trifluoroacetate complex (**54**), followed by trifluoroacetate group abstraction by $\text{B}(\text{C}_6\text{F}_5)_3$ in the presence of SMe_2 to give the gold-dimethyl sulphide adduct **56** (Pathway II). (Scheme 43)

While both pathways ultimately proved to be efficient to generate gold(III) cations, the chloride removal reaction proved to be the rate determining step which resulted in long reaction times (> 48 h). The reduced solubility of $(\text{C}^{\wedge}\text{N}^{\wedge}\text{C})^{\text{H}}\text{AuCl}$ **53** in the reaction solvent (CH_2Cl_2) also contributed to the slow reaction rates. In order to optimise the reaction, heating the reaction mixtures was attempted. In the case of Pathway I, heating the gold chloride (**53**) in the presence of the thallium(I) amidodiborane salt²¹⁵ and SMe_2 yielded a

mixture of products probably as a result of the thermal instability of the resulting cationic product **55**.

On the other hand, heating mixtures of the $(C^{\wedge}N^{\wedge}C)^H AuCl$ (**53**) and $AgOAc^F$ at 40 °C for 16 h resulted in clean conversions to the gold trifluoroacetate $(C^{\wedge}N^{\wedge}C)^H Au(OAc^F)$ (**54**). No side products were observed, probably due to the greater thermal stability of **54** when compared to the dimethyl sulphide adducts. The subsequent trifluoroacetate group abstraction by $B(C_6F_5)_3$ in the presence of SMe_2 instantaneously generates the gold-dimethylsulphide adduct **55** as observed by 1H NMR spectroscopy. In this respect, Pathway II was preferred to generate gold(III) olefin complexes by employing alkenes as neutral ligands.



Scheme 43 Pathways for the synthesis of gold(III) dimethylsulphide adducts

Complexes **54** – **56** have been characterised by 1H NMR spectroscopy and X-ray crystallography. The dimethylsulphide adducts **55** and **56** display a characteristic singlet for the SMe_2 group at δ_H 3.23 (CD_2Cl_2) which is shifted downfield from the one of ‘free’ dimethylsulphide (δ_H 2.37, CD_2Cl_2). The ^{19}F NMR spectrum of **56** also suggests a 1:1 ratio between the resonances corresponding to the CF_3 group of OAc^F (δ_F -76.94) and the resonances of the C_6F_5 groups in $B(C_6F_5)_3$ (See also Experimental, Chapter 5).

The trifluoroacetate **54** was recrystallised by slow evaporation of a CH_2Cl_2 solution at room temperature and its structure was determined by X-ray crystallography. The geometrical

parameters are very similar to the gold trifluoroacetate **4** bearing the *tert*-butyl substituted ($C^{\wedge}N^{\wedge}C$) ligand. The distance between two fluorine atoms (of the CF_3 groups) of neighbouring molecules is 2.910(3) Å, slightly shorter than the sum of the van der Waals radii (2.94 Å).⁸³ (Figure 55)

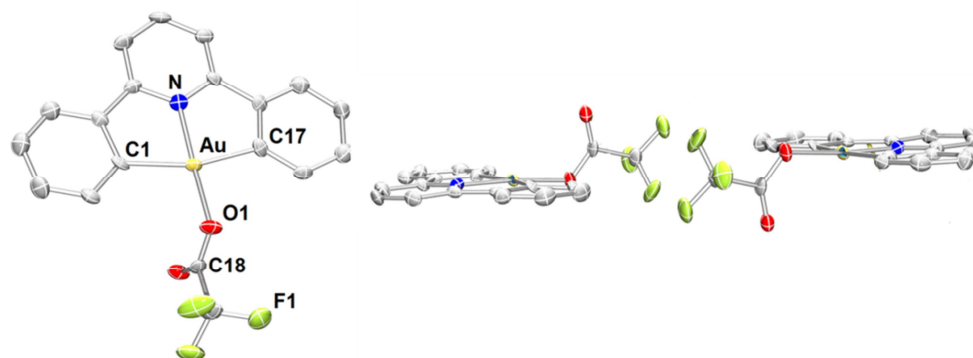


Figure 55 Molecular structure of $(C^{\wedge}N^{\wedge}C)^H Au(OAc^F)$ (**54**) (50% probability ellipsoids shown). Hydrogen atoms were omitted. Selected bond distances (Å) and angles ($^{\circ}$): Au—N 1.961(3), Au—C(1) 2.072(4), Au—C(17) 2.063(3), Au—O1 2.025(4), N—Au—O(1), 174.99 (23) C1—Au—C17 162.97(41). (left) F...F contacts between the CF_3 groups of neighbouring molecules. (right)

Both gold(III) dimethylsulfide adducts **55** and **56** were recrystallised by layering CH_2Cl_2 solutions with light petroleum (1:1). The geometrical parameters for the $[(C^{\wedge}N^{\wedge}C)^H Au(SMe_2)]^+$ fragment in **55** and **56** are very similar having the Au—S distances of 2.294 Å and (C18)—S(1)—C(19) angle of 99° , which is typical for R_2S fragments. (Fig. 56).

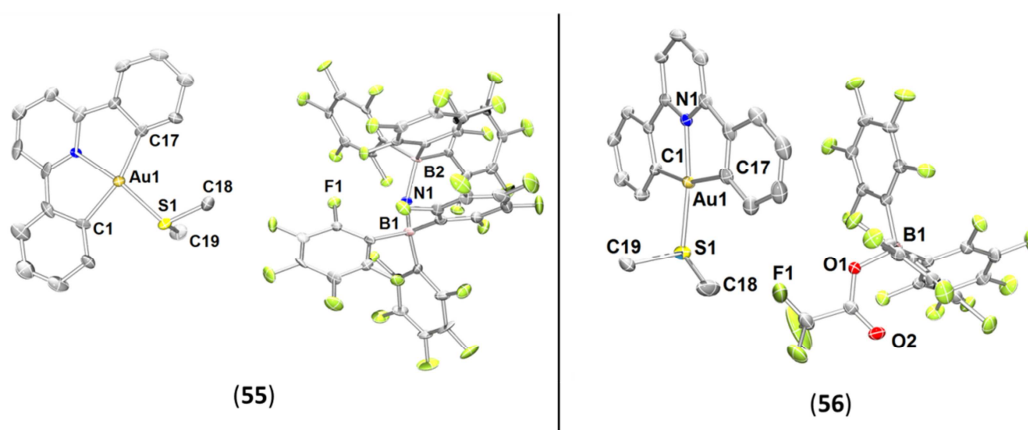
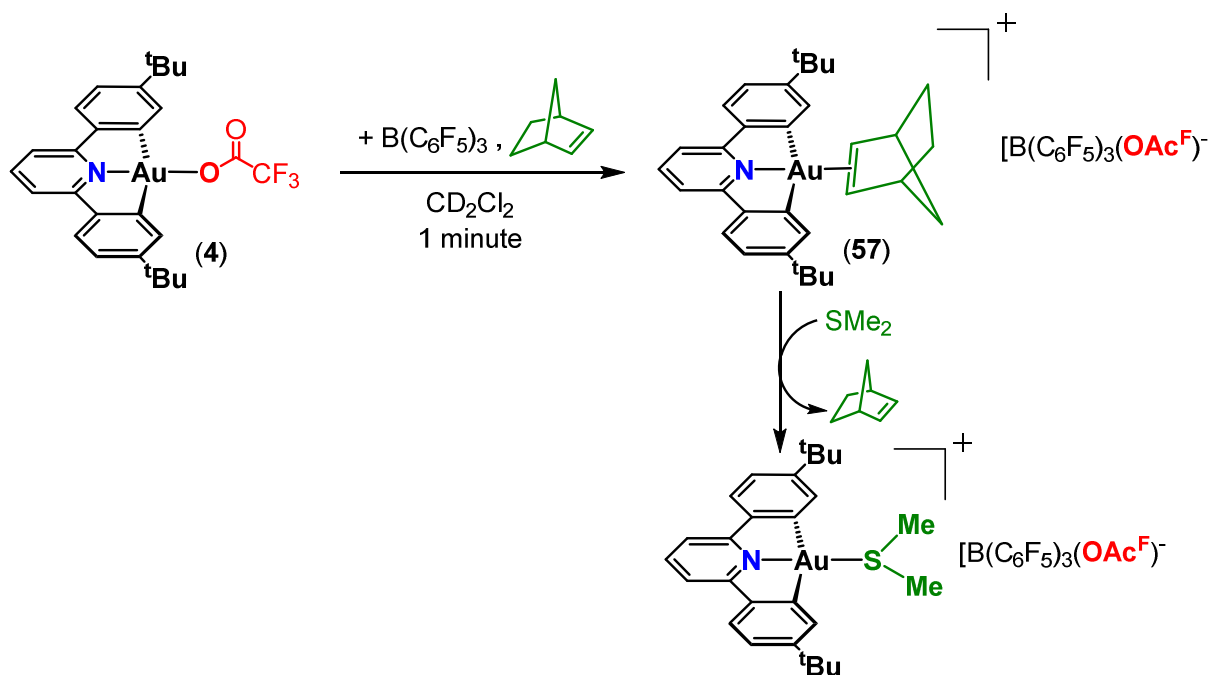


Figure 56 Molecular structure of $[(C^{\wedge}N^{\wedge}C)^H Au(SMe_2)][A]$ where $A = H_2N\{B(C_6F_5)_3\}_2$ (**55**· CH_2Cl_2) and $(OAc^F)\{B(C_6F_5)_3\}$ (**56**) (50% probability ellipsoids shown). Hydrogen atoms and solvent molecules were omitted. Only one of the two molecules in the asymmetric unit shown. Selected bond distances (Å) and angles ($^{\circ}$) **55** : Au(1)—N(1) 1.984(6), Au—C(1) 2.071(10), Au—C(17) 2.093(8), Au—S1 2.293(2), N(1)—Au(1)—S(1), 170.10 (19) C1—Au—C17 163.2(3), C(18)—S(1)—C(19) 98.2(6) . **56** : Au—N 2.003(3), Au—C(1) 2.102(4), Au—C(17) 2.081(3), Au—S1 2.2978(9), N—Au—S(1), 170.31 (9) C1—Au—C17 162.87(51) , C(18)—S(1)—C(19) 100.10(19).

4.T1.2 Reactions with olefins

Since tridentate diphenylpyridine ligands are able to stabilise gold(III) cations in the presence of weak σ -donors, we decided to generate gold(III) cations *via* Pathway II (Scheme 41) in the presence of alkenes. Cyclic alkenes are known to have an enhanced ability to coordinate to a metal centre due to their ring-strain²¹⁶ which upon coordination is released. Coordination ability is also enhanced by the pyramidalisation of the alkene carbon atom which is accompanied by a decrease in energy of the LUMO π^* and an increase in energy of the HOMO π . In this respect, norbornene was chosen for the initial tests. The diphenyl pyridine ligand seems suitable for the stabilisation of a gold(III) olefin complex since the ligand *trans* to the $(\eta^2\text{-olefin})\text{Au}$ fragment would be pyridine which only exerts a moderate *trans* influence. Since the substituted 2,6-bis(4-*t*BuC₆H₃)₂ pyridine supported trifluoroacetate shows better solubility in the reaction solvent (CD₂Cl₂), (C[^]N[^]C)Au(OAc^F) **4** was further chosen as the starting gold precursor.

Therefore, treating a mixture of (C[^]N[^]C)Au(OAc^F) **4** and norbornene (1.2 eq) in CD₂Cl₂ with B(C₆F₅)₃ instantly gave rise to a new compound which we formulate as the cationic gold(III)-norbornene complex **57** as observed by ¹H NMR spectroscopy. (Scheme 44) We also noted that adding B(C₆F₅)₃ to (C[^]N[^]C)Au(OAc^F) **4** solutions in CD₂Cl₂ at room temperature without norbornene or any other ligands present gives rise to a complicated ¹H NMR spectrum consisting of broad, undefined resonances. We therefore rationalise that the reaction solvent alone (CD₂Cl₂) is not capable of stabilising the [(C[^]N[^]C)Au]⁺ cation at room temperature, even though stabilisation can be achieved below -20 °C to give the dichloromethane adduct [(C[^]N[^]C)Au(CH₂Cl₂)]⁺.⁸⁰



Scheme 44 Synthesis of **57** and reaction with SMe₂

Upon addition of B(C₆F₅)₃ to a mixture of **4** and norbornene, an immediate change in the ¹H NMR pattern of the (C[∧]N[∧]C) ligand was observed. Most notably, the doublet resonance corresponding to the protons attached to the α-Carbon atom with respect to the gold centre (Red in Figure 57 and expansion) is significantly shifted downfield ($\Delta\delta_{\text{H}} = 0.9$). A downfield shift is also observed for the resonance corresponding to the *tert*-butyl groups ($\Delta\delta_{\text{H}} = 0.11$).

Upon coordination, the chemical shift of the olefinic signals of norbornene in **57** does not change significantly when compared from the one in ‘free’ norbornene (H^a in Figure 57). The chemical shift of H^a is influenced both by the π-donation of the olefin to the cationic gold centre and also by the back-donation from the metal centre to the π* (LUMO) of the norbornene. Since the change is negligible, it is assumed that both the π-donation and back donation cancel each other out (see also subsequent discussion). Unequivocal evidence for coordination could be provided by the chemical shift of the protons in the 5- and 6- positions (H^c) which display a pronounced downfield shift ($\Delta\delta_{\text{H}} = 0.72$ for H^c) in complex **57** when compared to free norbornene. A similar shift is also observed for the bridgehead protons (H^b) which are shifted downfield upon coordination ($\Delta\delta_{\text{H}} = 0.42$). (Table 17, Entries 1 and 3; Figure 57)

The olefin is readily displaced by SMe₂: the reaction of [(C[∧]N[∧]C)Au(η²-C₇H₁₀)]⁺ **57** with SMe₂ instantly produces [(C[∧]N[∧]C)Au(SMe₂)]⁺ together with free norbornene as established by ¹H NMR spectroscopy. (Scheme 44)

The difference in chemical shift of the olefinic protons ($\Delta\delta_{\text{H}}$) alongside the shift in olefinic carbon atoms ($\Delta\delta_{\text{C}}$) has been proposed to be diagnostic of the extent of π -back donation in Pd, Pt²¹⁷ and Au(I) complexes.^{210,218} Thus, a higher degree in back-donation results in olefinic protons further being shifted upfield. This correlation is also supported by computational studies.^{210,218} In this respect, upon comparing the spectroscopic data for the olefinic protons in coordinated norbornene to gold centres in **57** ($\Delta\delta_{\text{H}} = -0.03$, Table 17, entry 6) with the data from platinum(II) complexes ($\Delta\delta_{\text{H}} -1.94$, Table 17, entry 5),²¹⁹ it can be inferred that back donation from platinum(II) complexes is significantly greater than in gold(III) complexes. This trend has also been confirmed by DFT studies performed by Tilset *et al.* on $[\text{Me}_2\text{Au}(\eta^4\text{-COD})]^+$ and $[\text{Me}_2\text{Pt}(\eta^4\text{-COD})]$ complexes.^{214,220} Since back donation contributes significantly to the stability of the metal-(η^2 -alkene) bond, it can be inferred that platinum(II)-olefin complexes should have increased stability when compared to their gold(III) analogues. This is indeed verified by the fact that while platinum(II) olefin complexes are known to be thermally stable, and are in fact the first metal olefin complexes to be isolated, the gold(III) norbornene complex **57** shows limited stability in solution and noticeable decomposition is observed after 12 h. The limited stability of gold(III) olefins in solution at room temperature was also observed by Tilset *et al.* in a subsequent study on $[\text{Me}_2\text{Au}(\eta^4\text{-COD})][\text{OTf}]$ complexes.²¹⁴

Table 17. Comparison of chemical shifts (δ_{H} , CD_2Cl_2) of coordinated norbornene in selected gold(I), silver(I), platinum (II) and gold (III) cationic complexes

Entry	Complex	H^a	$\Delta\delta_{\text{H}}(\text{H}^a)$	H^c	H^b	Ref
1	'free' norbornene	5.99	-	2.84	1.61	-
2	$[\text{Ag}(\eta^2\text{-C}_7\text{H}_{10})_3]^+$	6.42	+0.43	3.20	1.77	221
3	$[\text{Au}(\eta^2\text{-C}_7\text{H}_{10})_3]^+$	5.53	-0.46	3.30	1.88	221
4	$[(\text{IPr})\text{Au}(\eta^2\text{-C}_7\text{H}_{10})]^+$	5.71	-0.28	2.90	2.40	222
5	$[\text{PtH}(\eta^2\text{-C}_7\text{H}_{10})(\text{PEt}_3)_2]^+$	4.05	-1.94	2.99	2.13	219
6	$[(\text{C}^{\wedge}\text{N}^{\wedge}\text{C})\text{Au}(\eta^2\text{-C}_7\text{H}_{10})]^+$ 57	5.96	-0.03	3.56	2.03	This work

$$\Delta\delta_{\text{H}} = \delta_{\text{H}}(\text{metal-norbornene complex}) - \delta_{\text{H}}(\text{free norbornene})$$

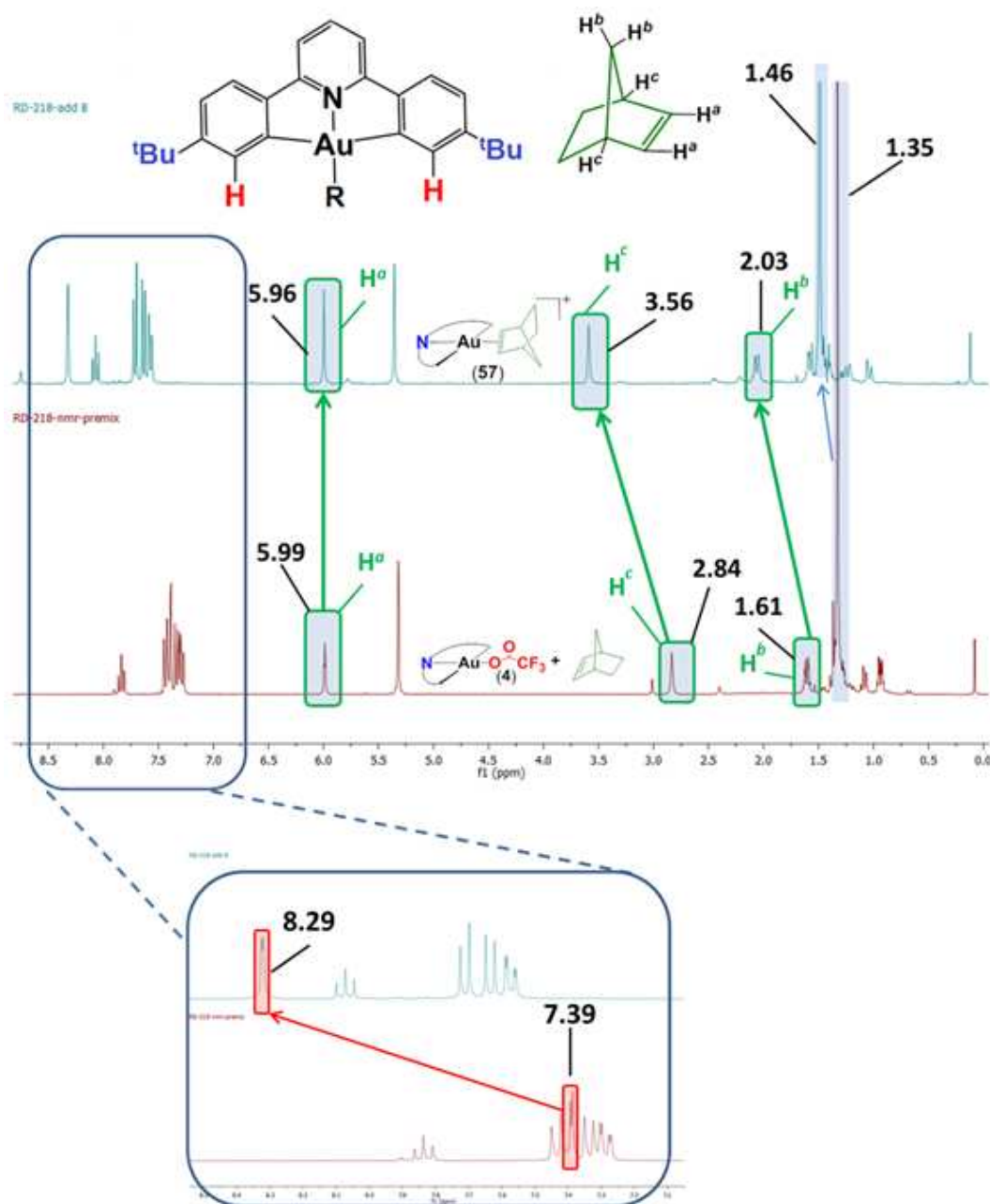


Figure 57 ^1H NMR spectra (300 MHz, RT, CD_2Cl_2) of a mixture of $(\text{C}^{\wedge}\text{N}^{\wedge}\text{C})\text{Au}(\text{OAc}^{\text{F}})$ **4** and norbornene (red) and of complex **57** (blue). R = OAc^{F} or norbornene

In a continuation of this work,²²³ Dr Nicky Savjani in our group showed that the same protocol that afforded the generation of $[(\text{C}^{\wedge}\text{N}^{\wedge}\text{C})\text{Au}(\eta^2\text{-C}_7\text{H}_{10})][(\text{OAc}^{\text{F}})\{\text{B}(\text{C}_6\text{F}_5)_3\}]$ **57** can also be used to generate the ethylene and cyclopentene complexes which, after subsequent solvent evaporation, were washed with light petroleum and isolated as solids. By performing ^1H NMR studies on the gold(III) norbornene, cyclopentene and ethylene complexes we established that while the norbornene complex is stable for hours at room temperature, the cyclopentene complex is stable up to 0°C and the ethylene complex shows signs of decomposition above -20°C . This observation is consistent with the fact that norbornene is a

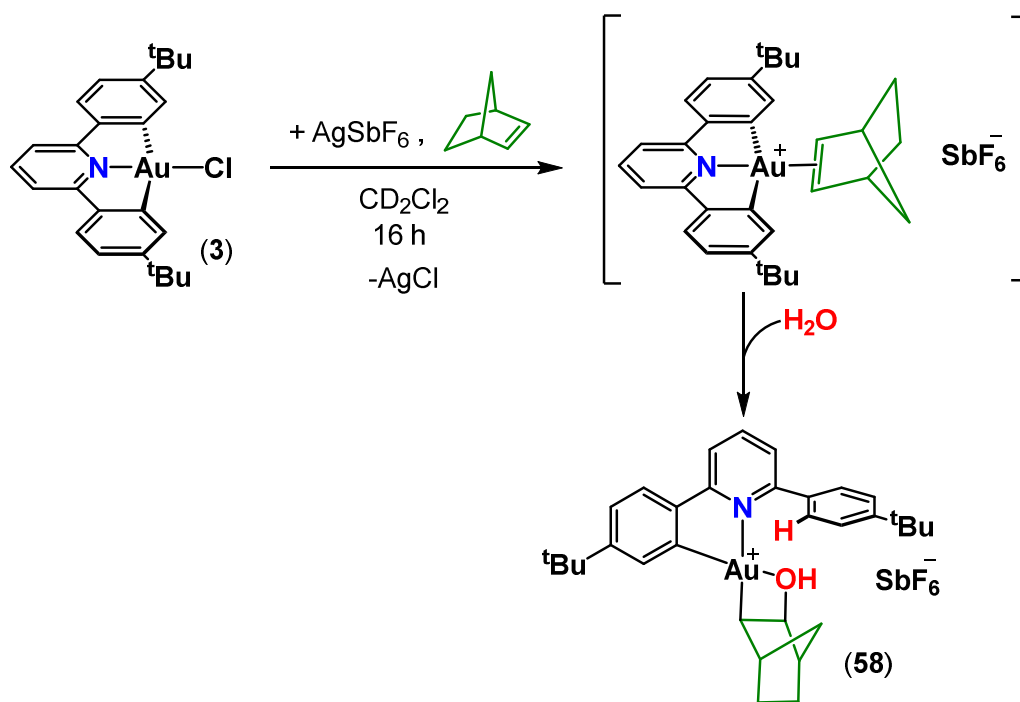
better π -acceptor than cyclopentene and both coordinate to the metal centre more strongly than ethylene due to the release of ring strain upon coordination. The strong coordination is also revealed by ^1H NMR titration experiments where adding an excess of free olefin does not promote exchange between free and coordinated olefin. In contrast, the gold(III) ethylene complex is more thermally and kinetically labile and olefin exchange between free and coordinated ethylene was observed over the temperature range of -70 to -10 $^\circ\text{C}$.

4.T1.3 Olefin Hydration

Attempts to obtain crystallographic confirmation of the complex $[(\text{C}^{\wedge}\text{N}^{\wedge}\text{C})\text{Au}(\eta^2\text{-C}_7\text{H}_{10})][(\text{OAc}^{\text{F}})\{\text{B}(\text{C}_6\text{F}_5)_3\}]$ **57** were so far unsuccessful. Since the anion can have an effect on packing modes in the crystal lattice, in an attempt to obtain single crystals of the cationic gold olefin complex we decided to generate the complex $[(\text{C}^{\wedge}\text{N}^{\wedge}\text{C})\text{Au}(\eta^2\text{-C}_7\text{H}_{10})](\text{SbF}_6)$ by chloride abstraction from $(\text{C}^{\wedge}\text{N}^{\wedge}\text{C})\text{AuCl}$ **3** in the presence of AgSbF_6 and norbornene.

Treating a mixture of $(\text{C}^{\wedge}\text{N}^{\wedge}\text{C})\text{AuCl}$ **3** and norbornene in CH_2Cl_2 with AgSbF_6 under the exclusion of light rapidly gave rise to a white precipitate (AgCl). After the removal of the precipitate by filtration, the solution was concentrated under vacuum, layered with light petroleum and stored at low temperature (-20 $^\circ\text{C}$). The resulting white crystalline blocks were then subjected to an X-ray diffraction study which revealed the structure of compound as the cationic gold norbornolyl complex **58**. (Scheme 45 and Figure 58)

A plausible route for the formation of **58** involves the initial coordination of norbornene to gold to give a cationic gold norbornene complex which would be susceptible to nucleophilic attack. Subsequent reaction with adventitious water led to a nucleophilic attack of HO^- on the coordinated norbornene while the gold—phenyl bond was protolysed. We have observed cleavage of the gold—phenyl bond in neutral $(\text{C}^{\wedge}\text{N}^{\wedge}\text{C})$ supported gold complexes but the reaction proceeded only with strong acids such as HOAc^{F} while weaker acids such as HOAc left the starting material unchanged. (See Chapter 1)



Scheme 45 Reaction of the gold(III) norbornene complex with H₂O to give the gold norbornolyl **58**.

While a number of transition metals, including Au(I)^{30,224} and Au(III)²²⁵ have proved to be efficient catalysts in alkyne or allene hydration reactions, alkene hydration still remains a challenging topic in terms of activity and selectivity.²²⁶ Often reaction protocols for alkyne hydration are not efficient for alkene hydration reactions.³⁰ Nevertheless, heavy metal (Hg, Tl, Pb) mediated alkene hydration reactions are well known, and β -hydroxyalkyl metal complexes have been long proposed as key intermediates in this process.²²⁷ β -hydroxyalkyl palladium(II) complexes have also been proposed as intermediates in the Wacker process, but were considered too reactive to be isolated.²²⁸

Gold(I) mediated intermolecular alkene hydroalkoxylation has been reported²²⁹ and is proposed to follow the general mechanism depicted in Scheme 41 where the alcohol acts as nucleophile. The only example of a structurally characterised olefin activation intermediate by a gold(III) complex was reported by Cinellu *et al.*⁶⁸ where the double oxo bridged Au(III) [(bipy)Au(μ -O)₂]²⁺ oxidises norbornene to give rise to an auroxoetane. (See Chapter 1, Introduction)

In this respect, the gold(III) norbornolyl complex **58** represents the first structurally characterised water addition product to a gold(III) olefin complex. We do note however that solution characterisation of gold (III) β -hydroxyalkyl complexes obtained by addition of water to *in situ* generated gold(III)-propylene and gold(III)-ethylene complexes have also

recently been reported.²³⁰ In principle, in the case of **58**, the alkene hydration reaction should be capable of proceeding under catalytic conditions, provided of course that the Au—C bond can be efficiently protolysed. In practise however, it was shown for Au(I) that protodeauration is often the rate determining step in Au(I) mediated organic transformations and it is strongly dependent on the ligand *trans* to the Au—C bond.²³¹ For **58** we suspect however that the pyridine N-donor is not strong enough to facilitate Au—C bond cleavage. This is confirmed by the fact that bidentate (HC-N[^]C)Au(Ar)(OAc^F) complexes are stable for hours at room temperature in HOAc^F/CH₂Cl₂ solvent mixtures (1 : 2). (See Section 1.1)

The solid state structure of **58** (Figure 58) shows that the norbornolyl fragment is bonded through its *exo* face, as it is usually observed. The OH functional group coordinates to the gold centre and the Au—O distance (2.159(2) Å) is comparable to the one in other gold(III) bidentate (HC-N[^]C) complexes where the O-ligand is *trans* to a phenyl group (for example Au—O in (HC-N[^]C)Au(Me)(OAc^F) **26**: 2.112(2) Å). The hydrogen atom of the OH group was located on the difference density map and shows a strong interaction with the SbF₆ anion (H(111)—F(6) : 1.1817 Å, $\Sigma_{\text{vdw}}(\text{H}, \text{F})$: 2.67 Å). H···F distances smaller than the sum of the van der Waals radii (2.484- 2.647 Å) can also be measured between the fluorine atoms of SbF₆ and aromatic hydrogen atoms of the neighbouring (C[^]N[^]C) fragments. The Au—C(26) distance (2.049(3) Å) is typical for a Au—C bond *trans* to a pyridine ligand (for example Au—C in (HC-C[^]N)Au(Me)(OAc^F) **26**: 2.031(4) Å).

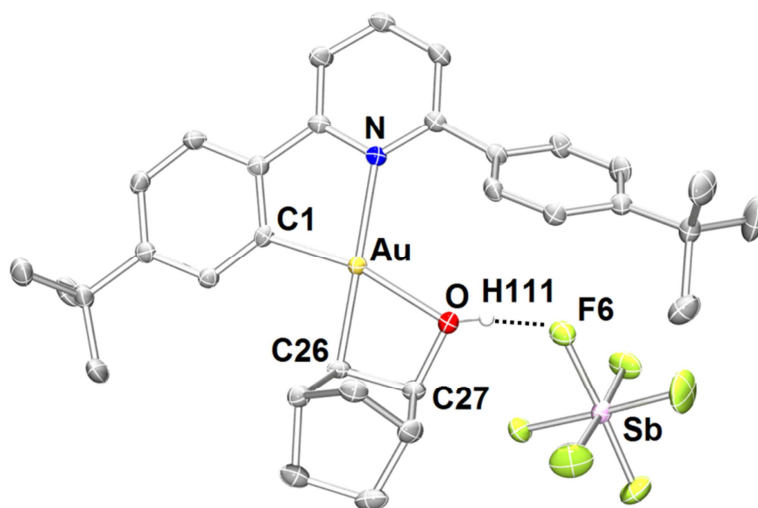


Figure 58 Molecular structure of **58** (50% probability ellipsoids shown). Hydrogen atoms (with the exception of the norbornolyl OH) were omitted. Selected bond distances (Å) and angles (°): Au—C(1) 1.995(3), Au—C(26) 2.049(3), Au—O(1) 2.159(2), Au—N 2.180(2), C(1)—Au—C(26) 98.23(11), C(1)—Au—O(1) 166.31(10), C(1)—Au—N 81.20(10), N—Au—C(26) 176.26(10), O(1)—Au—N 112.42(8)

This work was continued by Dr Nicky Savjani who showed that methanol can also act as a nucleophile and its reaction with $[(C^{\wedge}N^{\wedge}C)Au(\eta^2-C_7H_{10})][{(OAc)^F}\{B(C_6F_5)_3\}]$ **57** generated the gold(III) norbornyl methyl ether derivative which is an analogue of the norbornolyl complex **58**.²²³

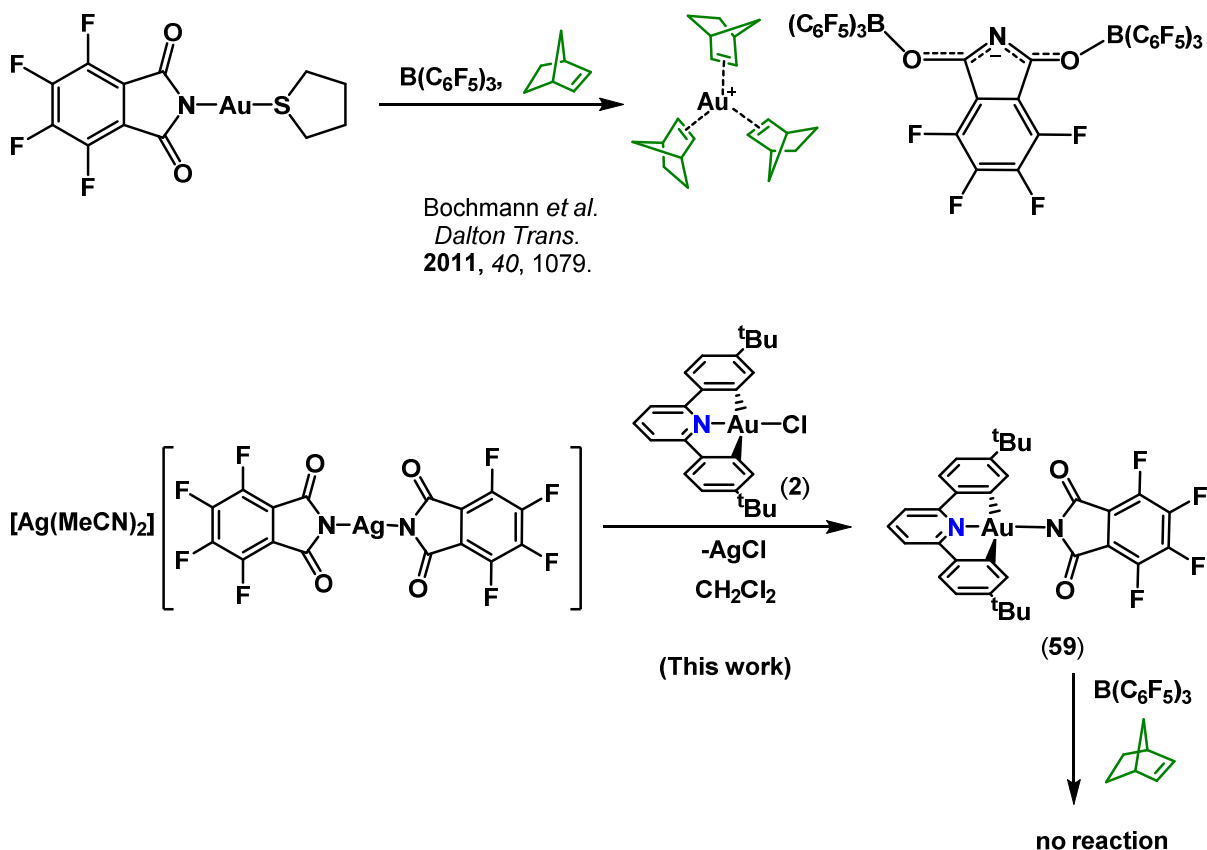
4.T1.4 Attempted Phthalimide Route

In order to obtain crystallographic confirmation for the $[(C^{\wedge}N^{\wedge}C)Au(\eta^2-C_7H_{10})]^+$ we envisaged that replacing the $[(B(C_6F_5)_3)(OAc)^F]$ with perfluorophthalimido-bridged diborane anion $[(B(C_6F_5)_3)_2(^F\text{phthalimide})]^-$ would aid the crystallisation of the resulting complex. Since the perfluorophthalimide fragment is essentially flat, it may allow better packing in the crystal lattice. This approach was previously used successfully to generate a gold(I) trisnorbornene complex $[Au^I(\eta^2-C_7H_{10})_3][\{B(C_6F_5)_3\}_2(^F\text{phthalimide})]$ by $B(C_6F_5)_3$ mediated perfluorophthalimide abstraction from a Au(I) centre in the presence of norbornene.²³² (Scheme 46, top)

In this respect, the Au(III) phthalimido $(C^{\wedge}N^{\wedge}C)Au(^F\text{phthalimide})$ **59** was synthesised by reacting the $(C^{\wedge}N^{\wedge})AuCl$ **3** with the silver salt of the perfluorophthalimide. (Scheme 46, bottom) The identity of the phthalimido complex **59** was confirmed by 1H and ^{19}F spectroscopy. (See Experimental, Chapter 5)

The phthalimido complex **59** was then treated with $B(C_6F_5)_3$ in the presence of norbornene in an attempt to generate the complex $[(C^{\wedge}N^{\wedge}C)Au(\eta^2-C_7H_{10})][\{B(C_6F_5)_3\}_2(^F\text{phthalimide})]$. A 1H and ^{19}F NMR investigation of the reaction mixture after 24 h revealed that no reaction had occurred and the starting materials were unchanged. It is known that while gold(I) is considered a 'soft' metal and binds nitrogen donor ligands (hard ligands) more weakly, gold(III) is harder according to the HSAB theory and thus would bind nitrogen donor ligands better.

Our observation therefore confirms that the Lewis acid $B(C_6F_5)_3$ is not strong enough to abstract the perfluorophthalimido ligand from $(C^{\wedge}N^{\wedge}C)Au(^F\text{phthalimide})$ **59**. (Scheme 46)



Scheme 46 Abstraction of the perfluorophthalimido ligand from Au(I) centres in the presence of norbornene (top) and synthesis of the perfluorophthalimido gold(III) complex **59** and attempted reaction with $\text{B}(\text{C}_6\text{F}_5)_3$ in the presence of norbornene (bottom).

CONCLUDING REMARKS AND PERSPECTIVES

We have shown that gold(III) olefin complexes can be efficiently generated in solution and are stable enough to be characterised, provided the gold(III) centre is efficiently stabilised. Based on ^1H NMR characterisation of the $[(\text{C}^{\wedge}\text{N}^{\wedge}\text{C})\text{Au}(\eta^2\text{-norbornene})]^+$ complex and on the small difference in chemical shift of the olefinic resonances between the coordinated and free norbornene we suggest that π -back donation from gold to the π^* MO of norbornene is less strong than in platinum(II) cationic complexes. The observation correlates directly with the reduced thermal stability of the gold olefin complexes when compared to the platinum(II) analogues.

Upon coordination, norbornene is susceptible to nucleophilic attack which was demonstrated by the crystallographic characterisation of a gold(III) norbornolyl complex. The gold β -hydroxylalkyl complex is stable towards further protolysis which precludes the olefin hydration reaction to proceed under catalytic conditions.

Attempts to obtain crystallographic confirmation for the $[(C^{\wedge}N^{\wedge}C)Au(\eta^2\text{-norbornene})]^+$ complex led us to investigate whether phthalimide displacement from a gold(III) centre in the presence of $B(C_6F_5)_3$ and norbornene would be a viable route for the synthesis of a Au-olefin complex that could be recrystallised. Our studies showed that despite the fact that this type of reaction proceeds smoothly for Au(I), $B(C_6F_5)_3$ is not Lewis acidic enough to displace a N-donor from a gold(III) centre.

Since gold(III) olefin complexes are often proposed as important intermediates in various catalytic cycles where ligand exchange reactions play a key role as a means of achieving selectivity, competition studies involving a variety of olefins and binding affinity studies are highly desirable.^{222,233} In particular, the olefin exchange reaction rates and reaction mechanism would shed more light in the nature of the gold(III) olefin interactions.

TOPIC 2: Gold azides

INTRODUCTION

Homoleptic anionic gold azides of the type $[Au(N_3)_2]^-$ and $[Au(N_3)_4]^-$ have been long known and have variable stability to detonation depending on the stabilising cation employed.²³⁴ In the case of gold(I), neutral heteroleptic complexes such as the phosphine supported R_3PAuN_3 have been reported as early as the 1970s²³⁵ as stable, non-explosive solids and their structure has been probed by IR spectroscopy where they display strong characteristic asymmetric ($2020 - 2060\text{ cm}^{-1}$) and symmetric ($1150\text{-}1300\text{ cm}^{-1}$) stretching frequencies. (Figure 59) Alongside the recently developed carbene supported analogues,^{236,237} the usefulness of gold(I) azides in building molecular architectures has been demonstrated in 'click' reactions with organic terminal acetylenes or isonitriles to give gold(I) C-triazoles or tetrazoles, in the absence of a catalyst.²³⁸

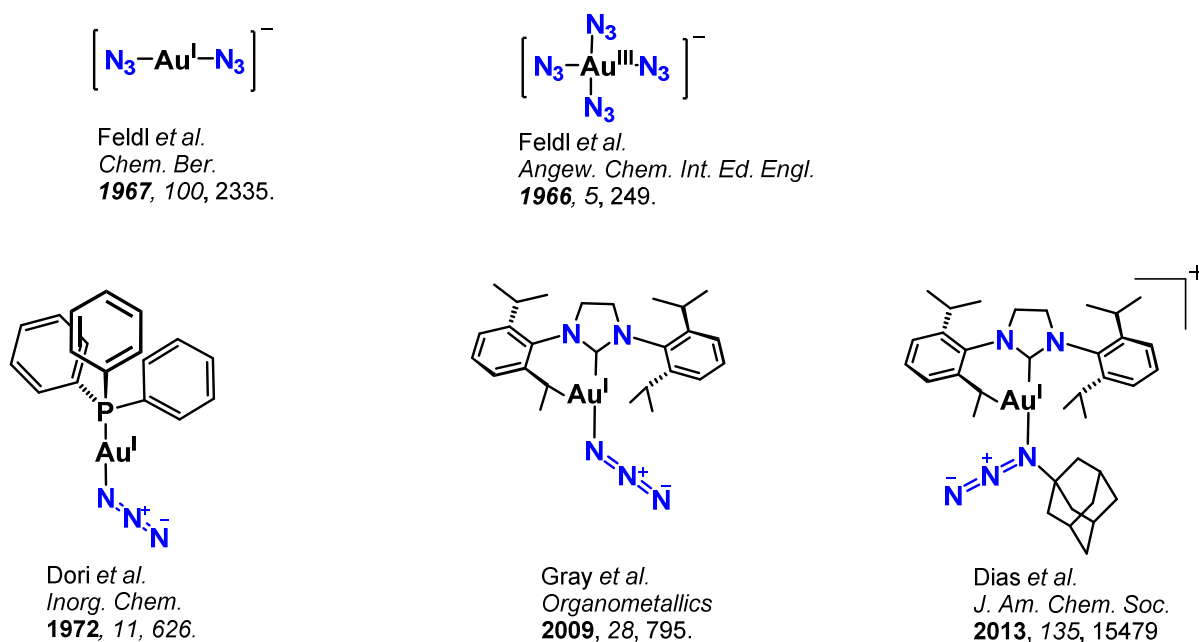
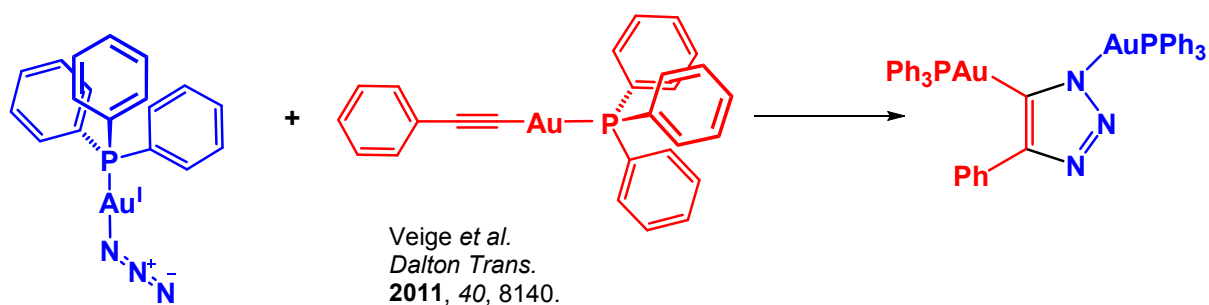


Figure 59 Homoleptic anionic Au(I) and Au(III) azides (top) and heteroleptic gold(I) azides (bottom)

Veige *et al.* also extended the cycloaddition ‘click’ reactions of gold(I) azides to metal acetylides and demonstrated that gold(I) azides are capable of reacting with gold acetylides to give di-gold functionalised triazoles in quantitative yields.²³⁹ (Scheme 47)



Scheme 47. Inorganic version of the click reaction (*iClick*) between gold(I) azides and gold(I) acetylides

Phosphine supported gold(I) azides can also perform cycloaddition reactions with nitrosonium cations to give rise to gold supported oxatetrazoles which immediately decompose to N_2 and N_2O to generate a ‘naked’ gold cation which can be trapped by a nucleophile such as a porphirin.²⁴⁰

Since previous work on gold(I) azides show that usually heteroleptic complexes are safer to manipulate and display interesting chemistry, we decided to employ the tridentate (C[^]N[^]C) pincer ligand to stabilise heteroleptic gold(III) azides, which to the best of our knowledge are so far not described. This section summarises our results in the synthesis of the first heteroleptic gold(III) azide. We also report the synthesis and initial reactivity studies of nitrosonium ions towards a carbene supported gold(I) azide.

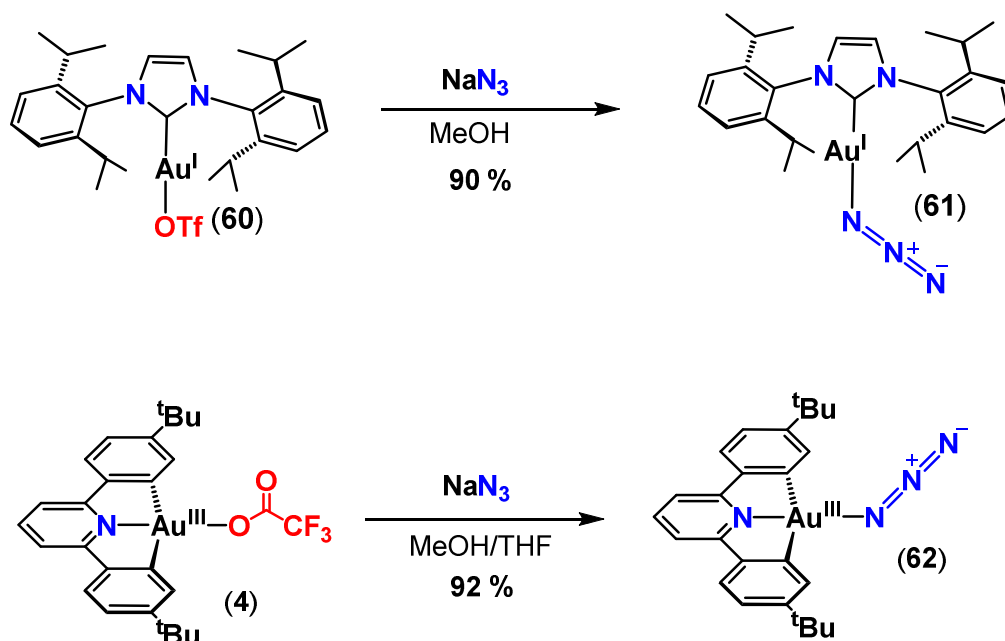
RESULTS AND DISCUSSION

4.T2.1. Synthesis and characterisation of Au(I) and Au(III) azides

The gold azides **61** and **62** were prepared by salt metathesis reactions from the corresponding gold(I) triflate **60**¹⁵³ and gold(III) trifluoroacetate **4**, respectively. In both cases the azides precipitate from the reaction mixtures enabling their isolation in nearly quantitative yields. (Scheme 48) In a separate attempt, Dr Dan Smith obtained the gold(III) azide **62** by reacting the dimethylsulphide adduct [(C[^]N[^]C)Au(SMe₂)](OTf) with NaN₃ in methanol.

Carbene and phosphine supported gold(I) azides have been known and studied (see Topic 2, Introduction in this Chapter) and their reported protocols often involve reactions of the gold precursors with AgN₃ which is known to detonate easily,^{236a} or with (Me₃Si)N₃ which is expensive.^{236b} In this respect, our reported protocol for the synthesis of (IPr)AuN₃ **61** is simpler since it affords the isolation of the azide without subsequent purification and uses NaN₃ as an azide transfer agent.

The (C[^]N[^]C) supported Au(III) complex **62** represents, to the best of our knowledge, the only reported heteroleptic gold(III) azide. Compared to the [Au(N₃)₄]⁻ complexes which are known to detonate if not efficient stabilisation is provided by the cation, (C[^]N[^]C)AuN₃ is remarkably stable for at least 16 h even in refluxing THF solutions. No detonation was observed upon impact or irradiation with UV light (365 nm).



Scheme 48 Synthesis of gold(I) and gold(III) azides

Both gold(I) and gold(III) azides were characterised by NMR spectroscopy where the resonances corresponding to the supporting ligands (IPr for **61** and (C[^]N[^]C) for **62**) show a significant shift when compared to the starting materials while the pattern remains essentially the same. A diagnostic method for characterising azide complexes was IR spectroscopy. The results are summarised in Table 18. Both complexes exhibited a strong absorption band around 2040 cm⁻¹ (2045 cm⁻¹ for **61** and 2042 cm⁻¹ for **62**) which we assign to the (N₃)⁻ asymmetric stretching. Upon comparison with the IR spectra of the starting materials, we could also tentatively assign the symmetric stretching modes of the (N₃)⁻ ligand at 1279 cm⁻¹ for **61** and 1284 cm⁻¹ for **62**. The stretching frequencies are typical for complexes bearing a terminal azide ligand and are comparable with the values for other gold azide complexes. (Table 18)

Table 18. Selected stretching frequencies for gold azido complexes

Entry	Complex	$\nu_{\text{as}}(\text{N}_3)^- (\text{cm}^{-1})$	$\nu_{\text{s}}(\text{N}_3)^- (\text{cm}^{-1})$	Reference
1	(Ph ₃ P)AuN ₃	2050	1175	234b
2	(SIPr)AuN ₃ ^b	2035	1271	236b
3	(IPr)AuN ₃ 61	2045	1279 ^a	This work
4	[Ph ₄ As][Au(N ₃) ₄]	2027	1250	234b
5	(C [^] N [^] C)AuN ₃ 62	2042	1284 ^a	This work

^a Assigned by comparison with the IR spectra of the starting materials

^b (SIPr) = 1,3-bis(2-6-diisopropyl-phenyl)imidazolidine

The molecular structure of complexes **61** and **62** was determined by X-ray crystallography. (Figure 60) In the crystal, the gold(I) azide **61** shows a linear geometry around the gold centre and the geometrical parameters are closely related to the ones of the (SIPr) supported gold azide reported by Gray *et al.*^{236b} The Au—N(3) distance in (IPr)AuN₃ **61** is shorter than in the corresponding (SIPr)AuN₃ (2.057(6) vs. 2.068(3) Å) which is a consequence of the stronger σ -donating capacity (thus stronger *trans* influence) of the saturated SIPr vs. the unsaturated IPr carbene ligand. The packing diagram of **61** displays hydrogen bonding between the terminal nitrogen of the azide group and the methylene protons of a NHC moiety from a neighbouring molecule. (Figure 60, right)

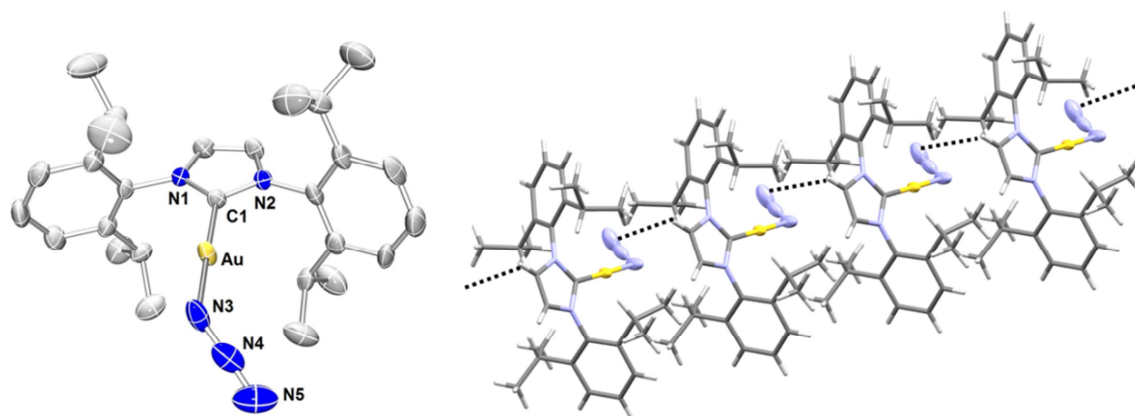


Figure 60 Molecular structure of **61** (50% probability ellipsoids shown). Hydrogen atoms were omitted. Selected bond distances (Å) and angles (°): C(1)—Au 1.977(6), Au—N3 2.057(6), N3—N4 1.238(10), N(4)—N(5) 1.165(11), C(1)—Au—N(3) 178.2(3), Au—N(3)—N(4) 115.6(5) (left); crystal packing showing hydrogen bonding between the N(5) of the N₃⁻ group and the carbene C—H atoms of a neighbouring molecule N(5)—H(24) 2.712(3)(right)

The crystal structure of the gold(III) (C[^]N[^]C)AuN₃ **62** (Figure 61) displays similar geometrical parameters for the AuN₃ fragment as complex **61**. In the case of the structurally characterised homoleptic [Au(N₃)₄]⁻ complexes, the Au—N bond length varies with the nature of the cation and typically ranges between 1.996(9) Å in [NMe₄][Au(N₃)₄]^{234a} and 2.033(2) Å in [Ph₄As][Au(N₃)₄].^{234b} Nevertheless, by comparison, the Au—N(2) distance in **62** is marginally longer. In the (C[^]N[^]C)Au fragment, the Au—N(1) distance between the metal centre and the pyridine ligand (1.955(10) Å) is similar to the Au—C(1) (1.965(10) Å) significantly longer than Au—Me (2.018(4) Å) distances in the isostructural (C[^]N[^]C)AuCl **2** and (C[^]N[^]C)AuMe **15** which suggests that the *trans* influence of the azide ligand is similar to the one of the chloride ligand and weaker than the one of a methyl ligand. The packing diagram of **62** displays hydrogen bonding between the terminal nitrogen of the azide

group and the aromatic protons from a pyridine fragment of a neighbouring molecule. (Figure 61, right)

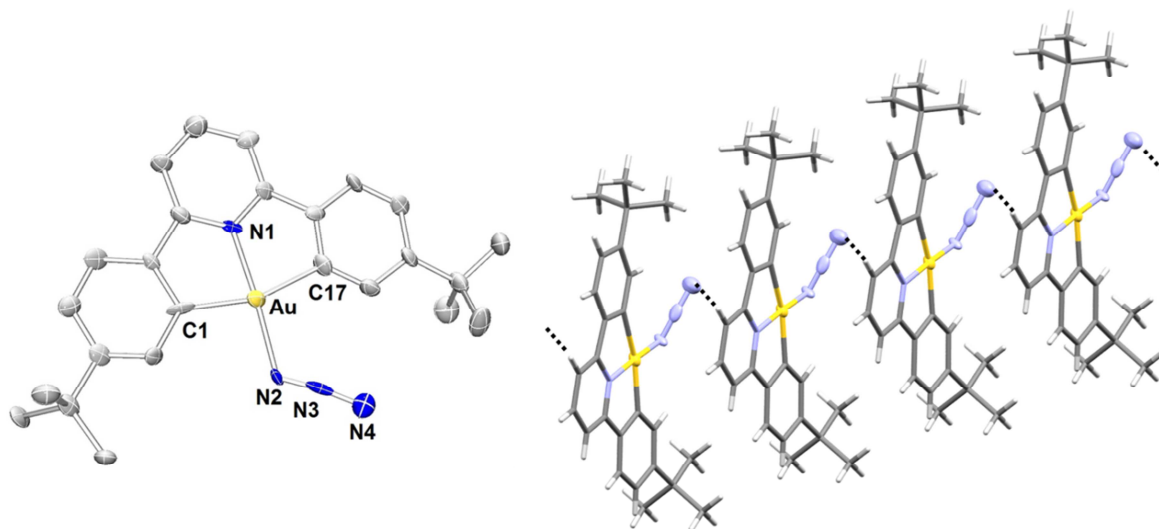


Figure 61 Molecular structure of **62** (50% probability ellipsoids shown). Hydrogen atoms were omitted. Selected bond distances (Å) and angles (°): Au—C(1) 2.042(16), Au—N(1) 1.955(10), Au—N(2) 2.057(11), N(2)—N(3) 1.134(17), N(1)—Au—N(2) 176.2(5), Au—N(2)—N(3) 120.0(9), C(1)—Au—C(17) 161.9(5) (left); crystal packing showing hydrogen bonding between the N(4) of the N₃⁻ group and the pyridine C—H atoms of a neighbouring molecule N(4)—H(10) 2.678(3) (right)

4.T2.2 Initial reactivity studies

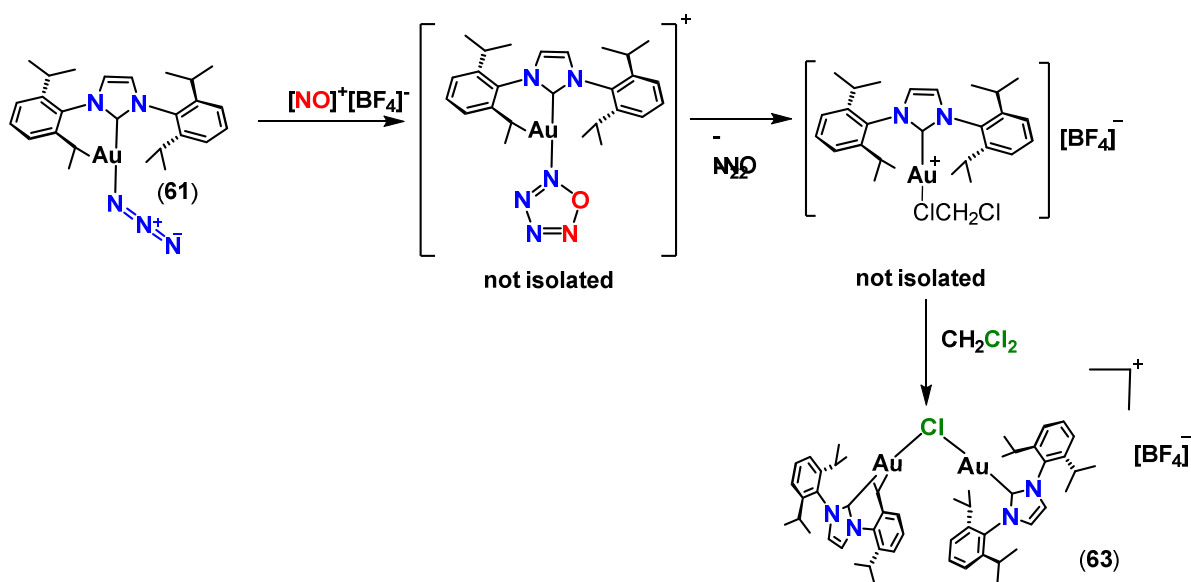
Since gold(I) azides are known to give triazolato complexes when reacted with terminal alkynes, we sought to extend this methodology by using NO⁺ as a [3+2] cycloaddition partner. Previous studies performed by Gray *et al.*²⁴⁰ showed that phosphine supported gold(I) azides such as (Cy₃P)AuN₃ are indeed able to react with nitrosonium cations to give a gold supported oxatetrazole which immediately decomposes to N₂O and N₂ to generate the a free gold(I) cation. The cation could be trapped by employing porphyrins such as octaethylporphyrin.²⁴⁰

Since N-heterocyclic carbenes have been shown to provide stabilisation gold(I) species such as terminal hydrides and hydroxides where phosphines proved to be inefficient, we envisaged that they would be good ancillary ligands for the isolation of highly reactive, energy rich species such as oxatetrazoles. Furthermore, decomposition of gold oxatetrazole complexes would be a clean pathway to generate ‘naked’ gold(I) cations’ (the by-products are gaseous) which are often invoked as primarily active species in catalytic transformations. Despite that, there is no structural evidence for such stable, isolable species.²⁴¹ Solution

characterisation of a ‘naked gold cation’ supported by a sterically demanding carbene ligand and a large borate anion $[\text{IPr}^{**}\text{Au}][\text{BAr}^{\text{F}}_{24}]$ ($\text{IPr}^{**} = 2,6\text{-bis}(\text{di-4-tert-butylphenyl})\text{methyl-4-methylphenyl}$) was proposed⁸⁵ but was not structurally confirmed.

Treatment of carbene supported gold(I) azide **61** with an excess of the nitrosonium salt $[\text{NO}][\text{BF}_4]$ rapidly leads to the clean formation of a new single product as indicated by ^1H NMR spectroscopy. Since the identity of the complex could not be established by NMR spectroscopy, we set forth in obtaining single crystals for X-ray diffraction studies.

Layering a CH_2Cl_2 solution of a mixture between **61** and $[\text{NO}][\text{BF}_4]$ with light petroleum at room temperature afforded the isolation of colourless crystals. X-ray diffraction studies established the identity of the complex as the cationic chloride-bridged digold complex $[\{(\text{IPr})\text{Au}\}_2(\mu\text{-Cl})][\text{BF}_4]$ (**63**). The cationic complex is the product of the electrophilic attack of the gold(I) cation $[(\text{IPr})\text{Au}]^+$ on the reaction solvent, CH_2Cl_2 . (Scheme 49)



Scheme 49 Reaction of **61** with NO^+ , synthesis of a chloro-bridged Au(I) cation.

The crystal structure of **63** (Figure 62) confirms the identity of the complex as a chloro-bridged digold cation. The geometry around each gold(I) centre is linear ($\text{C}(1)\text{—Au}(1)\text{—Cl}(1)$ $174.7(2)^\circ$). The $\text{Au}(1)\text{—Cl}(1)\text{—Au}(2)$ angle is considerably wider than in related chloro-bridged phosphine supported gold(I) cations²⁴¹ ($109.94(8)^\circ$ vs. $94.7 - 97.5^\circ$) and narrower than the $\text{Au}\text{—O(H)\text{—Au}}$ angle in the bridging hydroxide digold cation reported by Nolan *et al.* ($129.5(3)^\circ$).⁵⁴ As a consequence, the $\text{Au}\cdots\text{Au}$ distance in the carbene supported cation **63** (3.823 \AA) appears much longer than in phosphine supported analogues

(3.48—3.54 Å),²⁴¹ where the Au...Au contacts have been classified as aurophilic interactions.

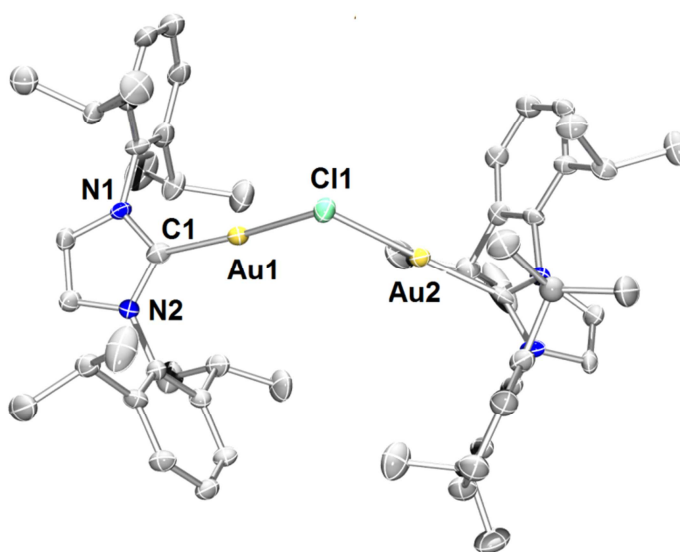


Figure 62 Molecular structure of **63** (50% probability ellipsoids shown). Hydrogen atoms and disordered BF_4 anion were omitted. Selected bond distances (Å) and angles ($^\circ$): C(1)—Au(1) 1.986(8), Au(1)—Cl(1) 2.336(2), Cl(1)—Au(2) 2.335(2), C(1)—Au(1)—Cl(1) 174.7(2), Au(1)—Cl(1)—Au(2) 109.94(8) (left), Au(1)··· Au(2) 3.823

CONCLUDING REMARKS AND PERSPECTIVES

We have shown that heteroleptic gold(I) and gold(III) azides could be readily obtained through salt metathesis reactions with sodium azide and can be safely manipulated at room temperature in small quantities. The gold(III) ($\text{C}^{\wedge}\text{N}^{\wedge}\text{C}$) AuN_3 complex **62** is to the best of our knowledge the first heteroleptic gold(III) azide complex to be reported.

Initial reactivity studies on the reactivity of carbene supported gold(I) azides shows that [3+2] cycloaddition reactions with NO^+ represents a clean way of generating carbene supported gold(I) cations which are often invoked in catalytic transformations. The reaction possibly proceeds via a gold oxatetrazole intermediate. ^{15}N labelling studies are necessary to study the stability of the oxatetrazole species. We are also investigating whether this methodology can be extended to the ($\text{C}^{\wedge}\text{N}^{\wedge}\text{C}$) supported gold(III) azide.

While it has been established that gold(I) azides react with terminal alkynes to give rise to gold(I) triazole complexes,²³⁸ our preliminary tests show that this is not the case for ($\text{C}^{\wedge}\text{N}^{\wedge}\text{C}$) AuN_3 **62** in the absence of a catalyst. Gold(III) complexes have established anti-tumour activity, and gold(III) aminoacid complexes may be suitable for anti-cancer cell

testing due to their solubility in polar solvents. In this respect, it remains to be established whether copper catalysed click reactions between gold(III) azides and alkyne functionalised aminoacids would be a viable method of obtaining gold-aminoacid complexes.

TOPIC 3: β -Diketiminato Ligands in Gold(III) Chemistry

INTRODUCTION

β -Diketiminato ligands have been widely used to stabilise and tune the reactivity of most metallic elements across the Periodic Table.²⁴² They are particularly attractive because of their ease of synthesis and because of their easily tuneable steric and electronic properties. Traditionally, the investigation of metal complexes of β -diketiminato anions have been focussed on non-functionalised ligand imino-enimine backbones but recent reports show that incorporating electron withdrawing CF_3 groups can aid in the stabilisation of several metal species.

For example, Daugulis and co-workers showed that while CH_3 functionalised imine-enamine backbone β -diketiminato ligands were incapable of stabilising monomeric Ag(I) species,²⁴³ the CF_3 analogues were employed successfully in the isolation of thermally stable monomeric stable silver species.²⁴⁴ A similar stabilisation effect was observed by Hill *et al.* in the isolation of indium(I) β -diketiminato complexes.²⁴⁵ (Figure 63) A DFT analysis of the frontier orbitals in the non-fluorinated and fluorinated indium(I) complexes show additional stabilisation of the HOMO by 21 kcal mol⁻¹ in the case of the latter.^{245b}

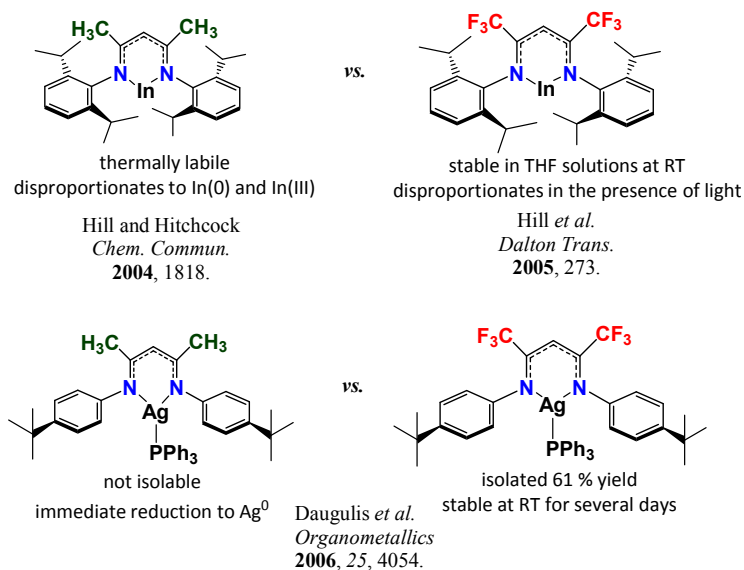


Figure 63 Stabilisation of In(I) and Ag(I) centres by electron withdrawing β -diketiminato complexes

In the case of gold, β -diketiminato anions have been generated used as supporting ligands in the Au(I) mediated catalytic oxidation of alcohols, however the β -diketiminato complex has been generated *in situ* and not characterised.²⁴⁶ Limited work has been reported on gold(I) β -diketiminato and the isolated complexes are depicted in Figure 64. All reported complexes are thermally robust, some even above 100 °C. The degree of fluorination of the supporting ligand has a substantial influence on the conformation of the isolated gold(I) complex. Similar to the case of silver,²⁴³ non-functionalised imine-enamine backbones give rise to dimeric gold(I) species,²⁴⁷ while incorporation of CF₃ groups in the ligand backbone dictates a monomeric, chelate structure.²⁴⁸ Further incorporation of CF₃ groups in the flanking aryl groups gives rise to a monomeric, open U-shaped conformation.²⁴⁹

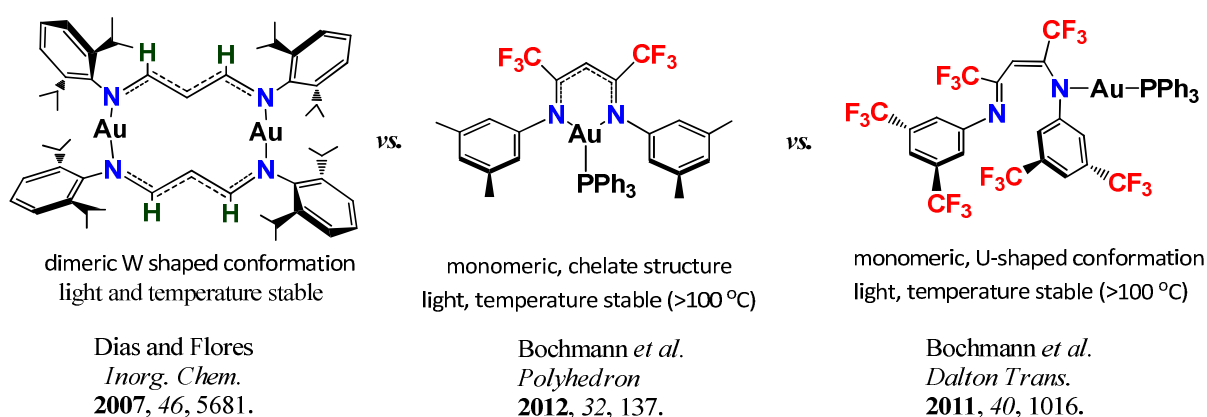
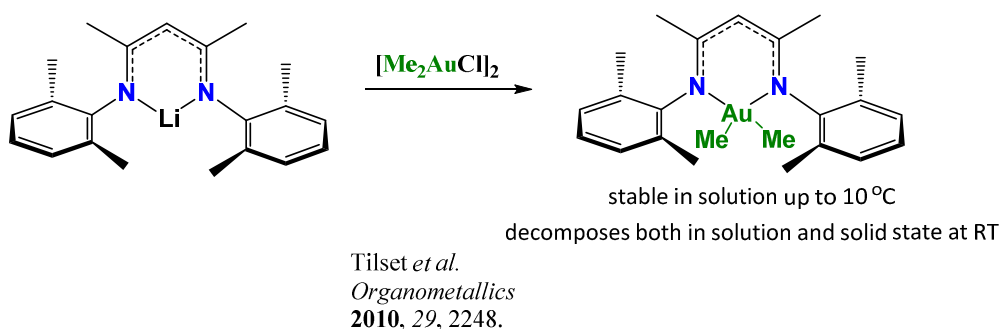


Figure 64 Isolated Au(I) β -diketiminato complexes showing conformation variation as a function of electronic properties of the ligand

The only previously reported gold(III) centre stabilised by a methyl functionalised β -diketiminato ligand (Scheme 50) had limited thermal stability, with decomposition occurring at room temperature even in solid state after 3 hours.²⁵⁰ Attempts to further cleave the Au-Me bond by employing a series of electrophiles proved unsuccessful and lead instead to attack on the supporting ligand or to reduction to Au(0).



Scheme 50. Synthesis of a gold(III) β -diketiminato complex²⁵⁰

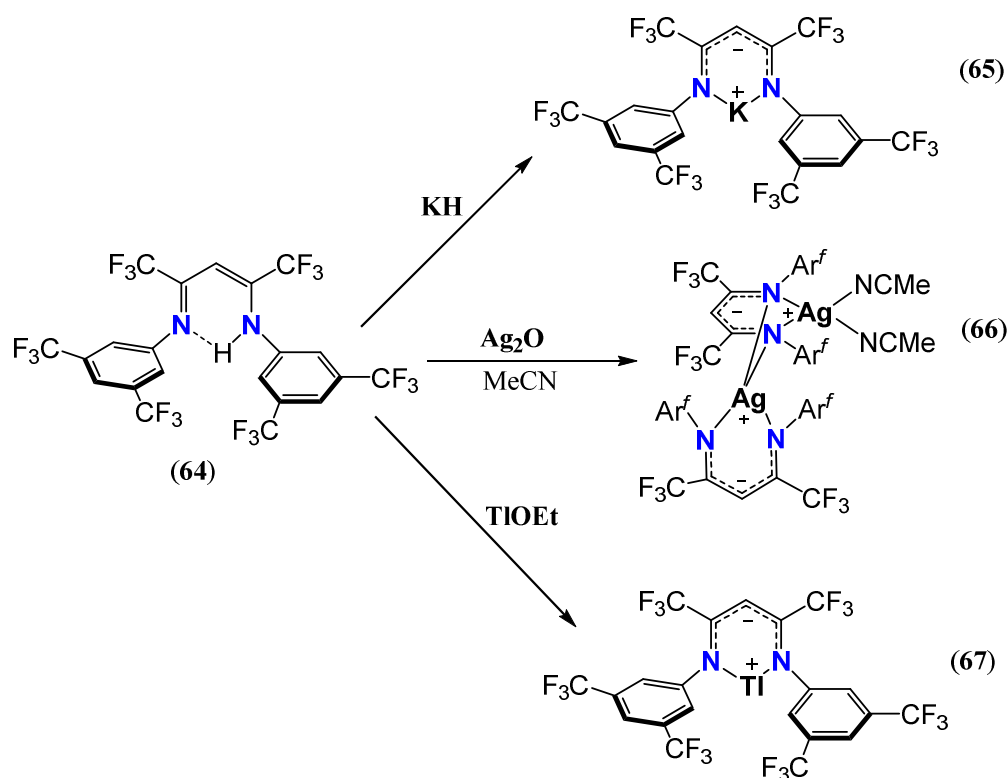
Given the tunability and steric versatility and ease of synthesis of β -diketiminato ligands, we decided to extend the our studies performed on diphenylpyridine gold(III) species to this class of ligands. Since electron deficient β -diketiminato complexes tend to be more stable than their more electron-rich counterparts, we decided to incorporate CF_3 groups on the ligand backbone and on the aryl flanking groups. This section summarises our attempts in the synthesis of these gold(III) complexes together with the synthesis of the transmetallation precursors.

RESULTS AND DISCUSSION

4.T3.1. Synthesis of precursors

The heavily fluorinated, electron poor β -diketiminato ligand **64** was prepared by an aza-Wittig condensation reaction following a protocol reported by Sadighi *et al.*²⁵¹

In our efforts to synthesise β -diketiminato supported gold(III) complexes, a series of salts capable to act as transmetallating agents were synthesised. The potassium salt **65** was obtained by deprotonating the β -diketiminato compound **64** in the presence of potassium hydride following a reported protocol.²⁴⁹ In a similar fashion, the pro-ligand **64** could be deprotonated by Ag_2O following the method of Daugulis *et al.*, to give rise to the silver salt **66**.²⁴⁴ (Scheme 51)



Scheme 51 Synthesis of K, Ag, and Tl β -diketiminato salts as transmetallating agents

There is an increasing interest in the heavier group 13 β -diketiminato compounds since indium and especially gallium β -diketiminato compounds have been shown to be isostructural and isolobal to N-heterocyclic carbenes.²⁵² Thallium analogues on the other hand are less studied and are not expected to show coordination or redox chemistry due to the low energy of their lone pairs.²⁵³ Nevertheless, probably because of their toxicity, they are not isolated but often generated *in situ* and used as transmetallating agents to take advantage of the insolubility of TlCl as a driving force for the formation of the desired product.²⁵⁴

In 2005, Hill and co-workers reported the synthesis of a β -diketiminato thallium(I) complex by reacting the free ligand with thallium(I) iodide in the presence of a $\text{K}[\text{N}(\text{SiMe}_3)_2]$.^{236b} The complex was reported to be light and thermally sensitive; C_6D_6 solutions of the complex are reported to deposit Tl metal over short periods of time. Furthermore, attempt to extend the reaction protocol to β -diketiminato ligands with a fluorinated backbone such as $[(\text{CH}(\text{CF}_3)_2\text{CN}-2,6\text{-}^i\text{Pr}_2\text{C}_6\text{H}_3)]$ led to the recovery of the starting materials even after prolonged heating to 70 °C.^{245b}

In contrast, we have found that thallium salts of heavily fluorinated β -diketiminato ligands can be cleanly accessed in high yield by deprotonation of **64** in the presence of thallium ethoxide.²⁵⁵ to give the thallium salt **67** as a yellow-orange powder. In contrast to the thallium salt isolated by Hill *et al.*,^{245b} complex **67** is stable at room temperature in the presence of ambient laboratory lighting in solid state and shows stability in solution for at least 16 h in the dark. The increased stability is a consequence of electron deficiency of the ligand backbone which is more capable of stabilising electrophilic metal centres.

The ^{19}F NMR spectrum of thallium complex **67** displayed a single resonance for the CF_3 groups of the back-bone and a single resonance for the CF_3 groups attached to the aromatic rings, confirming the C_{2v} -symmetric structure in solution, as expected for a chelating κ^2 - β -diketiminato Tl(I) complex.

The identity of the complex was also confirmed by single crystal X-ray diffractometry. Complex **67** was recrystallised from a concentrated light petroleum solution at -20 °C and the molecular structure is depicted in Figure 65. Despite crystal twinning which precluded detailed analysis of bond lengths, unambiguous connectivity could be established. In solid state, complex **67** has a monomeric structure with no $\text{Tl}\cdots\text{Tl}$ or $\text{Tl}\cdots\pi$ arene interactions which are usually characteristic for thallium complexes.²⁵⁶ The mononuclear constitution is probably a consequence of the steric demands of the β -diketiminato ligand which contains bulky 3,5- $\text{CF}_3\text{C}_6\text{H}_3$ flanking groups. The individual monomer units possess V-geometry

around the thallium centre. The geometrical parameters of **67** are, within error, similar to the non-fluorinated β -diketiminato thallium(I) complex reported by Hill *et al.*^{245b}

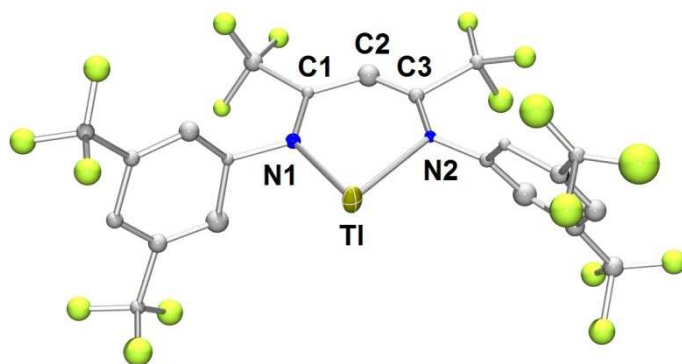
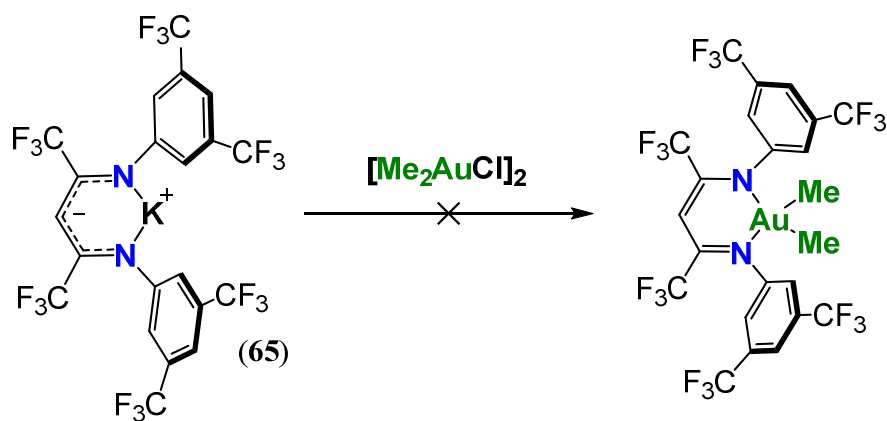


Figure 65 Molecular structure of **67** (thallium atom represented as 50% probability ellipsoid, the rest of the atoms were modelled isotropically due to twinning). Hydrogen atoms were omitted. Only one of the two molecules in the asymmetric unit shown. Selected bond distances (Å) and angles (°): Tl(1)—N1(1) 2.55(3), Tl(1)—N2(1) 2.39(3), N(1)—C(1) 1.39(4), C(1)—C(2) 1.28(6), C(2)—C(3) 1.56(5), N(1)—C(1)—C(2) 130(3), Tl(1)—N(1)—C(1) 126.7(17), C(1)—C(2)—C(3) 130(4) N(1)—Tl(1)—N(2) 72.6(8), Tl...Tl 8.30

4.T3.1. Reactivity towards Au(III)

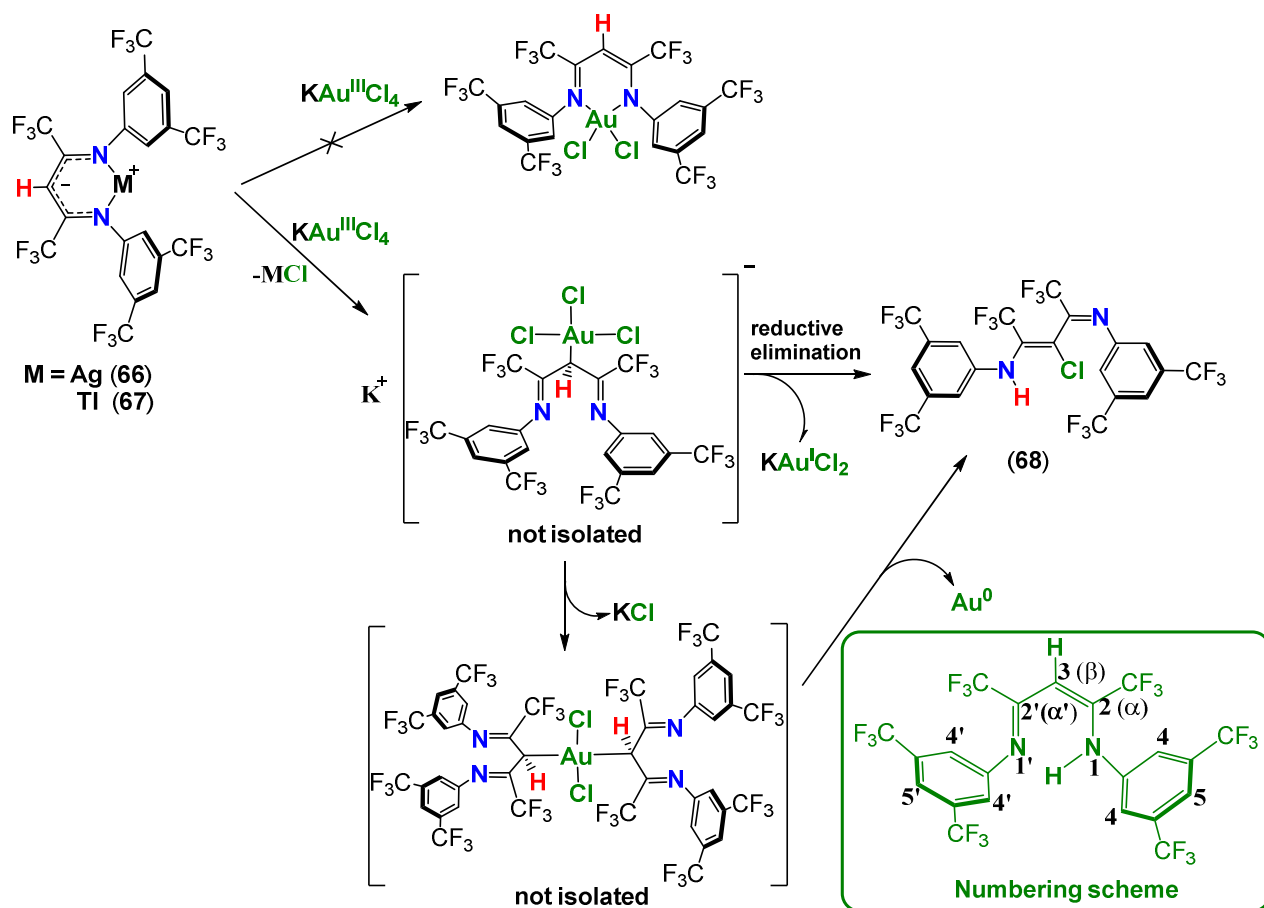
The highly fluorinated β -diketiminato salts **65** – **67** were tested as transmetallating agents to gold(III). Since the reaction of the potassium salt **65** with the $\text{Au}^{\text{I}}\text{Cl}(\text{PPh})_3$ proved to be a suitable way to obtain gold(I) β -diketiminato complexes,²⁴⁹ we envisaged that the potassium β -diketiminato would be a suitable material for the synthesis of the gold(III) analogue. A reaction between alkali salts of β -diketiminato ligands and $[\text{Me}_2\text{AuCl}]_2$ was also used by Tilset *et al.* in the synthesis of non-fluorinated β -diketiminato of gold(III)²⁵⁰ (see also Introduction to Topic 3). Compound **65** was reacted with $[\text{Me}_2\text{Au}^{\text{III}}\text{Cl}]_2$ ²⁵⁷ at -78 °C followed by warming the mixture to room temperature. (Scheme 52) During the course of the reaction, precipitation of gold metal was observed. Investigation of the reaction outcome by ^1H NMR spectroscopy revealed the free ligand as the major reaction product.



Scheme 52 Attempted reaction between the potassium β -diketiminato and $[\text{Me}_2\text{AuCl}]_2$

Since the potassium salt may be too electrophilic and thus facilitates reduction of the Au(III) centre we have switched to the silver **66** and thallium **67** salts as milder transmetallating agents. Also, we decided to employ the potassium tetrachloroaurate as a gold starting material since it is more thermally robust than $[\text{Me}_2\text{AuCl}]_2$. Treatment of acetonitrile solutions of the salts **66** and **67** with KAuCl_4 at room temperature in the dark rapidly gave rise to a purple precipitate. Continuous stirring for 16 h and filtration followed by recrystallisation from light petroleum at low temperature afforded the isolation of **68** as a colourless crystalline material.

A ^{19}F NMR investigation of **68** revealed the presence of four distinct signals for each CF_3 group suggesting that the compound generated does not possess C_{3v} symmetry, which implies that it does not adopt a chelate structure as would be expected for a gold(III) β -diketiminato complex. The ^1H NMR spectrum of the isolated material suggested that the reaction outcome was not simple hydrolysis of the Ag or Tl salts as indicated by the absence of the characteristic low field resonance (δ_{H} 11.11, C_6D_6) assigned for the NH group in the ligand **64** (H1, Scheme 53 for numbering scheme). The ^1H NMR spectrum of **68** also revealed the absence a singlet resonance around 5.87 ppm which was previously assigned to the H3 in **64** and a doubling of the expected aromatic resonances (H4 and H5 are no longer equivalent to H4' and H5'). This led us to propose that **68** is a C-ligated β -diketiminato which does not adopt a chelate structure.



Scheme 53 Reaction of Tl and Ag β -diketiminato salts with KAuCl₄, synthesis of a C-chloro-functionalised β -diketiminato ligand.

The molecular structure of **68** confirmed its identity as C-ligated β -diketiminato analogue, with a chlorine atom attached to the (β) C3 atom, adopting a *Z, Z* configuration. (Figure 66, top) The amine NH is engaged in strong intermolecular hydrogen bonding with the CF₃ attached to the aromatic ring of an adjacent molecule (H \cdots F 2.193 Å, $\Sigma_{\text{vdW}}(\text{H},\text{F})$ 2.67). (Figure 66, bottom) This arrangement is possibly dictated by the steric repulsion between the Cl atom and the CF₃ group which prevents the compound from adopting chelate-type structure. In contrast, the β -diketiminato ligand containing a hydrogen atom attached to the C3 (β) (**64**) adopts a *C*_{3v} symmetry and engages in intramolecular hydrogen bonding between the amine NH and imine nitrogen atom.^{249,255} (Figure 67) This difference in structure is also reflected by ¹H NMR spectroscopy in the chemical shift of the NH group. Therefore, in **68** which adopts an open structure, the NH chemical shift appears significantly at a lower frequency when compared to **68** which adopts a closed structure (δ_{H} 4.5 vs. 11.11).

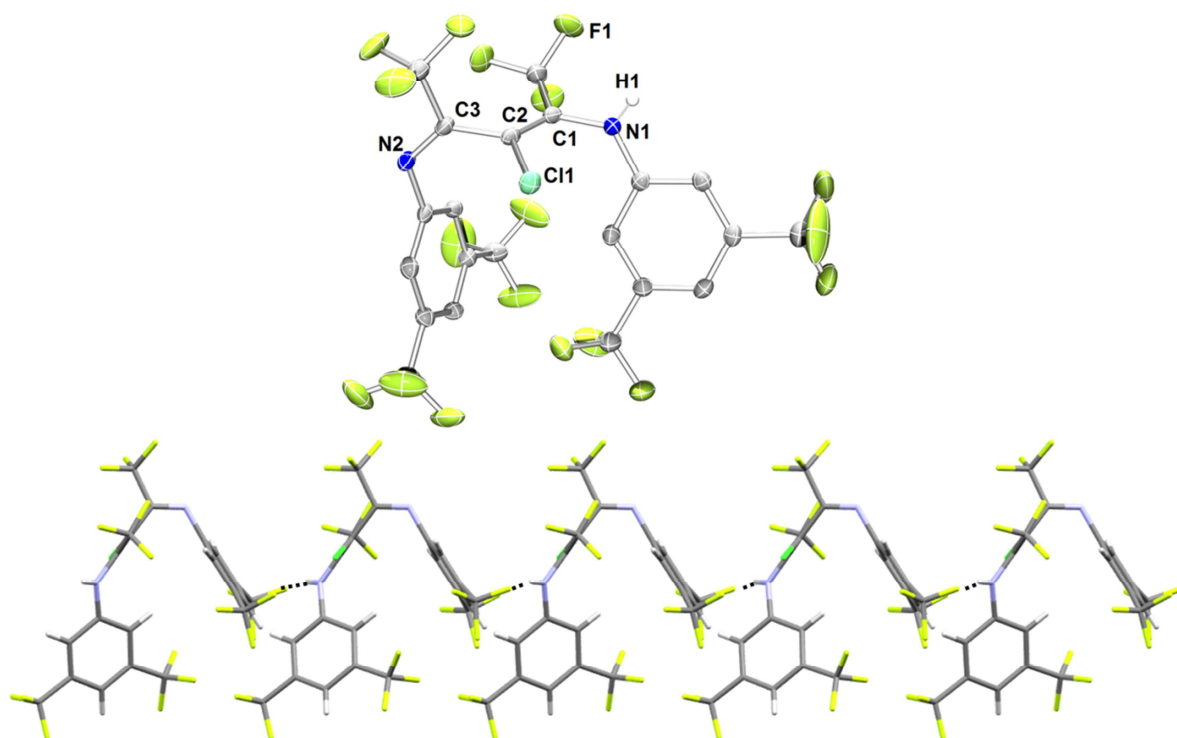


Figure 66 Molecular structure of **68** (*Z,Z* isomer) (50% probability ellipsoids shown). Hydrogen atoms except the H atom bound to N(1) were omitted. Selected bond distances (Å) and angles (°): N(1)—C(1) 1.381(3), C(1)—C(2) 1.324(3), C(2)—C(3) 1.496(3), C(3)—N(2) 1.266(2), N(1)—C(1)—C(2) 126.92(19), C(1)—C(2)—Cl(1) 110.77(15) (top); view along *c* axis depicting NH...*F* intermolecular hydrogen bonding

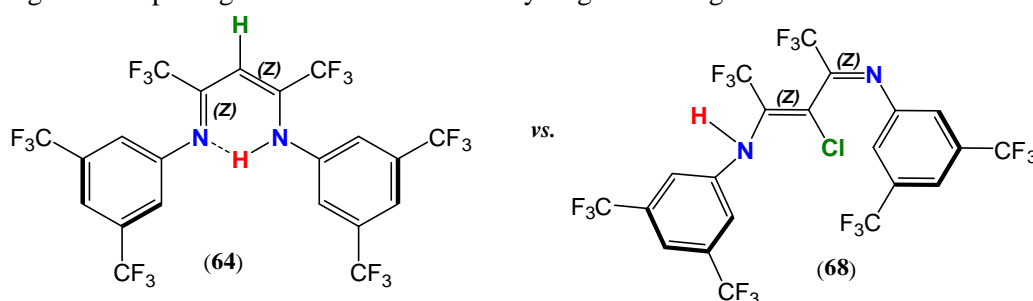


Figure 67 Open vs. closed conformation in β -diketiminates as a function of the substituent in at (β)C

While we have not been able to isolate any intermediates in the synthesis of **68**, it seems reasonable to propose an activation of the β -carbon atom (C3, Scheme 53) of β -diketiminato salt by KAuCl_4 to give rise to an anionic C-ligated $[(\beta\text{-diketiminato})(\text{AuCl}_3)]^-$ complex. The complex can then undergo reductive elimination concomitant with diimine to imine-enamine isomerisation, to give complex **68** and Au(I). (Scheme 53) However, we cannot exclude the reduction of KAuCl_4 to Au(I) in the presence of salts **66** and **67** which can then attack the C3 position as observed for the isoelectronic Cu(I) complexes. (*vide supra*)

No gold mediated activation of the β -carbon atom (C3, Scheme 54) of β -diketiminate ligands or complexes has been previously reported, but similar activation pathways have been shown for other late transition metals. It has been reported that GeCl_4 complexes can react with β -diketiminate pro-ligands to give rise to (β)C-ligated GeCl_3 diimine complexes²⁵⁸ while HgCl_2 and CuI react with lithium β -diketiminate complexes to give rise to β -C-ligated metal heterobimetallic or diimine complexes.²⁵⁹ Chloride functionalisation of the (β)C3 position has been reported in the presence of organic reagents such as triflyl chloride^{260a} or as a product of the reaction between the N-ligated Pd(II) $[(\beta\text{-diketiminate})\text{Pd}](\mu\text{-Cl}_2)$ and an oxidising agent such as $\text{PhI}(\text{OAc})_2$.^{260b}

CONCLUDING REMARKS

We have shown that thallium β -diketiminate complexes are useful transmetallating agents and can be stabilised by functionalising the imine-enamine ligand backbone with electron withdrawing CF_3 groups.

Attempts to use the same electron withdrawing β -diketiminate ligand to stabilise gold(III) centres lead to reduction if the potassium salt was used as a starting material, whereas milder transmetallating agents such as thallium or silver β -diketiminate lead to the isolation of a chloride C-bound β -diketiminate proligand. The reaction possibly proceeded by the gold activation of the β -carbon atom of the ligand backbone followed by reductive elimination.

CHAPTER 5
EXPERIMENTAL

GENERAL CONSIDERATIONS

Unless otherwise stated, all experiments were performed in air using bench solvents. In such exceptions, manipulations were performed using standard Schlenk techniques under dry nitrogen or a Saffron Scientific glovebox. Nitrogen was purified by passing through columns of supported P₂O₅, with moisture indicator, and activated 4 Å molecular sieves. Anhydrous solvents were freshly distilled from appropriate drying agents. (C[^]N[^]C)AuCl (**2**),⁵¹ (C[^]N[^]C)^HAuCl (**53**),⁵⁰ IPrAuH (**40**),⁴⁴ IPrAuOH (**48**),⁵⁸ IPrAuOTf (**60**),⁴⁴ **64**,²⁵¹ **65**,²⁴⁹ **66**,²⁴⁴ [Ti(OEt₂)₂][[H₂N{B(C₆F₅)₃}₂]²¹⁵ and tris(pentafluorophenyl)boron²⁶¹ were prepared using literature methods. AgOAc^F (Aldrich), AgOTf (Aldrich), CsOH·H₂O (Aldrich), phenylacetylene (Aldrich), pentafluorobenzene (Aldrich), 1,2,4,5- tetrafluorobenzene (Alfa Aesar), the boronic acids (Aldrich), LiHBEt₃ (1M solution in THF) (Aldrich), LiDBEt₃ (1M solution in THF) (Aldrich), cobaltocene (Aldrich), phenylacetylene (Aldrich), 3-hexyne (Lancaster Synthesis), dimethyl acetylenedicarboxylate (Aldrich), cyclohexylallene (Aldrich), 3,3-dimethylallene (Alfa Aesar), tBuOOH (5-6 M in dodecane, Aldrich), H₂O₂ (30% aq, Fisher), Galvinoxyl (Aldrich), TEMPO (Aldrich), H₂¹⁸O (Apollo Scientific) and the phoshines (Aldrich) were commercially available and used as received. Na¹⁸OH was prepared by reacting sodium with H₂¹⁸O in THF. Complexes **15**, **16**, **20**, **30**, **33** and **62** were first synthesised by Dr Dan Smith with suitable crystals for X-ray diffraction obtained by the author.

¹H, ¹³C{¹H} and ¹⁹F NMR spectra were recorded using a Bruker DPX300 spectrometer. ²D (77 MHz) and DOSY NMR spectra were recorded on a Bruker 500 Avance spectrometer. ¹H NMR spectra (300.13 MHz) were referenced to the residual protons of the deuterated solvent used. ¹³C{¹H} NMR spectra (75.47 MHz) were referenced internally to the D-coupled ¹³C resonances of the NMR solvent. ¹⁹F (282.4 MHz) NMR spectra were referenced externally to CFC₃ and internally to C₆F₆ (δ_F -164.9 ppm). Elemental analyses were performed by London Metropolitan University.

UV-Vis spectra were collected on a Perkin Elmer Lambda 34 UV-Vis spectrometer. Photoluminescence measurements were recorded on a Perkin Elmer LS55 Fluorescence Spectrometer with a solids mount attachment where appropriate. Time resolved fluorescence data were collected on a TCSPC Fluorolog Horiba Jobin Yvon spectrofluorimeter using Horiba Jobin Yvon DataStation v2.4 software. A NanoLED of 370 nm was used as excitation source with a repetition rate of 1 MHz and a full width at half maximum of 1.2 ns. The collected data were analysed using a Horiba Jobin Yvon DAS6 v6.3 software.

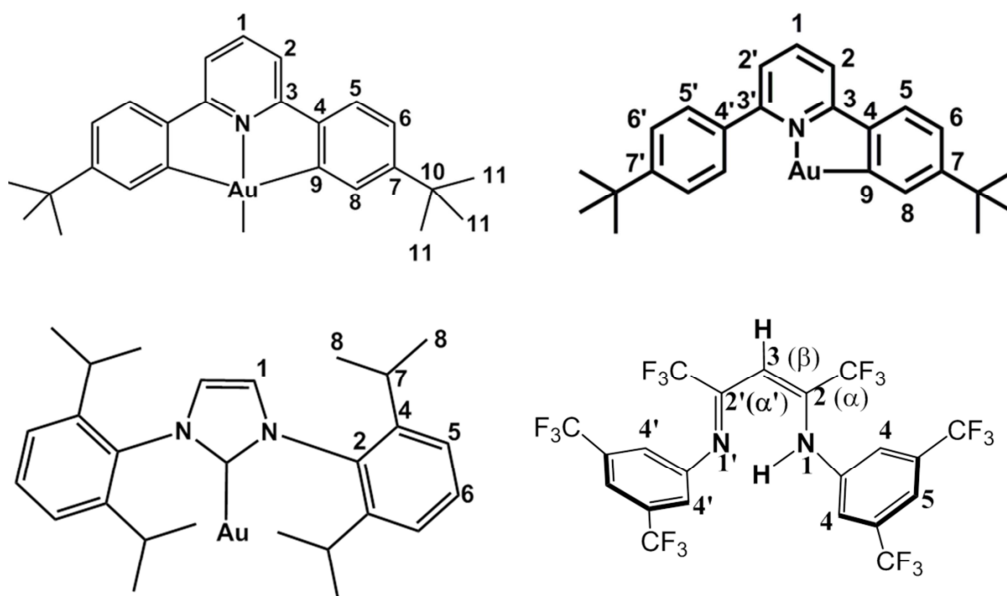


Figure E1: Numbering scheme for ^1H and ^{13}C peak assignment in tridentate ($\text{C}^{\wedge}\text{N}^{\wedge}\text{C}$)Au, bidentate ($\text{HC}-\text{N}^{\wedge}\text{C}$)Au, (NHC)Au and β -diketiminato complexes

SYNTHESIS OF COMPLEXES

1. Synthesis of chloride-free gold precursors

($\text{C}^{\wedge}\text{N}^{\wedge}\text{C}$) H_2 (**1**)

Under an atmosphere of dry nitrogen, 4-tertbutylboronic acid (15 g, 84 mmol), 2,6-dichloropyridine (4.15 g, 28 mmol) and K_3PO_4 (11.92g, 56 mmol) were mixed together in a flask. To this $\text{Pd}(\text{PPh}_3)_4$ (1.4 mol%, 480 mg, 0.4 mmol) and 300 mg degassed isopropanol were added and the mixture was heated to reflux for 12 h. The volatile components were then removed *in vacuo* and the solid residue was dissolved in dichloromethane and passed through a silica plug. The solvent was removed then *in vacuo* yielding **1** as a white powder. (8.2 g, 85%) The ^1H NMR data matched the one reported in the literature.⁷⁹

($\text{C}^{\wedge}\text{N}^{\wedge}\text{C}$)AuOH (**3**)

Method 1:

($^t\text{BuPh}_2\text{Py}$)AuCl (500 mg, 0.871 mmol) **2** and $\text{CsOH}\cdot\text{H}_2\text{O}$ (731 mg, 4.33 mmol) were charged in a flask and a mixture of THF, toluene and water (100 mL, 1:1:1) was added. The mixture was stirred for 16 h at 60°C after which the organic layer was separated and washed with 2 x 100 mL water. The volatiles were then removed under vacuum resulting in a mixture of **3**

and the analogous anhydride **45** [(C^NC)Au]₂(μ-O). Stirring the mixture in dichloromethane/water (60 mL, 1:1) for an additional 12 h followed by separation of the organic layer and removal of the volatiles yields **3** as a yellow powder (411 mg, 85%). Single crystals suitable for X-ray diffraction of **3**·H₂O were obtained by slow evaporation of a dichloromethane solution of **3**.

Method 2:

(C^NC)AuOAc^F **4** (100 mg, 0.153 mmol) and KOH (45 mg, 0.802 mmol) were charged in a flask and a mixture of toluene and water (30 mL, 1:1) was added. The mixture was stirred for 16 h at 60 °C after which the organic layer was separated and washed with water (2 x 10 mL). The volatile components were then removed under vacuum resulting in a mixture of **3** and the analogous anhydride [(C^NC)Au]₂(μ-O). Stirring the mixture in dichloromethane/water (20 mL, 1:1) for an additional 12h followed by separation of the organic layer and removal of the volatile components yields **3** as a yellow powder (69 mg, 81%).

¹H NMR (300 MHz, CD₂Cl₂) δ 7.83 (t, 8.0 Hz, *J* = 1H, H¹, pyridyl), 7.62 (d, *J* = 1.9 Hz, 2H, H⁸, phenyl), 7.54 (d, *J* = 8.2 Hz, 2H, H⁵, phenyl), 7.42 (d, *J* = 8.0 Hz, 2H, H², pyridyl), 7.31 (dd, *J* = 8.2, 2.0 Hz, 2H, H⁶, phenyl), 1.37 (s, 18H, H¹¹, ^tBu). ¹³C{¹H} NMR (75 MHz, CD₂Cl₂) δ 169.30 (C^NC ipso), 164.74 (C^NC ipso), 155.10 (C^NC ipso), 145.63 (C^NC ipso), 142.43 (C¹), 128.74 (C⁸), 125.18 (C⁵), 124.46 (C⁶), 116.48 (C²), 35.72 (C¹⁰), 31.33 (C¹¹). IR (ATR, cm⁻¹) 2480 (br, ν_{OH}). Anal. Calcd. (found) for C₂₅H₂₈AuNO: C, 54.06(54.17); H, 5.08(5.17); N, 2.52(2.46).

Preparation of (C^NC)AuOD (**3-d₁**)

To a solution of (C^NC)AuOH (200 mg, 0.36 mmol) in CH₂Cl₂ (40 mL) was added D₂O (15 mL, 833 mmol) and the mixture was stirred at room temperature for 16h. The organic layer was separated, D₂O (15 mL, 833 mmol) was added and the mixture was stirred again for 16 h. After separation of the organic layer, the volatile components were removed *in vacuo*, yielding (C^NC)AuOD (180 mg, 0.32 mmol, 90 %, 85% D) as a yellow powder. The compound was identical by ¹H NMR spectroscopy to the previously reported LAu¹⁶OH. The deuterium percentage was determined by reacting (C^NC)AuOD with P(*p*-Me-C₆H₄)₃ in toluene-*d*₈ to give **34** and integrating the residual hydride resonance (δ = -5.62) versus the H⁸ resonance of the (C^NC)AuOD(H) (δ = 8.40). IR (ATR, cm⁻¹) 2553 cm⁻¹ (v br, ν_{OD}).

Preparation of (C^NC)Au¹⁸OH (3-¹⁸O)

To a solution of (C^NC)Au(OAc^F) (200 mg, 0.306 mmol) in a mixture of THF and toluene (20 mL, 1:1) was added Na¹⁸OH (38.5 mg, 0.918 mmol). The mixture was stirred for 16h at 60 °C. Removal of the volatile components *in vacuo* and extraction with CH₂Cl₂ yielded (C^NC)AuO¹⁸H as a yellow powder (136 mg, 0.245 mmol, 80 %). The compound was identical by ¹H NMR spectroscopy (CD₂Cl₂) to the previously reported (C^NC)Au¹⁶OH. IR (ATR, cm⁻¹) = 3456 (v br, ν_{18OH})

(C^NC)AuOAc^F (4)

(C^NC)AuCl (500 mg, 0.871 mmol) **2** and AgOAc^F (192.4 mg, 1.31 mmol) were charged in a flask and dichloromethane (100 mL) was added. The mixture was shielded from light and was stirred at room temperature for 2 h during which precipitation of AgCl was observed. The mixture was filtered, the volatile components were removed *in vacuo* and the resulting yellow powder was dissolved in toluene (50 mL) and stirred for 12 h in the presence of light. Filtration and removal of the volatile components *in vacuo* yielded **4** as a bright yellow powder (499 mg, 88%). Single crystals suitable from X-ray diffraction were obtained by layering a concentrated dichloromethane solution of **4** with light petroleum.

¹H NMR (300 MHz, CD₂Cl₂) δ 7.71 (t, *J* = 8.0 Hz, 1H, H¹, pyridyl), 7.33 (d, *J* = 1.7 Hz, 2H, H⁸, phenyl), 7.30 – 7.11 (m, 6H, phenyl + pyridyl, overlapping), 1.33 (s, 18H, H¹¹). ¹³C{¹H} NMR (75 MHz, CDCl₃) δ (C=O and CF₃ not observed) 169.93 (C^NC ipso), 165.62 (C^NC ipso), 155.99 (C^NC ipso), 143.98 (C^NC ipso), 143.78 (C¹), 129.72 (C⁸), 125.13 (C⁵), 124.76 (C⁶), 116.34 (C²), 35.56 (C¹⁰), 31.17 (C¹¹). ¹⁹F NMR (282 MHz, CD₂Cl₂) δ -73.74 (s). Anal. Calcd for C₂₇H₂₇AuF₃NO₂ (found): C, 49.78(49.85); H, 4.18(4.21); N, 2.15(2.02).

(C^NC)AuOMe (5)

Under a dry N₂ atmosphere, (C^NC)AuOAc^F **4** (100 mg, 0.153 mmol) and dry KOMe (54 mg, 0.765 mmol) were charged in a Schlenk flask and dry MeOH (30 mL) was added. The mixture was stirred at room temperature for 12 h during which a black precipitate was observed. The solvent was removed under vacuum and the mixture was extracted with dry dichloromethane (30 mL). Removal of the solvent under vacuum yielded **5** as a yellow powder (48 mg, 55%)

^1H NMR (300 MHz, CD_2Cl_2) δ 7.82 (d, 1.9 Hz, $J = 2\text{H}$, H^8 , phenyl), 7.79 (t, $J = 7.9\text{ Hz}$, 1H, H^1 pyridyl), 7.52 (d, $J = 8.1\text{ Hz}$, 2H, H^5 , phenyl), 7.40 (d, $J = 8.0\text{ Hz}$, 2H, H^2 , pyridyl), 7.30 (dd, $J = 8.2\text{ Hz}$, 2.0 Hz, 2H, H^6 , phenyl), 4.14 (s, 3H, OCH_3), 1.38 (s, 18H, H^{11}). $^{13}\text{C}\{^1\text{H}\}$ NMR (75 MHz, CD_2Cl_2) δ 170.84 ($\text{C}^{\wedge}\text{N}^{\wedge}\text{C}$ ipso), 164.75 ($\text{C}^{\wedge}\text{N}^{\wedge}\text{C}$ ipso), 155.14 ($\text{C}^{\wedge}\text{N}^{\wedge}\text{C}$ ipso), 145.49 ($\text{C}^{\wedge}\text{N}^{\wedge}\text{C}$ ipso), 142.49 (C^1), 129.61 (C^8), 124.90 (C^5), 124.39 (C^6), 116.35 (C^2), 61.48 (OCH_3), 35.68 (C^{10}), 31.34 (C^{11}). Anal. Calcd. (found) for $\text{C}_{26}\text{H}_{30}\text{AuNO}$: C, 54.83(54.77); H, 5.31(5.25); N, 2.46(2.53).

($\text{C}^{\wedge}\text{N}^{\wedge}\text{C}$)Au(OCOH) (6)

To a solution of ($\text{C}^{\wedge}\text{N}^{\wedge}\text{C}$)AuOH (100 mg, 0.18 mmol) (**3**) in dichloromethane, formic acid (2 eq, 13.6 μL , 0.36 mmol) was added. The mixture was stirred for 5 minutes at room temperature and the volatile components were removed *in vacuo*. The resulting solid was triturated with light petroleum (3 x 5mL) affording **7** as a yellow powder. (89 mg, 85%)

^1H NMR (300 MHz, CD_2Cl_2) δ 8.60 (s, 1H, OCOH), 7.83 (t, $J = 8.0\text{ Hz}$, 1H, H^1), 7.48 (d, $J = 2\text{ Hz}$, 2H, H^8), 7.42 (d, $J = 8\text{ Hz}$, 2H, H^5), 7.33 (d, $J = 8.0\text{ Hz}$, 2H, H^2), 7.28 (dd, $J = 8$, 2 Hz, 2H, H^6), 1.38 (s, 18H, H^{11}). $^{13}\text{C}\{^1\text{H}\}$ NMR (75 MHz, CD_2Cl_2) δ 170.74 (OCOH) 169.35 (C^9), 165.25 (C^3), 155.41 (C^7), 144.52 (C^4), 143.27 (C^1), 130.01 (C^8), 124.91 (C^5), 124.41 (C^6), 116.31 (C^2), 35.28 (C^{10}), 30.86 (C^{11}). Anal. Calcd. (found) for $\text{C}_{26}\text{H}_{28}\text{AuNO}_2$: C 53.52 (53.61), H 4.84 (4.72), N 2.40 (2.48).

($\text{C}^{\wedge}\text{N}^{\wedge}\text{C}$)AuOAc (7)

Method 1: A mixture of ($\text{C}^{\wedge}\text{N}^{\wedge}\text{C}$)AuCl (152 mg, 0.349 mmol) and AgOAc (45 mg, 0.384 mmol) in dichloromethane (100 mL) was stirred at room temperature for 36 h in the dark. The precipitate of AgCl was filtered off and volatiles were removed *in vacuo* to yield ($\text{C}^{\wedge}\text{N}^{\wedge}\text{C}$)AuOAc as a bright yellow powder (196 mg, 88%).

Method 2: To a solution of ($\text{C}^{\wedge}\text{N}^{\wedge}\text{C}$)AuOH (100 mg, 0.18 mmol) (**3**) in dichloromethane, HOAc (2 eq, 20 μL , 0.36 mmol) was added. The mixture was stirred for 5 minutes at room temperature and the volatile components were removed *in vacuo*. The resulting solid was triturated with light petroleum (3 x 5mL) affording **7** as a yellow powder. (95mg, 88 %)

^1H NMR (300 MHz, CD_2Cl_2) δ 7.85 (t, $J = 8\text{ Hz}$, 1H, H^1), 7.54 – 7.45 (m, 4H, $\text{H}^8 + \text{H}^5$), 7.39 (d, $J = 8\text{ Hz}$, 2H, H^2), 7.32 (dd, $J = 8.2$, 2 Hz, 2H, H^6), 2.34 (s, 3H, OCOCH_3), 1.38 (s, 18H, H^{11}). $^{13}\text{C}\{^1\text{H}\}$ NMR (75 MHz, CD_2Cl_2) δ 174.25 (O=C), 169.50 (C^9), 165.21 (C^3), 155.22 (C^7), 144.56 (C^4), 143.15 (C^1), 129.80 (C^8), 124.82 (C^5), 124.37 (C^6), 116.24 (C^2), 35.23

(C¹⁰), 30.86 (C¹¹), 22.36 (OCOCH₃). Anal. Calcd. (found) for C₂₇H₃₀AuNO₂: C 56.34 (56.45), H 5.67 (5.50), N 2.19 (2.31).

2. Synthesis of Au(III) aryl and alkyl and Au—N complexes

(C^{N^C})AuC₆F₅ (**8**)

Method 1: Under a dry N₂ atmosphere, (C^{N^C})AuOMe **5** (47 mg, 0.082 mmol) was dissolved in dry toluene (20 mL) and C₆F₅H (18.5 μL, 28 mg, 0.164 mmol) added. The mixture was stirred at 110°C for 48 h after which the volatile components were removed under vacuum and the resulting solid was washed with light petroleum (5 mL). The solid was dried under vacuum giving **8** as a pale yellow powder (55 mg, 95%)

Method 2:

(C^{N^C})AuOH **3** (30 mg, 0.054 mmol) was dissolved in toluene (20 mL) and C₆F₅H (12 μL, 18 mg, 0.108 mmol) was added. The mixture was stirred at 110°C for 48 h after which the volatile components were removed under vacuum and the resulting solid was washed with 10 mL light petroleum. The solid was dried under vacuum giving **8** as a pale yellow powder (36 mg, 95%)

Method 3:

Under a dry N₂ atmosphere, (C^{N^C})AuOH **3** (40 mg, 0.072 mmol) and B(C₆F₅)₃ (37 mg, 0.072 mmol) were charged in a Schlenk flask and dry, degassed toluene (20 mL) added. The mixture was stirred for 12 h at room temperature after which the volatile components were removed *in vacuo*. The solid residue was dissolved in CH₂Cl₂ (10 mL) and passed through a silica plug. Removal of the solvent yielded **8** as a pale yellow powder (46 mg, 90%)

¹H NMR (300 MHz, CD₂Cl₂) δ 7.83 (t, *J* = 8.2 Hz, 1H, H¹, pyridyl), 7.53 (d, *J* = 8.1 Hz, 2H, H⁵, phenyl), 7.43 (d, *J* = 8.1 Hz, 2H, H², pyridyl), 7.26 (dd, *J* = 8.1 Hz, 2.2 Hz, 2H, H⁶, phenyl), 7.15 (d, *J* = 2.0 Hz, 2H, H⁸, phenyl), 1.22 (s, 18H, H¹¹). ¹³C{¹H} NMR (75 MHz, CD₂Cl₂) δ C(ipso, pentafluorophenyl, not observed) 165.98 (C^{N^C} ipso), 164.52 (C^{N^C} ipso), 155.56 (C^{N^C} ipso), 147.22 (C^{N^C} ipso), 143.06 (C¹), 133.09 (C⁸), 124.98 (C⁵), 124.28 (C⁶), 116.83 (C²), 35.37 (C¹⁰), 31.25 (C¹¹). (C-F not observed) ¹⁹F NMR (282 MHz, CD₂Cl₂) δ -118.18 – -120.91 (m, 2F), -159.76 (t, 19.7 Hz, 1F, p-F), -162.35 – -163.59 (m, 2F).

(C¹³N¹⁵C)AuC₆F₄H (9)

Under a dry N₂ atmosphere, (C¹³N¹⁵C)AuOMe **5** (15 mg, 0.027 mmol) was charged in a J-Young NMR tube and dry toluene-*d*₈ (0.6 mL) and 1,2,4,5 – tetrafluorobenzene (6.0 μL, 8.1 mg, 0.054 mmol) were added. The mixture was heated at 110°C and the reaction was monitored by ¹⁹F NMR spectroscopy. Complete conversion was observed after 72 h. The volatile components were removed *in vacuo* and the mixture was redissolved in CD₂Cl₂.

¹H NMR (300 MHz, CD₂Cl₂) δ 7.88 (t, *J* = 8.0 Hz, 1H, H¹, pyridyl), 7.56 (d, *J* = 8.3 Hz, 2H, H⁵, phenyl), 7.48 (d, 8.0 Hz, 2H, H², pyridyl), 7.28 (dd, *J* = 8.2, 2.0 Hz, 2H, H⁶, phenyl), 7.20 (d, *J* = 1.8 Hz, 2H, H⁸, phenyl), 7.17 – 7.10 (m, 1H, CH from C₆F₄H) 1.23 (s, 18H, H¹¹). ¹³C{¹H} NMR (75 MHz, CD₂Cl₂) δ (C ipso C₆F₄H carbon atoms not observed), 165.61 (C¹⁵N¹⁵C ipso), 164.12 (C¹³N¹⁵C ipso), 155.08 (C¹³N¹⁵C ipso), 146.86 (C¹³N¹⁵C ipso), 142.53 (C¹), 132.80 (C⁸), 125.21 (C⁵), 123.82 (C⁶), 116.36 (C²), 34.92 (C¹⁰), 30.72 (C¹¹). (C-F not observed) ¹⁹F NMR (282 MHz, CD₂Cl₂) δ -121.93 (qt, 60.1, 30.0 Hz, 2F), -140.29 – -141.37 (m, 2F).

(C¹³N¹⁵C)AuCCPh (10)

(C¹³N¹⁵C)AuOH **3** (97 mg, 0.175 mmol) was dissolved in toluene (20 mL) and phenylacetylene (40 μL, 18 mg, 0.350 mmol) was added. The mixture was stirred at 110°C for 12 h after which the volatile components were removed under vacuum and the resulting solid was washed with light petroleum (10 mL). The solid was dried under vacuum giving **10** as a yellow powder (100 mg, 90%). ¹H NMR spectroscopy matches the one reported by Yam *et al.*⁵¹

(C¹³N¹⁵C)Au(acetate) (11)

(C¹³N¹⁵C)AuOH **3** (100 mg, 0.18 mmol) was dissolved in acetone (20 mL) and was refluxed for 16 h during which a yellow precipitate was formed. Isolation of the precipitate by filtration followed by drying *in vacuo* afforded the isolation of **11** as a yellow powder (75 mg, 70%)

¹H NMR (300 MHz, CD₂Cl₂) δ 7.96 (d, *J* = 2 Hz, 2H, H⁸), 7.76 (t, *J* = 8 Hz, 1H, H¹), 7.52 (d, *J* = 8 Hz, 2H, H⁵), 7.39 (d, 8 Hz, *J* = 2H, H¹), 7.27 (dd, *J* = 8.0, 2 Hz, 2H, H⁶), 3.01 (s, 2H, Au-CH₂), 2.22 (s, 3H, OC-CH₃), 1.39 (s, 18H, H¹¹). ¹³C{¹H} NMR (75 MHz, CD₂Cl₂) δ 209.42 (C=O), 166.45 (C⁹), 162.90 (C³), 154.37 (C⁷), 147.56 (C⁴), 141.76 (C¹), 130.94 (C⁸),

124.98 (C⁵), 123.41 (C⁶), 116.06 (C²), 35.38 (C¹⁰), 34.63 (Au-CH₂), 31.01 (C¹¹), 30.43 (OC-CH₃). Anal. Calcd. (found) for C₂₇H₃₀AuNO: C 55.77 (55.02), H 5.20 (5.10), N 2.41 (2.66)

(C^NC)Au(3,5-dmpyr) (12)

(^tBuPh₂Py)AuOH **3** (40 mg, 0.072 mmol) and 3,5-dimethylpyrazole (7 mg, 0.072 mmol) were charged in a flask and toluene (30 mL) was added. The mixture was stirred at 110°C for 12 h after which the volatile components were removed under vacuum and the resulting solid was washed with light petroleum (5 mL). The solid was dried under vacuum giving **12** as a light yellow powder (44 mg, 95%).

¹H NMR (300 MHz, CD₂Cl₂) δ 7.84 (t, *J* = 8.0 Hz, 1H, H¹), 7.47 (d, *J* = 8.1 Hz, 2H, H⁵, phenyl), 7.39 (d, *J* = 8.1 Hz, 2H, H²), 7.24 (dd, *J* = 8.0 Hz, 2.1 Hz, 2H, H⁶), 7.19 (d, *J* = 2.0 Hz, 2H, H⁸, phenyl), 6.00 (s, 1H, pyrazolyl) 2.34 (s, 3H, Me), 2.26 (s, 3H, Me), 1.24 (s, 18H, H¹¹#). ¹³C{¹H} NMR (75 MHz, CD₂Cl₂) δ 169.69 (C^NC ipso), 165.60 (C^NC ipso), 155.61 (C^NC ipso), 149.87 (C^NC ipso), 145.82 (C ipso pyrazolyl), 143.44 (C1), 143.10 (pyrazolyl), 131.94 (C8), 125.08 (C5), 124.47 (C6), 116.66 (C2), 103.60 (pyrazolyl), 35.50 (C10), 31.16 (C11), 14.42 (CH₃, pyrazolyl), 14.12 (CH₃, pyrazolyl).

(C^NC)Au(imidazole) (13)

(C^NC)AuOH **3** (40 mg, 0.072 mmol) and imidazole (5 mg, 0.072 mmol) were charged in a flask and toluene (30 mL) was added. The mixture was stirred at 110°C for 12 h after which the volatile components were removed under vacuum. The solid was dried giving **13** as a light yellow powder (40 mg, 92%)

¹H NMR (300 MHz, CD₂Cl₂) δ 7.85 (t, *J* = 8.0 Hz, 1H, H¹, pyridyl), 7.65 (br s, 1H, imidazolyl), 7.50 (d, *J* = 8.0 Hz, 2H, H⁵), 7.40 (d, *J* = 8.0 Hz, 2H, H²), 7.33 (dd, *J* = 8.3, 1.9 Hz, 2H, H⁶), 7.28 (d, *J* = 1.9 Hz, 2H, H⁸), 7.20 (br s, 2H, imidazolyl), 1.28 (s, 18H, H¹¹). ¹³C{¹H} NMR (75 MHz, CD₂Cl₂) δ 168.91 (C^NC ipso), 165.50 (C^NC ipso), 156.01 (C^NC ipso), 145.82 (C^NC ipso), 143.48 (C1), 141.48 (ipso, imidazolyl), 130.89 (C8), 128.46 (imidazolyl), 125.48 (C5), 124.81 (C6), 124.04 (imidazolyl), 116.84 (C2), 35.72 (C10), 31.22 (C11). Anal. Calcd. (found) for C₂₈H₃₀AuN₃: C, 55.54(55.56); H, 4.99(4.93); N, 6.94(7.05).

(C^NC)Au(Benzotriazole) (14)

(C^NC)AuOH **3** (42 mg, 0.076 mmol) and benzotriazole (9 mg, 0.076 mmol) were charged in a flask and toluene (30 mL) was added. The mixture was stirred at 60°C for 12 h after which the volatile components were removed under vacuum. The solid was redissolved in a minimum amount of dichloromethane (2 mL), layered with light petroleum and left at -20°C overnight. **14** was isolated light yellow crystals consisting of a mixture of both 2H (**14a**) and 1H (**14b**) isomers in a 6:1 ratio (44 mg, 89%).

¹H NMR (300 MHz, CDCl₃) δ 8.25 – 8.16 (m, 1H), 8.02 – 7.84 (m, 3H), 7.72 – 7.59 (m, 1H), 7.50 – 7.38 (m, 2H), 7.39 – 7.24 (m, 7H), 7.17 (dd, 8.2, 1.9 Hz, 2H, H⁶), 7.11 (d, 1.9 Hz, 2H, H⁸), 1.38 (s, 3H, ^tBu, isomer 14b), 1.12 (s, 18H, ^tBu, isomer 14a). ¹³C NMR (75 MHz, CDCl₃) δ 170.62 (C^NC ipso 14b), 168.52 (C^NC ipso 14a), 165.52 (C^NC ipso 14b), 165.10 (C^NC ipso 14a), 155.83 (C^NC ipso 14a), 155.74 (C^NC ipso 14b), 145.68 (benzotriazole CH), 145.14 (benzotriazole CH), 145.11 (C^NC ipso 14a), 145.04 (C^NC ipso 14b), 143.83 (C¹, 14a), 143.07 (C¹, 14b), 139.34 (CH benzotriazole), 131.94 (C⁸, 14a), 130.91 (C⁸, 14b), 125.22 (C⁶ or CH benzotriazole), 124.97 (C⁶ or CH benzotriazole), 124.82 (C⁵ or CH benzotriazole), 124.49 (C⁶ or CH benzotriazole), 124.26 (C⁶ or CH benzotriazole), 123.08 (C⁶ or CH benzotriazole), 119.12 (CH benzotriazole), 116.62 (C², 14a), 116.32 (C², 14b), 114.37 (CH, benzotriazole), 113.68 (CH benzotriazole), 35.75(C¹⁰, 14b), 35.40(C¹⁰, 14a), 31.37 (C¹¹, 14b), 31.04 (C¹¹, 14a). Anal. Calcd. (found) for C₃₁H₃₁AuN₄: C, 56.71(56.77); H, 4.76(4.70); N, 8.53(8.45).

(C^NC)Au(Me) (15)

Under a dry nitrogen atmosphere a toluene solution of complex **4** (85 mg, 0.13 mmol) was added to trimethylaluminium (0.075 mL, 1.4 mmol) and the reagents shaken briefly upon transfer. After 10 min, with the reaction remaining under nitrogen, distilled water (10 mL) was slowly added, shaken and allowed to settle for 30 mins. Separation of the organic phase, removal of the volatile components and washing with hexanes gave **15** as a pale yellow solid (43 mg, 60 %). Single crystals suitable for X-ray diffraction were obtained by slow evaporation of a CH₂Cl₂ solution of **15** at room temperature.

¹H NMR (300 MHz, CD₂Cl₂) δ: 7.81 (1H, t, *J* = 8 Hz, H¹), 7.74 (2H, d, *J* = 2 Hz, H⁸), 7.60 (2H, d, *J* = 8 Hz, H⁵), 7.49 (2H, d, *J* = 8 Hz, H²), 7.28 (2H, dd, *J* = 8, 2 Hz, H⁶), 1.37 (18H, s, H¹¹), 1.33 (3H, s, AuCH₃). ¹³C{¹H} NMR (75 MHz, CD₂Cl₂) δ: 167.2 (s), 162.7 (s), 154.1 (s), 148.5 (s), 141.5 (C¹), 130.5 (C⁸), 125.4 (s, C⁵), 123.5 (s, C⁶), 116.3 (s, C²), 35.6 (s,

CCH₃), 31.5 (s, CCH₃), 2.6 (s, AuCH₃). Anal. calc (found) C, 56.42 (56.52); H, 5.46 (5.46); N, 2.53 (2.64).

(C^NC)Au(Et) (16)

Under a dry nitrogen atmosphere a toluene solution of complex **3** (110 mg, 0.19 mmol) was added to a stirred solution of triethylaluminium (0.13 mL, 1.4 mmol) in toluene (10 mL) at 0 °C. After 20 min, with the reaction remaining under nitrogen, distilled water (10 mL) was slowly added with stirring. Separation of the organic phase, removal of the volatile components and washing with cold hexanes gave a pale yellow solid. Due to the compounds partial solubility in hexanes additional material could be obtained recrystallisation of the washings. Total yield (53 mg, 40 %).

¹H NMR (300 MHz, CD₂Cl₂) δ: 7.80 (2H, d, *J* = 2 Hz, H⁸), 7.67 (1H, t, *J* = 8 Hz, H¹), 7.52 (2H, d, *J* = 8 Hz, H⁵), 7.36 (2H, d, *J* = 8 Hz, H²), 7.26 (2H, dd, *J* = 8, 2 Hz, H⁶), 1.98 (2H, q, *J* = 8 Hz, CH₂ of Et), 1.56 (3H, t, *J* = 8 Hz, CH₂CH₃), 1.42 (18H, s, H¹¹). ¹³C{¹H} NMR (75 MHz, CD₂Cl₂) δ: 167.8 (s), 162.5 (s), 154.2 (s), 148.4 (s), 141.5 (s, C¹), 130.5 (s, C⁸), 125.4 (s, C⁵), 123.5 (s, C⁶), 116.3 (s, C²), 35.6 (s, CCH₃), 31.5 (s, CCH₃), 19.4 (s, CH₂CH₃), 15.9 (s, CH₂CH₃). Anal. calc (found) C, 57.14 (56.96); H, 5.68 (5.61); N, 2.47 (2.57).

General protocol for the reactions of (C^NC)AuOH with ArB(OH)₂

(C^NC)AuOH **3** (1 eq) and ArB(OH)₂ (1 eq) were charged in a flask and toluene (20 mL) was added. The mixture was stirred at 60°C for 12 h after which the volatile components were removed under vacuum. The resulting solid was washed with light petroleum (2 x 3 mL) and dried under vacuum, yielding the corresponding gold aryl. Additional purification can be achieved by passing a dichloromethane solution of the isolated gold aryl through a silica plug.

(C^NC)Au(C₆H₅) (17)

(C^NC)AuOH **3** (70 mg, 0.126 mmol) and (C₆H₅)B(OH)₂ (16 mg, 0.13 mmol). **18** isolated as a yellow powder (70 mg, 90%).

¹H NMR (300 MHz, CDCl₃) δ 7.81 (t, *J* = 8.0 Hz, 1H, H¹), 7.73 (dd, *J* = 9.5, 8.4 Hz, 2H, H⁶), 7.58-7.54 (m, 4H), 7.47 (d, *J* = 8.0 Hz, 2H, H⁵), 7.40 – 7.21 (m, 4H, C₆H₅), 1.28 (s, 18H, H¹¹). ¹³C NMR (75 MHz, CDCl₃) δ 168.45 (C^NC ipso), 163.26 (C^NC ipso), 154.42 (C₆H₅), 147.97 (C⁷), 147.17 (C₆H₅), 141.42 (C¹), 134.29 (C₆H₅), 132.71 (C⁸), 128.54

(C₆H₅), 124.73 (C⁵), 123.27 (C⁶), 115.79 (C²), 35.30 (C¹⁰), 31.16 (C¹¹). Anal. Calcd. (found) for C₃₁H₃₂AuN: C, 60.49(60.58); H, 5.24(5.25); N, 2.28(2.30).

(C^NC)Au(*p*-F-C₆H₄) (**18**)

(C^NC)AuOH **3** (40 mg, 0.072 mmol) and (C₆H₄F)B(OH)₂ (10 mg, 0.072 mmol). **18** isolated as a yellow powder (42 mg, 92%). Suitable crystals for X-ray analysis were obtained by layering a CH₂Cl₂ solution of **18** with light petroleum.

¹H NMR (300 MHz, CDCl₃) δ 7.81 (t, *J* = 8.0 Hz, 1H, H¹), 7.64 (dd, *J* = 8.5, 6.4 Hz, 2H, *m*-C₆H₄F), 7.56 (d, *J* = 8.2 Hz, 2H, H⁵), 7.47 (d, *J* = 8.0 Hz, 2H, H²), 7.45 (d, *J* = 1.8 Hz, 2H, H⁸), 7.23 (dd, *J* = 8.0 Hz, 2.1 Hz, 2H, H⁶), 7.07 (t, *J* = 9.1 Hz, 2H, *o*-C₆H₄F), 1.26 (s, 18H, H¹¹). ¹³C{¹H} NMR (75 MHz, CDCl₃) δ 168.24 (C^NC ipso), 166.81 (CF, 259 Hz), 163.34 (C^NC ipso), 154.57 (C^NC ipso), 147.17 (C^NC ipso), 141.52 (C¹), 135.00 (d, 6 Hz, Ph^F), 132.50 (C⁸), 129.07 (Ph^F), 124.81 (C⁵), 123.40 (C⁶), 115.86 (C²), 115.28 (d, *J* = 20 Hz, Ph^F), 35.31 (C¹⁰), 31.14 (C¹¹). ¹⁹F NMR (282 MHz, CDCl₃) δ -119.62 (m). Anal. Calcd. (found) for C₃₁H₃₁AuFN: C, 58.77(58.64); H, 4.93(4.84); N, 2.21(2.23).

(C^NC)Au(*p*-^tBu-C₆H₄) (**19**)

(C^NC)AuOH **3** (40 mg, 0.072 mmol) and (^tBu-C₆H₄)B(OH)₂ (13 mg, 0.072 mmol). **19** isolated as a yellow powder (46 mg, 92%).

¹H NMR (300 MHz, CDCl₃) δ 7.76 (t, *J* = 7.9 Hz, 1H, H¹), 7.65 (dd, *J* = 7.1 Hz, 5.5 Hz, 2H, *m*-C₆H₄^tBu), 7.59 (d, *J* = 2 Hz, 2H, H⁸), 7.54 (d, *J* = 8.1 Hz, 2H, H⁵), 7.49 – 7.35 (m, 4H, H² and H⁶, overlapping), 7.25 (d, 2H, *o*-C₆H₄^tBu, overlapping with residual CHCl₃), 1.45 (s, 9H, C₆H₄^tBu), 1.31 (s, 18H, H¹¹). ¹³C{¹H} NMR (75 MHz, CDCl₃) δ 168.54 (C^NC ipso), 163.11 (C^NC ipso), 154.21 (C^NC ipso), 147.17 (C^NC ipso), 147.06 (^tBuPh), 143.99 (^tBuPh), 141.33 (C¹), 133.88 (^tBuPh), 132.68 (C⁸), 125.34 (C⁵ or ^tBuPh), 124.68 (C⁵ or C⁶ or ^tBuPh), 123.19 (C⁶ or ^tBuPh), 115.73 (C²), 35.29 (C₆H₄C(CH₃)₃), 34.32 (C¹⁰), 31.52 (C₆H₄C(CH₃)₃), 31.14 (C¹¹).

(C^NC)Au(*p*-vinyl-C₆H₄) (20)

(C^NC)AuOH **3** (40 mg, 0.072 mmol) and (*p*-vinyl-C₆H₄)B(OH)₂ (11 mg, 0.08 mmol). **20** isolated as a yellow powder (41 mg, 88%).

¹H NMR (300 MHz, CD₂Cl₂) δ 7.77 (t, *J* = 7.9 Hz, 1H, H¹), 7.68 (d, *J* = 8 Hz, 2H, H⁵), 7.54 – 7.49 (m, 2H), 7.42 (dd, 2H, *J* = 8, 2 Hz, H⁶) 7.27 – 7.21 (m, 4H), 5.84 (d, *J* = 17.6 Hz, 1H, vinyl), 5.32 – 5.24 (m, 2H, CH=CH₂), 1.27 (s, 18H, H¹¹). ¹³C{¹H} NMR (75 MHz, CD₂Cl₂) δ 168.62 (C^NC ipso), 163.49 (C^NC ipso), 154.68 (C^NC ipso), 148.57 (C^NC ipso), 147.60 (^{vinyl}Ph), 142.04 (C¹) 137.93 (^{vinyl}Ph), 134.99 (^{vinyl}Ph), 134.28 (HC=CH₂), 132.72 (C⁸), 129.38 (^{vinyl}Ph s), 128.57 (^{vinyl}Ph), 126.70 (C⁵ or ^{vinyl}Ph), 125.21 (C⁵ or C⁶ or ^{vinyl}Ph), 123.64 (C⁶ or ^{vinyl}Ph), 116.41 (C²), 111.97 (HC=CH₂), 35.58 (C¹⁰), 31.34 (C¹¹). Anal. Calcd. (found) for C₃₃H₃₄AuN: C, 61.78(61.85); H, 5.34(5.37); N, 2.18(2.20).

(C^NC)Au(*p*-formyl -C₆H₄) (21)

(C^NC)AuOH **3** (150 mg, 0.27 mmol) and (*p*-formyl-C₆H₄)B(OH)₂ (41 mg, 0.30 mmol). **21** isolated as a yellow powder (147 mg, 85%).

¹H NMR (300 MHz, CD₂Cl₂) δ 10.03 (s, 1H, HC=O), 7.88 (d, *J* = 8.2 Hz, 2H, *p*-formyl-phenyl), 7.81 (dd, *J* = 8 Hz, 2 Hz, 2H, *p*-formyl-phenyl), 7.53 (d, *J* = 8 Hz, 1H, H²), 7.44 (d, *J* = 8 Hz, 2H, H⁵), 7.32 (t, *J* = 8 Hz, 1H, H¹), 7.25 (dd, *J* = 8.1, 2.1 Hz, 2H, H⁶), 1.22 (s, 18H). ¹³C{¹H} NMR (75 MHz, CD₂Cl₂) δ 192.74 (HC=O), 167.68 (C⁹), 163.21 (C³), 158.13 (C-*p*-formyl-phenyl), 154.51 (C⁷), 147.06 (C⁴), 141.84 (C¹), 134.95 (C⁸), 133.56 C-*p*-formyl-phenyl), 132.23 (C-*p*-formyl-phenyl), 129.49 (C-*p*-formyl-phenyl), 124.92 (C⁵), 123.45 (C⁶), 116.14 (C²), 35.14 (C¹⁰), 30.85 (C¹¹). Anal. Calcd. (found) for C₃₂H₃₂AuNO: C 59.72(59.57), H 5.01 (4.93), N 2.18(2.07)

(C^NC)Au(5-acenaphthene) (22)

(C^NC)AuOH **3** (40 mg, 0.072 mmol) and (5-acenaphthene)B(OH)₂ (14 mg, 0.072 mmol). **22** isolated as a pale yellow powder (44 mg, 88%).

¹H NMR (300 MHz, CD₂Cl₂) δ 7.86 (t, *J* = 8.0 Hz, 1H, H1, pyridyl), 7.75 (d, *J* = 7.0 Hz, 1H, acenaphthene), 7.65 (d, *J* = 7.2 Hz, 1H, acenaphthene), 7.60 (d, *J* = 8.1 Hz, 2H, H5, phenyl), 7.53 (d, *J* = 8.0 Hz, 2H, H2, pyridyl), 7.31 (d, *J* = 7.0 Hz, 1H, acenaphthene), 7.27 – 7.21 (m, 3H, phenyl + acenaphthene, overlapping) 7.21 – 7.16 (m, 3H, phenyl + acenaphthene,

overlapping), 3.44 (br s, 4H, CH₂ acenaphtene), 1.07 (s, 18H, H¹¹, ^tBu). ¹³C{¹H} NMR (75 MHz, CD₂Cl₂) δ 167.88 (C^{N^C} ipso), 163.18 (C^{N^C} ipso), 154.05 (C^{N^C} ipso), 147.46 ((C^{N^C} ipso or CH acenaphtene), 145.78 ((C^{N^C} ipso or CH acenaphtene), 143.90 ((C^{N^C} ipso or CH acenaphtene), 142.20 ((C^{N^C} ipso or CH acenaphtene), 141.67 ((C^{N^C} ipso or CH acenaphtene), 140.53 (CH acenaphtene), 134.43 (CH acenaphtene), 133.32 (C⁸), 132.04 (CH acenaphtene), 127.69 (CH acenaphtene), 125.70 (CH acenaphtene), 124.70 (C⁵), 123.07 (C⁶), 120.40 (CH acenaphtene), 118.20 (CH acenaphtene), 116.02 (C²), 34.87 (C¹⁰), 30.67 (C¹¹), 30.50 (CH₂ acenaphtene), 29.97 (CH₂ acenaphtene). Anal. Calcd. (found) for C₃₇H₃₆AuN: C, 64.25(64.09); H, 5.25(5.36); N, 2.03(2.14).

(C^{N^C})Au(2-furanyl) (**23**)

(C^{N^C})AuOH **3** (40 mg, 0.072 mmol) and (2-furanyl)B(OH)₂ (8.7 mg, 0.072 mmol). The isolated powder was redissolved in dichloromethane and passed through a silica plug. The solvent was removed under vacuum, yielding **23** as a pale yellow powder (37 mg, 85%).

¹H NMR (300 MHz, CD₂Cl₂) δ 8.08 (d, *J* = 8.6 Hz, 1H, furanyl), 7.91 (d, *J* = 2.0 Hz, 2H, H⁸, phenyl), 7.84 (t, *J* = 8.0 Hz, 2H, H¹, pyridyl), 7.68 (d, *J* = 7.5 Hz, 1H, furanyl), 7.47 (d, *J* = 8.2 Hz, 2H, H⁵, phenyl), 7.40 (d, *J* = 8.0 Hz, 2H, H², pyridyl), 7.29 (dd, *J* = 8.2 Hz, 2.0 Hz, 2H, H⁶, phenyl), 1.37 (s, 18H, H¹¹, ^tBu). ¹³C{¹H} NMR (75 MHz, CD₂Cl₂) δ C(ipso and a CH furanyl resonance not observed) 170.29 (C^{N^C} ipso) 164.93 (C^{N^C} ipso), 155.52 (C^{N^C} ipso), 145.22 (C^{N^C} ipso), 142.91 (C¹), 130.41 (C⁸), 126.51 (CH furanyl), 125.57 (CH furanyl), 124.90 (C⁵), 124.26 (C⁶), 116.41 (C²), 35.46 (C¹⁰), 30.92 (C¹¹).

(C^{N^C})Au(2-thienyl) (**24**)

(C^{N^C})AuOH **3** (40 mg, 0.072 mmol) and (2-thienyl)B(OH)₂ (9.2 mg, 0.072 mmol). **24** isolated as a bright yellow powder (48 mg, 95%).

¹H NMR (300 MHz, CD₂Cl₂) δ 7.86 (t, *J* = 8.0 Hz, 1H, H¹, pyridyl), 7.72 – 7.63 (m, 3H, H⁸ phenyl + CH thienyl, overlapping), 7.56 (d, *J* = 8.2 Hz, 2H, H⁵, phenyl), 7.48 (d, *J* = 8.0 Hz, 2H, H², pyridyl), 7.35 – 7.26 (m, 3H, H⁶ + CH thienyl, overlapping), 7.23 (dd, *J* = 3.4 Hz, 1.0 Hz, 1H, CH thienyl), , 1.31 (s, 18H, H¹¹). ¹³C{¹H} NMR (75 MHz, CD₂Cl₂) δ 167.83 (C^{N^C} ipso), 164.02 (C^{N^C} ipso), 154.86 (C^{N^C} ipso), 147.52 (C^{N^C} ipso), 142.39 (C¹), 140.18 (C ipso, thienyl), 132.83 (C⁸), 129.17 (CH thienyl), 127.76 (CH thienyl), 126.31

(CH thienyl), 125.32 (C⁵), 123.88 (C⁶), 116.51 (C²), 35.59 (C¹⁰), 31.30 (C¹¹). Anal. Calcd. (found) for C₂₉H₃₀AuNS: C, 56.04(55.90); H, 4.86(5.00); N, 2.25(2.29).

(^tBuPh₂Py)Au(benzo[b]thienyl) (25):

(^tBuPh₂Py)AuOH **3** (92 mg, 0.166 mmol) and (2-benzo[b]thienyl)B(OH)₂ (29.5 mg, 0.166 mmol). The isolated powder was redissolved in dichloromethane and passed through a silica plug. The solvent was removed under vacuum, yielding **25** as a pale yellow powder (102 mg, 92%).

¹H NMR (300 MHz, CD₂Cl₂) δ 7.93 (d, *J* = 8.0 Hz, 1H, benzo[b]thienyl), 7.86 (t, *J* = 8.1 Hz, 1H, H^{1#}), 7.85 (d, *J* = 8.1 Hz, 1H, benzo[b]thienyl), 7.65 (d, *J* = 2.0 Hz, 2H, H^{8#}), 7.57 (d, *J* = 8.2 Hz, 2H, H⁵, phenyl), 7.49 (d, *J* = 8.0 Hz, 2H, H²), 7.40 (s, 1H, benzo[b]thienyl), 7.36 – 7.30 (m, 2H, benzo[b]thienyl), 7.27 (dd, *J* = 8.1 Hz, 2.1 Hz, 2H, H⁶), 1.23 (s, 18H, H¹¹). ¹³C{¹H} NMR (75 MHz, CDCl₃) δ 167.63 (C^NC ipso), 163.88 (C^NC ipso), 154.96 (C^NC ipso), 147.09 (C^NC ipso), 143.82 (CH benzothienyl), 143.03 (CH benzothienyl), 142.26 (C¹ or CH benzothienyl), 142.08 (C¹ or CH benzothienyl), 133.04 (C⁸), 125.31 (CH benzothienyl), 125.08 (C⁵), 123.67 (C⁶), 123.39 (CH benzothienyl), 122.18 (CH benzothienyl), 121.97 (CH benzothienyl), 121.94 (CH benzothienyl), 116.10 (C²), 35.47 (C¹⁰), 31.31 (C¹¹). Anal. Calcd. (found) for C₃₂H₃₂AuNS:C,59.01(59.13); H, 4.80 (4.69); N, 2.09(2.15).

3. Synthesis of gold bidentate complexes

(HC-N^C)Au(Me)(OAc^F) (26)

To a solution of **15** (20 mg, 0.036 mmol) in CH₂Cl₂ (20 mL), 10 eq HOAc^F (20 μL, 0.36 mmol) were added and stirred for 3 min at room temperature. The solvent was removed and the residue was dissolved in toluene (5 mL). Removal of the volatile components *in vacuo* afforded the isolation of **26** as a colourless solid. (22 mg, 91 %)

Single crystals suitable for an X-ray diffraction study were obtained by slow evaporation of a C₆D₆ solution of **26** at room temperature.

¹H NMR (300 MHz, CD₂Cl₂) δ: 8.02 (1H, t, *J* = 8 Hz, H¹), 7.94 (1H, dd, *J* = 8, *J* = 1, H²), 7.74 (1H, d, *J* = 8 Hz, H⁵), 7.48-7.60 (6H, m, ArH), 7.43 (1H, dd, *J* = 8, 2 Hz, H⁶), 1.47 (3H, s, AuCH₃), 1.38 (9H, s, H¹¹), 1.36 (9H, s, H¹¹). ¹³C{¹H} NMR (75 MHz, CD₂Cl₂) δ: 161.4

(s), 161.0 (s), 154.7 (s), 153.7 (s), 141.8 (s), 141.0 (s, C¹) 135.5 (quatern), 135.1 (quatern), 128.7 (CH), 126.2 (C⁵H), 126.2 (CH), 126.2 (CH), 125.4 (s, CH), 125.4 (s, C⁶), 118.1 (s, C²), 35.8 (s, CCH₃), 35.1 (s, CCH₃), 31.3 (s, CCH₃), 31.3 (s, CCH₃), 14.7 (s, AuCH₃). ¹⁹F NMR (282 MHz, CD₂Cl₂) δ: -74.0 (s). Anal. calc (found) C, 50.38 (50.46); H, 4.67 (4.68); N, 2.10 (2.19).

(HC-N[^]C)Au(Et)(OAc^F) (27)

Same method as for complex **26**. Complex **27** (47 mg, 0.083 mmol), 3 equivalents of HOAc^F. Yield (53 mg, 94 %).

¹H NMR (300 MHz, CD₂Cl₂) δ: 8.00 (1H, t, *J* = 8 Hz, H¹), 7.94 (1H, d, *J* = 8 Hz, H²), 7.75 (1H, d, *J* = 8 Hz, H⁵), 7.63 (1H, d, *J* = 2 Hz, H⁸), 7.48-7.61 (5H, m, ArH), 7.44 (1H, dd, *J* = 8, *J* = 2 Hz, H⁶), 2.25 (2H, q, *J* = 8 Hz, CH₂), 1.40 (9H, s, H¹¹), 1.37 (9H, s, H^{11'}), 1.15 (3H, t, *J* = 8 Hz, CH₂CH₃). ¹³C{¹H} NMR (75 MHz, CD₂Cl₂) δ: 161.1 (s), 161.0 (s), 154.9 (s), 153.6 (s), 141.7 (s), 140.8 (s, C¹) 135.5 (s), 135.2 (s), 128.7 (s), 128.5 (s, C⁸), 126.1 (s), 125.9 (s, C⁵), 125.3 (s, C⁶), 125.1 (s), 118.1 (s, C²), 35.7 (s, CCH₃), 35.1 (s, CCH₃), 34.3 (s, CH₂CH₃), 31.3 (s, CCH₃), 31.3 (s, CCH₃), 15.5 (s, CH₂CH₃). ¹⁹F NMR (282 MHz, CD₂Cl₂) δ: -74.0 (s). Anal. calc (found) C, 51.11 (51.26); H, 4.88 (4.94); N 2.06 (2.13).

(HC-N[^]C)Au(C₆H₄F)(OAc^F) (28)

Method 1:

To a mixture of complex **4** (140 mg, 0.215 mmol), AgOAc^F (24 mg, 0.108 mmol) and (HO)₂BC₆H₄F (32 mg, 0.226 mmol) was added DCM (20 mL) and solution stirred for 24 h. Removal of the volatile components and extraction of the residue with toluene gave a colourless solution. Recrystallisation of toluene/petrol solutions at low temperature gave a colourless crystalline solid (122 mg, 76 %). Single crystals suitable for an X-ray diffraction study were grown from dichloromethane solution layered with petroleum ether.

Method 2:

To a solution of **18** (100 mg, 0.158 mmol) in CH₂Cl₂ (20 mL), 10 eq HOAc^F (0.9 mL, 1.58 mmol) were added and stirred for 3 min at room temperature. The solvent was removed and the residue was dissolved in toluene (5 mL). Removal of the volatile components *in vacuo* afforded the isolation of **28** as a colourless solid. (112 mg, 95%)

^1H NMR (300 MHz, CD_2Cl_2) δ : 8.06 (1H, t, $J = 8$ Hz, H^1), 7.97 (1H, d, $J = 8$ Hz, H^2), 7.35-7.74 (9H, m, ArH), 6.90-7.03 (2H, m, Ph^{F}), 6.85 (1H, d, $J = 2$ Hz, H^8), 1.35 (9H, s, CH_3), 1.14 (9H, s, CH_3). $^{13}\text{C}\{^1\text{H}\}$ NMR (75 MHz, CD_2Cl_2) δ : 162.0 (s), 161.6 (s), 154.9 (s), 153.8 (s), 141.4 (s, C^1), 140.9 (s), 134.8 (s), 133.0 (s), 132.6 (s, C^8), 129.3 (s), 128.7 (s), 128.5 (s), 126.2 (s), 125.6 (s), 125.6 (s), 125.4 (s), 118.3 (s, C^2), 115.8 (d, $J = 76$, Ph^{F}), 35.4 (s, CCH_3), 35.1 (s, CCH_3), 31.2 (s, CH_3), 30.9 (s, CH_3). ^{19}F NMR (282 MHz, CD_2Cl_2) δ : -74.07 (3F, s, CF_3), -117.27 (1F, m, $\text{C}_6\text{H}_4\text{F}$). Anal. calc (found) C, 53.02 (52.87); H, 4.31 (4.40); N, 1.87 (1.76).

((HC-N[^]C)Au(*p*-^tBu-C₆H₄F)(OAc^F)) (29)

Following *Method 1* for the synthesis of **28**, compound **4** (150 mg, 0.236 mmol), AgOAc^{F} (26 mg, 0.118 mmol) and (*p*-^tBu-C₆H₄)B(OH)₂ (43 mg, 0.240 mmol) were reacted in CH_2Cl_2 (30 mL) to give **29** as a colourless powder. (139 mg, 75%)

^1H NMR (300 MHz, CD_2Cl_2) δ 8.04 (t, $J = 8$ Hz, 1H, H^1), 7.97 (d, $J = 8$ Hz, 1H, H^2), 7.72 – 7.61 (m, 9H, ArH), 7.59 – 7.49 (m, 2H, Ph^{tBu}), 7.38 – 7.29 (m, 2H, Ph^{tBu}), 7.23 (dd, $J = 8.8$, 2.0 Hz, 2H), 6.79 (d, $J = 1.9$ Hz, 1H, H^8), 1.36 (s, 9H, Ph^{tBu}), 1.31 (s, 9H, H^{11} or $\text{H}^{11'}$), 1.10 (s, 9H, H^{11} or $\text{H}^{11'}$). $^{13}\text{C}\{^1\text{H}\}$ NMR (75 MHz, CD_2Cl_2) δ 161.88 (s), 161.50 (s), 154.68 (s), 153.78 (s), 149.76 (s), 142.48 (s), 141.21 (C^1), 140.81 (s), 138.32 (s), 134.93 (s), 132.91 (C^8), 131.29 (s), 128.72 (s), 126.35 (s), 126.19 (s), 125.49 (s), 125.39 (s), 125.22 (s), 118.27 (C^2), 35.43 (C^{11}), 35.09 ($\text{C}^{11'}$), 34.58 (CH_3), 31.45 (CH_3), 31.25 (CH_3), 30.89 (CH_3). ^{19}F NMR (282 MHz, CD_2Cl_2) δ -73.87 (s).

((HC-N[^]C)Au(*p*-vinyl-C₆H₄F)(OAc^F)) (30)

Following *Method 1* for the synthesis of **28**, compound **4** (150 mg, 0.236 mmol), AgOAc^{F} (26 mg, 0.118 mmol) and (*p*-vinyl-C₆H₄)B(OH)₂ (35.5 mg, 0.240 mmol) were reacted in CH_2Cl_2 (30 mL) for 3 days to give **30** as a colourless powder. (125 mg, 70%)

^1H NMR (300 MHz, CD_2Cl_2) δ 8.09 (t, $J = 7.8$ Hz, 1H, H^1), 8.00 (d, $J = 8.0$ Hz, 2H, H^2), 7.80 – 7.50 (m, 9H, ArH), 7.50 – 7.25 (m, 4H, ^{vinyl}Ph), 6.98 (d, $J = 1.8$ Hz, 1H, H^8), 5.82 (t, $J = 18.3$ Hz, 2H), 5.25 (d, $J = 10.9$ Hz, 1H), 1.39 (s, 9H, H^{11} or $\text{H}^{11'}$), 1.16 (s, 9H, H^{11} or $\text{H}^{11'}$). ^{19}F NMR (282 MHz, CD_2Cl_2) δ -73.85 (s).

(HC-N[^]C)Au(C₆F₅)(OAc^F) (31)

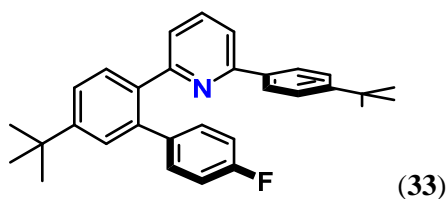
To a deuterated dichloromethane solution (0.8 mL) of complex (HC-N[^]C)Au(C₆F₅) (25 mg, 0.037 mmol) was added HOAc^F (28 μL, 0.37 mmol) and shaken briefly. After 5 mins the ¹H NMR spectrum was recorded and complete consumption of starting material observed. Toluene was added to the solution and the volatile components removed. The addition and removal of toluene was repeated once more to ensure that excess acid was no longer present. Dissolution, filtration through Celite and removal of the volatile components gave a pale yellow solid (26 mg, 90 %).

¹H NMR (300 MHz, CD₂Cl₂) δ: 8.13 (1H, t, *J* = 8 Hz, H¹), 7.95 (1H, dd, *J* = 8 Hz, *J* = 1 Hz, H²), 7.52-7.70 (6H, m, ArH), 7.44 (1H, dd, *J* = 8, 2 Hz H⁶), 6.68 (1H, d, *J* = 2 Hz, H⁸) 1.35 (9H, s, H¹¹), 1.18 (9H, s, H^{11'}). ¹³C{¹H} NMR (75 MHz, CD₂Cl₂) δ: 162.7 (s), 161.7 (s), 155.6 (s), 154.6 (s), 142.3 (s, C¹), 137.0 (s), 134.3 (s), 131.5 (s), 129.4 (s), 128.8 (s), 126.6 (s), 126.5 (s), 126.4 (s), 126.2 (s), 118.6 (s, C²), 35.5 (s, CCH₃), 35.2 (s, CCH₃), 31.2 (s, CH₃), 30.1 (s, CH₃). ¹⁹F NMR (282 MHz, CD₂Cl₂) δ: -73.81 (3F, s, CF₃), -122.69 (2F, m, CF), -156.54 (1F, t, *J* = 20, p-CF), -161.37 (2F, m, CF). Anal. calc (found) C, 48.36 (48.44); H, 3.44 (3.51); N, 1.71 (1.82).

(HC-N[^]C)Au(C₄H₃S)(OAc^F) (32)

Same method as for complex **18** (HC-N[^]C)Au(C₄H₃S) (25 mg, 0.036 mmol), 10 equivalents of HOAc^F, yellow solid. Yield (23 mg, 88 %).

¹H NMR (300 MHz, CD₂Cl₂) δ: 8.07 (1H, t, *J* = 8 Hz, H¹), 7.96 (1H, dd, *J* = 8, 1 Hz, ArH), 7.49-7.70 (7H, m, Ar), 7.38 (1H, dd, *J* = 8, *J* = 2, ArH), 7.06-7.16 (2H, m, Ar), 6.88 (1H, d, *J* = 2 Hz, H⁸), 1.36 (9H, s, H¹¹), 1.16 (9H, s, H^{11'}). ¹³C{¹H} NMR (75 MHz, CD₂Cl₂) δ: 162.5 (s), 161.7 (s), 155.2 (s), 154.1 (s), 141.7 (s, C¹), 140.9 (s), 138.2 (s), 136.2 (s), 134.7 (s), 132.7 (s), 128.7 (s), 128.1 (s), 127.0 (s), 126.7 (s), 126.3 (s), 126.0 (s), 125.8 (s), 125.7 (s), 118.4 (s, C²), 35.5 (s, C¹¹), 35.1 (s, C^{11'}), 31.2 (s, CH₃), 31.0 (s, CH₃). ¹⁹F NMR (282 MHz, CD₂Cl₂) δ: -73.9 (s). Anal. calc (found) C, 50.62 (50.70); H, 4.25 (4.29); N, 1.90 (1.86).



To a solution of $(\text{HC-N}^{\wedge}\text{C})\text{Au}(\text{C}_6\text{H}_4\text{F})(\text{OAc}^{\text{F}})$ (50 mg, 0.067 mmol) (**28**) in CH_2Cl_2 (30 mL), an excess of SMe_2 (5 eq, 25.6 μL , 0.334 mmol) was added. The mixture was stirred at room temperature and the volatile components were removed *in vacuo*. The residue was then extracted with light petroleum and was taken to dryness yielding **32** as a white powder. Crystals suitable for X-ray analysis were obtained by slow evaporation of a light petroleum solution of **32** at room temperature.

^1H NMR (300 MHz, CDCl_3) δ 7.81 – 7.83 (m, 4H), 7.62 – 7.43 (m, 6H), 7.31 – 7.18 (m, 3H), 7.08 – 6.91 (m, 3H), 1.43 (s, 9H), 1.38 (s, 9H). $^{13}\text{C}\{^1\text{H}\}$ NMR (75 MHz, CDCl_3) δ 163.52, 160.26, 158.64, 156.71, 152.08, 151.69, 139.43, 138.35 (d, $J = 3.3$ Hz), 136.83, 136.41, 131.35, 131.24, 130.50, 127.63, 126.71, 125.54, 124.79, 122.98, 117.81, 115.07, 114.79, 34.74, 34.67, 31.37, 31.31. ^{19}F (282 MHz, CDCl_3) 121.45 (m, $\text{C}_6\text{H}_4\text{F}$)

4. Synthesis and chemistry of the $(\text{C}^{\wedge}\text{N}^{\wedge}\text{C})\text{AuH}$

$(\text{C}^{\wedge}\text{N}^{\wedge}\text{C})\text{AuH}$ (**34_H**)

$(\text{C}^{\wedge}\text{N}^{\wedge}\text{C})\text{AuOH}$ (287 mg, 0.51 mmol) (**3**) was dissolved in toluene (30 mL) and at -78°C LiHBEt_3 (517 μL , 0.51 mmol, 1M solution in THF) was added. The mixture was stirred in the dark at -78°C for 5 min and at room temperature for another 15 min. The colour of the mixture changed from yellow to dark yellow and a white precipitate was observed. The supernatant was filtered off, the solvent was removed *in vacuo* and the yellow powder was washed with light petroleum (10 mL), to give **34_H** as a dark yellow powder (209 mg, 0.38 mmol, 75 %). Crystals suitable for X-ray diffraction were grown from a concentrated CH_2Cl_2 solution at -28°C .

^1H NMR (300 MHz, CD_2Cl_2) δ 8.05 – 7.92 (m, 2H, H^8), 7.83 (t, $J = 8$ Hz, 1H, H^1), 7.59 (d, $J = 8$ Hz, 2H, H^5), 7.47 (dd, $J = 8$ Hz, $J = 1$ Hz, 2H, H^2), 7.29 (dd, $J = 8$ Hz, $J = 2$ Hz, 2H, H^6), 1.38 (s, 18H, H^{11}), -6.51 (s, 1H, Au-H). $^{13}\text{C}\{^1\text{H}\}$ NMR (75 MHz, CD_2Cl_2) δ 165.77 (C^9), 163.19 (C^3), 154.82 (C^7), 147.78 (C^4), 141.54 (C^1), 137.62 (C^8), 124.81 (C^5), 122.75 (C^6), 115.89 (C^2), 34.85 (C^{10}), 30.92 (C^{11}). IR: $\nu_{\text{Au-H}} = 2188\text{ cm}^{-1}$. Anal. Calcd. (found) for $\text{C}_{25}\text{H}_{28}\text{AuN}$: C, 55.66 (55.46); H, 5.23 (5.16); N, 2.60 (2.48).

(C¹³N¹⁵C)AuD (**34_D**)

Following the protocol for **34_H**, (C¹³N¹⁵C)AuOH (100 mg, 0.18 mmol) (**3**) was treated with LiDBEt₃ (180 μL, 0.18 mmol, 1M solution in THF) in toluene (15 mL) at -78°C. **34_D** was isolated as a dark yellow powder (28 mg, 0.11 mmol, 60 %).

¹H NMR (300 MHz, CD₂Cl₂) δ 7.98 (d, *J* = 2 Hz, 2H, H⁸), 7.83 (t, *J* = 8 Hz, 1H, H¹), 7.59 (d, *J* = 8 Hz, 2H, H⁵), 7.47 (d, *J* = 8 Hz, 2H, H²), 7.29 (dd, *J* = 8 Hz, *J* = 2 Hz, 2H, H⁶), 1.38 (s, 18H, H¹¹). ²H NMR (77 MHz, CH₂Cl₂) δ -6.58 (s, Au-D).

(C¹³N¹⁵C)Au(CMe=CMe₂) (**35**)

In a J-Young NMR tube, to a solution of (C¹³N¹⁵C)AuH **34_H** (7.5 mg, 0.014 mmol) in C₆D₆ (0.8 mL), 3,3-dimethylallene (2 μL, 0.020 mmol) was added and the NMR tube was shaken and kept in the dark. The reaction was monitored by ¹H NMR spectroscopy. After 20h, full conversion to **35** was noted. The volatile components were removed *in vacuo* yielding a yellow solid (7.7 mg, 0.013 mmol, 92%). The solid residue was dissolved in CD₂Cl₂. Single crystals were obtained by layering a solution of **35** with light petroleum at -28 °C.

¹H NMR (300 MHz, CD₂Cl₂) δ 7.80 (t, *J* = 8 Hz, 1H, H¹), 7.66 (d, *J* = 2 Hz, 2H, H⁸), 7.57 (d, *J* = 8 Hz, 2H, H⁵), 7.48 (d, *J* = 8 Hz, 2H, H²), 7.25 (dd, *J* = 8, 2 Hz, 2H, H⁶), 2.30 (s, 3H, CH₃), 1.87 (s, 3H, CH₃), 1.76 (s, 3H, CH₃), 1.33 (s, 18H, H¹¹). ¹³C{¹H} NMR (75 MHz, CD₂Cl₂) δ 167.90 (C⁹), 163.09 (C³), 154.54 (C⁷), 147.84 (C⁴), 141.68 (C¹), 138.28 (vinyl), 133.35 (C⁸), 125.13 (C⁵), 123.32 (C⁶), 122.12 (vinyl), 116.24 (C²), 35.32 (C¹⁰), 31.37 (C¹¹), 29.81 (Me), 22.89 (Me), 20.05 (Me). Anal. Calcd. (found) for C₃₀H₃₆AuN: C, 59.30 (59.27); H, 5.97 (6.01); N, 2.31 (2.41).

(C¹³N¹⁵C)Au(CMe=CHCy) (**36**)

To a solution of (C¹³N¹⁵C)AuH **34_H** (10 mg, 0.018 mmol) in C₆D₆ (0.8 mL) in a J-Young NMR tube was added cyclohexyl allene (3.5 μL, 0.024 mmol). The mixture was shaken briefly and then kept in the dark. The reaction was monitored by ¹H NMR spectroscopy and after 72 h, the conversion to **3a** was found to be 90%. The remaining 10% of the reaction mixture consisted of unreacted **34_H** and **37** which formed during the reaction. The volatile components were removed *in vacuo* and the solid residue was dissolved in CD₂Cl₂.

^1H NMR (300 MHz, CD_2Cl_2) δ 7.80 (t, $J = 8$ Hz, 1H, H^1), 7.74 (d, $J = 2$ Hz, 2H, H^8), 7.58 (d, $J = 8$ Hz, 2H, H^5), 7.48 (d, $J = 8$ Hz, 2H, H^2), 7.25 (dd, $J = 8$ Hz, $J = 2$ Hz, 2H, H^6), 6.02 (d, $J = 8$ Hz, 1H, vinyl), 2.29 (s, 3H, CH_3), 1.83 – 1.45 (m, 6H, Cy), 1.34 (s, 18H, H^{11}), 1.26 – 1.03 (m, 5H, Cy). $^{13}\text{C}\{^1\text{H}\}$ NMR (75 MHz, CD_2Cl_2) δ 167.70 (C^9), 163.06 (C^3), 154.63 (C^7), 147.85 (C^4), 145.41 (C^1), 141.75 (C^8), 133.64 (vinyl), 129.88 (vinyl), 125.16 (C^5), 123.23 (C^6), 116.29 (C^2), 44.32 (Cy), 35.47 (C^{10}), 33.53 (Cy), 31.37 (C^{11}), 28.25 (CH_3), 26.68 (Cy), 26.33 (Cy). Anal. Calcd. (found) for $\text{C}_{34}\text{H}_{42}\text{AuN}$: C, 61.72 (61.62); H, 6.40 (6.51); N, 2.12 (2.15).

5. Synthesis and reactivity of the Au(II) dimer

$[(\text{C}^{\wedge}\text{N}^{\wedge}\text{C})\text{Au}]_2$ (**37**)

Method 1: $(\text{C}^{\wedge}\text{N}^{\wedge}\text{C})\text{AuH}$ (**34_H**) (7.0 mg, 0.013 mmol), C_6Me_6 (1.5 mg, 0.009 mmol, internal standard) and $(\text{C}^{\wedge}\text{N}^{\wedge}\text{C})\text{AuOH}$ (**3**) (7.2 mg, 0.013 mmol) were charged in a J-Young NMR tube and C_6D_6 (0.8 mL) was added. The mixture was kept in the dark and was monitored by ^1H NMR spectroscopy. Full conversion was observed after 60 h. The solvent was removed *in vacuo* and the yellow solid was dissolved in CH_2Cl_2 and passed through a silica plug to remove trace amounts of **3**. Removal of the solvent *in vacuo* followed by washing the residue with light petroleum (5 mL) yielded **37** as a yellow powder (9 mg, 0.008 mmol, 64%). Crystals suitable for X-ray diffraction were obtained by storing a C_6D_6 solution of **37** at room temperature.

Method 2: $(\text{C}^{\wedge}\text{N}^{\wedge}\text{C})\text{AuH}$ **34_H** (7 mg, 0.013 mmol) and $(\text{C}^{\wedge}\text{N}^{\wedge}\text{C})\text{AuOAc}^{\text{F}}$ (8.2 mg, 0.013 mmol) (**4**) were charged in a J-Young NMR tube and CD_2Cl_2 (0.6 mL) was added. The NMR tube was shaken and kept in the dark. After 5 minutes, **34_H** had been fully consumed with 75% conversion to **37**.

Method 3: To a toluene (25 mL) solution of $(\text{C}^{\wedge}\text{N}^{\wedge}\text{C})\text{AuOAc}^{\text{F}}$ (165 mg, 0.26 mmol) (**4**) was added a toluene solution (15 mL) of cobaltocene (49 mg, 0.26 mmol). The mixture was stirred in the dark for 4 h. After filtration through Celite, the volatile components were removed *in vacuo*. The solid residue was washed with light petroleum (10 mL) to give **37** as a yellow powder (118 mg, 0.22 mmol, 85%).

^1H NMR (300 MHz, CD_2Cl_2) δ 8.12 (d, $J = 2$ Hz, 1H, H^8), 7.85 (t, $J = 8$ Hz, 1H, H^1), 7.57 (d, $J = 8$ Hz, 2H, H^5), 7.53 (d, $J = 8$ Hz, 2H, H^2), 7.14 (dd, $J = 8$ Hz, $J = 2$ Hz, 2H, H^6), 1.01 (s, 18H, H^{11}). $^{13}\text{C}\{^1\text{H}\}$ NMR (75 MHz, CD_2Cl_2) δ 171.84 (C^9), 164.69 (C^3), 155.68 (C^7), 149.77 (C^4), 143.40 (C^1), 142.66 (C^8), 126.06 (C^5), 123.69 (C^6), 117.39 (C^2), 36.49 (C^{10}),

32.69 (C¹¹). Anal. Calcd. (found) for C₅₀H₅₄Au₂N₂: C, 55.76 (55.63); H, 5.05 (5.17); N, 2.60 (2.73).

Control reaction:

(¹BuPh₂Py)AuH **2-H** (7 mg, 0.013 mmol) and C₆Me₆ (3 mg, 0.018 mmol, internal standard) were charged in a J-Young NMR tube and C₆D₆ (0.6 mL) was added. The mixture was kept in the dark and was monitored by ¹H NMR spectroscopy. No conversion to **4** was observed after 60 h.

(C[^]N[^]C)AuI (**38**)

In a J-Young NMR tube, I₂ (2.5 mg, 0.01 mmol) was added to a solution of **37** (10 mg, 0.009 mmol) in CD₂Cl₂ (0.6 mL). The NMR tube was shaken briefly. After 10 minutes, ¹H NMR spectroscopy indicated full conversion of **37** to (¹BuPh₂Py)AuI.

¹H NMR (300 MHz, CD₂Cl₂) δ 7.98 (d, *J* = 2 Hz, 2H, H⁸), 7.85 (t, *J* = 8 Hz, 2H, H¹), 7.53 (d, *J* = 8 Hz, 2H, H⁵), 7.53 – 7.49 (m, 4H, H² and H⁶), 1.35 (s, 18H, H¹¹). ¹³C NMR (75 MHz, CD₂Cl₂) δ 168.36 (C⁹), 164.82 (C³), 155.98 (C⁷), 146.49 (C⁴), 142.42 (C¹), 130.08 (C⁸), 125.24 (C⁵), 123.52 (C⁶), 116.27 (C²), 35.47 (C¹⁰), 30.91 (C¹¹).

Au^{III}₄/Au^I₄ Macrocycle (**39**)

[(C[^]N[^]C)Au]₂ (**37**) (40 mg, 37.1 μmol) was placed in a Schlenk flask sealed with a J-Young valve and dissolved in 30 mL C₆H₆. The solution was degassed by three freeze-pump-thaw cycles and then placed under a UV lamp (365 nm) for 30 minutes. The color of the mixture changed from pale yellow-green to orange-brown. The solvent was removed *in vacuo* and the dark orange residue extracted with light petroleum (2 x 30 mL, bp 40-60 °C). The solvent was then evaporated *in vacuo*, affording the isolation of **2** as a pale-yellow powder. (26 mg, 65 %) Layering a dichloromethane solution of **2** with light petroleum and cooling to -20 °C gave **5** as yellow blocks which were characterised by X-ray crystallography.

IPrAuIPr⁺(Galvinoxyl)⁻ (41)

To a solution of IPrAuH (**40**) (100 mg, 0.171 mmol) in CH₂Cl₂ (30 mL) galvinoxyl (72 mg, 0.171 mmol) was added. The mixture immediately changed colour from pale yellow to purple. Stirring was continued at room temperature for 30 min followed by solvent evaporation. Trituration of the resulting solid with light petroleum (3 x 5 mL) afforded the isolation of **41** as a purple solid (73 mg). Crystals suitable for X-ray diffraction were obtained by storing benzene solutions of **41** at room temperature.

¹H NMR (300 MHz, CD₂Cl₂) δ 7.51 (t, *J* = 8 Hz, 4H, C⁵), 7.40 (s, 4H, phenyl in galvinoxyl), 7.25 (s, 4H, H¹), 7.22 (d, *J* = 4.0 Hz, 4H, H⁴) 7.03 (s, 1H, HC=C bridge in galvinoxyl), 2.36 (sept, *J* = 7 Hz, 8H, H⁶), 1.36 (s, 36H, *t*-butyl of galvinoxyl), 1.16 (d, *J* = 6.9 Hz, 24H), 1.03 (d, *J* = 6.9 Hz, 24H).

6. Synthesis and reactivity of gold(III) peroxides

(C[^]N[^]C)AuOO[^]Bu (42).

Under an atmosphere of nitrogen, (C[^]N[^]C)AuOH (**3**) (200 mg, 0.36 mmol) and 4 Å molecular sieves were charged into a Schlenk flask and toluene (20 mL) was added. ^tBuOOH (5 M in dodecane, 100 μL, 0.5 mmol) was injected and the mixture was stirred at room temperature for 12 h. The mixture was filtered and the volatile components were removed *in vacuo*. The solid residue was washed with light petroleum (2 x 5 mL) and dried under vacuum to give **2** as a yellow powder (180 mg, 80%). Recrystallization from CH₂Cl₂: light petroleum (1:1) at -20 °C gave **2** as yellow blocks.

¹H NMR (300 MHz, CD₂Cl₂) δ 7.91 (d, *J* = 2 Hz, 2H, H⁸), 7.79 (t, *J* = 8.0 Hz, 1H, H¹), 7.49 (d, *J* = 8 Hz, 2H, H⁵), 7.38 (d, *J* = 8 Hz, 1H, H²), 7.28 (dd, *J* = 8, 2 Hz, 2H, H⁶), 1.40 (s, 9H, OOCMe₃), 1.36 (s, 18H, C¹¹). ¹³C{¹H} NMR (75 MHz, CD₂Cl₂) δ 170.80 (C⁹), 164.41 (C³), 154.96 (C⁷), 145.45 (C⁴), 142.42 (C¹), 130.65 (C⁸), 124.82 (C⁵), 124.36 (C⁶), 116.30 (C²), 79.68 (OOCMe₃), 35.75 (C¹⁰), 31.33 (C¹¹), 26.49 (OOCMe₃). IR: 831, 844, 878 cm⁻¹. Anal. Calcd. (found) for C₂₉H₃₆AuNO₂: C, 55.50 (55.59); H, 5.78 (5.80); N, 2.23 (2.34).

(C^NC)AuOOH (43).

(C^NC)AuOH (200 mg, 0.26 mmol) (**3**) was dissolved in toluene (30 mL) and H₂O₂ (30% aq, 82 μL, 0.52 mmol) was added. A yellow precipitate was immediately observed. The mixture was stirred for 30 minutes at room temperature, after which the supernatant was decanted and the yellow precipitate was washed with acetonitrile (5 mL) and light petroleum (5 mL) to afford **3** as a yellow powder (95.6 mg, 65%). . Recrystallisation from CH₂Cl₂: light petroleum (1:1) at +5 °C overnight gave **3** as yellow blocks which were analysed by X-ray diffraction.

¹H NMR (300 MHz, CD₂Cl₂) δ 8.26 (s, 1H, OOH), 7.83 (t, *J* = 8 Hz, 1H, H¹), 7.62 (d, *J* = 2 Hz, 2H, H⁸), 7.52 (d, *J* = 8 Hz, 2H, H⁵), 7.41 (d, *J* = 8. Hz, 2H, H²), 7.30 (dd, *J* = 8, 2 Hz, 2H, H⁶), 1.36 (s, 18H, H¹¹). ¹³C data could not be obtained because of the degradation of (C^NC)AuOOH in solution. IR: 825 cm⁻¹ Anal. Calcd. (found) for C₂₅H₂₈AuNO₂: C, 53.54 (52.91); H, 4.94 (4.80); N 2.45 (2.35).

(C^NC)AuOOAu(C^NC) (44).

Under nitrogen, a solution of (C^NC)AuOOH (150 mg, 0.25 mmol) (**43**) in dry THF (10 mL) was kept in the dark at room temperature. After 3 days, yellow crystalline blocks were observed. The supernatant was filtered off and the residue dried *in vacuo*, giving **4** as yellow crystals. An additional crop of crystals could be obtained by concentrating the mother liquor and leaving the solution to stand at room temperature. Total yield: 81 mg, 55%. The crystals obtained were suitable for X-ray diffraction.

¹H NMR (300 MHz, CD₂Cl₂) δ 8.23 (d, *J* = 2 Hz, 2H, H⁸), 7.80 (t, *J* = 8 Hz, 1H, H¹), 7.51 (d, *J* = 8 Hz, 2H, H⁵), 7.41 (d, *J* = 8 Hz, 1H, H²), 7.23 (dd, *J* = 8, 2 Hz, 2H, H⁶), 1.14 (s, 18H, H¹¹). ¹³C{¹H} NMR (75 MHz, CD₂Cl₂) δ 170.14 (C⁹), 163.45 (C³), 154.41 (C⁷), 145.48 (C⁴), 141.63 (C¹), 129.99 (C⁸), 124.35 (C⁵), 123.71 (C⁶), 115.73 (C²), 35.27 (C¹⁰), 30.91 (C¹¹). IR: 823, 828, 844 cm⁻¹. Anal. Calcd. (found) for C₅₀H₅₄Au₂N₂O₂: C 54.16 (54.00); H 4.91 (5.01); N, 2.53 (2.59).

(C^NC)AuOAu(C^NC) (45).

A solution of (C^NC)AuOH (100 mg, 0.18 mmol) (**3**) in dry acetone (20 mL) was stirred for 16 h at 60 °C. The resulting precipitate was collected and was washed with acetone (5 mL) and light petroleum (5 mL) to give **5** as a yellow powder (49 mg, 50%). Crystals

suitable for X-ray diffraction were obtained by layering a dichloromethane solution of **5** with light petroleum at -25 °C.

^1H NMR (300 MHz, CD_2Cl_2) δ 8.32 (d, 2.0 Hz, 2H, pyridyl), 7.77 (t, J = 8.0 Hz, 1H, pyridyl), 7.50 (d, J = 8 Hz, 2H, phenyl), 7.41 (d, 8.0 Hz, 2H, phenyl), 7.20 (dd, J = 8, 2 Hz, 2H, phenyl), 1.08 (s, 18H, ^tBu). $^{13}\text{C}\{^1\text{H}\}$ NMR (75 MHz, CD_2Cl_2) δ 173.73 (C^9), 164.16 (C^3), 154.85 (C^7), 145.26 (C^4), 141.33 (C^1), 131.18 (C^8), 124.16 (C^5), 123.22 (C^6), 115.57 (C^2), 35.18 (C^{10}), 30.80 (C^{11}). Anal. Calcd. For $\text{C}_{50}\text{H}_{54}\text{Au}_2\text{N}_2\text{O}$ (found): C 54.95 (55.03); H 4.98 (5.09); N, 2.56 (2.66).

Reaction of $(\text{C}^{\wedge}\text{N}^{\wedge}\text{C})\text{AuOAc}^{\text{F}}$ with KO_2 and isolation of $(\text{C}^{\wedge}\text{N}^{\wedge}\text{C})\text{AuO}(\text{C}_4\text{H}_7\text{O})$ (**49**)

Under an atmosphere of oxygen, to a solution of $(\text{C}^{\wedge}\text{N}^{\wedge}\text{C})\text{AuOAc}^{\text{F}}$ (100 mg, 0.157 mmol) (**4**) in a toluene/THF mixture (1:1 v/v) were added potassium superoxide (23 mg, 0.32 mmol) and 4 Å molecular sieves. The mixture was stirred at 40 °C for 16 h in the absence of light. Filtration, evaporation of the volatiles *in vacuo* followed by washing with light petroleum (5 mL) afforded a white powder. Recrystallization from CH_2Cl_2 : light petroleum (1:1) at -20 °C afforded the furanolato complex **9** as yellow blocky crystals (20 mg, 20 %). The crystals were suitable for X-ray diffraction studies.

^1H NMR (300 MHz, CD_2Cl_2) δ 7.88- &.82 (m, 3H, $\text{H}^1 + \text{H}^8$), 7.55 (d, J = 8 Hz, 2H, H^5), 7.44 (d, J = 8 Hz, 2H, H^2), 7.33 (dd, J = 8, 2Hz, 2H, H^6), 5.75 – 5.72 (m, 1H, CH furanolate), 3.85 – 3.81 (m, 2H, CH_2 , furanolate), 2.16 – 1.95 (m, 3H, CH_2 , furanolate) 1.86 – 1.76 (m, 1H, CH_2 , furanolate) 1.39 (s, 18H, H^{11}). $^{13}\text{C}\{^1\text{H}\}$ NMR (75 MHz, CD_2Cl_2) δ 170.21 (C^9), 164.15 (C^3), 154.63 (C^7), 145.00 (C^4), 142.20 (C^1), 129.89 (C^8), 124.53 (C^5), 124.09 (C^6), 116.00 (C^2), 108.02 (furanolate), 67.24 (furanolate), 35.30 (C^{10}), 30.98 (C^{11}), 29.49 (furanolate).

Reaction of $(\text{C}^{\wedge}\text{N}^{\wedge}\text{C})\text{AuOOBu}^{\text{t}}$ **42** with HOAc

To a solution of $(\text{C}^{\wedge}\text{N}^{\wedge}\text{C})\text{AuOOBu}^{\text{t}}$ **42** (5 mg, 7.96 μmol) in C_6D_6 (0.5 mL), HOAc (5 μL , 83.82 μmol) was added. Full conversion to the $(\text{C}^{\wedge}\text{N}^{\wedge}\text{C})\text{AuOAc}$ alongside with the formation of $\text{HOO}^{\text{t}}\text{Bu}$ was observed after 6 h by ^1H NMR spectroscopy.

Reaction of LAuOOAuL **44** with Me₃SiBr

Adding Me₃SiBr (3 μL, 23 μmol) to a solution of (C^N^C)AuOOAu(C^N^C) **44** (7 mg, 6.31 μmol) in CD₂Cl₂ (0.5 mL) gave an instant quantitative conversion to LAuBr together with Me₃SiOOSiMe₃ (65%) and Me₃SiOSiMe₃ (35%), identified by ¹H NMR spectroscopy.

Reaction of (C^N^C)AuOO^tBu (**42**) with acetaldehyde

A mixture of **42** (10 mg, 15.93 μmol) and acetaldehyde (9 μL, 160 μmol) in C₆D₆ (0.5 mL) was kept at 60 °C for 16h. ¹H NMR spectroscopy confirmed quantitative conversion to (C^N^C)AuOAc (**7**).

Reaction of (C^N^C)AuOO^tBu (**42**) with P(*p*-tolyl)₃

To a solution of (C^N^C)AuOO^tBu **42** (10 mg, 15.93 μmol) in C₆D₆ (0.5 mL) at room temperature was added a solution of P(*p*-tolyl)₃ (145 μL, 110 mM, 12.74 μmol) in C₆D₆. Quantitative conversion to (C^N^C)AuO^tBu (**46**) and O=P(*p*-tolyl)₃ was observed by ¹H and ³¹P{¹H} NMR spectroscopy after 16 h.

Reaction of (C^N^C)AuOOH (**43**) with P(*p*-tolyl)₃

Adding a solution of P(*p*-tolyl)₃ (127 μL, 110 mM, 14 μmol) in CD₂Cl₂ to a solution of (C^N^C)AuOOH (**43**) (10 mg, 17.5 μmol) in CD₂Cl₂ (0.5 mL) resulted in an immediate quantitative conversion to (C^N^C)AuOH (**3**) and O=P(*p*-tolyl)₃, as confirmed by ¹H (disappearance of the OOH resonance) and ³¹P{¹H} NMR spectroscopy.

Reaction of (C^N^C)AuOOAuL (**44**) with P(*p*-tolyl)₃

To a solution of (C^N^C)AuOOAu(C^N^C) (**44**) (10 mg, 9 μmol) in CD₂Cl₂ (0.5 mL), a solution of P(*p*-tolyl)₃ (123 μL, 110 mM, 4.3 μmol) in CD₂Cl₂ was added. After 16 h, a mixture of products was observed which contained (C^N^C)AuOOAu(C^N^C) (21 %), (C^N^C)AuCl (**2**) (17%) and the gold(II) complex [(C^N^C)Au]₂ (**37**) (25 %) as the major components, alongside O=P(*p*-tolyl)₃ and P(*p*-tolyl)₃ (ratio 1:1).

Reaction of (C^NC)AuO₂AuL (**45**) with P(*p*-tolyl)₃

To a solution of LAuO₂AuL (**45**) (10 mg, 9.14 μmol) in CD₂Cl₂ (0.5 mL) was added a solution of P(*p*-tolyl)₃ (100 μL, 110 mM, 11 μmol) in CD₂Cl₂. ¹H and ³¹P{¹H} NMR spectroscopy showed quantitative conversion to (LAu)₂ and O=P(*p*-tolyl)₃ after 16 h.

7. Synthesis of gold(I) peroxides

IPrAuOOH (**50**)

A solution of IPrAuH (**40**) (2 mg, 3.41 μmol) in C₆D₆ (0.5 mL) was subjected to three freeze-pump-thaw cycles and was backfilled with O₂ (1 atm). The reaction was monitored by ¹H NMR spectroscopy showing the disappearance of the hydride resonance (δ_H 5.11) and clean conversion to a new compound. Storing a solution of **40** in C₆D₆ under O₂ produced single crystals of **51** while storing a solution of **40** in C₆D₆ under air produced crystals of the carbonate **52**.

¹H NMR (300 MHz, C₆D₆) δ 7.18- 7.16 (t, overlapping with residual C₆H₆ signal, H⁶) 7.15 (d, *J* = 7.3 Hz, 2H, H⁵), 6.36 (s, 1H, H¹), 2.71 (sept, *J* = 8 Hz 1H), 1.53 (d, *J* = 6.5 Hz, 12H), 1.18 (d, *J* = 6.5 Hz, 12H). ¹³C Spectra could not be obtained due to the fast disproportionation of **50** into **48**.

8. Synthesis of chloride-free starting materials bearing the non-substituted (C^NC)^HAu fragment

(C^NC)^HAuOAc^F (**54**)

The protocol for the synthesis of **4** was followed, starting from (C^NC)^HAuCl (**53**) (200 mg, 0.433 mmol) and AgOAc^F in MeCN (40 mL). Isolated yield : 175 mg, 80%. Crystals suitable for X-ray diffraction were obtained by layering a CH₂Cl₂ solution of **54** with light petroleum at room temperature.

¹H NMR (300 MHz, CD₂Cl₂) δ 7.90 (t, *J* = 8.0 Hz, 1H), 7.52 (dd, *J* = 7.7, 1.2 Hz, 2H), 7.43 (d, *J* = 8.0 Hz, 1H), 7.37 (dd, *J* = 7.3, 1.3 Hz, 1H), 7.31 (d, *J* = 1.3 Hz, 2H), 7.28 (t, *J* = 1.6 Hz, 1H), 7.25 (d, *J* = 1.4 Hz, 1H), 7.23 (d, *J* = 1.4 Hz, 1H). ¹³C NMR (75 MHz, CD₂Cl₂) δ 143.76 (s), 132.34 (s), 131.88 (s), 127.67 (s), 125.32 (s), 117.23 (s). ¹⁹F NMR (282 MHz, CD₂Cl₂) δ -73.62 (s). due to the reduced solubility of the sample, the ipsoC signals were not observed

$[(C^{\wedge}N^{\wedge}C)^H AuSMe_2][(NH_2)\{B(C_6F_5)_3\}_2]$ (**55**)

A solution of $(C^{\wedge}N^{\wedge}C)^H AuCl$ (**53**) (100 mg, 0.216 mmol) in CH_2Cl_2 (40 mL) was treated with $[Ti(OEt_2)_2][[H_2N\{B(C_6F_5)_3\}_2]$ (294 mg, 0.216 mmol) and SMe_2 (3 mL). The mixture was stirred at room temperature for 16 h during which a white precipitate ($TiCl$) was observed. The mixture was filtered and the supernatant was taken to dryness giving a yellow waxy solid. The solid was then triturated with light petroleum (3 x 10 mL) to afford the isolation of **55** as a yellow powder. (254 mg, 75%) Single crystals suitable for an X-ray diffraction study were obtained by layering a CH_2Cl_2 solution of **55** with light petroleum at room temperature.

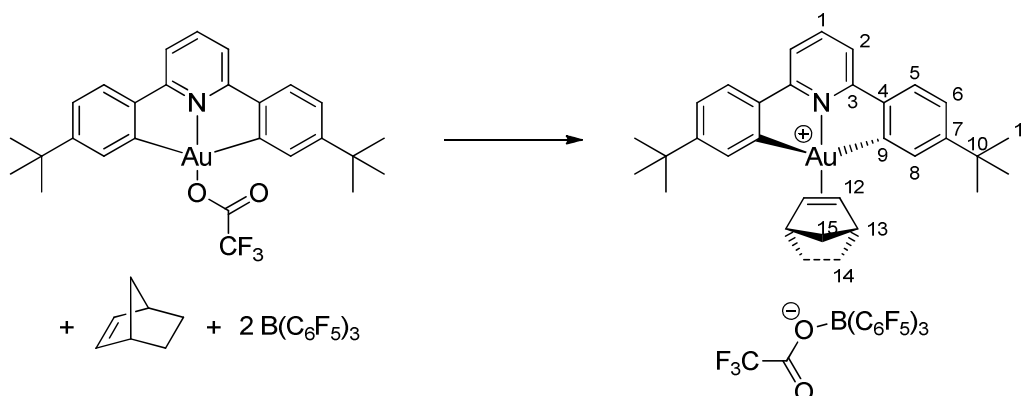
1H NMR (300 MHz, CD_2Cl_2) δ 8.09 (t, $J = 8.0$ Hz, 1H), 7.75 (dd, $J = 7.7, 1.3$ Hz, 2H), 7.73 – 7.62 (m, 4H), 7.56 (td, $J = 7.4, 1.4$ Hz, 2H), 7.53 – 7.41 (m, 2H), 5.71 (s, 2H), 3.25 (s, 6H). ^{19}F NMR (282 MHz, CD_2Cl_2) δ -133.28 (t, $J = 137.4$ Hz), -160.19 (t, $J = 20.3$ Hz), -165.72 (d, $J = 19.7$ Hz).

$[(C^{\wedge}N^{\wedge}C)^H AuSMe_2][(OAc^F)\{B(C_6F_5)_3\}]$ (**56**)

To a suspension of $(C^{\wedge}N^{\wedge}C)^H AuOAc^F$ (**54**) (150 mg, 0.298 mmol) and SMe_2 (3 mL) in toluene, $B(C_6F_5)_3$ (153 mg, 0.298 mmol) was added. The solution immediately became clear and was stirred for 16 h at room temperature. The volatile components were removed *in vacuo* and the resulting waxy solid was washed with light petroleum (3 x 5 mL) to give **56** as a yellow powder. (276 mg, 80%) Single crystals suitable for an X-ray diffraction study were obtained by layering a CH_2Cl_2 solution of **56** with light petroleum at room temperature.

1H NMR (300 MHz, CD_2Cl_2) δ 8.09 (t, $J = 8.0$ Hz, 1H), 7.75 (dt, $J = 7.8, 3.9$ Hz, 2H), 7.71 – 7.62 (m, 4H), 7.56 (td, $J = 7.4, 1.4$ Hz, 2H), 7.47 (td, $J = 7.5, 1.3$ Hz, 2H), 3.23 (s, 6H). ^{19}F NMR (298 MHz, CD_2Cl_2): δ -76.8 (3F, s, $^{\ominus}OAc^F$), -135.3 (6F, d, $J_{FF} = 21.7$ Hz, *o*- C_6F_5), -160.8 (3F, t, $J_{FF} = 20.9$ Hz, *p*- C_6F_5), -165.9 (6F, m, *m*- C_6F_5).

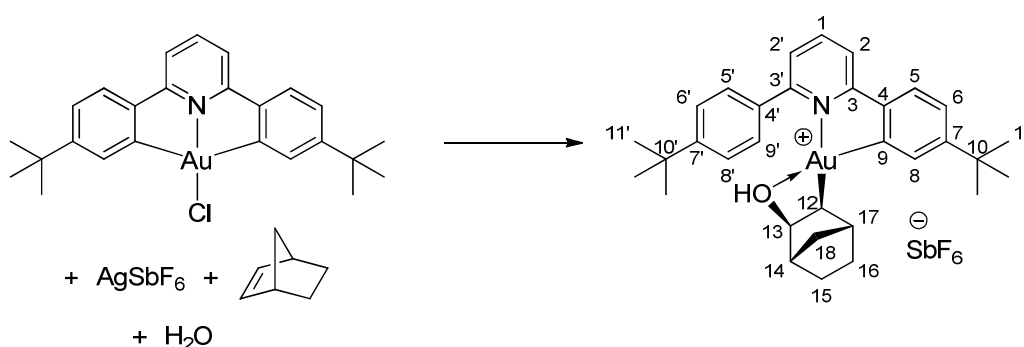
9. Synthesis and reactivity of a gold(III) norbornene complex



A 5 mm NMR tube with a J. Young valve was charged with $\text{B}(\text{C}_6\text{F}_5)_3$ (15.4 mg, 0.030 mmol) and norbornene (2.0 mg, 0.020 mmol) and cooled to $-78\text{ }^\circ\text{C}$. A solution of **4** (10.0 mg, 0.015 mmol) in dichloromethane- d_2 (0.6 mL) was added slowly. The mixture was warmed to room temperature. Dichloromethane- d_2 and excess norbornene were then removed *in vacuo* at $0\text{ }^\circ\text{C}$. The residue was left under reduced pressure for 10 min. Nitrogen was admitted, and the solids were washed with light petroleum ($6 \times 3\text{ mL}$) at $0\text{ }^\circ\text{C}$ and dried *in vacuo* to yield **57** (17.6 mg, 0.014 mmol, 94 %) as a yellow solid.

^1H NMR (CD_2Cl_2 , $-40\text{ }^\circ\text{C}$): δ 8.22 (2H, s, H^8), 7.98 (1H, t, $J_{\text{HH}} = 8.0\text{ Hz}$, H^1), 7.63-7.48 (6H, m, 2,5, H^6), 5.97 (2H, s, H^{12}), 3.49 (2H, s, H^{13}), 1.94 (1H, s, $\text{H}^{15\text{a}}$), 1.90 (1H, s, $\text{H}^{15\text{b}}$), 1.41 (18H, s, H^{11}); note, the signals corresponding to 13 and 14-H were too difficult to distinguish from the residual norbornene and ^1Bu signals. ^{19}F NMR (CD_2Cl_2 , $-40\text{ }^\circ\text{C}$): δ -76.8 (3F, s, OAc^{F}), -135.3 (6F, d, $J_{\text{FF}} = 21.7\text{ Hz}$, *o*- C_6F_5), -160.8 (3F, t, $J_{\text{FF}} = 20.9\text{ Hz}$, *p*- C_6F_5), -165.9 (6F, m, *m*- C_6F_5). $^{13}\text{C}\{^1\text{H}\}$ NMR (CD_2Cl_2 , $-40\text{ }^\circ\text{C}$): δ 164.5 (9-C), 163.6 (3-C), 157.1 (7-C), 146.9 (4-C), 144.3 (1-C), 133.3 (12-C), 133.0 (8-C), 127.0 (5-C), 126.0 (6-C), 118.4 (*ipso*-C, C_6F_5), 116.7 (2-C), 45.5 (15-C), 41.9 (13-C), 35.9 (10-C), 30.8 (11-C), 24.2 (14-C); no defined signals were observed corresponding to the carbon atoms of C-F or C=O bonds.

[HC-N⁺C)Au(κ^2 -norbornol)]SbF₆ (58)



To a solution of (C^NC)*AuCl (100 mg, 0.186 mmol) in CH₂Cl₂ (15 mL) was added norbornene (41 mg, 0.435 mmol) followed by AgSbF₆ (64 mg, 0.186 mmol). A white precipitate (AgCl) formed slowly. The mixture was stirred in the dark for 16 h. The white precipitate was then filtered off. The filtrate was concentrated *in vacuo* to 5 mL, layered with light petroleum (10 mL) and kept at -25 °C. After 48 h colourless prisms were collected, suitable for X-ray diffraction.

¹H NMR (CD₂Cl₂) δ 8.12 (1H, t, *J*_{HH} = 8 Hz, H¹), 7.98 (1H, dd, *J*_{HH} = 8, 1 Hz, H²), 7.73-7.54 (6H, m, 5, 5', 6, 6', 8' and 9'-H), 7.49 (1H, dd, *J* = 8, 2 Hz, H^{2'}), 7.35 (1H, d, *J* = 2 Hz, H⁸), 3.06 (1H, d, *J* = 4 Hz, H¹³), 2.71 (1H, *J* = 4 Hz, H¹⁴), 2.48 (1H, dd, *J* = 6, 3 Hz, H¹²), 2.20 (1H, s, H^{18a}), 2.14 (1H, s, H^{18b}), 1.74-1.11 (4H, 4 × m, 15, 16 and 17-H), 1.40 (9H, s, H¹¹), 1.37 (9H, s, H^{11'}); note, the proton signals for 15, 16 and 17-H protons of the norbornol moiety could not be unambiguously assigned. IR (ATR, cm⁻¹): 3379 cm⁻¹ (ν_{OH})

(C^NC)Au(^Fphtalimide) (59)

Silver perfluorophthalimide [Ag(MeCN)₂] [(^Fphtalimide)₂Ag] (64 mg, 0.087 mmol) and (C^NC)AuCl **2** (100 mg, 0.174 mmol) were charged in a Schlenk flask and CH₂Cl₂ (40 mL) was added. The formation of a white precipitate (AgCl) was immediately observed. The mixture was stirred at room temperature for 16 h followed by filtration. The supernatant was then taken to dryness to afford the isolation of **59** as a yellow powder. (112 mg, 85 %)

¹H NMR (300 MHz, CD₂Cl₂) δ 7.87 (t, *J* = 8.0 Hz, 1H, H¹), 7.45 (d, *J* = 8.0 Hz, 2H, H²), 7.38 (d, *J* = 8.0 Hz, 2H, H⁵), 7.27 – 7.24 (m, 4H), 1.25 (s, 18H, H¹¹). ¹⁹F NMR (282 MHz, CD₂Cl₂) δ -139.39 – -139.63 (m, 2F), -146.24 – -146.45 (m, 2F).

10. Synthesis of gold azides

IPrAuN₃ (61)

A solution of IPrAuOTf (**60**) (100 mg, 0.136 mmol) in MeOH (20 mL) was treated with NaN₃ (13 mg, 0.200 mmol). The mixture was stirred for 3 h at room temperature during which the formation of a white precipitate could be observed. The precipitate was collected by filtration and washed with light petroleum to give **61** as a colourless powder. (77 mg, 90%) Crystals suitable for X-ray diffraction were obtained by layering a CH₂Cl₂ solution of **61** with light petroleum at 5 °C.

¹H NMR (300 MHz, CD₂Cl₂) δ 7.58 (t, *J* = 8 Hz, 2H, H⁵), 7.35 (d, *J* = 8 Hz, 2H, H⁴), 7.23 (s, 2H, C¹), 2.53 (sept, *J* = 7 Hz, 2H, C⁶), 1.32 (d, *J* = 7 Hz, 12H, C⁷), 1.22 (d, *J* = 6.9 Hz, 12H, H⁸). ¹³C{¹H} NMR (75 MHz, CD₂Cl₂) δ 172.89 (C⁸), 145.71 (C³), 133.92 (C²), 130.71 (C⁵), 124.27 (C⁴), 123.50 (C¹), 28.78 (C⁶), 24.17 (C⁷), 23.72 (C⁸). IR (ATR, cm⁻¹): 2045 (ν_{as}), 1279 (ν_s) Anal. Calcd. (found) for C₂₇H₃₇AuN₃: C 51.59 (51.63), H 5.93 (6.15), N 11.14 (10.23)

(C[^]N[^]C)AuN₃ (62)

A solution of (C[^]N[^]C)AuOAc^F (**4**) (100 mg, 0.157 mmol) in MeOH (20 mL) was treated with NaN₃ (13 mg, 0.200 mmol) The mixture was stirred for 1 h at room temperature during which the formation of a yellow precipitate was observed. The precipitate was collected by filtration and washed with light petroleum to give **62** as a yellow powder. (84 mg, 92%) Crystals suitable for X-ray diffraction were obtained by layering a THF solution of **61** with light petroleum at 5 °C.

¹H NMR (300 MHz, CD₂Cl₂) δ 7.92 – 7.78 (t+d, 3H, H¹ + H²), 7.51 (d, *J* = 8.1 Hz, 2H, H⁵), 7.41 (d, *J* = 8.0 Hz, 1H), 7.31 (dd, *J* = 8.1, 1.9 Hz, 2H, H⁶), 1.37 (s, 18H). IR (ATR, cm⁻¹): 2042 (ν_{as}), 1284 (ν_s) Anal. Calcd. (found) for C₂₅H₂₇AuN₄: C 51.73 (51.82), H 4.69 (4.72), N 9.65 (9.70)

[(IPrAu)₂](μ-Cl) (**63**)

Under a dry atmosphere of nitrogen, in a J-Young NMR tube, a solution of IPrAuN₃ (**61**) (10 mg, 0.016 mmol) in CD₂Cl₂ (0.6 mL) was treated with [NO]BF₄ (2 mg, 0.017). The mixture briefly shaken and the ¹H NMR spectrum was recorded. An instant conversion of the azide **61** was noted. The CD₂Cl₂ solution was then layered with light petroleum at 5 °C to afford colourless needles suitable for an X-ray diffraction study.

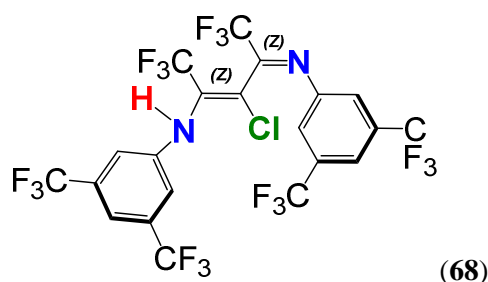
¹H NMR (300 MHz, CD₂Cl₂) δ 7.62 (t, *J* = 7.8 Hz, 2H, H⁵), 7.45 – 7.29 (m, 6H, C¹+C⁴), 2.52 (d, *J* = 6.2 Hz, 2H, H⁶), 1.36 (d, *J* = 7 Hz, 12H, H⁷), 1.27 (d, *J* = 7 Hz, 12H, H⁸).

11. Betadiketiminato complexes

β-diketiminato thallium(I) (**67**)

Under a dry dinitrogen atmosphere and in the absence of light, to a solution of the β-diketiminato proligand **64** (300 mg, 0.476 mmol) in THF (40 mL) a solution of thallium ethoxide (118.73 mg, 0.476 mmol) in THF (10 mL) was added. A colour change from pale yellow to intense orange was noted. The mixture was stirred at room temperature for 16 h followed by evaporation of the volatile components *in vacuo* to give **67** as an orange powder (293 mg, 74%). Single crystals suitable for X-ray diffraction were obtained from a concentrated solution of **67** in light petroleum at 5 °C.

¹H NMR (300 MHz, C₆D₆) δ 7.58 (s, 2H, H⁵), 7.21 (s, 4H, H⁴), 5.90 (s, 1H, H³). ¹⁹F NMR (282 MHz, C₆D₆) δ -60.06 (6F, s), -62.63 (6F, s).



Under a dry dinitrogen atmosphere, to a solution of β-diketiminato silver salt (146.2 mg, 0.198 mmol) (**66**) or thallium salt (165 mg, 0.198 mmol) (**67**) in acetonitrile, KAuCl₄ (75 mg, 0.198 mmol) was added. The mixture was stirred for 16 h at room temperature during which a purple precipitate was formed. The solution was filtered and the supernatant was taken to dryness. Extraction with light petroleum (20 mL) followed by evaporation of the volatile components *in vacuo* afforded the isolation of **68** as a colourless powder. (26 mg,

20%) Crystals suitable for X-ray diffraction were obtained from a concentrated solution of **68** in light petroleum at -20 °C.

¹H NMR (300 MHz, C₆D₆) δ 7.71 (s, 1H, H⁵ or H^{5'}), 7.36 (s, 1H, H⁵ or H^{5'}), 7.13 (s, 2H, H⁴ or H^{4'}), 6.36 (s, 2H, H^{4'} or H⁴), 4.42 (s, br, NH, 1H). ¹⁹F NMR (282 MHz, C₆D₆) δ -62.92 (s, 6F, CF₃), -63.03 (s, 6F, CF₃), -65.49 (q, *J* = 3.0 Hz, 3F), -69.50 (q, *J* = 3.2 Hz, 3F).

KINETICS

Kinetics of O-abstraction from **1 with phosphines.** Stock solutions of **3** (14.4 mM), PR₃ (151 mM) and 18-crown-6 (internal standard, 300 mM) in toluene-*d*₈ were prepared. To a solution of **3** (0.5 mL, 14.4 mM, 7.2 μmol) in toluene-*d*₈ was added a solution of 18-crown-6 (20 μL, 300 mM, 6 μmol). The mixture was cooled at -78 °C. Under light exclusion an appropriate amount of a pre-cooled solution of (p-tolyl)₃P (151 mM) was added. The NMR tube was briefly shaken before being inserted into the NMR probe which was pre-cooled to the appropriate temperature. The reaction was monitored by ¹H NMR spectroscopy. Data points were collected at regular intervals (typically 120 s, with D1 = 1 s, AQ = 5.3 s and NS = 16 scans) Observed rates were determined under pseudo-first order conditions by monitoring the disappearance of the resonance of H⁸ for **3**, (δ = 8.13), the increase of the resonance of H⁸ for (C^{^N^C})AuH **34_H** (δ = 8.40) and aromatic proton signals for O=P(*o*-tolyl)₃ (δ = 7.79) versus the resonance of the internal standard (δ = 3.51). Spectra were integrated automatically using the multi_integ3 command in TopSpin and the baseline correction was done manually.

2.4 Presence vs absence of radical inhibitors

Presence of TEMPO

To a solution of LAuOH **3** (0.5 mL, 14.4 mM, 7.2 μmol) in toluene-*d*₈ was added a solution of internal standard 18-crown-6 (20 μL, 300 mM, 6 μmol) and TEMPO (1.2 mg, 7.7 μmol). The mixture was cooled at -78 °C. Under exclusion of light, a pre-cooled solution of P(*p*-MeC₆H₄)₃ (151 mM) was added. The NMR tube was shaken briefly before being introduced into the NMR probe which was pre-cooled at -30 °C. The observed rate constant was

extracted from the plot of $\ln([\text{LAuOH}]_t/[\text{LAuOH}]_0)$ vs reaction time, $k_{\text{obs}} = 5.01(9) \times 10^{-4} \text{ s}^{-1}$ ($[\text{LAuOH}]_0 : [\text{P}(p\text{-Me-C}_6\text{H}_4)_3]_0 = 1 : 12.3$ determined by NMR).

Absence of TEMPO

Following the protocol described above but without the addition of TEMPO, at $-30 \text{ }^\circ\text{C}$, $k_{\text{obs}} = 4.82(5) \times 10^{-4} \text{ s}^{-1}$ ($[\text{LAuOH}]_0 : [\text{PR}_3]_0 = 1 : 10.5$ determined by NMR).

Control reactions

Under exclusion of light, in an NMR tube, to a solution of LAuOH **3** (4 mg, 7.2 μM) in toluene- d_8 (0.5 mL) was added TEMPO (1.2 mg, 7.7 μmol). No reaction was observed over the course of 24 h.

$\text{P}(p\text{-Me-C}_6\text{H}_4)_3$ (10 mg, 32.86 μmol) was loaded into an NMR tube and toluene- d_8 (0.5 mL) was added. Under light exclusion, TEMPO (5.2 mg, 33.28 μmol) was added. No reaction was observed by ^1H NMR spectroscopy over the course of 24 h.

LAuH **34_H** (7 mg, 13.0 μmol) was loaded in an NMR tube and toluene- d_8 (0.5 mL) was added. Under light exclusion, TEMPO (2 mg, 12.9 μmol) was added. No reaction was observed by ^1H NMR spectroscopy over the course of 24 h.

LAuH **34_H** (7 mg, 13.0 μmol) was loaded in an NMR tube and toluene- d_8 (0.5 mL) was added. Under light exclusion, galvinoxyl (5.5 mg, 13.0 μmol) was added. Full conversion of the LAuH **34_H** to the $(\text{LAu})_2$ **37** was noted after 5 h as indicated by ^1H NMR spectroscopy.

Table 19. Kinetic data for the reaction between LAuOH and PR₃

Temp (K)	[3] ₀ (mM)	[PR ₃] ₀ (mM)	[3] ₀ : [PR ₃] ₀	k _{obs} x10 ⁴ (s ⁻¹)	Obs
223	14.4	599	41.6	2.82(3)	R = <i>p</i> -Me-C ₆ H ₄
223	14.4	482.8	33.53	2.45(1)	R = <i>p</i> -Me-C ₆ H ₄
223	14.4	351.36	24.4	1.62(4)	R = <i>p</i> -Me-C ₆ H ₄
223	14.4	151.2	10.5	0.78(1)	R = <i>p</i> -Me-C ₆ H ₄
263	14.4	152.3	10.58	17.33(3)	R = <i>p</i> -Me-C ₆ H ₄
253	14.4	152.3	10.58	8.23(6)	R = <i>p</i> -Me-C ₆ H ₄
243	14.4	152.3	10.58	4.34(5)	R = <i>p</i> -Me-C ₆ H ₄
233	14.4	152.3	10.58	2.06(1)	R = <i>p</i> -Me-C ₆ H ₄
243	14.4	177.12	12.3	5.01(9)	R = <i>p</i> -Me-C ₆ H ₄ , TEMPO added
243	14.4	152.3	10.58	6.43(6)	R = <i>p</i> -MeOC ₆ H ₄
243	14.4	152.3	10.58	0.94(1)	R = C ₆ H ₅
243	14.4	152.3	10.58	0.621(7)	R = <i>p</i> -FC ₆ H ₄
253	14.4	155.2	10.8	5.49(3)	LAuOD used

Mass Spectrometry sample preparation

To a precooled (-60 °C) toluene-*d*₈ (0.5 mL) solution of LAu¹⁸OH or LAu¹⁶OH (5 mg, 9 μmol) **3** was added (*p*-tolyl)₃P (2.8 mg, 9 μmol). The reaction was kept at low temperature until all the (*p*-tolyl)₃P was oxidised, as confirmed by ¹H NMR spectroscopy. The volatile components were then removed *in vacuo* and the phosphine oxide was extracted with acetonitrile. The extract was analysed by atmospheric pressure chemical ionisation mass spectrometry (APCI(+)-MS). Since the sample preparation did not allow for rigorous exclusion of oxygen, some ¹⁶O contamination of the ¹⁸O labelled sample may have occurred while the sample was nebulised in the mass spectrometer (T = 673 K). Nevertheless, the mass spectrum shows unequivocal ¹⁸O incorporation.

For the ¹⁶O sample, m/z: 321.1 (100%, ¹⁶O=P(*p*-MeC₆H₄)₃ + [H⁺]), 322.1 (60%, ¹⁶O=P(*p*-MeC₆H₄)₃ + [H⁺]), 323.1 (8%, ¹⁶O=P(*p*-MeC₆H₄)₃ + [H⁺]).

For the ¹⁸O sample, m/z: 321.1 (94%, ¹⁶O=P(*p*-MeC₆H₄)₃ + [H⁺]); 322.1 (25%, ¹⁶O=P(*p*-

$\text{MeC}_6\text{H}_4)_3 + [\text{H}^+]$); 323.1 (100%, $^{18}\text{O}=\text{P}(p\text{-MeC}_6\text{H}_4)_3 + [\text{H}^+]$); 324.1 (25%, $^{18}\text{O}=\text{P}(p\text{-MeC}_6\text{H}_4)_3 + [\text{H}^+]$), 325.1 (4%, $^{18}\text{O}=\text{P}(p\text{-MeC}_6\text{H}_4)_3 + [\text{H}^+]$).

X-RAY CRYSTALLOGRAPHY

Crystals of each sample were mounted in oil on glass fibres and fixed in the cold nitrogen stream on a diffractometer. Diffraction intensities for compounds **2—5**, **14**, **15**, **26**, **33**, **34**, **37**, **42**, **44**, **45**, **58**, **61**, **62** and **68** were recorded at 140(2)K on an Oxford Diffraction Xcalibur-3/Sapphire3-CCD diffractometer, equipped with Mo-K α radiation and graphite monochromator. Data were processed using the CrystAlisPro-CCD and –RED software.²⁶² Intensities for compounds **18**, **35**, **39**, **41**, **51** and **67** were collected at 100(2)K on a Bruker-Nonius Roper CCD diffractometer, equipped with Mo-K α radiation and graphite monochromator at the EPSRC National Crystallography service, Southampton, UK.²⁶³

Data were processed using CrystalClear-SM Expert 3.1 b21 (Rigaku, 20112) programs.

The structures of all samples were determined by the direct methods routines in the SHELXS program and refined by full-matrix least-squares methods on F^2 in SHELXL.²⁶⁴ Non-hydrogen atoms were generally refined with anisotropic thermal parameters. Hydrogen atoms were included in idealised positions. No missed symmetry was reported by PLATON.²⁶⁵ Computer programs used in this analysis were run through WinGX.²⁶⁶ Scattering factors for neutral atoms were taken from reference 267.

Compound	2	3	4	14
Reference	Dragos15	RD-237	RD-217	RD-260
Formula weight	573.68	555.13	651.25	656.32
Crystal system	Triclinic	Monoclinic	Triclinic	Triclinic
Space group	P -1	P21/c	P -1	P -1
Unit cell dimensions				
a (Å)	6.9059(3)	14.9668(4)	10.822(3)	9.0201(7)
b	10.0278(7)	11.3514(3)	15.703(5)	10.8043(10)
c	16.1442(9)	12.9152(4)	16.449(5)	13.2449(11)
α (°)	82.537(5)	90	111.656(4)	88.580(7)
β	78.028(5)	99.366(3)	91.252(2)	89.946(7)
γ	81.304(5)	90	109.791(4)	81.414(7)
Volume (Å ³)	1075.49(11)	2164.97(11)	2409.9(13)	1275.93(19)
Z	2	4	4	2
Calculated density (Mg/m ³)	1.772	1.753	1.795	1.708
F(000)	560	1120.0	1272	648
Absorption coefficient μ (mm ⁻¹)	6.974	6.816	6.152	5.793
Crystal colour	Yellow needle	Yellow block	Yellow block	Yellow block
Crystal size (mm ³)	0.40 x 0.04 x 0.03	0.20 x 0.15 x 0.10	0.3 x 0.2 x 0.2	0.20 x 0.20 x 0.10
θ range (°)	3.40 to 29.23	3.46 to 27.48	2.94 to 27.48	3.52 to 27.48
No. of unique reflections, R_{int}	5088 [R(int) = 0.0970]	4938 [R(int) = 0.0457]	10964 [R(int) = 0.0233]	5732 [R(int) = 0.1168]
Data/restraints/parameters	5088 / 0 / 223	4938 / 0 / 263	10964 / 0 / 625	5732 / 0 / 325
Final R indices ('observed' data)	R1 = 0.0707, wR2 = 0.1768	R1 = 0.0236, wR2 = 0.0547	R1 = 0.0195, wR2 = 0.0379	R1 = 0.0483, wR2 = 0.1145
Final R indices (all data)	R1 = 0.0809, wR2 = 0.1806	R1 = 0.0277, wR2 = 0.0569	R1 = 0.0246, wR2 = 0.0390	R1 = 0.0549, wR2 = 0.1209
Largest diff. peak and hole (e Å ⁻³)	5.384 and -2.863	1.375 and -1.083	0.710 and -0.946	2.871 and -3.456

Compound	15	18	28
Reference	Dragos53	2012ncs0289a-sr	rd-226
Formula weight	553.48	633.53	718.36
Crystal system	Triclinic	Triclinic	Triclinic
Space group	P-1	P-1	P-1
Unit cell dimensions			
a (Å)	7.0563(2)	12.5555(3)	11.3438(9)
b	10.0663(3)	15.8095(4)	11.7899(7)
c	16.1346(4)	15.9066(11)	13.5826(7)
α (°)	81.314(2)	116.260(8)	114.937(5)
β	77.672(2)	93.596(7)	91.198(5)
γ	77.709(2)	112.304(8)	112.676(7)
Volume (Å ³)	1087.25(5)	2516.44(19)	1482.90(17)
Z	2	4	2
Calculated density (Mg/m ³)	1.690	1.672	1.609
<i>F</i> (000)	544	1248	678
Absorption coefficient μ (mm ⁻¹)	6.776	5.873	5.000
Crystal colour	Yellow needle		Colourless block
Crystal size	0.40 x 0.40 x 0.10	0.27 x 0.17 x 0.16	0.20 x 0.20 x 0.10
θ range (°)	3.01 to 27.48	3.03 to 27.49	3.48 to 29.39
No. of unique reflections, <i>R</i> _{int}	4977 [R(int) = 0.0464]	11468 [R(int) = 0.0425]	7067 [R(int) = 0.0811]
Data/restrains/parameters	4977 / 0 / 253	11468 / 66 / 613	7067 / 0 / 370
Final <i>R</i> indices ('observed' data)	R1 = 0.0259, wR2 = 0.0776	R1 = 0.0277, wR2 = 0.0614	R1 = 0.0513, wR2 = 0.1263
Final <i>R</i> indices (all data)	R1 = 0.0271, wR2 = 0.0781	R1 = 0.0318, wR2 = 0.0629	R1 = 0.0609, wR2 = 0.1341
Largest diff. peak and hole (e Å ⁻³)	1.485 and -1.817	1.179 and -1.937	3.454 and -2.460

Compound	33	34_H	35	37 · 2C₆H₆
Reference	das_009	rd-293a	rd-339	Dragos51
Formula weight	437.32	539.23	607.56	1233.11
Crystal system	monoclinic	monoclinic	Monoclinic	monoclinic
Space group	C 2/c	P 21/c	C 2/c	P 21/c
Unit cell dimensions				
a (Å)	32.491	13.0685(4)	22.26(3)	12.609(2)
b	6.466	13.3073(3)	12.790(14)	26.9775(15)
c	28.498	12.2361(4)	9.053(10)	17.476(2)
α(°)	90	90	90	90
β	124.23	101.582(3)	98.763(19)	121.135(8)
γ	90	90	90	90
Volume (Å ³)	4949.5	2084.61(10)	2547(5)	5088.3(10)
Z	8	4	4	4
Calculated density (Mg/m ³)	1.174	1.718	1.584	1.610
F(000)	1872	1056	1208	2440
Absorption coefficient μ (mm ⁻¹)	0.072	7.066	5.792	5.798
Crystal colour	Colourless block	Yellow block	Yellow block	Yellow needle
Crystal size	0.20 x 0.15 x 0.10	0.20 x 0.15 x 0.10	0.14 x 0.10 x 0.06	0.15 x 0.05 x 0.05
θ range (°)	3.46 to 27.48	3.40 to 27.48	3.04 to 27.48	2.94 to 25.00
No. of unique reflections, R _{int}	5651 [R(int) = 0.0650]	4727 [R(int) = 0.0398]	2790 [R(int) = 0.0854]	8940 [R(int) = 0.0610]
Data/restraints/parameters	5651 / 0 / 354	4727 / 2 / 254	2790 / 15 / 157	8940 / 66 / 595
Final R indices ('observed' data)	R1 = 0.0537, wR2 = 0.1076	R1 = 0.0273, wR2 = 0.0590	R1 = 0.1029, wR2 = 0.2687	R1 = 0.0347, wR2 = 0.0810
Final R indices (all data)	R1 = 0.0898, wR2 = 0.1241	R1 = 0.0329, wR2 = 0.0611	R1 = 0.1198, wR2 = 0.2943	R1 = 0.0417, wR2 = 0.0843
Largest diff. peak and hole (e Å ⁻³)	0.161 and -0.206	1.944 and -0.974	1.190 and -3.314	2.812 and -1.474

Compound	39	41	42-0.3 CH₂Cl₂	43
Reference	2012ncs0923	2013ncs0543	rd-277	2013ncs0112p
Formula weight	4081.84	1173.11	1909.16	1142.91
Crystal system	tetragonal	Monoclinic	Triclinic	Triclinic
Space group	P 4/n	P2	P -1	P -1
Unit cell dimensions				
a (Å)	26.9936(10)	15.1887(11)	16.4552(2)	7.161(3)
b	26.9936(10)	24.4609(17)	16.4939(3)	18.056(8)
c	12.952(5)	24.3362(17)	17.0121(3)	19.494(8)
α(°)	90	90	75.695(2)	111.221(6)
β	90	94.2700(10)	79.5930(10)	92.691(6)
γ	90	90	87.6340(10)	97.596(6)
Volume (Å ³)	9438(4)	9016.5(11)	4400.47(12)	2316.7(17)
Z	2	8	2	2
Calculated density (Mg/m ³)	1.436	1.728	1.441	1.635
F(000)	3767	4672	1861.8	1120
Absorption coefficient μ (mm ⁻¹)	6.239	6.543	5.051	6.369
Crystal colour	Yellow block	Pink needle	Yellow block	Yellow needle
Crystal size	0.6 x 0.6 x 0.3	0.16 x 0.3 x 0.1	0.4 x 0.3 x 0.2	0.16 x 0.08 x 0.02
θ range (°)	3.02 to 27.48	2.93 to 27.48	3.38 to 25.00	3.53 to 25.00
No. of unique reflections, <i>R</i> _{int}	10770 [R(int) = 0.1255]	19858 [R(int) = 0.1166]	15473 [R(int) = 0.0477]	8069 [R(int) = 0.0424]
Data/restraints/parameters	10770 / 0 / 520	19858 / 0 / 850	15473 / 0 / 936	8069 / 0 / 560
Final <i>R</i> indices ('observed' data)	R1 = 0.0726, wR2 = 0.1735	R1 = 0.1240, wR2 = 0.3469	R1 = 0.0317, wR2 = 0.0772	R1 = 0.0677, wR2 = 0.1561
Final <i>R</i> indices (all data)	R1 = 0.0806, wR2 = 0.1778	R1 = 0.1715, wR2 = 0.3841	R1 = 0.0433, wR2 = 0.0805	R1 = 0.0784, wR2 = 0.1632
Largest diff. peak and hole (e Å ⁻³)	3.269 and -2.122	7.781 and -3.549	1.260 and -0.579	5.864 and -5.338

Compound	44·0.56CH₂Cl₂	45	49	51·2C₆H₆
Reference	2012ncs0922	2013ncs0034	dragos50-sr	
Formula weight	1219.74	1146.51	609.41	1281.20
Crystal system	Monoclinic	Orthorhombic	Monoclinic	Monoclinic
Space group	P 21/c	P bca	P 21/c	I 2/a
Unit cell dimensions				
a (Å)	14.3276(2)	17.5176(6)	14.8206(18)	15.3438(11)
b	18.9625(3)	16.4061(5)	7.1285(3)	19.5250(14)
c	17.9763(12)	33.695(2)	25.4028(10)	19.6769(14)
α(°)	90	90	90	90
β	102.313(7)	90	104.134(7)	92.122(5)
γ	90	90	90	90
Volume (Å ³)	4771.6(3)	9683.8(7)	2602.5(3)	5890.9(7)
Z	4	8	4	4
Calculated density (Mg/m ³)	1.698	1.573	1.555	1.445
F(000)	2386.2	4487	1176	2560
Absorption coefficient μ (mm ⁻¹)	6.249	6.091	5.676	5.017
Crystal colour	Yellow block	Yellow block	Yellow Block	Colourless block
Crystal size	0.06 x 0.05 x 0.05	0.07 x 0.03 x 0.02	0.2 x 0.1x 0.1	0.1 x 0.1x 0.07
θ range (°)	3.09 to 25.00	3.00 to 27.48	2.91 to 32.65	2.07 to 25.00
No. of unique reflections, R _{int}	8379 [R(int) = 0.0355]	11068 [R(int) = 0.0866]	8928 [R(int) = 0.0712]	5175 [R(int) = 0.0355]
Data/restraints/parameters	8379 / 0 / 576	11068 / 0 / 567	8928 / 0 / 261	5175 / 11 / 297
Final R indices ('observed' data)	R1 = 0.0278, wR2 = 0.0649	R1 = 0.0448, wR2 = 0.1080	R1 = 0.0963, wR2 = 0.1070	R1 = 0.0760, wR2 = 0.1762
Final R indices (all data)	R1 = 0.0339, wR2 = 0.0676	R1 = 0.0667, wR2 = 0.1175	R1 = 0.1384, wR2 = 0.1101	R1 = 0.0775, wR2 = 0.1767
Largest diff. peak and hole (e Å ⁻³)	1.364 and -0.633	1.688 and -2.675	3.408 and -2.022	4.772 and -3.310

Compound	52	54	55· CH ₂ Cl ₂	56
Reference	2013ncs0542	dragos11-sr-sr	2011ncs0069	dragos10d
Formula weight	982.13	539.17	1440.90	2226.50
Crystal system	monoclinic	Triclinic	Triclinic	Monoclinic
Space group	P 21/n	P -1	P -1	P 21/c
Unit cell dimensions	a (Å)	8.5879(7)	11.5727(2)	20.4811(2)
	b	41.783(3)	14.4911(3)	15.95290(10)
	c	21.4315(15)	18.4696(4)	26.5706(3)
	α (°)	90	107.1780(10)	90
	β	94.2010(10)	90.8280(10)	123.0080(10)
	γ	90	91.6190(10)	90
Volume (Å ³)	11145.2(14)	971.30(11)	2957.18(10)	7280.24(12)
Z	8	2	2	4
Calculated density (Mg/m ³)	1.171	1.844	1.618	2.031
F(000)	4072	508	1372	4287
Absorption coefficient μ (mm ⁻¹)	2.675	7.611	2.825	4.232
Crystal colour	Colourless needle	Yellow needle	Yellow block	Yellow block
Crystal size	0.26 x 0.06 x 0.04	0.18 x 0.12 x 0.05	0.25 x 0.2 x 0.12	0.35 x 0.21 x 0.15
θ range (°)	2.93 to 27.49	3.45 to 29.08	2.93 to 27.48	3.40 to 29.28
No. of unique reflections, R_{int}	25376 [R(int) = 0.0983]	4552 [R(int) = 0.0871]	25043 [R(int) = 0.0573]	18143 [R(int) = 0.0446]
Data/restraints/parameters	25376 / 0 / 921	4552 / 0 / 235	25043 / 3 / 1762	18143 / 0 / 1163
Final R indices ('observed' data)	R1 = 0.0737, wR2 = 0.1961	R1 = 0.0456, wR2 = 0.1051	R1 = 0.0552, wR2 = 0.1357	R1 = 0.0329, wR2 = 0.0686
Final R indices (all data)	R1 = 0.1172, wR2 = 0.2256	R1 = 0.0585, wR2 = 0.1112	R1 = 0.0682, wR2 = 0.1420	R1 = 0.0446, wR2 = 0.0738
Largest diff. peak and hole (e Å ⁻³)	2.230 and -3.037	2.635 and -2.751	4.657 and -1.585	4.200 and -3.530

Compound	58	61	62	63
Reference	dragos19-sr	dragos69	dragos62	2013ncs0371
Formula weight	886.06	583.39	553.26	717.45
Crystal system	Monoclinic	Monoclinic	Triclinic	monoclinic
Space group	P 21/c	P 21/a	P -1	
Unit cell dimensions				
a (Å)	11.6305(2)	16.7246(2)	6.9221(6)	18.2569(13)
b	19.8302(2)	9.42270(10)	10.0600(13)	16.7694(11)
c	14.7618(2)	19.6220(4)	16.109(2)	20.7931(15)
α (°)	90	90	85.875(12)	90
β	108.5560(10)	105.000(2)	77.626(10)	115.624(4)
γ	90	90	86.297(9)	90
Volume (Å ³)	3227.59(8)	2986.88(8)	1091.5(2)	5739.9(7)
Z	4	5	2	8
Calculated density (Mg/m ³)	1.823	1.622	1.683	1.660
F(000)	1720	1400	514	2738
Absorption coefficient μ (mm ⁻¹)	5.437	6.176	6.755	5.181
Crystal colour	Colourless block	Colourless block	Yellow needle	Colourless needle
Crystal size	0.20 x 0.20 x 0.10	0.25 x 0.23 x 0.15	0.15 x 0.05 x 0.03	0.1 x 0.03 x 0.03
θ range (°)	3.39 to 27.48	2.99 to 27.48	3.02 to 26.37	2.93 to 27.49
No. of unique reflections, R_{int}	7340 [R(int) = 0.0410]	6847 [R(int) = 0.0787]	4464 [R(int) = 0.1453]	12740 [R(int) = 0.0563]
Data/restraints/parameters	7340 / 0 / 385	6847 / 0 / 318	4464 / 6 / 271	12740 / 0 / 570
Final R indices ('observed' data)	R1 = 0.0217, wR2 = 0.0443	R1 = 0.0430, wR2 = 0.1123	R1 = 0.0755, wR2 = 0.1661	R1 = 0.0480, wR2 = 0.1284
Final R indices (all data)	R1 = 0.0255, wR2 = 0.0458	R1 = 0.0606, wR2 = 0.1271	R1 = 0.1042, wR2 = 0.1831	R1 = 0.0823, wR2 = 0.1451
Largest diff. peak and hole (e Å ⁻³)	0.941 and -0.684	2.362 and -1.126	4.600 and -2.393	5.956 and -2.373

Compound	67	68
Reference	rd73	dragosr1
Formula weight	784.57	1329.47
Crystal system	triclinic	orthorhombic
Space group	P 1	P bca
Unit cell dimensions		
a (Å)	8.0144(7)	16.2766(9)
b	9.6552(10)	12.0597(8)
c	16.8626(17)	24.0159(14)
α (°)	91.793(3)	90
β	93.038(5)	90
γ	112.876(4)	90
Volume (Å ³)	1198.6(2)	4714.1(5)
Z	2	4
Calculated density (Mg/m ³)	2.174	1.873
<i>F</i> (000)	724	2608
Absorption coefficient μ (mm ⁻¹)	6.886	0.321
Crystal colour	Orange block	Colourless block
Crystal size	0.2 x 0.22 x 0.18	0.22 x 0.21 x 0.13
θ range (°)	3.04 to 27.48	3.46 to 25.00
No. of unique reflections, R_{int}	5427 (twin)	4146 [R(int) = 0.0781]
Data/restrains/parameters	5427 / 3 / 398	4146 / 0 / 463
Final <i>R</i> indices ('observed' data)	R1 = 0.0811, wR2 = 0.2081	R1 = 0.0323, wR2 = 0.0623
Final <i>R</i> indices (all data)	R1 = 0.0852, wR2 = 0.2138	R1 = 0.0658, wR2 = 0.0690
Largest diff. peak and hole (e Å ⁻³)	3.944 and -5.738	0.222 and -0.190

REFERENCES AND NOTES

- 1 H. Schmidbaur *Interdiscip. Sci. Rev.* **1992**, *17*, 213.
- 2 N. N. Greenwood, A. Earnshaw, *Chemistry of the Elements* Pergamon Press, Oxford, **1984**, pp.1365-1368.
- 3 H. Schmidbaur *Angew. Chem. Int. Ed. Engl.* **1976**, *15*, 728.
- 4 G. J. Hutchings, M. Brust, H. Schmidbaur *Chem. Soc. Rev.* **2008**, *37*, 1759.
- 5 E. Zintl, J. Goubeau, W. Z. Dullenkopf *Z. Phys. Chem. A.* **1931**, *154*, 1. b) W. Biltz, F. Weibke *Z. Anorg. Allg. Chem.* **1938**, *236*, 12. c) A. Sommer *Nature* **1943**, *152*, 215.
- 6 H. Schmidbaur, S. Cronje, B. Djordjevic, O. Schuster *Chem. Phys.* **2005**, *311*, 151.
- 7 P. Pyykkö, J.-P. Desclaux *Acc. Chem. Res.* **1979**, *12*, 276.
- 8 For a review on relativistic effects on the chemistry of Pt, Au and Hg see A. Corma *Angew. Chem. Int. Ed.* **2012**, *51*, 614.
- 9 N. Shapiro, F. D. Toste *Synlett.* **2010**, *5*, 675.
- 10 N. Barlett, *Gold Bull.* **1998**, *31*, 22.
- 11 (a) P. Pyykkö, *Chem. Soc. Rev.* **2008**, *37*, 1967. (b) P. Pyykkö *Angew. Chem. Int. Ed.* **2004**, *43*, 4412. (c) P. Pyykkö *Inorg. Chim. Acta* **2005**, *358*, 4113.
- 12 A. Bard, R. Parsons *Standard Potentials in Aqueous Solutions*, Marcel Dekker, New York, **1985**.
- 13 For a recent review on Au—H and Au···H—X type complexes see H. Schmidbaur, H. G. Raubenheimer, L. Dobrzanska *Chem. Soc. Rev.* **2013**, *43*, 345.
- 14 D. M. Mingos *J. Chem. Soc. Dalton Trans.* **1996**, 561.
- 15 Selected reviews: a) Y. Lu, W. Chen *Chem. Soc. Rev.* **2012**, *41*, 3594. b) H. Qian, M. Zhu, Z. Wu, R. Jin *Acc. Chem. Res.* **2012**, *45*, 1470. c) P. Schwerdtfeger *Angew. Chem. Int. Ed.* **2003**, *42*, 1892. d) H. Häkkinen *Nat. Chem.* **2012**, *4*, 443.
- 16 H. G. Raubenheimer, H. Schmidbaur *Organometallics*, **2012**, *31*, 2507.
- 17 H. Schmidbaur *Pure Appl. Chem.* **1993**, *65*, 691.
- 18 M. C. Gimeno, A. Laguna *Chem. Soc. Rev.* **2008**, *37*, 1952.
- 19 H. Schmidbaur, A. Schier *Chem. Soc. Rev.* **2012**, *41*, 370.
- 20 *Modern Supramolecular Gold Chemistry: Gold-Metal Interactions and Applications* Antonio Laguna ed., Wiley-VCH, Weinheim, 2008, pp. 347-401.
- 21 L. H. Doerrer *Dalton Trans.* **2010**, *39*, 3543.
- 22 F. Mendizabal, P. Pyykkö *Phys. Chem. Chem. Phys.* **2004**, *6*, 900.
- 23 C. Bronner, O. S. Wenger *Dalton Trans.* **2011**, *40*, 12409.

- 24 A. Bayler, A. Schier, G. A. Bowmaker, H. Schmidbaur *J. Am. Chem. Soc.* **1996**, *118*, 7006.
- 25 D. J. Gorin, F. D. Toste *Nature*, **2007**, *446*, 395.
- 26 S. P. Nolan *Nature*, **2007**, *445*, 496.
- 27 H. Schmidbaur, A. Schier *Arab. J. Sci. Eng.* **2012**, *37*, 1187.
- 28 R. O. C. Norman, W. J. E. Parr, C. B. Thomas *J. Chem. Soc. Perkin Trans. 1*, **1976**, 1983.
- 29 G. J. Hutchins *J. Catal.* **1985**, *96*, 292.
- 30 See for example a) A.S.K. Hashmi *Chem. Rev.* **2007**, *107*, 3180. b) E. Mizushima, K. Sato, T. Hayashi, M. Tanaka *Angew. Chem. Int. Ed.* **2002**, *41*, 4563.
- 31 A. S. K. Hashmi *Angew. Chem. Int. Ed.* **2010**, *49*, 5232.
- 32 *Modern Supramolecular Gold Chemistry: Gold-Metal Interactions and Applications* Antonio Laguna (ed.) Wiley-VCH, Weinheim, **2008**, pp. 41-63.
- 33 B. Armer, H. Schmidbaur *Angew. Chem. Int. Ed. Engl.* **1970**, *9*, 101.
- 34 W. J. Pope, C. S. Gibson *J. Chem. Soc.* **1907**, *91*, 2061.
- 35 S. Komiya, T. A. Albright, R. Hoffmann, J. K. Kochi *J. Am. Chem. Soc.* **1976**, *98*, 7255.
- 36 M. S. Kharasch, H. S. Isbell *J. Am. Chem. Soc.* **1931**, *53*, 3053.
- 37 For a review on cyclometallated gold(III) complexes, see: W. Henderson *Adv Organomet. Chem.* **2006**, *54*, 207.
- 38 *Comprehensive Coordination Chemistry* 2nd Edition, Elsevier, New York, Vol 6, pp 717-720.
- 39 For comprehensive reviews see a) H. Schmidbaur, A. Schier "Gold Organometallics" in *Comprehensive Organometallic Chemistry III*, vol. 2. Elsevier, Amsterdam, **2007**. b) B. K. Min, C. M. Friend *Chem. Rev.* **2007**, *107*, 3180.
- 40 P. Schützenberger, *Bull. Soc. Chim. de Paris* **1868**, *10*, 188.
- 41 a) J. Chatt, L. A. Duncanson, B. L. Shaw *Proc. Chem. Soc.* **1957**, 329. b) J. Chatt, B. L. Shaw *J. Chem. Soc.* **1962**, 5075. c) J. Chopoorian, R. S. Nyholm, J. Lewis, *Nature* **1961**, *190*, 528-529.
- 42 Q. Xu, Y. Souma, *Top. Catal.* **1998**, *6*, 17.
- 43 a) W.C. Zeise *Poggendorfs Ann. Phys.* **1827**, *9*, 632. b) W. C. Zeise *Poggendorfs Ann. Phys.* **1831**, *21*, 497. Nevertheless, its structure was not recognised until 50 years later: c) J. A. Wunderlich, D. P. Mellor *Acta Crystallogr.* **1954**, *7*, 130.
- 44 E. Y. Tsui, P. Müller, J. P. Sadighi *Angew. Chem. Int. Ed.* **2008**, *47*, 8937.
- 45 J. Browning, M. Green, B. R. Penfold, J. L. Spencer, F. G. A. Stone, *J. Chem. Soc., Chem. Commun.*, **1973**, 31-32.

- 46 E. Herrero-Gomez, C. Nieto-Oberhuber, S. Lopez, J. Benet-Buchholz, A. M. Echavarren *Angew. Chem. Int. Ed.* **2006**, *45*, 5455.
- 47 First structurally characterised Au(I) alkene: a) D. B. Dell'Amico; F. Calderazzo, R. Dantona, J. Strähle, H. Weiss *Organometallics* **1987**, *6*, 1207. First structurally characterised Au(I) alkyne complex: b) D. M. Mingos, J. Yau, S. Menzer, D. J. Williams *Angew. Chem. Int. Ed. Engl.* **1995**, *34*, 1894.
- 48 Selected reviews: a) A. S. K. Hashmi *Angew. Chem. Int. Ed.* **2010**, *49*, 5232. b) I. Larrosa *Chem. Soc. Rev.* **2011**, *40*, 1910. See also c) A. Comas-Vives, C. González-Arellano, A. Corma, M. Iglesias, F. Sánchez, G. Ujaque *J. Am. Chem. Soc.* **2006**, *128*, 4756. d) A. Comas-Vives, G. Ujaque *J. Am. Chem. Soc.* **2013**, *135*, 1295.
- 49 *Gold Chemistry*. Fabian Mohr (ed.), Wiley-VCH, **2009**, pp. 47-91.
- 50 K-H. Wong, K.-K. Cheung, M. C.-W. Chan, C.-M. Che *Organometallics* **1998**, *17*, 3505.
- 51 K. M.-C. Wong, L.-L. Hung, W. H. Lam, N. Zhu, V. W.-W. Yam *J. Am. Chem. Soc.* **2007**, *129*, 4350.
- 52 H. W. Roesky, S. Singh, K. K. M Yusuff, J. A. Maguire, N. S. Hosmane *Chem. Rev.*, **2006**, *106*, 3813.
- 53 A. N. Nesmeyanov, E. G. Perevalova, Y. T. Struchkov, M. Y. Antipin, K. I. Grandberg, V. P. Dyadchenko *J. Organomet. Chem.* **1980**, *201*, 343.
- 54 S. Gaillard, J. Bosson, R. S. Ramon, P. Nun, A. M.Z. Slawin, S. N. Nolan *Chem. Eur. J.* **2010**, *16*, 13729.
- 55 Y. Tang, B. Yu *RSC Adv.* **2012**, *2*, 12686.
- 56 Y. Yang, P. R. Sharp *J. Am. Chem. Soc.* **1994**, *116*, 6983.
- 57 H. Schmidbaur, S. Hofreiter, A. Paul *Nature* **1995**, *377*, 503.
- 58 a) S. Gaillard, A. M. Z. Slawin, S. P. Nolan *Chem. Commun.* **2010**, *46*, 2742. b) A. Gómez-Suárez, R. S. Ramón, A. M. Z. Slawin, S. P. Nolan *Dalton Trans.* **2012**, *41*, 5461.
- 59 R. S. Ramón, S. Gaillard, A. Poater, L. Cavallo, A. M. Z. Slawin, S. P. Nolan *Chem. Eur. J.* **2011**, *17*, 1238.
- 60 I. I. F. Boogaerts, S. P. Nolan *J. Am. Chem. Soc.* **2010**, *132*, 8858.
- 61 S. Dupuy, F. Lazreg, A. M. Z. Slawin, C. S. J. Cazin, S.P. Nolan *Chem. Commun.* **2011**, *47*, 5455.
- 62 S. Gaillard, P. Nun, A. M. Z. Slawin, S. P. Nolan *Organometallics* **2011**, *29*, 5402.
- 63 E. Brulé, S. Gaillard, M.-N. Rager, T. Roisnel, V. Guérineau, S. P. Nolan, C. M. Thomas *Organometallics* **2011**, *30*, 2650.
-

- 64 M. A. Cinellu, G. Minghetti, N. V. Pianna, S. Stoccoro, A. Zucca, M. Manassero *Chem. Commun* **1998**, 2397.
- 65 M. A. Cinellu, G. Minghetti, M. V. Pianna, S. Stoccoro, A. Zucca, M. Manassero, M. Sansoni *J. Chem. Soc. Dalton Trans.* **1998**, 1735.
- 66 For a review on gold(III) complexes with anionic oxygen donor ligands see: M. A. Cinellu, G. Minghetti *Gold Bull.* **2002**, 35, 11. and references therein
- 67 M. A. Cinellu, G. Minghetti, S. Stoccoro, A. Zucca, M. Manassero *Chem. Commun.* **2004**, 1618.
- 68 M. A. Cinellu, G. Minghetti, F. Cocco, S. Stoccoro, A. Zucca, M. Manassero *Angew. Chem. Int. Ed.* **2005**, 44, 6892.
- 69 M. A. Cinellu, L. Maiore, M. Manassero, A. Casini, N. Arca, H.-H. Fiebig, G. Kelter, E. Micheluci, G. Pieraccini, C. Gabbiani, L. Messori *ACS. Med. Chem. Lett.* **2010**, 1, 336.
- 70 J. A. T. O'Neill, G. M. Rosair, A.-L. Lee *Catal. Sci. Technol.* **2012**, 2, 1818.
- 71 a) M. G. Miles, G. E. Glass, R. S. Tobias *J. Am. Chem. Soc.* **1966**, 88, 5738.
b) G. E. Glass, J. H. Konnert, M. G. Miles, D. Britton, R. S. Tobias *J. Am. Chem. Soc.* **1968**, 90, 1131.
- 72 a) G. Jander, G. Krien *Z. Anorg. Allg. Chem.* **1960**, 304, 154. b) P. G. Jones, G. M. Sheldrick *Acta. Crystallogr.* **1984**, C40, 1776.
- 73 M. A. Cinellu, G. Minghetti, M. V. Pinna, S. Stoccoro, A. Zucca, M. Manassero *J. Chem. Soc., Dalton Trans.* **2000**, 1261.
- 74 B. Pitteri, G. Marangoni, F. Visentin, T. Bobbo, V. Bertolasi, P. Gilli *J. Chem. Soc., Dalton Trans.* **1999**, 677.
- 75 M. A. Cinellu, G. Minghetti, M. V. Pinna, S. Stoccoro, A. Zucca, M. Manassero *Eur. J. Inorg. Chem.* **2003**, 2304.
- 76 M. A. Cinellu, G. Minghetti, M. V. Pinna, S. Stoccoro, A. Zucca, M. Manassero *J. Chem. Soc., Dalton Trans.* **1999**, 2823.
- 77 G. Marcon, S. Carotti, M. Coronello, L. Messori, E. Mini, P. Orioli, T. Mazzei, A. A. Cinellu, G. Minghetti *J. Med. Chem.* **2002**, 45, 1672.
- 78 V. K.-M. Au, K. M.-C. Wong, N. Zhu, V. W.-W. Yam *J. Am. Chem. Soc.* **2009**, 131, 9076.
- 79 F. Kröhnke *Synthesis* **1976**, 1.
- 80 We have found that the (C^NC)Au⁺ cation can only be stabilised by the solvent (CH₂Cl₂) at temperatures below -10 °C. Above this temperature notable decomposition and reduction is observed by ¹H NMR spectroscopy.
-

- 81 A. Venugopal, Z. P. Shaw, K. W. Törnroos, R. H. Heyn, M. Tilset *Organometallics* **2011**, *30*, 3250.
- 82 S. Komiya, J. C. Huffman, J. K. Kochi *Inorg. Chem* **1977**, *16*, 2138.
- 83 A. Bondi *J. Phys. Chem.* **1964**, *68*, 441.
- 84 a) K. Shen, Y. Fu, J.-N. Li, L. Liu, Q.-X. Guo *Tetrahedron* **2007**, *63*, 1568.
b) W. S. Matthews, J. E. Bares, J. E. Bartmess, F. G. Bordwell, F. J. Cornforth, G. E. Drucker, Z. Margolin, R. J. McCallum, G. J. McCollum, N. R. Vainer *J. Am. Chem. Soc.* **1975**, *97*, 7006. c) F. G. Bordwell *Acc. Chem. Res.* **1998**, *21*, 456.
- 85 a) S. G. Weber, D. Zahner, F. Rominger, B. F. Straub *Chem. Commun.* **2012**, *48*, 11325.
- 86 D. V. Partyka, M. Zeller, A. D. Hunter, T. G. Gray *Angew. Chem. Int. Ed.* **2006**, *45*, 8188.
- 87 E. Langseh, C. H. Görbitz, R. H. Heyn, M. Tilset *Organometallics* **2012**, *31*, 6567.
- 88 V. W.-W. Yam, K. M.-C. Wong *Chem. Commun.* **2011**, *47*, 11579.
- 89 W.-P. To, G. S.-M. Tong, W. Lu, C. Ma, J. Liu, A. L.-F. Chow, C.-M. Che *Angew. Chem. Int. Ed.* **2012**, *51*, 2654.
- 90 V. W.-W. Yam, K. M.-C. Wong, L.-L. Hung, N. Zhu *Angew Chem. Int. Ed* **2005**, *44*, 3107.
- 91 V. K.-M. Au, K. M.-C. Wong, N. Zhu, V. W.-W. Yam *Chem. Eur. J.* **2011**, *17*, 130.
- 92 J. A. Garg, O. Blacque, K. Venkatesan *Inorg. Chem.* **2011**, *50*, 5430.
- 93 V. W.-W. Yam, S. W.-K. Choi, T.-F. Lai, W.-K. Lee *J. Chem. Soc., Dalton Trans.* **1993**, 1001.
- 94 J. A. Garg, O. Blacque, T. Fox, K. Venkatesan *Inorg. Chem.* **2010**, *49*, 11463.
- 95 a) J. N. Demas, G. A. Crosby *J. Phys Chem.* **1971**, *75*, 991. b) J. van Houten, R. Watts *J. Am. Chem. Soc.* **1976**, *98*, 4853.
- 96 B. Cornilis, W. A. Herrmann, *Applied Homogeneous Catalysis with Organometallic Compounds*, Wiley-VCH, Weinheim, **1996**.
- 97 M.-J. Crawford, T. M. Klapötke *Angew. Chem. Int. Ed.* **2002**, *41*, 2269.
- 98 a) For a review see A. S. K. Hashmi *Angew. Chem. Int. Ed.* **2006**, *45*, 7896.
b) B. Alcaide, P. Almendros, T. Martines del Campo, I. Fernández *Chem. Commun.* **2011**, *47*, 9054.
- 99 a) A. Negoï, S. Wuttke, E. Kemnitz, D. Macovei, V. I. Parvulescu, C. M. Teodorescu, S. M. Coman *Angew. Chem. Int. Ed.* **2010**, *49*, 8134. b) C. Gonzáles-Arellano,

- A. Corma, M. Iglesias, F. Sánchez *Chem. Commun.* **2005**, 3451. c) A. Arnanz, C. González-Arrelano, A. Juan, A. Corma, M. Iglesias, F. Sánchez *Chem. Commun.* **2010**, 46, 3001.
- 100 a) H. Ito, T. Saito, T. Miyahara, C. Zhong, M. Sawamura *Organometallics* **2009**, 28, 4829. b) S. Labouille, A. Escalle-Lewis, Y. Jean, N. Mézailles, P. Le Floch *Chem. Eur. J.* **2011**, 17, 2256.
- 101 J. Xie, H. Li, J. Zhou, Y. Cheng, C. Zhu *Angew. Chem. Int. Ed.* **2012**, 51, 1252.
- 102 a) X. Wang, L. Andrews *J. Am. Chem. Soc.* **2001**, 123, 12899. b) X. Wang, L. Andrews *Angew. Chem. Int. Ed.* **2003**, 42, 5201. c) L. Andrews, X. Wang *J. Am. Chem. Soc.* **2003**, 125, 11751. d) L. Andrews *Chem. Soc. Rev.* **2004**, 33, 123. See also ref. 13 and references therein.
- 103 See for example a) M. Green, A. G. Orpen, I. D. Salter, F. G. A. Stone *J. Chem. Soc. Dalton Trans.* **1984**, 2497. b) A. Albinati, F. Demartin, P. Janser, L. F. Rhodes, L. M. Venanzi *J. Am. Chem. Soc.* **1989**, 111, 2115. c) M. Crespo, J. Sales *J. Chem. Soc. Dalton Trans.* **1989**, 1089. d) A. Albinati, S. Chaloupka, A. Currao, W. T. Klooster, T. K. Koetzle, R. Nesper, L. M. Venanzi *Inorg. Chem. Acta* **2000**, 300-302, 903.
- 104 A. Escalle, G. Mora, F. Gagosz, N. Mézailles, X. F. Le Goff, Y. Jean, P. Le Floch *Inorg. Chem.* **2009**, 48, 8415.
- 105 G. N. Khairallah, R. A. J. O'Hair, M. I. Bruce *Dalton Trans.* **2006**, 3699.
- 106 G. Klatt, R. Xu, M. Pernpointner, L. Molinari, T. Q. Hung, F. Rominger, A. S. K. Hashmi, H. Köppel *Chem. Eur. J.* **2013**, 19, 3954.
- 107 H. Lv, J.-H. Zhan, Y.-B. Cai, Y. Yu, B. Wang, J.-L. Zhang *J. Am. Chem. Soc.* **2012**, 134, 16216.
- 108 E. Wiberg, H. Neumaier *Inorg. Nucl. Chem. Lett* **1965**, 1, 35.
- 109 Y. Ruiz-Morales, G. Schreckenbach, T. Ziegler *Organometallics* **1996**, 15, 3920.
- 110 a) P. Hrobárik, V. Hrobárikova, F. Meier, M. Repiský, S. Komorovský, M. Kaupp *J. Phys. Chem. A.* **2011**, 115, 5654. b) P. Hrobárik, V. Hrobárikova, A. H. Greif, M. Kaupp *Angew. Chem. Int. Ed.* **2012**, 51, 10844.
- 111 M. Kaupp Relativistic Effects on NMR Chemical Shifts. *Relativistic Electroic Structure Theory II: Applications*; P. Schwerdfeger, Ed. Elsevier: Amsterdam, 2004, Chapter 9, pp 552-597.
- 112 a) PhHgH : Z. Zhu, M. Brynda, R. J. Wright, R. C. Fischer, W. A. Merrill, E. Rivard, R. Wolf, J. C. Fettinger, M. M. Olmstead, P. P. Power *J. Am. Chem. Soc.* **2007**, 129, 10847. b) (IPr)CuH: N. P. Mankad, D. S. Laitar, J. P. Sadighi *Organometallics* **2004**, 23, 3369. c) Pt(II)H : A. L. Seligson, R. L. Cowan, W. C. Trogler *Inorg. Chem.* **1991**, 30,

3371. d) Ir(III)H : H. D. Empsall, E. M. Hyde, E. Mentzer, B. L. Shaw, M. F. Uttely *J. Chem. Soc. Dalton Trans.* **1976**, 2069.
- 113 K. P. Huber, G. Hertzberg *Molecular Spectra and Molecular Structure IV. Constants of Diatomic Molecules*; Van Nostrand Reinhold, New York, **1979**, pp.54-56.
- 114 A. Zucca, S. Stoccoro, M. A. Cinellu, G. L. Petretto, G. Minghetti *Organometallics* **2007**, *26*, 5621.
- 115 a) G. M. Whitesides, J. F. Gaasch, E. R. Stedronsky *J. Am. Chem. Soc.* **1972**, *94*, 5258. b) T. J. McCarthy, R. G. Nuzzo, G. M. Whitesides *J. Am. Chem. Soc.* **1981**, *103*, 1676.
- 116 Nevertheless, five coordinated gold(III) complexes are rare but not unknown: S. M. Godfrey, N. Ho, C. A. McAuliffe, R. G. Pritchard *Angew. Chem. Int. Ed. Engl.* **1996**, *33*, 2344.
- 117 M. H. Chisholm, H. C. Clark *Acc. Chem. Res.* **1973**, *6*, 202.
- 118 L.-P. Liu, G. B. Hammond *Chem. Soc. Rev.* **2012**, *41*, 3129.
- 119 O. A. Egorova, H. Seo, Y. Kim, D. Moon, Y. M. Rhee, K. H. Ahn *Angew. Chem. Int. Ed.* **2011**, *50*, 11446.
- 120 A. Besora, A. Lledos, F. Maseras *Chem. Soc. Rev.* **2009**, *38*, 957.
- 121 S. J. Lancaster, A. Rodriguez, A. Lara-Sanchez, M. D. Hannat, D. A. Walker, D. L. Hughes, M. Bochmann *Organometallics* **2002**, *21*, 451.
- 122 a) P. Pyykkö *Chem. Soc. Rev.* **2008**, *37*, 1967. b) P. Pyykkö *Angew. Chem. Int. Ed.* **2004**, *43*, 4412. c) P. Pyykkö *Inorg. Chem. Acta* **2005**, *358*, 4113.
- 123 A. Laguna, M. Laguna *Coord. Chem. Rev.* **1999**, *193-195*, 837.
- 124 For Au(II) compounds by metal oxidants see for example: a) H. H. Murray, A. M. Mazany, J. P. Fackler, Jr. *Organometallics* **1985**, *4*, 154.; b) V. W.-W. Yam, S. W.-K. Choi, K.-K. Cheung, *J. Chem. Soc., Chem. Commun.* **1996**, 1173; c) V. W.-W. Yam, C.-K. Li, C.-L. Chan, K.-K. Cheung, *Inorg. Chem.* **2001**, *40*, 7054; d) M. D. Irwin, H. E. Abdou, A. A. Mohamed, J. P. Fackler, Jr. *Chem. Commun.* **2003**, 2882; e) D. Y. Melgarejo, G. M. Chiarella, J. P. Fackler, Jr., L. M. Perez, A. Rodrigue-Witchel, C. Reber, *Inorg. Chem.* **2011**, *50*, 4238.
- 125 For Au(II) compounds by oxidative addition see for example: a) H. Schmidbaur, J. R. Mandl, A. Frank, G. Huttner, *Chem. Ber.* **1976**, *109*, 466; b) D. C. Calabro, B. A. Harrison, G. T. Palmer, M. K. Moguel, R. L. Rebbert, J. L. Burmeister, *Inorg. Chem.* **1981**, *20*, 4311; c) H. H. Murray, J. P. Fackler, Jr., *Organometallics* **1984**, *3*, 821.; d) J. D. Basil, H. H. Murray, J. P. Fackler, Jr., J. Tocher, A. M. Mazany, B. T. Bancroft, H. Knachel, D. Dudis, T. J. Delord, D. O. Marler, *J. Am. Chem. Soc.* **1985**, *107*, 6908; e) R. Usón, A. Laguna, M. Laguna, M. N. Fraile, *J. Chem. Soc., Dalton Trans.* **1986**, 291; f) H. H. Murray, J. P. Fackler, Jr., L. C. Porter, D. A. Briggs, M. A. Guerra, R. J. Lagow, *Inorg.*

- Chem.* **1987**, *26*, 357; g) C. King, D. D. Heinrich, G. Garzon, J. C. Wang, J. P. Fackler, Jr., *J. Am. Chem. Soc.* **1989**, *111*, 2300; h) R. Usón, A. Laguna, M. Laguna, J. Jimenez, P. G. Jones, *J. Chem. Soc., Dalton Trans.* **1991**, 1361; i) M. C. Gimeno, J. Jimenez, P. G. Jones, A. Laguna, M. Laguna, *Organometallics* **1994**, *13*, 2508. j) M. Bardaji, N. G. Connelly, M. C. Gimeno, P. G. Jones, A. Laguna, M. Laguna, *J. Chem. Soc., Dalton Trans.* **1995**, 2245; k) H. E. Abdou, A. A. Mohamed, J. P. Fackler, Jr. *Inorg. Chem.* **2007**, *46*, 9692.
- 126 For Au(II) compounds by comproportionation see: J. Coetzee, W. F. Gabrielli, K. Coetzee, O. Schuster, S. D. Nogai, S. Cronje, H. G. Raubenheimer, *Angew. Chem. Int.Ed.* **2007**, *46*, 2497.
- 127 C. M. Fafard, D. Adhikari, B. M. Foxman, D. J. Mindiola, O. V. Ozerov, *J. Am. Chem. Soc.* **2007**, *129*, 10318.
- 128 a) S. N. Mendiara, M. E. J. Coronel *Appl. Magn. Res.* **2008**, *33*, 341. b) L.R. Mahoney, G. D. Mendenhall, K. U. Ingold *J. Am. Chem. Soc.* **1973**, *95*, 8610.
- 129 J. A. Martinho Simoes, J. S. Beauchamp *Chem. Rev.* **1990**, *90*, 629.
- 130 D.-A. Rosca, J. A. Wright, D. L. Hughes, M. Bochmann *Nat. Commun.* **2013**, *4*, 2167. doi: 10.10138/ncomms3167.
- 131 E. Tkatchouk, N. P. Mankad, D. Benitez, W. A. Goddard III, F. D. Toste *J. Am. Chem. Soc.* **2011**, *133*, 14293.
- 132 B. Sahoo, M. N. Hopkinson, F. Glorius *J. Am. Chem. Soc.* **2013**, *135*, 5505.
- 133 A. J. Blake, J. A. Grieg, A. J. Holder, T. I. Hyde, A. Taylor, M. Schröder *Angew. Chem. Int. Ed. Engl.* **1990**, *29*, 197.
- 134 E. W. Y. Wong, A. Miura, M. D. Wright, Q. He, C. J. Walsby, S. Shimizu, N. Kobayashi, D. B. Leznoff *Chem. Eur. J.* **2012**, *18*, 12404.
- 135 The authors of ref 133 have used the same ligand environment to stabilise monomeric “Pd(III)” complexes. Nevertheless, DFT calculations reveal that the SOMO contains 26-27% metal character and a “significant contribution from the S donors of the macrocyclic ligand” See E. Stephen, A. J. Blake, E. Carter, D. Collison, E. S. Davies, R. Edge, W. Lewis, D. M. Murphy, C. Wilson, R. O. Gould, A. J. Holder, J. McMaster, M. Schröder, *Inorg. Chem.* **2012**, *51*, 1450.
- 136 S. Seidel, K. Seppelt *Science* **2000**, *290*, 117.
- 137 D. Zopes, C. Hegemann, W. W. Tyrra, S. Mathur *Chem. Commun.* **2012**, *48*, 8805.
- 138 T. Dann, D.-A. Rosca, J. A. Wright, G. G. Wildgoose, M. Bochmann *Chem. Commun.* **2013**, *49*, 10169.
-

- 139 a) A. A. Mohamed, H. E. Abdou, A. Mayer, J. P. Fackler Jr. *J. Cluster Sci.* **2008**, *19*, 551. b) M. A. Bennerr, S. K. Bhargava, N. Mirzadeh, S. H. Priver, J. Wagler, A. C. Willis *Dalton Trans.* **2009**, 7537.
- 140 J. R. Walensky, C. M. Fafard, C. Guo, C. M. Brammell, B. M. Foxman, M. B. Hall, O. V. Ozerov *Inorg. Chem.* **2013**, *52*, 2317.
- 141 S. A. Yurin, D. A. Lemenovskii, K. I. Grandberg, I. G. Il'ina, L. G. Kuz'mina *Russ. Chem. Bull. Int. Ed.* **2003**, *52*, 2752.
- 141 a) J. Kordis, K. A. Ginerich, R. J. Seyse *J. Chem. Phys.* **1974**, *61*, 5114. b)
- 142 Luo, Y. R. *Comprehensive Handbook of Chemical Bond Energies*, CRC Press, Boca Raton, FL, **2007**.
- 143 X.-G. Xiong, P. Pyykkö *Chem. Commun.* **2013**, *49*, 2103.
- 144 R. Huacuja, D. J. Graham, C. M. Fafard, C.-H. Chen, B. M. Foxman, D. E. Herbert, G. Alliger, C. M. Thomas, O. V. Ozerov *J. Am. Chem. Soc.* **2011**, *133*, 3820.
- 145 E. S. Borren, A. F. Hill, R. Shang, M. Sharma, A. C. Willis *J. Am. Chem. Soc.* **2013**, *135*, 4942.
- 146 T. K.M. Lee, N. Zhu, V. W.-W. Yam *J. Am. Chem. Soc.* **2010**, *132*, 17646.
- 147 S.-Y. Yu, Z.-X. Zhang, E. C.-C. Cheng, Y.-Z. Li, V. W.-W. Yam, H.-P. Huang, R. Zhang. c) A. A. Mohamed, H. E. Abdou, M. D. Irwin, J. M. Lopez-de-Luzuriaga, J. P. Fackler Jr. *J. Cluster Sci.* **2003**, *14*, 253.
- 148 a) S. Bhargava, K. Kitadai, T. Masashi, D. W. Drumm, S. P. Russo, V. W.-W. Yam, R. K.-K. Lee, J. Wagler, N. Mirzadeh *Dalton Trans.* **2012**, *41*, 4789. b) S. Cronje, H. G. Raubenheimer, H. S.C. Spies, C. Esterhuysen, H. Schmidbaur, A. Schier, G. J. Kruger *Dalton Trans.* **2003**, 2859. c) J. H. K. Yip, J. Prabhavanthy *Angew. Chem. Int. Ed.* **2001**, *40*, 2159. d) C. Yang, M. Messerschmidt, P. Coppens, M. A. Omary *Inorg. Chem.* **2006**, *45*, 6592. e) E. M. Lane, T. W. Chapp, R. P. Hughes, D. S. Glueck, B. C. Feland, G. M. Bernard, R. E. Wasylshen, A. L. Rheingold *Inorg. Chem.* **2010**, *49*, 3950. f) D. M. P. Mingos, J. Yau, S. Menzer, D. J. Williams *Angew. Chem. Int. Ed. Engl.* **1995**, *34*, 1894.
- 149 a) A. A. Herzing, C. J. Kiely, A. F. Carley, P. Landon, G. J. Hutchings *Science*, **2008**, *321*, 1331. b) Chunyan Liu, Y. Tan, S. Lin, H. Li, X. Wu, L. Li, Y. Pei, X. C. Zeng *J. Am. Chem. Soc.* **2013**, *135*, 2583.
- 150 S. Lee, L. M. Molina, M. J. Lopez, J. A. Alonso, B. Hammer, B. Lee, S. Seifert, R. E. Winans, J. W. Elam, M. J. Pellin, S. Vajda *Angew. Chem. Int. Ed.* **2009**, *48*, 1467.
- 151 J. Guzman, B. C. Gates *Angew. Chem. Int. Ed.* **2003**, *42*, 690.
- 152 A. Corma, P. Concepcion, M. Boronat, M. J. Sabater, J. Navas, M. J. Yacaman, E. Larios, A. Posadas, M. A. Lopez-Quintela, D. Buceta, E. Mendoza, G. Guilera, A. Mayoral *Nat. Chem.* **2013**, *5*, 775.

- 153 T. J. Robilotto, J. Bacsa, T. G. Gray, J. P. Sadighi *Angew. Chem. Int. Ed.* **2012**, *51*, 12077.
- 154 E. Zeller, H. Beruda, H. Schmidbaur *Inorg. Chem.* **1993**, *32*, 3203.
- 155 a) Clive E. Briant, K. P. Hall, D. M. P. Mingos *J. Organomet. Chem.* **1983**, *254*, C18. b) V. Ramamoorthy, Z. Wu, Y. Yi, P. R. Sharp *J. Am. Chem. Soc.* **1992**, *114*, 1526.
- 156 a) E. S. Smirnova, A. M. Echavarren, *Angew. Chem. Int. Ed.* **2013**, *52*, 9023. b) P. Bellon, M. Monassero, M. Sansoni *J. Chem. Soc. Dalton Trans.* **1973**, 2423.
- 157 J. P. Fackler Jr. *Polyhedron* **1996**, *16*, 1.
- 158 S. Goel, K. A. Velizhanin, A. Pirytinski, S. Tretiak, S.A. Ivanov *J. Phys Chem. Lett.* **2010**, *1*, 927.
- 159 a) T. Dröge, F. Glorius *Angew. Chem. Int. Ed.* **2010**, *49*, 6940 b) O. Back, M Henry-Ellinger, C. D. Martin, D. Martin, G. Bertrand *Angew. Chem. Int. Ed.* **2013**, *52*, 2939.
- 160 D. Canseco-Gonzales, A. Petronilho, H. Mueller-Bunz, K. Ohmatsu, T. Ooi, M. Albrecht *J. Am. Chem. Soc.* **2013**, *135*, 13193.
- 161 D. S. Weinberger, M. Melaimi, C. E. Moore, A. L. Rheingold, G. Frenking, P. Jerbek, G. Bertrand *Angew. Chem. Int. Ed.* **2013**, *34*, 8964.
- 162 W. Nam, *Acc. Chem. Res.* **2007**, *40*, 465 and review articles in the special issue
- 163 For selected reviews see a) C. J. Cramer *Acc. Chem. Res.* **2007**, *40*, 601. b) J. A. Labinger, J. E. Bercaw *Nature* **2002**, *417*, 507. c) A. N. Vedernikov *Acc. Chem. Res.* **2012**, *45*, 803. d) K. Ray, F. Heims, F. F. Pfaff *Eur. J. Inorg. Chem.* **2013**, 3784. e) P. R. Sharp *J. Chem. Soc. Dalton. Trans.* **2000**, 2647. See also f) N. M. Weljange, E. Szuromi, P. R. Sharp *J. Am. Chem. Soc.* **2009**, *131*, 8736. g) E. Szuomi, H. Shan, P. R. Sharp *J. Am. Chem. Soc.* **2003**, *125*, 10522 h) M. Ahijado, T. Braun, D. Noveski, N. Kocher, B. Neumann, D. Stalke, H.-G. Stammer *Angew. Chem. Int. Ed.* **2005**, *44*, 6947. For oxygen transfer to inorganic substrates see i) A. Bakac *Coord. Chem. Rev.* **2006**, *250*, 2046.
- 164 a) C. N. Cornell, M. S. Sigman *Inorg. Chem.* **2007**, *46*, 1903. b) K. M. Gligorich, M. S. Sigman *Chem. Commun.* **2009**, 3854. c) T. Nishimura, T. Onoue, K. Ohe, S. Uemura *J. Org. Chem.* **1999**, *64*, 6750. d) S.-I. Murahashi, N. Komiya, H. Terai, T. Nakae *J. Am. Chem. Soc.* **2003**, *125*, 15312.
- 165 R. A. Taylor, D. J. Law, G. J. Sunley, A. J. P. White, G. J. P. Britovsek *Angew. Chem. Int. Ed.* **2009**, *48*, 5900.
- 166 M. C. Gimeno, A. Laguna *Comprehensive Coordination Chemistry II*. Vol. 6 (J. A. McCleverty, T. J. Meyer eds.) Elsevier, **2003**, p.911-1145.
- 167 R. H. Holm *Chem. Rev.* **1987**, *87*, 1401.

- 168 E. Poverenov, I. Efremenko, A. I. Frenkel, Y. Ben-David, L. J. W. Shimon, G. Leitus, L. Konstantinovski, J. M. L. Martin, D. Milstein *Nature* **2008**, *455*, 1093.
- 169 K. P. O'Halloran, C. Zhao, N. S. Ando, A. J. Schultz, T. F. Koetzle, P. M. B. Piccoli, B. Hedman, K. O. Hodgson, E. Bobyr, M. L. Kirk, S. Knottenbelt, E. C. Depperman, B. Stein, T. M. Anderson, R. Cao, Y. V. Geletii, K. I. Hardcastle, D. G. Musaev, W. A. Neiwert, X. Fang, K. Morokuma, S. Wu, P. Kögerler, C. L. Hill *Inorg. Chem.* **2012**, *51*, 7025.
- 170 A. Corma, I. Dominiguez, A. Domenech, V. Fornes, C. J. Gomez-Garcia, T. Rodenas, M. J. Sabater *J. Catal.* **2009**, *265*, 238.
- 171 M. Haruta, T. Kobayashi, H. Sano, N. Yamada *Chem. Lett.* **1987**, 405.
- 172 M. Chen, D. W. Goodman *Chem. Soc. Rev.* **2008**, *37*, 1860.
- 173 See for example a) M. S. Chen, D. W. Goodman *Science* **2004**, *306*, 252. b) G. Bond, D. T. Thompson *Gold Bull.* **2000**, *32*, 41. c) M. Valden, D. W. Goodman *Science* **1998**, *281*, 1647.
- 174 P. Lakshmanan, F. Averseng, N. Bion, L. Delannoy, J.-M. Tatibouet, C. Louis *Gold Bull.* **2013**, doi:10.1007/s13404-013-013-z
- 175 R. Meyer, C. Lemire, S. K. Shaikhutdinov, H.-J. Freund *Gold Bull.* **2004**, *37*, 72.
- 176 a) L. D. Socaciu, J. Hagen, T. M. Bernhardt, L. Wöste, U. Heiz, H. Häkkinen, U. Landman *J. Am. Chem. Soc.* **2003**, *125*, 10437. b) A. P. Woodham, G. Meijer, A. Fielicke *Angew. Chem. Int. Ed.* **2012**, *51*, 4444. c) Y. Gao, X. C. Zeng *ACS Catal.* **2012**, *2*, 2614.
- 177 A. P. Woodham, G. Meijer, A. Fielicke *J. Am. Chem. Soc.* **2013**, *135*, 1727.
- 178 a) J. Guzman, B. C. Gates *J. Am. Chem. Soc.* **2004**, *126*, 2672. b) G. J. Hutchings, M. S. Hall, A. F. Carley, P. Landon, B. E. Solsona, C. J. Kiely, A. Herzing, M. Makkee, J. A. Moulijn, A. Overweg, J. C. Fierro-Gonzalez, J. Guzman, B. C. Gates *J. Catal.* **2006**, *242*, 71.
- 179 a) A. M. Joshi, N. Delgass, K. M. Thomson *J. Phys. Chem. B* **2006**, *110*, 2572. b) K. L. Howard, D. J. Willock *Faraday Discuss.* **2011**, *152*, 135, and cites references.
- 180 K. Bobuatong, S. Karanjit, R. Fukuda, M. Ehara, H. Sakurai *Phys. Chem. Chem. Phys.* **2012**, *14*, 3103.
- 181 O. Diaz-Morales, F. Calle-Vellejo, C. de Munck, M. T. M. Koper *Chem. Sci.* **2013**, *4*, 2334.
- 182 a) M. C. Denney, N. A. Smythe, K. L. Cetto, R. A. Kemp, K. I. Goldberg *J. Am. Chem. Soc.* **2006**, *128*, 2508. b) D. D. Wick, K. I. Goldberg *J. Am. Chem. Soc.* **1999**, *121*, 11900. c) L. Boisvert, K. I. Goldberg *Acc. Chem. Res.* **2012**, *45*, 899. d) V. V. Rostovtsev, L. M. Henling, J. A. Labinger, J. E. Bercaw *Inorg. Chem.* **2002**, *41*, 3608.

- 183 a) T. S. Teets, D. G. Nocera *J. Am. Chem. Soc.* **2011**, *133*, 17796. b) T. S. Teets, D. G. Nocera *Dalton Trans.* **2013**, *42*, 3521.
- 184 J. M. Keith, R. P. Muller, R. A. Kemp, K. I. Goldberg, W. A. Goddard III, J. Oxgaard *Inorg. Chem.* **2006**, *45*, 9631.
- 185 J. Yoon, A. W. Czarnik *J. Am. Chem. Soc.* **1992**, *114*, 5874.
- 186 G. Strukul *Catalytic Oxidations with Hydrogen Peroxide as Oxidant*, Springer, **1993**, p. 59
- 187 A. Collado, A. Gomez-Suarez, Y. Oonishi, A. M.Z. Slawin, S. P. Nolan *Chem. Commun.* **2013**, *49*, 10745.
- 188 G. Strukul, R. A. Michelin, J. D. Orbell, L. Randaccio *Inorg. Chem.* **1983**, *22*, 3706.
- 189 T. Miyaji, M. Kujime, S. Hikichi, Y. Moro-oka, M. Akita *Inorg. Chem.* **2002**, *41*, 5286.
- 190 a) L. Boisvert, M. C. Denney, S. Kloek Hanson, K. I. Goldberg *J. Am. Chem. Soc.* **2009**, *131*, 15802. b) K. A. Grace, K. I. Goldberg *Organometallics* **2009**, *28*, 953.
- 191 Jacox, M. E. *NIST Chemistry WebBook, NIST Standard Reference Database Number 69*. (eds P. J. Linstrom & W. G. Mallard) (National Institute of Standards and Technology 20899, 2011) <http://webbook.nist.gov>
- 192 B. S. Yeo, S. L. Klaus, P. N. Ross, R. A. Mathies, A. T. Bell *ChemPhysChem* **2010**, *11*, 1854.
- 193 S. C. Abrahams, R. L. Collin, W. N. Lipscomb *Acta. Cryst.* **1951**, *4*, 15.
- 194 a) J. R. Barker, S. W. Benson, D. M. Golden *Int. J. Chem. Kinet.* **1977**, *9*, 31. b) X. Luo, P. R. Fleming, T. R. Rizzo *J. Chem. Phys.* **1992**, *96*, 5659.
- 195 A substoichiometric amount of phosphine was used to avoid over-reduction of (C^NC)AuOH
- 196 a) G. Strukul, R. Ros, R. A. Michelin *Inorg. Chem.* **1982**, *21*, 495. b) G. Strukul, R. A. Michelin *J. Am. Chem. Soc.* **1985**, *107*, 7563.
- 197 M. Akita, T. Miyaji, S. Hikichi, Y. Moro-oka *Chem. Commun.* **1998**, 1005.
- 198 N. A. Smythe, K. A. Grace, B. S. Williams, K. I. Goldberg *Organometallics* **2009**, *28*, 277.
- 199 S. K. Tahmassebi, R. R. Conry, J. M. Mayer *J. Am. Chem. Soc.* **1993**, *115*, 7553.
- 200 a) R. Gerber, T. Fox, C. M. Frech *Chem. Eur. J.* **2010**, *16*, 6771. b) G. R. Fulmer, A. N. Herndon, W. Kaminsky, R. A. Kemp, K. I. Goldberg *J. Am. Chem. Soc.* **2011**, *133*, 17713.

- 201 a) R. Cao, W. Lai, O. Du *Energy Environ. Sci.* **2012**, 5, 8134. b) D. G. Hetterscheid, J. N. H. Reek *Angew. Chem. Int. Ed.* **2012**, 51, 9740.
- 202 S. W. Kohl, L. Weiner, L. Schartsburd, L. Konstantinovski, L. J. Shimon, Y. Ben-David, M. A. Iron, D. Milstein *Science* **2009**, 324, 74.
- 203 Despite numerous attempts and methods, a maximum deuteration of 85% could only be achieved
- 204 P.W. Atkins *Physical Chemistry* Oxford University Press, Oxford **1998** p. 833.
- 205 For a discussion on Secondary Kinetic Isotope Effects relevant to organometallic compounds see M. Gomez-Gallego, M. A Sierra *Chem. Rev.* **2011**, 111, 4857.
- 206 Hammett parameters taken from O. Exner *Correlation Analysis of Chemical Data*, Plenum Press, New York, **1988**. p. 61-62.
- 207 Since the sample preparation did not allow for rigorous exclusion of oxygen, some ^{16}O contamination of the ^{18}O labelled sample may have occurred while the sample was nebulised in the mass spectrometer ($T = 673\text{ K}$). Nevertheless, the mass spectrum shows unequivocal ^{18}O incorporation.
- 208 See for example H. Schmidbaur, A. Schier *Organometallics* **2010**, 29, 2.
- 209 X. Cai, S. Majumdar, G. Fortman, C. S. J. Cazin, A. M. Z. Slawin, C. Lhermitte, R. Prabhakar, M. E. Germain, T. Pallucio, S. P. Nolan, E. V. Rybak-Akimova, M. Temprado, B. Captain, C. D. Hoff *J. Am. Chem. Soc.* **2011**, 133, 1290.
- 210 a) M. Deward *Bull. Soc. Chim. Fr.* **1951**, 18, C79. b) J. Chatt, L. A. Duncanson, L. M. Venanzi *J. Chem. Soc.* **1955**, 4456. For a review on coinage metal alkene complexes see c) H.V. Rasika Dias, J. Wu *Eur. J. Inorg. Chem.* **2008**, 509-522.
- 211 a) R. O. C. Norman, W. E. Parr, C. B. Thomas, *J. Chem. Soc. Perkin Trans I* **1976**, 811. b) B. Armer, H. Schmidbaur *Angew. Chem. Int. Ed. Engl.* **1970**, 9, 101. c) P. K. Monaghan, R. J. Puddephatt *Inorg. Chim. Acta.* **1975**, 15, 231.
- 212 A. J. Chalk *J. Am. Chem. Soc.* **1964**, 86, 4733.
- 213 a) M. S. Nechaev, V. M. Rayon, G. Frenking *J. Phys. Chem. A.* **2004**, 108, 3134. b) M. Garcia-Mota, N. Cabello, F. Maseras, A. M. Echavarren, J. Perez-Ramirez, N. Lopez *ChemPhysChem* **2008**, 9, 1624. c) M. Pernpointner, A.S.K. Hashmi *J. Chem. Theory Comput.* **2009**, 5, 2717.
- 214 E. Langseth, M. L. Scheuermann, D. Balcells, W. Kaminsky, K. I. Goldberg, O. Eisenstein, R. H. Heyn, M. Tilset *Angew. Chem. Int. Ed.* **2013**, 52, 1660.
- 215 Y. Sarazin, D. L. Hughes, N. Kaltsoyannis, J. A. Wright, M. Bochmann *J. Am. Chem. Soc.* **2007**, 129, 881.
- 216 C. A. Tolman *J. Am. Chem. Soc.* **1974**, 96, 2780.

- 217 F. P. Fanizzi, F. P. Intini, L. Maresca, G. Natile, M. Lanfranchi, A. Tiripicchio *J. Chem. Soc. Dalton Trans.* **1991**, 1007.
- 218 M. A. Cinellu, G. Minghetti, F. Cocco, S. Stoccoro, A. Zucca, M. Monassero, M. Arca *Dalton Trans.* **2006**, 5703.
- 219 A. D. Hennis, J. D. Polley, G. S. Long, A. Sen *Organometallics* **2001**, *20*, 2802.
- 220 Nevertheless, caution should be taken when comparing directly cationic and neutral complexes since in cationic complexes the MOs reduce in size leading to a smaller degree of overlap.
- 221 M. Fianchini, H. Dai, H. V. Rasika Dias *Chem. Commun.* **2009**, 6373.
- 222 T. J. Brown, M. G. Dickens, R. A. Widenhoeffer *J. Am. Chem. Soc.* **2009**, *131*, 6350
- 223 N. Savjani, D.-A. Rosca, M. Schormann, M. Bochmann *Angew. Chem. Int. Ed.* **2013**, *52*, 874.
- 224 Z. Zhang, S. Du Lee, A. S. Fisher, R. A. Widenhoeffer *Tetrahedron* **2009**, *65*, 1794.
- 225 R. Casado, M. Contel, M. Laguna, P. Romero, S. Sanz *J. Am. Chem. Soc.* **2003**, *125*, 11925.
- 226 K. Weissermel, H.-J. Arpe, *Industrial Organic Chemistry*, 2003, Wiley-VCH, New York, ed. 4
- 227 a) J. Chatt *Chem. Rev.* **1951**, *48*, 7. b) R. Grinstead *J. Org. Chem.* **1961**, *26*, 238. c) P. M. Henry *J. Am. Chem. Soc.* **1965**, *87*, 990. d) W. Kruse, T. M. Bednarski *J. Org. Chem.* **1971**, *36*, 1154. e) J. Byrd, J. Halpern *J. Am. Chem. Soc.* **1973**, *95*, 2586.
- 228 J. Smidt, W. Hafner, R. Jira, R. Sieber, J. Sedlmeier, A. Sabel *Angew. Chem. Int. Ed. Engl.* **1962**, *1*, 80. b) J. E. Baeckvall, B. Akermark, S. O. Ljunggren *J. Am. Chem. Soc.* **1979**, *101*, 2411. c) J. K. Stille, R. Divakaruni *J. Am. Chem. Soc.* **1978**, *100*, 1303. d) S. A. Beyrambadi, H. Eshtigah-Hosseini, M. R. Housaindokht, A. Morsali *Organometallics* **2008**, *27*, 72.
- 229 C.-G. Yang, C. He *J. Am. Chem. Soc.* **2005**, *127*, 6966.
- 230 C. E. Rezsnyak, J. Autschbach, J. D. Atwood, S. Moncho *J. Coord. Chem.* **2013**, *66*, 1153.
- 231 W. Wang, G. B. Hammond, B. Xu *J. Am. Chem. Soc.* **2012**, *134*, 5697.
- 232 N. Savjani, S. J. Lancaster, S. Bew, D. L. Hughes, M. Bochmann *Dalton Trans.* **2011**, *40*, 1079.
- 233 M. R. Plutino, L. Fenech, S. Stocoro, S. Rizzato, C. Castellano, A. Albinati *Inorg. Chem.* **2010**, *49*, 407.

- 234 a) T. M. Klapötke, B. Krumm, J.-C. Galvez-Ruiz, H. Nöth *Inorg. Chem.* **2005**, *44*, 9625. b) W. Beck, T. M. Klapötke, P. Klüfers, G. Kramer, C. M. Rienäcker *Z. Anorg. Allg. Chem.* **2001**, *627*, 1669 and references therein c) W. Beck, E. Schuierer, K. Feldl *Angew. Chem. Int. Ed. Engl.* **1966**, *5*, 249.
- 235 R. F. Ziolo, J. A. Thich, Z. Dori *Inorg. Chem.* **1972**, *11*, 626.
- 236 a) M. V. Baker, P. J. Barnard, S. K. Brayshaw, J. L. Hickey, B. W. Skelton, A. H. White *Dalton Trans.* **2005**, *37*. b) D. V. Partyka, T. J. Robilotto, J. B. Updegraff III, M. Zeller, A. D. Hunter, T. G. Gray *Organometallics* **2009**, *28*, 795.
- 237 C. Dash, M. Yousufuddin, T. R. Cundari, H. V. Rasika Dias *J. Am. Chem. Soc.* **2013**, *135*, 15479.
- 238 a) W. Beck, K. Burger, W. P. Fehlhammer *Chem. Ber.* **1971**, *104*, 1816. b) D. V. Partyka, J. B. Updegraff III, M. Zeller, A. D. Hunter, T. G. Gray *Organometallics* **2007**, *26*, 183. c) T. Robilotto, D. S. Alt, H. A. van Recum, T. G. Gray *Dalton Trans.* **2011**, *40*, 8083. d) T. J. Robilotto, N. Deligonul, J. B. Updegraff III, T. G. Gray *Inorg. Chem.* **2013**, *52*, 9659.
- 239 T. J. Del Castillo, S. Sarkar, K. A. Abboud, A. S. Veige *Dalton Trans.* **2011**, *40*, 8140. See also A. R. Powers, X. Yang, T. J. Del Castillo, I. Ghirviriga, K. A. Abbud, A. S. Veige *Dalton Trans.* **2013**, *42*, 14963
- 240 D. V. Partyka, T. J. Robilotto, M. Zeller, M. Zeller, A. D. Hunter, T. G. Gray *Proc. Natl. Acad. Sci.* **2008**, *105*, 14293.
- 241 A. Homms, I. Escofet, A. M. Echavarren *Org. Lett.* **2013**, *15*, 5782.
- 242 L. Bourget-Merle, M. F. Lappert, J. R. Severn *Chem. Rev.* **2002**, *102*, 3031.
- 243 An earlier report however shows the isolation of a dimeric silver(I) species supported by a non-functionalised β -diketiminatate ligand. See C. Shimokawa, S. Itoh *Inorg. Chem.* **2005**, *44*, 3031.
- 244 H. A. Chiong, O. Daugulis *Organometallics* **2006**, *26*, 4054.
- 245 a) M. S. Hill, P. B. Hitchcock *Chem. Commun.* **2004**, 1818. b) M. S. Hill, P. B. Hitchcock, R. Pongtavornpinyo *Dalton Trans.* **2005**, 273.
- 246 B. Guan, D. Xing, G. Cai, X. Wan, N. Yu, Z. Fang, L. Yang, Z. Shi *J. Am. Chem. Soc.* **2005**, *127*, 18004.
- 247 H. V. Rasika Dias, J. A. Flores *Inorg. Chem.* **2007**, *46*, 5841.
- 248 N. Savjani, M. Schormann, M. Bochmann *Polyhedron* **2012**, *137*.
- 249 N. Carrera, N. Savjani, J. Simpson, D. L. Hughes, M. Bochmann *Dalton Trans.* **2011**, *40*, 1016.
- 250 A. Venguopal, M. K. Ghosh, H. Jürgens, K. W. Törnroos, O. Swang, M. Tilset, R. H. Heyn *Organometallics* **2010**, *29*, 2248.

- 251 D. S. Laitar, C. J. N. Mathison, W. M. Davis, J. P. Sadighi *Inorg. Chem.* **2003**, *42*, 7354.
- 252 For a review see a) R. J. Baker, C. Jones *Coord. Chem. Rev.* **2005**, *249*, 1857. See also b) G. J. Moxey, C. Jones, A. Stasch, P. C. Junk, G. B. Deacon, W. D. Woodul, P. R. Drago *Dalton Trans.* **2009**, 2630. c) M. S. Hill, P. B. Hitchcock, R. Pongtavornpinyo *Dalton Trans.* **2008**, 2854.
- 253 Y.-C. Tsai *Coord. Chem. Rev.* **2012**, *256*, 722.
- 254 See for example a) X. Dai, T. H. Warren *Chem. Commun.* **2001**, 1998. b) P. L. Holland, T. R. Cundari, L. L. Perez, N. A. Eckert, R. J. Lachiotte *J. Am. Chem. Soc.* **2002**, *124*, 14416. c) Z. J. Tonzetich, A. J. Jiang, R. R. Schrock, P. Müller *Organometallics* **2007**, *26*, 3771. d) E. Kogut, H. L. Wiencko, L. Zhang, D. E. Cordeau, T. H. Warren *J. Am. Chem. Soc.* **2005**, *127*, 11248.
- 255 While this work was in progress, Phillips *et al.* reported the *in situ* generation of **67** and suggests the confirmation of its identity by independent synthesis. Nevertheless, no stability or characterisation data (solution or solid state) is presented. See D. F. Scheriber, Y. Ortin, H. Müller-Bunz, A. D. Phillips *Organometallics* **2011**, *30*, 5381.
- 256 a) L. H. Gade *Dalton Trans.* **2003**, 267. b) H. V. Rasika Dias, S. Singh, T. R. Cundari *Angew. Chem. Int. Ed.* **2005**, *44*, 4907 and references therein.
- 257 A number of methods for the synthesis of [Me₂AuCl]₂ were explored. We have found that by far, the most reliable method was the one described in M. Paul, H. Schmidbaur *Z. Naturforsch. B.* **1994**, *49*, 647. However, the isolated yield (20 %) was lower than the one reported (45%) and extensive reduction to gold metal was observed.
- 258 B. Räke, F. Zülch, D. J. Prust, H. W. Roesky, M. Noltemeyer, H.-G. Schmidt *Z. Anorg. Allg. Chem.* **2001**, *627*, 836.
- 259 a) J. Prust, H. Hohmeister, A. Stasch, H. W. Roesky, J. Magull, E. Alexopoulos, I. Uson, H.-G. Schmidt, M. Noltemeyer *Eur. J. Inorg. Chem.* **2002**, 2156. b) L. Ferro, M. P. Coles, I. J. Day, J. Robin Fulton *Organometallics* **2010**, *29*, 2911.
- 260 a) B. A. Jazdzewski, P. L. Holland, M. Pink, V. G. Young Jr., D. J. E. Spencer, W. B. Tolman *Inorg. Chem.* **2001**, *40*, 6097. b) A. Hadzovic, D. Song *Organometallics* **2008**, *27*, 1290.
- 261 S. J. Lancaster <http://cssp.chemspider.com/Article.aspx?id=215>
- 262 *Programs CrysAlisPro*, Oxford Diffraction Ltd., Abingdon, UK (2010)
- 263 S.J. Coles, P. Gale *Chem. Sci.* **2012**, *3*, 683.
- 264 G. M. Sheldrick *Acta Cryst.* **2008**, *A64*, 112.
- 265 A. L. Spek (2006) PLATON – A Multipurpose Crystallographic Tool, Utrecht University, Utrecht, The Netherlands. A. L. Spek, *Acta Cryst.*, **1990**, *A46*, C34
- 266 Farrugia, L. J. *J. Appl. Crystallogr.*, **1999**, *32*, 837.

267 *'International Tables for X-ray Crystallography'*, Kluwer Academic
Publishers, Dordrecht (1992). Vol. C, pp. 500, 219 and 193.